

AEDC-TR-95-12

Equations for Store Separation Motion Simulations and
Instrumented Model Data Reduction



K. S. Keen
Micro Craft Technology/AEDC Group

August 1996

Final Report for Period October 1993 through January 1995

Approved for public release; distribution is unlimited.

19960903 074

**ARNOLD ENGINEERING DEVELOPMENT CENTER
ARNOLD AIR FORCE BASE, TENNESSEE
AIR FORCE MATERIEL COMMAND
UNITED STATES AIR FORCE**

DTIC QUALITY INSPECTED 1

NOTICES

When U. S. Government drawings, specifications, or other data are used for any purpose other than a definitely related Government procurement operation, the Government thereby incurs no responsibility nor any obligation whatsoever, and the fact that the Government may have formulated, furnished, or in any way supplied the said drawings, specifications, or other data, is not to be regarded by implication or otherwise, or in any manner licensing the holder or any other person or corporation, or conveying any rights or permission to manufacture, use, or sell any patented invention that may in any way be related thereto.

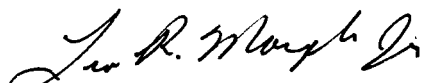
Qualified users may obtain copies of this report from the Defense Technical Information Center.

References to named commercial products in this report are not to be considered in any sense as an endorsement of the product by the United States Air Force or the Government.

This report has been reviewed by the Office of Public Affairs (PA) and is releasable to the National Technical Information Service (NTIS). At NTIS, it will be available to the general public, including foreign nations.

APPROVAL STATEMENT

This report has been reviewed and approved.



LEO R. MARPLE, JR
Aircraft Systems Test Division
Test Operations Directorate

Approved for publication:

FOR THE COMMANDER



EUGENE J. SANDERS
Technical Director, Aircraft Sys Test Division
Test Operations Directorate

REPORT DOCUMENTATION PAGE			Form Approved OMB No. 0704-0188
<p>Public reporting burden for this collection of information is estimated to average 1 hour per response, including the time for reviewing instructions, searching existing data sources, gathering and maintaining the data needed, and completing and reviewing the collection of information. Send comments regarding this burden estimate or any other aspect of this collection of information, including suggestions for reducing this burden, to Washington Headquarters Services, Directorate for Information Operations and Reports, 1215 Jefferson Davis Highway, Suite 1204, Arlington, VA 22202-4302, and to the Office of Management and Budget, Paperwork Reduction Project (0704-0188), Washington, DC 20503.</p>			
1. AGENCY USE ONLY (Leave blank)	2. REPORT DATE	3. REPORT TYPE AND DATES COVERED	
	August 1996	Final Report for Period October 1993 - January 1995	
4. TITLE AND SUBTITLE		5. FUNDING NUMBERS	
Equations for Store Separation Motion Simulations and Instrumented Model Data Reduction		PN - 0675	
6. AUTHOR(S)			
Keen, K. Scott, Micro Craft Technology/AEDC Operations			
7. PERFORMING ORGANIZATION NAME(S) AND ADDRESS(ES)		8. PERFORMING ORGANIZATION (REPORT NUMBER)	
Arnold Engineering Development Center/DOT Air Force Materiel Command Arnold Air Force Base, TN 37389-9011		AEDC-TR-95-12	
9. SPONSORING/MONITORING AGENCY NAMES(ES) AND ADDRESS(ES)		10. SPONSORING/MONITORING AGENCY REPORT NUMBER	
Aeronautical Systems Center/YFT Wright-Patterson Air Force Base, OH 45433			
11. SUPPLEMENTARY NOTES			
Available in Defense Technical Information Center (DTIC).			
12A. DISTRIBUTION/AVAILABILITY STATEMENT		12B. DISTRIBUTION CODE	
Approved for public release; distribution is unlimited.			
13. ABSTRACT (Maximum 200 words)			
<p>The mathematical equations of motion for ground simulation of the separation trajectories of stores from aircraft are developed in this document. The equations have application to both analytical and wind tunnel captive trajectory store separation testing. The equations of motion as presented here include features not previously available in AEDC analytical and wind tunnel simulations such as arbitrary aircraft maneuvers, more rigorous models of the specific pivot hardware used by some aircraft, and downrail motions with all components of kinematic acceleration (including Coriolis effects) modeled. The data reduction equations for free-falling instrumented store models are also included.</p>			
14. SUBJECT TERMS		15. NUMBER OF PAGES	
store separation, motion simulation, trajectory simulation, trajectory analysis, telemetry, axis systems, accelerometers, captive trajectory testing		233	
		16. PRICE CODE	
17. SECURITY CLASSIFICATION OF REPORT	18. SECURITY CLASSIFICATION OF THIS PAGE	19. SECURITY CLASSIFICATION OF ABSTRACT	20. LIMITATION OF ABSTRACT
UNCLASSIFIED	UNCLASSIFIED	UNCLASSIFIED	SAME AS REPORT

PREFACE

The work reported herein was conducted at the Arnold Engineering Development Center (AEDC), Air Force Materiel Command (AFMC). The major portion of the effort was sponsored by the store separation effort for the F-22 aircraft at the request of the Aeronautical Systems Center (ASC/YFT), AEDC Project Number 0675. The ASC/YFFIT Project Manager was Mr. Pete Amstutz. The results were obtained by Micro Craft Technology, technical services contractor for the Aerospace Flight Dynamics effort at the AEDC, AFMC, Arnold Air Base, TN. The work was conducted during the period October 1, 1993 through December 31, 1994, and the manuscript was submitted for publication on March 25, 1996.

This report is intended to summarize a broad range of topics in the numerical simulation, testing, and measurement of flight motions, and the author wishes to acknowledge the invaluable assistance of several colleagues who contributed greatly to the final product. Special thanks go to Mr. C. H. Morgret, whose unparalleled understanding of both the kinematics and aerodynamics of motion simulation were often called upon. Messrs. T. F. Langham, G. H. Saunders, and B. H. Hall developed the nomenclature system which is so integral a part of the equation development. Mr. D. A. Moore contributed to the modeling of accelerometer measurements. Dr. S. L. Keeling straightened out the math for the rotational motion equations about a moving pivot point. Finally, the combined experience of the captive trajectory testing group at AEDC and especially the kinematic expertise of Mr. J. B. Carman, Jr., lead CTS engineer, was invaluable.

CONTENTS

	<u>Page</u>
1.0 REFERENCE FRAMES AND MOTION PARAMETERS	7
1.1 Primary Axis Systems	7
1.2 Primary Motion Quantities.....	9
1.3 Projection Transformations for Vector Motion Properties.....	12
1.4 Derivatives of Rotational Transformations and Vector Quantities Projected into Rotating Reference Frames.....	16
1.5 Alternate Projection Transformations for Angular Velocity and Acceleration Vectors.....	18
2.0 ACCELEROMETER DESCRIPTION	19
3.0 ACCELERATION TRANSFER EQUATIONS	21
4.0 STORE EQUATIONS OF MOTION IN TRADITIONAL BODY-AXIS PROJECTION FORM	24
4.1 Translational Equations of Motion.....	24
4.1.1 Translational Equations for Unrestricted Motion	26
4.1.2 Translational Equations for Restricted Motion	28
4.2 Rotational Equations of Motion.....	31
4.2.1 Rotational Equations for Unrestricted Motion.....	33
4.2.2 Rotational Equations for Restricted Motion	41
4.2.3 Angular Orientations and Their Derivatives	53
4.3 Math Models of Physical Restraints for Restricted Motion (Boundary Conditions). .	85
4.3.1 Accelerations, Velocities, and Flight Path of a Wings-Level Constant Load Factor Aircraft Pitch-Plane Maneuver.....	86
4.3.2 Accelerations of a Fixed or Moving Hook Axis System Attached to a Maneuvering Aircraft	89
4.3.3 The Simple Pivot Rotational Constraint	95
4.3.4 True Pivot Rotational Constraint (F-16 Type)	98
4.3.5 True Pivot Rotational Constraint (F-15/F-18 Type)	105
4.3.6 Modified F-15 Pivot without Offset Roll Joint.....	125
4.3.7 Rail Constraints.....	130
4.3.8 Cradle Launcher Restraint (Motion Restricted to Ejector Plane)	136
4.3.9 Accelerations, Velocities, and Flight Path of an Aircraft Undergoing an Arbitrary Non-Idealized Maneuver.....	147
4.3.10 Strapdown Equations.....	155
4.4 Initial Conditions for Store-Separation Trajectory Simulations.....	158
4.4.1 Initial Conditions for Simulations from Carriage	158
4.4.2 Initial Conditions for Re-Started Simulations.....	161
4.4.3 Initial Conditions for Simulations Started at End-Of-Stroke or at Downrail Positions	161

	<u>Page</u>
5.0 DATA REDUCTION EQUATIONS FOR CALCULATION OF TRADITIONAL MOTION PROPERTIES FROM MEASUREMENTS OF FORWARD- AND AFT-MOUNTED ACCELEROMETERS	163
6.0 APPROXIMATING DYNAMIC STORE SEPARATION EVENTS USING STEADY-STATE WIND TUNNEL FORCE AND MOMENT MEASUREMENTS ..	174
6.1 Flow-Field, Translational, and Rotational Aerodynamics -	
The "Induced-Angle" Approximation	174
6.2 The "Non-Rotating Aircraft" Approximation for Constant Load-Factor Maneuvers	179
6.3 Extraction of Tested Model Orientations from Wind Tunnel Captive Trajectories..	180
7.0 CONCLUDING REMARKS	183
REFERENCES	183

ILLUSTRATIONS

<u>Figure</u>	<u>Page</u>
1. Operationally Inertial Axis Systems for Atmospheric Motion Simulations	185
2. The "Earth" Axis System for Store Separation	188
3. Store-Separation Inertial Axes	189
4. Store Body-Axis Coordinate System	191
5. Yaw-Pitch-Roll Rotation Sequence	192
6. Yaw-Pitch-Roll Rotation Sequence Shown on a Unit Sphere	193
7. The Effects of Two Rotations Performed in Opposite Orders	196
8. Pitch-Yaw-Roll Rotation Sequence	197
9. Physical Approximation of a "Tri-Axial" Accelerometer	198
10. An Idealized Accelerometer	199
11. Body, Hook, and Inertial Axis Systems	200
12. Moment Arms of Point P Relative to Body, Hook, and Inertial Axes	201
13. Schematic of the Derivative of a Vector	202
14. Velocities of Unit Vectors Fixed in a Rotating Body	202
15. Depiction of Euler Axis and Arbitrary Point "P" Before and After Euler Rotation ..	203
16. View of Euler Rotation Looking Down Euler Axis	204
17. Idealized Constant-Load-Factor Maneuver	205
18. Trajectory-Axis Coordinate Directions	206
19. Relationship Between Various Trajectory Axes for Pitch-Plane-Only Rotations ..	209
20. F-16 Pivot Fitting	210
21. F-15 Pivot Fitting	211
22. Relationship Between Body, Roll, and Hook Axes for F-15 Pivot	212
23. Free-Body Diagram for F-15 Pivot	213
24. Phases of Release Motion for F-15 Pivot Mechanism	215
25. Motion Parameters for Numerical Experiment	216
26. Free-Body Diagram of Tank at Instant RZS = 0	221

<u>Figure</u>	<u>Page</u>
27. AMRAAM/MRL Physical Interface	222
28. Ejector-Plane Motion	224
29. Instrumentation Axes for F-22 Drop Tanks.....	225
30. Sources of Aerodynamic Loads	226
31. Example of "Induced Angle" Approximation	227
32. Non-Rotating Aircraft Approximation.....	230

INTRODUCTION

The equations of motion used to numerically model free-flight, restricted pivot releases, and rail releases of stores from arbitrarily maneuvering aircraft are developed in this document. Also the equations modeling the operation, transfer of measurements, and data reduction necessary for fully instrumenting flight and drop models for store separation are developed and presented herein.

The document begins in Section 1.0 with a brief background discussion of rotating and inertial reference frames and some of the vector math necessary to provide a foundation for the developments which will follow. A description of the operation of accelerometer instrumentation and a mathematical description of the physical quantities measurable by accelerometers is provided in Section 2.0. Section 2.0 provides some of the background information necessary to understand how flight and wind tunnel test models may be instrumented to measure motion properties. The relationships for transforming measured accelerations from the point of measurement to another point on a rigid body are developed in Section 3.0. Derivations of the equations of motion as used in separation trajectory simulations and as used in inverse form in programs designed to extract the aerodynamic properties which cause a given flight or wind tunnel free-drop motion are presented in Section 4.0. The Section 4.0 equations represent an upgrade to the equation-of-motion package which has traditionally been used for captive trajectory store separation wind tunnel testing at the AEDC since the late 1970's (Ref. 1). The upgraded capabilities include more rigorous models of accelerations for rail-launched missiles which include all Coriolis acceleration components downrail, more rigorous models of pivot constraints (a decoupled, "simple" constraint had been used previously), more rigorous models of ejector cradle devices which restrict early store motion to the ejector plane, use of quaternions to describe angular orientations (which avoids numerical problems at certain rotation angles), and provision for including arbitrary aircraft maneuvers in the motion simulations. Specification of initial conditions for numerical trajectory simulations is also described in Section 4.0. The data reduction equations required to reduce the output from a pair of three-axis linear accelerometers (one mounted forward in the store and one mounted aft) into store linear and angular accelerations, velocities, and positions at the store center of gravity are presented in Section 5.0. The equations developed in Section 5.0 form the basis of the data reduction package used to reduce telemetered motion information during a recent F-22 tank drop test. Finally, an analysis of approximations which are necessary when attempting to model dynamic store separation events using steady-state wind tunnel measurements is presented in Section 6.0.

1.0 REFERENCE FRAMES AND MOTION PARAMETERS

1.1 PRIMARY AXIS SYSTEMS

The fundamental axis system relative to which all motion parameters are defined and relative to which the equations of motion are derived must be inertially fixed. An inertial or Newtonian system is simply a coordinate system which is not allowed to rotate or linearly accelerate. The Newtonian (Force = Mass * Acceleration) relations from which the equations of motion are developed do not hold if the axis systems in which the force or acceleration properties

are measured are, themselves, accelerating. All physical processes such as forces, moments, velocities, and accelerations occur fundamentally within inertial space. Although inertial quantities may be expressed in terms of components measured in a non-inertial system, only in the inertial system do they have true physical meaning.

The first issue to be addressed in any motion simulation is the selection of a proper inertial axis system. It is, of course, not possible to define a true inertially fixed reference base anywhere in the known universe, but so-called "operationally inertial" frames can be defined which are (at least) inertial enough to allow solution of certain classes of motion problems. For example, in interplanetary flight simulations, the inertial axes can be sun-centered and fixed relative to certain "fixed" stars. At a slightly lower level, the inertial axes for simulations of satellites and spacecraft in earth orbit can be fixed at the center of the earth with the axes fixed relative to the fixed stars but with the earth rotating about the inertial axes once per day. Four different levels of successively less sophisticated operationally inertial systems for atmospheric motion simulations are shown in Fig. 1. The "navigation" axis system of Fig. 1d, which is based on local earth latitude and longitude coordinates, is most often used for simulation of aircraft flight motions for significant distances over the earth. (Note that the definitions for the local longitude, latitude, and altitude above the earth surface become slightly more complicated than the spherical-earth relations presented in Fig. 1 if the oblateness or bulging of the earth at the equator is included in the model).

For store separation motion simulations (which are normally of small time duration), the true local earth surface can be operationally replaced with a "flat earth" approximation. The inertial system is often taken to be fixed relative to the local tangent to the earth surface. One special case of earth-fixed "flat earth" inertial axes is generally referred to as "earth" axes and will be designated herein by the letter "E". The ZE-axis is usually directed downward along the gravity vector from the aircraft or store center of gravity and the XE-YE plane is parallel to the local tangent to the earth's surface. The XE direction is usually aligned with the projection of the aircraft flight velocity at the initial time onto the local earth horizontal plane, and YE is perpendicular to the XE and ZE axes. Generally, the origin of the earth axis system is coincident with the center-of-gravity position of the aircraft (or the store on the aircraft) at the start of the simulation, although sometimes the point on the earth's surface directly below the initial position of the aircraft is used. The earth-axis system is often used as the inertial system for aircraft motion simulations (sometimes including correction terms to roughly account for errors associated with not using the rotating round earth model). Less often, earth axes are used as the inertial system in store separation simulations. When earth axes are selected as the inertial system for a store separation trajectory analysis, separate motion simulations are required for the motion of the store relative to earth axes and for the motion of the parent aircraft relative to earth axes so that the difference between the two simulations can be used to define the trajectory of the store relative to the aircraft. Earth axes are illustrated in Fig. 2.

The inertial system most commonly used in store separation analyses is one step in sophistication below earth axes and is defined relative to the air mass (which may be moving relative to the earth if atmospheric winds are included in the simulation). The special separation inertial axis system is designated by the letter "I" and will be the primary system for all trajectory problems

analyzed herein. This axis system is not fixed in the air mass but is aligned with the tangent to the parent aircraft flight path at the instant of store release and is translating at a constant free-stream velocity within the air mass (not linearly accelerating) along the initial flight-path tangent. This inertial system is particularly convenient for wind tunnel simulations of flight separation events because the XI axis is aligned with the tunnel centerline (and, therefore, the tunnel free-stream velocity), and the system is operationally fixed relative to the moving air mass in the tunnel. The specialized store separation inertial axes allow modeling of the store separation event as a single "relative" trajectory (store relative to aircraft) rather than as the differences between two separate "absolute" trajectories for store and aircraft. The inertial axes are pitched relative to earth axes by the simulated aircraft climb angle and rolled by the simulated aircraft bank angle, making XI positive forward along the free-stream velocity vector at the instant of release, ZI positive down parallel to the plane of symmetry of the parent aircraft, and YI perpendicular to the XI and ZI directions to the pilot's right. The inertial origin can be arbitrary, but for separation studies, it is usually defined to be coincident with the store center-of-gravity (cg) position at the instant of release. The common store separation inertial axes are illustrated in Fig. 3.

For convenience, several other non-inertial axis systems have been defined which are sometimes useful in the development of motion equations. It should always be remembered, however, that forces, velocities, and accelerations are fundamentally inertial quantities. One important secondary coordinate reference frame is the store body-axis system (Fig. 4) - a store body-fixed right-handed system with origin at the store center of gravity and which will be designated herein by the letter "B". The store body axes are a rotating frame of reference moving with the store during its motion. Body axes are sometimes more convenient than inertial systems in the development of store equations of motion because store mass properties such as moments and products of inertia are not dependent on store attitude when they are defined in this system. When a fundamentally inertial quantity (such as a velocity) is measured in or projected into the coordinate directions of a non-inertial system such as body axes, it is sometimes said to be "coordinatized" in that system.

Another useful set of coordinate systems for instrumented stores are additional body-fixed systems which are aligned with the acceleration and rate measurement instrumentation. The "transducer" systems will be denoted by the letter "T". The system for each transducer may be translated and rotated relative to the cg-fixed body-axis system.

A whole series of trajectory axis systems will be introduced to describe the motion of a separating store body relative to an aircraft in Section 4.0. Common trajectory axes include flight axes, aircraft axes, pylon axes, and carriage axes (denoted by "F", "A", "P", and "C", respectively) along with several hook and rail-fixed axes necessary to describe physical motion restraints. These trajectory axis systems will be described as needed in Section 4.0.

1.2 PRIMARY MOTION QUANTITIES

A special nomenclature has been developed to denote the fundamental motion quantities in the derivations presented in this report. Use of the nomenclature greatly simplifies the development of motion and data reduction equations and also greatly aids in developing an understanding of the physical meaning of various motion parameters. Most importantly, the

nomenclature provides a consistent system for defining all types of trajectory motions in a unified manner. The importance of the nomenclature system should not be underestimated. The interrelations of kinematic quantities can be very complicated, and erroneous mathematical relationships are surprisingly common throughout much of the available literature. In several cases in the present effort, errors in the mathematical formulations of "textbook" equations were identified simply because the names of various terms in the equations were inconsistent when they were adapted to the new nomenclature. Another strong feature of the nomenclature is that it adapts directly to computer coding without any need to relate program variable names to some external nomenclature or variable definition table. In a very real sense, the computer coding for the motion equations using the new nomenclature as developed herein can be considered to be "self-commented."

Up to three different axis systems may be involved in completely defining many important motion quantities. One important system is the one in whose coordinate directions the property is measured. The second system is the system of interest (that is, the system representing the body which is moving). The final system is the system relative to which the motion of the system of interest is defined. Each of these systems is identified within the variable name of the motion property when the new nomenclature is used.

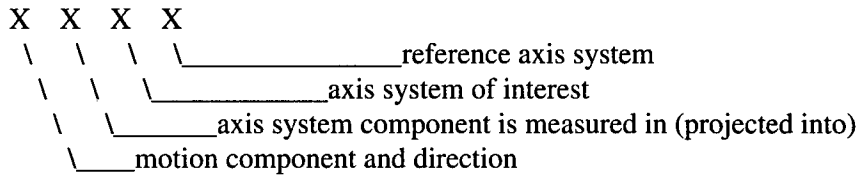
The primary translational motion quantities are:

1. The three components defined in the coordinate directions of some measurement axis system of the displacement (linear position) of the origin of the coordinate system of interest relative to the reference system ($\bar{r} = \{X, Y, Z\}$),
2. The three components defined in the coordinate directions of some measurement axis system of the linear velocity of the origin of the coordinate system of interest relative to the reference system ($\bar{v} = \{U, V, W\}$), and
3. The three components defined in the coordinate directions of some measurement axis system of the linear acceleration of the origin of the coordinate system of interest relative to the reference system ($\bar{a} = \{\alpha X, \alpha Y, \alpha Z\}$).

The primary rotational motion quantities are:

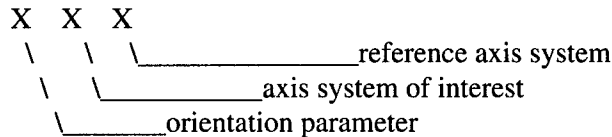
1. The angular orientation of the axis system of interest relative to the reference system. This orientation may be defined alternately by three successive rotation angles (Ψ, θ , and ϕ), or by four Euler parameters or quaternions (E_0, E_1, E_2 , and E_3), or by a nine-element transformation matrix (TRN),
2. The three components defined in the coordinate directions of some measurement axis system of the angular velocity of the coordinate system of interest relative to the reference system ($\bar{\omega} = \{P, Q, R\}$), and
3. The three components defined in the coordinate directions of some measurement axis system of the angular acceleration of the coordinate system of interest relative to the reference system ($\bar{\alpha} = \{\alpha X, \alpha Y, \alpha Z\}$).

The special nomenclature developed for motion terms incorporates identifiers for each axis system involved in defining each motion property. The full names of the motion quantities make use of a coding process which takes the following form for all linear terms and angular velocity and acceleration terms:



For example, the full motion quantity name UBBI would be decoded as "the x-component of the velocity of the body axis system relative to the inertial axis system as measured in (projected into) the body-axis component directions."

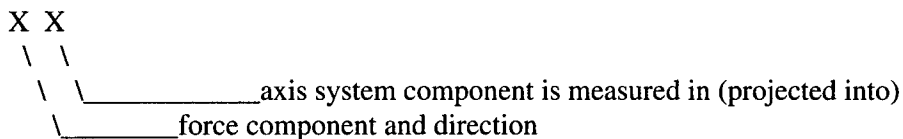
Orientation parameters include only reference-system and system-of-interest indicators:



For example, the full motion quantity name THAIE (or θ_{IE}) would be decoded as "the pitch angle of the inertial axis system relative to the earth axis system." Similarly, the term TRNBI represents "the transformation matrix describing the orientation of the body axis system relative to the inertial axis system."

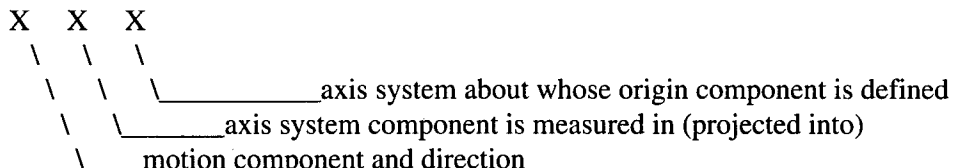
In addition to the motion terms, naming conventions have also been defined for the applied forces and moments (and related terms such as linear and angular momentum) which cause the motion.

Force terms are coded with indicators for only the component and the axis system of projection:



For example, the full force quantity name FXB would be decoded as "the x-component of the force applied onto the store as measured in (projected into) the body-axis component directions."

Moments and products of inertia must specify the measurement axis system and the axis system about whose origin point the moments are defined:



For example, the full quantity name I_{xxIB} , would be decoded as “the x-component of the moment of inertia about the body-axis origin point as measured in (projected into) the inertial-axis component directions.”

1.3 PROJECTION TRANSFORMATIONS FOR VECTOR MOTION PROPERTIES

The equations for coordinate projection transformations and their derivatives are developed in this section. More in-depth discussions of rotations will also be provided later in Section 4.2.3. At the present point, however, only the level of detail necessary to allow development of the basic motion equations will be presented.

Rotations are commonly represented by rotational transformations which project the pre-rotation coordinates of an object to post-rotation coordinates. A yaw rotation through an angle ψ about the Z-axis of a coordinate system can, for example, be represented by a transformation of the form:

$$\begin{aligned} x_{\text{new}} &= x_{\text{old}} * \cos \psi + y_{\text{old}} * \sin \psi \\ y_{\text{new}} &= -x_{\text{old}} * \sin \psi + y_{\text{old}} * \cos \psi \\ z_{\text{new}} &= z_{\text{old}} \end{aligned} \quad (1.3.1)$$

where the coordinates of each point measured in the old axis system are rotated to define coordinates in the new axis system. This transformation can also be written in matrix form as

$$\{\bar{x}_{\text{new}}\} = [\text{TRNz}(\psi)] \{\bar{x}_{\text{old}}\} \quad (1.3.2)$$

where

$$[\text{TRNz}(\psi)] = \begin{bmatrix} \cos \psi & \sin \psi & 0 \\ -\sin \psi & \cos \psi & 0 \\ 0 & 0 & 1 \end{bmatrix} \quad (1.3.3)$$

$$\{\bar{x}_{\text{new}}\} = \begin{vmatrix} x_{\text{new}} \\ y_{\text{new}} \\ z_{\text{new}} \end{vmatrix} \quad \text{and } \{\bar{x}_{\text{old}}\} = \begin{vmatrix} x_{\text{old}} \\ y_{\text{old}} \\ z_{\text{old}} \end{vmatrix} \quad (1.3.4)$$

Similarly, a rotation through a pitch angle θ about the coordinate Y-axis can be represented by the rotation matrix:

$$[\text{TRNy}(\theta)] = \begin{bmatrix} \cos \theta & 0 & -\sin \theta \\ 0 & 1 & 0 \\ \sin \theta & 0 & \cos \theta \end{bmatrix} \quad (1.3.5)$$

and a rotation through a roll angle ϕ about the coordinate X-axis can be represented by:

$$[\text{TRNx}(\phi)] = \begin{bmatrix} 1 & 0 & 0 \\ 0 & \cos \phi & \sin \phi \\ 0 & -\sin \phi & \cos \phi \end{bmatrix} \quad (1.3.6)$$

The complete rotational transformation, assuming the rotations are applied in sequence first about the z axis, then about the resulting new y axis, then about the resulting new x axis (yaw-pitch-roll sequence) becomes

$$\{\bar{x} \text{ new}\} = [\text{TRNx}(\phi)] [\text{TRNy}(\theta)] [\text{TRNz}(\psi)] \{\bar{x} \text{ old}\} = [\text{TRN}(\psi, \theta, \phi)] \{\bar{x} \text{ old}\} \quad (1.3.7)$$

The terms of the complete rotation matrix (which are sometimes called direction cosines, as will be shown in Section 4.2.3) are obtained by carrying out the matrix multiplication in Eq. (1.3.7):

$$\begin{aligned} [\text{TRN}(\psi, \theta, \phi)] &= \begin{bmatrix} \text{TRN}(1,1) & \text{TRN}(1,2) & \text{TRN}(1,3) \\ \text{TRN}(2,1) & \text{TRN}(2,2) & \text{TRN}(2,3) \\ \text{TRN}(3,1) & \text{TRN}(3,2) & \text{TRN}(3,3) \end{bmatrix} \quad (1.3.8) \\ &= \begin{bmatrix} \cos \theta \cos \psi & \cos \theta \sin \psi & -\sin \theta \\ \sin \phi \sin \theta \cos \psi - \cos \phi \sin \psi & \sin \phi \sin \theta \sin \psi + \cos \phi \cos \psi & \sin \phi \cos \theta \\ \cos \phi \sin \theta \cos \psi + \sin \phi \sin \psi & \cos \phi \sin \theta \sin \psi - \sin \phi \cos \psi & \cos \phi \cos \theta \end{bmatrix} \end{aligned}$$

The three sequential rotations for orienting the body axis system relative to the inertial axis system are illustrated in Fig. 5 and are shown on a unit sphere in Fig. 6.

Given a rotational matrix of the form of Eq. (1.3.8) above, it is also sometimes necessary to extract the sequential yaw-pitch-roll rotation angles which correspond to that matrix. This can be accomplished by forming ratios of appropriate terms in the matrix:

$$\begin{aligned} \psi &= \tan^{-1} \{\text{TRN}(1,2)/\text{TRN}(1,1)\}, & -180 < \psi < 180 \\ \theta &= \sin^{-1} \{-\text{TRN}(1,3)\} & -90 < \theta < 90 \\ \phi &= \tan^{-1} \{\text{TRN}(2,3)/\text{TRN}(3,3)\} & -180 < \phi < 180 \end{aligned} \quad (1.3.9)$$

The expression $\psi = \sin^{-1} \{\text{TRN}(1,2)/\cos(\theta)\}$ is sometimes found in the literature, but this form is not as mathematically rigorous because $1/\cos(\theta)$ is undefined when θ is ± 90 deg.

Note that the order in which rotational matrices are applied is vitally important. Matrix multiplication is not commutative and, in general, the yaw-pitch-roll matrix product $\{[\text{TRNx}(\phi)] [\text{TRNy}(\theta)] [\text{TRNz}(\psi)]\}$ which was used to form the terms in Eq. (1.3.8) does not result in the same orientation matrix as the pitch-yaw-roll $\{[\text{TRNx}(\omega)] [\text{TRNz}(\eta)] [\text{TRNy}(\nu)]\}$ product (or, in alternate words, the yaw-pitch-roll sequence angles extracted from a given transformation matrix are not necessarily the same as the pitch-yaw-roll sequence angles that would be extracted from the same matrix). For this reason, the pitch-yaw-roll sequence angles are given the different symbols ν , η , and ω . (Note that the rotation angle ω is not to be confused with the angular velocity vector ω). The observation that the resultant of a series of finite rotations is dependent on the order of rotations can be vividly demonstrated by a simple experiment. Figure 7 illustrates the

results of yawing and pitching versus pitching and yawing a body through angles of 90 deg. The final orientations in the two cases are obviously markedly different. The yaw-pitch-roll sequence has been adopted as the primary sequence for actual implementation of the motion equations in most motion analyses - the pitch-yaw-roll angles are normally provided only as alternate output parameters. (In some texts, the yaw-pitch-roll sequence angles are somewhat misleadingly referred to as the "Euler" angles - actually the term "Euler angle" is literally reserved for the single equivalent rotation fundamental to the definition of quaternions and the sequential angles are more properly referred to as "modified Euler" angles- see Section 4.2.3).

Because the pitch-yaw-roll sequence angles are sometimes useful in describing the motion of objects such as pivoted fuel tanks which exhibit predominantly pitch motion, the equations for this alternate sequence will also be presented before concluding this section. The direction cosine matrix given a rotation sequence of pitch first through an angle ν about the y axis, then yaw through an angle η about the resulting new z axis, and then roll through an angle ω about the resulting new x axis (pitch-yaw-roll sequence) can be written as:

$$\{\bar{x}\text{ new}\} = [\text{TRNx}(\omega)] [\text{TRNz}(\eta)] [\text{TRNy}(\nu)] \{\bar{x}\text{ old}\} = [\text{TRN}(\nu, \eta, \omega)] \{\bar{x}\text{ old}\} \quad (1.3.10)$$

The terms of the complete rotation matrix are again obtained by matrix multiplication:

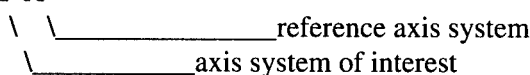
$$\begin{aligned} [\text{TRN}(\nu, \eta, \omega)] &= \begin{bmatrix} \text{TRN}(1,1) & \text{TRN}(1,2) & \text{TRN}(1,3) \\ \text{TRN}(2,1) & \text{TRN}(2,2) & \text{TRN}(2,3) \\ \text{TRN}(3,1) & \text{TRN}(3,2) & \text{TRN}(3,3) \end{bmatrix} \quad (1.3.11) \\ &= \begin{bmatrix} \cos\nu \cos\eta & \sin\eta & -\sin\nu \cos\eta \\ \sin\omega \sin\nu - \cos\omega \cos\nu \sin\eta & \cos\omega \cos\eta & \cos\omega \sin\nu \sin\eta + \cos\nu \sin\omega \\ \sin\omega \cos\nu \sin\eta + \cos\omega \sin\nu & -\sin\omega \cos\eta & \cos\omega \cos\nu - \sin\omega \sin\nu \sin\eta \end{bmatrix} \end{aligned}$$

If, given a rotational matrix, it is necessary to extract the pitch-yaw-roll sequence angles which correspond to that matrix, ratios of appropriate terms in the matrix can again be used:

$$\begin{aligned} \nu &= \tan^{-1} \{-\text{TRN}(1,3)/\text{TRN}(1,1)\}, & -180 < \nu < 180 \\ \eta &= \sin^{-1} \{\text{TRN}(1,2)\} & -90 < \eta < 90 \\ \omega &= \tan^{-1} \{-\text{TRN}(3,2)/\text{TRN}(2,2)\} & -180 < \omega < 180 \end{aligned} \quad (1.3.12)$$

The pitch-yaw-roll sequence for the orientation of body axes relative to inertial axes is illustrated in Fig. 8.

Rotational transformation matrices have also been included in the special nomenclature developed for motion analyses. Transformation matrices are identified by:

TRN X X

 reference axis system
 axis system of interest

As an example, the name TRNTI would be decoded as "the transformation matrix describing the orientation of the transducer axis system relative to the inertial axis system."

It is important to emphasize that the matrices used to describe the orientation of one system relative to another are fundamentally different physically from the vectors used to describe the other motion properties of the systems. In other words, orientation is a matrix property and cannot be represented by a single vector in three-dimensional space, even though the other major kinematic properties (linear position, velocity, and acceleration as well as angular velocity and acceleration) are vector quantities. The fact that orientation is a matrix rather than a vector while angular velocity is a vector instead of a matrix has enormous implications when angular orientation is to be updated in time within a time-dependent numerical trajectory simulation. Update of angular orientations in a numerical simulation will, therefore, be treated in detail in Section 4.2.3 later in this report.

Orientation matrices can be used to project any of the major kinematic vector quantities to other measurement directions. For example, the matrix defining the orientation of an axis system of interest relative to a reference system may be used to project reference-axis vector quantities to components aligned with the axes of interest. True inertial accelerations, for instance, can be mapped into the components that would be measured by an onboard body-fixed acceleration transducer by the transformation:

$$\begin{vmatrix} \text{AXTTI} \\ \text{AYTTI} \\ \text{AZTTI} \end{vmatrix} = [\text{TRNTI}] \begin{vmatrix} \text{AXITI} \\ \text{AYITI} \\ \text{AZITI} \end{vmatrix} \quad (1.3.13)$$

Two or more transformation matrices can be "concatenated" together by simple matrix multiplication to form cumulative transformations. For example, the matrix [TRNTI] above can be formed from the matrix product:

$$[\text{TRNTI}] = [\text{TRNTB}] [\text{TRNBI}] \quad (1.3.14)$$

where [TRNTB] defines the orientation of the accelerometer transducer axes relative to body axes and [TRNBI] defines the orientation of body axes relative to inertial axes.

Rotational transformation matrices belong to a special class of matrices known as orthogonal matrices. Because the rotational matrix is formed by sequential rotations about orthogonal axes, no shearing or deformation of vectors in space occurs. An orthogonal matrix has the unique and useful mathematical property that its inverse is identically equal to its transpose. In mathematical terms, if $\text{TRN} = [\text{TRN}(i,j)]$ then, for an orthogonal matrix,

$$\text{TRN}^{-1} = \text{TRN}^T = [\text{TRN}(j,i)] \quad (1.3.15)$$

where i and j are the row and column indices, respectively, of the original rotation matrix. In terms of the special motion nomenclature for a transformation from inertial axes to body axes, the relationship can be illustrated by the expressions:

$$\text{TRNBI}^{-1} = \text{TRNBI}^T = \text{TRNIB} \quad (1.3.16)$$

The proof of Eq. (1.3.16) will be left until Section 4.3.2.

1.4 DERIVATIVES OF ROTATIONAL TRANSFORMATIONS AND VECTOR QUANTITIES PROJECTED INTO ROTATING REFERENCE FRAMES

Several very important rules concerning vector and matrix calculus for kinematic properties are presented and emphasized in this section. These rules will be followed in all derivations in subsequent sections.

1. Whenever possible, derivatives should only be taken of quantities measured in inertial components. Derivatives of transformation matrices or rotating reference frames are not necessary in such cases.
2. If derivatives are taken of quantities measured in non-inertial coordinate directions, the rotating coordinate frames will introduce additional terms which must be accounted for.
3. If the reference system relative to which the property is defined is non-inertial, additional terms must also be accounted for.
4. Vector derivative operations are not commutative, i.e., the derivative of the projection of a vector into a non-inertial axis system is not equivalent to the projection of the derivative of the original inertial vector.

Because vectors have both magnitude and direction, the derivative of a vector must account for both change in magnitude and change in direction. When, however, the system relative to which the vector directions are specified is itself rotating, vector derivative operations can become extremely confusing. The primary difficulty in taking the derivatives of a linear motion term which is actually a projection of an inertial term into a non-inertial measurement axis system is that the rotational transformation matrices used to form the projections also have derivatives. Because of the important implications of the four rules, an illustrative example involving different methods of expressing velocity as the derivative of position will be examined. The fundamental position quantities for a store are the inertial components of the position of the store body axes relative to the inertial axes (XIBI, YIBI, and ZIBI). Two cases will be examined. For the first case, the derivatives of the positions will be obtained and then projected into body axis components. In the second case, the positions will be projected into body axes and then the derivatives will be obtained.

By the first rule, derivatives of properties measured in the inertial directions relative to the origin of the inertial system can be taken directly. Thus, the inertial velocities (UIBI, VIBI, and WIBI) are obtained as $UIBI = d(XIBI) / dt$, etc. The projections into body axes are then:

$$\begin{vmatrix} UBBI \\ VBBI \\ WBBI \end{vmatrix} = [TRNBI] \begin{vmatrix} UIBI \\ VIBI \\ WIBI \end{vmatrix} \quad (1.4.1)$$

For the second case, the projections of the inertial positions are:

$$\begin{vmatrix} XBBI \\ YBBI \\ ZBBI \end{vmatrix} = [TRNBI] \begin{vmatrix} XIBI \\ YIBI \\ ZIBI \end{vmatrix} \quad (1.4.2)$$

The derivatives of the projected positions (using the chain rule) are:

$$\frac{d}{dt} \begin{vmatrix} XBBI \\ YBBI \\ ZBBI \end{vmatrix} = \frac{d}{dt} [TRNBI] \begin{vmatrix} XIBI \\ YIBI \\ ZIBI \end{vmatrix} + [TRNBI] \frac{d}{dt} \begin{vmatrix} XIBI \\ YIBI \\ ZIBI \end{vmatrix} \quad (1.4.3)$$

or:

$$\begin{aligned} \begin{vmatrix} DXBBI \\ DYBBI \\ DZBBI \end{vmatrix} &= \frac{d}{dt} [TRNBI] \begin{vmatrix} XIBI \\ YIBI \\ ZIBI \end{vmatrix} + [TRNBI] \begin{vmatrix} UIBI \\ VIBI \\ WIBI \end{vmatrix} \\ &= \frac{d}{dt} [TRNBI] \begin{vmatrix} XIBI \\ YIBI \\ ZIBI \end{vmatrix} + \begin{vmatrix} UBBI \\ VBBI \\ WBBI \end{vmatrix} \end{aligned} \quad (1.4.4)$$

Note that derivatives of projected terms do not have specific names in the new extended motion nomenclature. Such terms actually have a fundamentally mathematical meaning and will be denoted by a "D" prefix added to the beginning of the name (or by a dot for the first derivative) and by a "DD" prefix (or double dot) for the second derivative. Note that the derivative of the XBBI vector (the DXBBI vector) in Eq. (1.4.4) is not the same as the UBBI vector in Eq. (1.4.1) because of the introduction of the additional term involving the derivative of [TRNBI]. Even more additional terms will be introduced if a second derivative is taken of Eq. (1.4.4) to get a measure of the "acceleration" vector {DDXBBI}.

The derivatives of transformation matrices such as those found in Eq. (1.4.4) can be determined by the matrix equations:

$$\frac{d}{dt} [TRNBI]^{-1} = [TRNBI]^{-1} [\tilde{\omega} BBI] \quad (1.4.5)$$

and

$$\frac{d}{dt} [TRNBI] = -[\tilde{\omega} BBI] [TRNBI] \quad (1.4.6)$$

where $[\tilde{\omega} BBI]$ represents the "skew-symmetric operator" defined by

$$[\tilde{\omega} BBI] = \begin{bmatrix} 0 & -RBBI & QBBI \\ RBBI & 0 & -PBBI \\ -QBBI & PBBI & 0 \end{bmatrix} \quad (1.4.7)$$

The actual derivations of Eqs. (1.4.5) and (1.4.6) will be saved for Section 4.2.3. For the present, the expressions for the transformation derivatives presented in Eqs. (1.4.5) and (1.4.6) will be used without proof. In so doing, it is possible to proceed with the development of the important motion equations without getting involved with complex rotational vector math. Given the above

formulas for the derivatives of the transformation matrices, almost all of the important acceleration and velocity kinematic motion equations can be developed by simply applying the "chain rule" for partial differentiation to the relationships between the positions of various axis systems just as has already been done to generate Eq. (1.4.4) from Eq. (1.4.2).

Using Eq. (1.4.6), Eq. (1.4.4) can be rewritten as:

$$\begin{aligned} \begin{vmatrix} \text{DXBBI} \\ \text{DYBBI} \\ \text{DZBBI} \end{vmatrix} &= -[\tilde{\omega}_{\text{BBI}}] [\text{TRNBI}] \begin{vmatrix} \text{XIBI} \\ \text{YIBI} \\ \text{ZIBI} \end{vmatrix} + \begin{vmatrix} \text{UBBI} \\ \text{VBBI} \\ \text{WBBI} \end{vmatrix} \\ &= -[\tilde{\omega}_{\text{BBI}}] \begin{vmatrix} \text{XBBI} \\ \text{YBBI} \\ \text{ZBBI} \end{vmatrix} + \begin{vmatrix} \text{UBBI} \\ \text{VBBI} \\ \text{WBBI} \end{vmatrix} \end{aligned} \quad (1.4.8)$$

The skew-symmetric operator of Eq. (1.4.7) can be recognized as the matrix equivalent of the vector cross-product operation:

$$[\tilde{\omega}_{\text{BBI}}] \begin{vmatrix} \text{XBBI} \\ \text{YBBI} \\ \text{ZBBI} \end{vmatrix} = \begin{vmatrix} \text{PBBI} \\ \text{QBBI} \\ \text{RBBI} \end{vmatrix} \times \begin{vmatrix} \text{XBBI} \\ \text{YBBI} \\ \text{ZBBI} \end{vmatrix} \quad (1.4.9)$$

Another interesting and sometimes useful property of the skew-symmetric matrix is that $[\tilde{\omega}_{\text{BBI}}] = -[\tilde{\omega}_{\text{BIB}}]$ since $\{\text{PBBI}\} = -\{\text{PBIB}\}$. This property can be readily observed by replacing the terms of the $\{\text{PBBI}\}$ vector with the terms of $-\{\text{PBIB}\}$ in Eq. (1.4.7) and will be used in the next section.

1.5 ALTERNATE PROJECTION TRANSFORMATIONS FOR ANGULAR VELOCITY AND ACCELERATION VECTORS

It was shown in Section 1.3 that the projection of a linear position, velocity, or acceleration vector or an angular velocity or acceleration vector from one axis system of measurement to another can be accomplished by pre-multiplying the vector by a rotational transformation matrix. An alternate formulation for projections of angular vectors is also sometimes useful. The alternate transformations for angular vectors can be derived from Eqs. (1.4.5) through (1.4.7).

From Eq. (1.4.6):

$$\frac{d}{dt} [\text{TRNBI}] = -[\tilde{\omega}_{\text{BBI}}] [\text{TRNBI}] \quad (1.5.1)$$

From Eq. (1.3.16):

$$\text{TRNBI} = \text{TRNIB}^{-1} \quad (1.5.2)$$

From Eq. (1.4.5):

$$\frac{d}{dt} [\text{TRNIB}]^{-1} = [\text{TRNIB}]^{-1} [\tilde{\omega}_{\text{IIB}}] \quad (1.5.3)$$

When Eqs. (1.5.1) through (1.5.3) are combined and rearranged (note that $[\tilde{\omega}_{\text{IBI}}] = -[\tilde{\omega}_{\text{IIB}}]$):

$$-[\tilde{\omega}_{\text{IIB}}] = [\tilde{\omega}_{\text{IBI}}] = [\text{TRNIB}] [\tilde{\omega}_{\text{BBI}}] [\text{TRNBI}] = [\text{TRNBI}]^{-1} [\tilde{\omega}_{\text{BBI}}] [\text{TRNBI}] \quad (1.5.4)$$

The projection of an angular velocity vector can, therefore, also be accomplished by forming the appropriate skew-symmetric matrix, pre- and post-multiplying by the rotational transformations out of and into the desired axis system (respectively), and extracting the new rotational vector from the resulting new skew-symmetric matrix as outlined in Eq. (1.5.4). Projections of this type are useful for some rotational matrix terms including, most notably, projections of the rotational inertia matrix to other axis systems, as will be described in Section 4.2.

2.0 ACCELEROMETER DESCRIPTION

As outlined in the previous sections, motion quantities are physically defined relative to inertial systems but are often presented in terms of measured components in a non-inertial system. This fact will be illustrated in this section by an examination of one of the most common and most useful types of motion instrumentation, the linear accelerometer.

A linear accelerometer is a transducer-type instrument which outputs a signal proportional to the acceleration sensed by the instrument. It is important to realize, however, that a single accelerometer mounted within a body cannot measure the total inertial acceleration of the body relative to inertially fixed space. The output of the accelerometer is, instead, related to the projection of the inertial acceleration onto the axis of sensitivity of the instrument (usually the x-axis of the transducer). Thus, while the true inertial acceleration at the transducer is represented by the vector (AXITI, AYITI, AZITI) which is obtained by taking the second derivative with respect to time of the inertial position vector (XITI, YITI, ZITI), an accelerometer would be sensitive only to the single component AXTTI as defined in the following projection relation:

$$\begin{vmatrix} \text{AXTTI} \\ \text{AYTTI} \\ \text{AZTTI} \end{vmatrix} = [\text{TRNTI}] \begin{vmatrix} \text{AXITI} \\ \text{AYITI} \\ \text{AZITI} \end{vmatrix} \quad (2.0.1)$$

where the transformation matrix TRNTI represents the projection from inertial components to transducer coordinates. Because all three terms in the {AXTTI} vector usually cannot be sensed by a single accelerometer, additional transducers in various mutually perpendicular orientations within the body are usually necessary to get the AYTTI and AZTTI components.

To simplify some of the derivations in the following sections, a fictitious, idealized instrument which will be referred to as a "tri-axial" accelerometer which consists of three

perpendicular accelerometers with a common point of sensitivity will be defined. The idealized tri-axial instrument will be assumed to be sensitive to all three components of the projected acceleration in Eq. (2.0.1) simultaneously. A close physical approximation to the idealized tri-axial case which was recently used in an instrumented model of the F-22 fuel tank is illustrated in Fig. 9. Three accelerometers are shown attached to a common mounting cube so that the axes of sensitivity of the accelerometers intersect at the center of the cube. In the absence of rotation, a true tri-axial measurement at the common point of sensitivity is obtained. When the entire assembly is rotating, however, some accounting of those portions of the measured accelerations which are attributable to the cross products of the rotational velocities and accelerations with the finite transfer distances from the common point to the location of each individual accelerometer must be made (see Section 5.0).

Other complications to the use of accelerometers to measure motion properties are introduced as a consequence of the physics behind how accelerometers work. Accelerometers cannot measure the full magnitude of the {AXTTI} vector components because they do not respond to the gravitational portion of the acceleration applied to the body. A description of the physics of accelerometers is necessary to help explain this point. An idealized accelerometer can be visualized as a simple system consisting of a support structure from which is suspended a mass attached to a linear spring (Fig. 10). When an acceleration is applied to the support structure, the inertia of the suspended mass will tend to cause it to resist motion which in turn will cause the spring to stretch. The spring displacement is proportional to the applied acceleration. An accelerometer is, therefore, sensitive only along the axis aligned with the spring (which necessitates the projection transformation in Eq. (2.0.1)). Gravitational acceleration is unique, however, because gravity acts on both the support structure and the suspended mass independently. In free fall near the earth's surface, for example, a vertically oriented accelerometer under the influence of earth gravity would be falling at a rate of approximately 32.174 ft/sec^2 (the nominal earth gravitational acceleration). However, both the accelerometer support structure and the suspended weight would be accelerating downward at the same rate so that no spring stretching would occur and the accelerometer would output a zero reading. Similarly, a vertically oriented accelerometer at rest on the earth's surface would be subject to gravitational acceleration pulling down on both the suspended mass and the support structure and a reaction force (sometimes called the "contact force") imparted by the earth's solid surface which prevents the support structure from moving downward but does not prevent the suspended mass from stretching the spring. At rest the accelerometer would, therefore, read approximately -32.174 ft/sec^2 or minus one "g" of upward, ground-imposed acceleration. The actual acceleration components measured by an idealized tri-axial accelerometer would then be (defining a new identifier, AXM, to mean AX "measured"):

$$\begin{vmatrix} AXMTTI \\ AYMTTI \\ AZMTTI \end{vmatrix} = \begin{vmatrix} AXTTI \\ AYTTI \\ AZTTI \end{vmatrix} - [TRNTE] \begin{vmatrix} 0.0 \\ 0.0 \\ GG \end{vmatrix} \quad (2.0.2)$$

$$\text{where } [TRNTE] = [TRNTI] [TRNIE] \quad (2.0.3)$$

and [TRNIE] is formed from the climb (THAIE) and bank (PHIIIE) angles of the aircraft inertial flight path relative to the earth horizontal tangent plane. The {AXMTTI} vector is sometimes referred to as the "specific" acceleration.

The GG term in Eq. (2.0.2) represents the local value of the gravitational acceleration (which decreases slightly as a function of altitude and latitude from the earth equator). To engineering accuracy in most simulations the "nominal" GG value of 32.174 ft/sec² can be used.

Acceleration equations are also often written in a special non-dimensional form (expressed in units of "g's) in which each term is divided by the nominal earth gravitational acceleration:

$$\begin{vmatrix} GAXMTTI \\ GAYMTTI \\ GAZMTTI \end{vmatrix} = \begin{vmatrix} AXMTTI / 32.174 \\ AYMTTI / 32.174 \\ AZMTTI / 32.174 \end{vmatrix} = \begin{vmatrix} GAXTTI \\ GAYTTI \\ GAZTTI \end{vmatrix} - [TRNTE] \begin{vmatrix} 0.0 \\ 0.0 \\ GG/32.174 \end{vmatrix} \quad (2.0.4)$$

where the character "G" denotes a reading in "g's."

3.0 ACCELERATION TRANSFER EQUATIONS

The equations for transfer of a measured acceleration from the point of measurement to another point on the body will be developed in this section. For purposes of the derivation, the accelerations will be transferred from the origin of the transducer axis system to the origin of the body axis system, and it will be assumed that a tri-axial 3-component measurement at the transducer-axis origin is available. If orthogonal accelerations at a common point are not available, the transfer equations derived herein will simply have to be applied for each separate transducer individually using the transfer distances associated with that transducer as outlined in Section 5.0.

Given a transducer axis system T and a body axis system B, the transfer distance from the cg (body-axis origin) to the transducer in body-axis components is {XBTB, YBTB, ZBTB}. Additionally, the transducer axis system may be rotated relative to the body axis system as represented by a transformation matrix [TRNBI]. Recalling that an accelerometer measures the projection of the second derivative of inertial position, the derivation begins with the relationship between inertial position of the transducer and inertial position of the body axes:

$$\begin{vmatrix} XITI \\ YITI \\ ZITI \end{vmatrix} = \begin{vmatrix} XIBI \\ YIBI \\ ZIBI \end{vmatrix} + [TRNBI]^{-1} \begin{vmatrix} XBTB \\ YBTB \\ ZBTB \end{vmatrix} \quad (3.0.1)$$

Taking the first derivative by the chain rule:

$$\frac{d}{dt} \begin{vmatrix} XITI \\ YITI \\ ZITI \end{vmatrix} = \frac{d}{dt} \begin{vmatrix} XIBI \\ YIBI \\ ZIBI \end{vmatrix} + \frac{d}{dt} [TRNBI]^{-1} \begin{vmatrix} XBTB \\ YBTB \\ ZBTB \end{vmatrix} + [TRNBI]^{-1} \frac{d}{dt} \begin{vmatrix} XBTB \\ YBTB \\ ZBTB \end{vmatrix} \quad (3.0.2)$$

or (noting that the transfer distance is not time varying) and using Eq. (1.4.5):

$$\begin{vmatrix} UITI \\ VITI \\ WITI \end{vmatrix} = \begin{vmatrix} UIBI \\ VIBI \\ WIBI \end{vmatrix} + [TRNBI]^{-1} [\tilde{\omega} BBI] \begin{vmatrix} XBTB \\ YBTB \\ ZBTB \end{vmatrix} \quad (3.0.3)$$

Now taking the second derivative by the chain rule:

$$\begin{aligned} \frac{d}{dt} \begin{vmatrix} \text{UITI} \\ \text{VITI} \\ \text{WITI} \end{vmatrix} &= \frac{d}{dt} \begin{vmatrix} \text{UIBI} \\ \text{VIBI} \\ \text{WIBI} \end{vmatrix} + \frac{d}{dt} [\text{TRNBI}]^{-1} [\tilde{\omega} \text{BBI}] \begin{vmatrix} \text{XBTB} \\ \text{YBTB} \\ \text{ZBTB} \end{vmatrix} \\ &+ [\text{TRNBI}]^{-1} \frac{d}{dt} [\tilde{\omega} \text{BBI}] \begin{vmatrix} \text{XBTB} \\ \text{YBTB} \\ \text{ZBTB} \end{vmatrix} + [\text{TRNBI}]^{-1} [\tilde{\omega} \text{BBI}] \frac{d}{dt} \begin{vmatrix} \text{XBTB} \\ \text{YBTB} \\ \text{ZBTB} \end{vmatrix} \quad (3.0.4) \end{aligned}$$

or (again realizing that the transfer distances are time-invariant):

$$\begin{aligned} \begin{vmatrix} \text{AXITI} \\ \text{AYITI} \\ \text{AZITI} \end{vmatrix} &= \begin{vmatrix} \text{AXIBI} \\ \text{AYIBI} \\ \text{AZIBI} \end{vmatrix} + [\text{TRNBI}]^{-1} [\tilde{\omega} \text{BBI}] [\tilde{\omega} \text{BBI}] \begin{vmatrix} \text{XBTB} \\ \text{YBTB} \\ \text{ZBTB} \end{vmatrix} \\ &+ [\text{TRNBI}]^{-1} \frac{d}{dt} [\tilde{\omega} \text{BBI}] \begin{vmatrix} \text{XBTB} \\ \text{YBTB} \\ \text{ZBTB} \end{vmatrix} \quad (3.0.5) \end{aligned}$$

Note that the third term on the right-hand side of Eq. (3.0.5) involves a skew-symmetric matrix consisting of the derivatives of rotational velocity terms which have been projected into a non-inertial system:

$$\frac{d}{dt} [\tilde{\omega} \text{BBI}] = [\text{D} \tilde{\omega} \text{BBI}] = \begin{bmatrix} 0 & -\text{DRBBI} & \text{DQBBI} \\ \text{DRBBI} & 0 & -\text{DPBBI} \\ -\text{DQBBI} & \text{DPBBI} & 0 \end{bmatrix} \quad (3.0.6)$$

Finally, the inertial measurements are projected into the transducer axis system by multiplying all terms by the projection matrix [TRNTI]:

$$\begin{aligned} \begin{vmatrix} \text{AXTTI} \\ \text{AYTTI} \\ \text{AZTTI} \end{vmatrix} &= [\text{TRNTI}] \begin{vmatrix} \text{AXIBI} \\ \text{AYIBI} \\ \text{AZIBI} \end{vmatrix} + [\text{TRNTI}] [\text{TRNBI}]^{-1} [\tilde{\omega} \text{BBI}] [\tilde{\omega} \text{BBI}] \begin{vmatrix} \text{XBTB} \\ \text{YBTB} \\ \text{ZBTB} \end{vmatrix} \\ &+ [\text{TRNTI}] [\text{TRNBI}]^{-1} [\text{D} \tilde{\omega} \text{BBI}] \begin{vmatrix} \text{XBTB} \\ \text{YBTB} \\ \text{ZBTB} \end{vmatrix} \quad (3.0.7) \end{aligned}$$

Noting that $[TRNTI] = [TRNTB][TRNBI]$, Eq. (3.0.7) becomes:

$$\begin{vmatrix} AXTTI \\ AYTTI \\ AZTTI \end{vmatrix} = [TRNTB][TRNBI] \begin{vmatrix} AXIBI \\ AYIBI \\ AZIBI \end{vmatrix} + [TRNTB][\tilde{\omega} BBI][\tilde{\omega} BBI] \begin{vmatrix} XBTB \\ YBTB \\ ZBTB \end{vmatrix} \\ + [TRNTB][D\tilde{\omega} BBI] \begin{vmatrix} XBTB \\ YBTB \\ ZBTB \end{vmatrix} \quad (3.0.8)$$

Equation (3.0.8) represents the full acceleration transfer equation for a "tri-axial" linear accelerometer at arbitrary position and orientation relative to body axes. In many applications, however, the accelerometer axes are aligned with the body axes. For such cases, the rotational transformation from transducer axes to body axes is an identity and the transfer equation reduces to:

$$\begin{vmatrix} AXBTI \\ AYBTI \\ AZBTI \end{vmatrix} = \begin{vmatrix} AXTTI \\ AYTTI \\ AZTTI \end{vmatrix} = \begin{vmatrix} AXBBI \\ AYBBI \\ AZBBI \end{vmatrix} + [\tilde{\omega} BBI][\tilde{\omega} BBI] \begin{vmatrix} XBTB \\ YBTB \\ ZBTB \end{vmatrix} + [D\tilde{\omega} BBI] \begin{vmatrix} XBTB \\ YBTB \\ ZBTB \end{vmatrix} \quad (3.0.9)$$

The middle term on the right-hand side of Eq. (3.0.9) represents the centripetal acceleration ($\bar{\omega} X \bar{\omega} X r$) and is directed toward the center of rotation. The final term is the tangential acceleration ($\dot{\bar{\omega}} X r$). Expanding out the matrices in Eq. (3.0.9) and subtracting the components of the acceleration of gravity (which are the same on both sides of the equations because of the lack of rotational offset) results in the more familiar expressions:

$$\begin{aligned} AXMTTI &= AXMBBI + XBTB^* (-RBBI^2 - QBBI^2) \\ &\quad + YBTB^* (PBBI^* QBBI - DRBBI) + ZBTB^* (RBBI^* PBBI + DQBBI) \\ AYMTTI &= AYMBBI + XBTB^* (PBBI^* QBBI + DRBBI) \\ &\quad + YBTB^* (-RBBI^2 - PBBI^2) + ZBTB^* (RBBI^* QBBI - DPBBI) \\ AZMTTI &= AZMBBI + XBTB^* (RBBI^* PBBI - DQBBI) \\ &\quad + YBTB^* (RBBI^* QBBI + DPBBI) + ZBTB^* (-QBBI^2 - PBBI^2) \end{aligned} \quad (3.0.10)$$

Finally, note that if the hypothesized idealized tri-axial accelerometer capable of measuring all three components of acceleration at a common point is not available, then three separate linear accelerometers placed at right angles to one another within the store and as closely spaced as possible are necessary. The relations of Eq. (3.0.10) for accelerometers aligned with the body axes must, in such cases, be rewritten by specifying separate transfer distances for the positions of the transducer axis systems for each accelerometer:

$$\begin{aligned} AXMT_{xT_xI} &= AXMBBI + XBT_xB^* (-RBBI^2 - QBBI^2) \\ &\quad + YBT_xB^* (PBBI^* QBBI - DRBBI) + ZBT_xB^* (RBBI^* PBBI + DQBBI) \\ AYMT_{yT_yI} &= AYMBBI + XBT_yB^* (PBBI^* QBBI + DRBBI) \\ &\quad + YBT_yB^* (-RBBI^2 - PBBI^2) + ZBT_yB^* (RBBI^* QBBI - DPBBI) \\ AZMT_{zT_zI} &= AZMBBI + XBT_zB^* (RBBI^* PBBI - DQBBI) \\ &\quad + YBT_zB^* (RBBI^* QBBI + DPBBI) + ZBT_zB^* (-QBBI^2 - PBBI^2) \end{aligned} \quad (3.0.11)$$

where the x, y, and z subscripts for each transducer axis system denote the accelerometer oriented to measure the acceleration component in that direction.

4.0 STORE EQUATIONS OF MOTION IN TRADITIONAL BODY-AXIS PROJECTION FORM

The basic equations of motion for modeling store-separation events with and without physical motion restraint are developed in this section. The separation dynamic equations (like all classical dynamic equations) are derived from fundamental physical principles first correctly stated by Sir Isaac Newton (1642-1727) for point-mass particles, and later extended by Euler to include systems of particles acting collectively as rigid bodies. The basic laws governing the classical motion of a particle were presented by Newton in his *Principia* (1687) (Ref. 2). Newton's laws of motion stated in modern terminology are:

Law I. A particle remains at rest or continues to move in a straight line with uniform velocity if there is no unbalanced force acting on it. (This is sometimes referred to as the principle of inertia).

Law II. The acceleration of a particle is proportional to the resultant force acting on it and is in the direction of this force. (Actually this is a popularized, simplified statement of the Second Law. The full law states that the derivative of the linear momentum of the particle is proportional to the force).

Law III. The forces of action and reaction between interacting particles are equal in magnitude and opposite in direction.

These laws have been proven by innumerable physical measurements and experiments and are only inapplicable for situations at which relativity becomes significant (such as speeds approaching the speed of light and sub-atomic scales).

The developments of the translational equations of motion are presented in Section 4.1, and the developments for rotational equations in Section 4.2. Separate developments are presented in each section for unrestricted movement (Sections 4.1.1 and 4.2.1) and for motion with some kind of physical restriction (Sections 4.1.2 and 4.2.2). The derivation of the unrestricted equations closely parallels similar derivations in a variety of texts. The unrestricted equation development is provided both in the interests of completeness and to provide a starting point for the development of the restricted equations of motion for which no satisfactory derivation was found in recent texts. Additional analyses of the concept of rotation are then provided in Section 4.2.3

4.1 TRANSLATIONAL EQUATIONS OF MOTION

It will be shown in this section that the forces on the body are directly related to its linear momentum. The important translational equations for unrestricted and restricted motion will be presented in Sections 4.1.1 and 4.1.2. First, a brief introductory will be presented to define some

of the basic translational terms and the most general form of the inertial translational motion equations.

The linear momentum of a rigid body is simply the sum of the linear momentums of each point in the body where the linear momentum of each point mass is the product of the infinitesimal mass of that point with its inertial velocity. Newton's Second Law of Motion states that the infinitesimal forces on a point are related to the derivative of linear momentum. Given an arbitrary point p with mass Δm in a rigid body and the inertial velocity of that point, Newton's Law for that point can be written as:

$$\begin{vmatrix} \Delta F_{XI} \\ \Delta F_{YI} \\ \Delta F_{ZI} \end{vmatrix} = \frac{d}{dt} \left(\Delta m \begin{vmatrix} U_{IpI} \\ V_{IpI} \\ W_{IpI} \end{vmatrix} \right) \quad (4.1.0.1)$$

where the term within the derivative operator is the linear momentum of the differential mass at point p. For rigid bodies, Eq. (4.1.0.1) can be summed for all mass elements in the body to obtain:

$$\Sigma \begin{vmatrix} \Delta F_{XI} \\ \Delta F_{YI} \\ \Delta F_{ZI} \end{vmatrix} = \frac{d}{dt} \left(\Sigma \Delta m \begin{vmatrix} U_{IpI} \\ V_{IpI} \\ W_{IpI} \end{vmatrix} \right) \quad (4.1.0.2)$$

where $\Sigma \{\Delta F_{XI}\}$ is the summation of all forces on all mass elements in the body. The internal forces within the body (forces exerted by one mass element on another) all occur in equal and opposite pairs by Newton's Third Law of Motion ("for every action there is an opposite and equal reaction") and, therefore, contribute nothing to the summation. Thus

$$\Sigma \{\Delta F_{XI}\} = \{FXI\} \quad (4.1.0.3)$$

is the resultant of the external forces acting on the body. The velocity of each element can be represented as:

$$\{U_{IpI}\} = \{U_{IBI}\} + \frac{d}{dt} \{X_{IpB}\} \quad (4.1.0.4)$$

where $\{U_{IBI}\}$ is the velocity of the mass center. Rewriting the linear momentum in Eq. (4.1.0.2):

$$\begin{aligned} \Sigma \left(\Delta m \begin{vmatrix} U_{IpI} \\ V_{IpI} \\ W_{IpI} \end{vmatrix} \right) &= \Sigma \Delta m \left(\begin{vmatrix} U_{IBI} \\ V_{IBI} \\ W_{IBI} \end{vmatrix} + \frac{d}{dt} \begin{vmatrix} X_{IpB} \\ Y_{IpB} \\ Z_{IpB} \end{vmatrix} \right) \\ &= m \begin{vmatrix} U_{IBI} \\ V_{IBI} \\ W_{IBI} \end{vmatrix} + \frac{d}{dt} \Sigma \begin{vmatrix} X_{IpB} \\ Y_{IpB} \\ Z_{IpB} \end{vmatrix} \Delta m \end{aligned} \quad (4.1.0.5)$$

But, since the body axis origin is at the mass center, the definition of mass center requires that:

$$\Sigma \begin{vmatrix} X_{IpB} \\ Y_{IpB} \\ Z_{IpB} \end{vmatrix} \Delta m = 0 \quad (4.1.0.6)$$

when summed over all mass elements. Substituting Eqs. (4.1.0.3), (4.1.0.5), and (4.1.0.6) into Eq. (4.1.0.2) leads to the inertial form of Newton's Law for a rigid body:

$$\begin{vmatrix} \Sigma F_{XI} \\ \Sigma F_{YI} \\ \Sigma F_{ZI} \end{vmatrix} = \frac{d}{dt} \left(m \begin{vmatrix} U_{IBI} \\ V_{IBI} \\ W_{IBI} \end{vmatrix} \right) \quad (4.1.0.7)$$

Equation (4.1.0.7) represents the most fundamental form of Newton's translational law for rigid-body motion.

4.1.1 Translational Equations for Unrestricted Motion

Motion simulations of translational motion are basically generated by solving Eq. (4.1.0.7) for the store accelerations which are then integrated over time to get velocities and positions. Beginning with the inertial form of Newton's Law:

$$\begin{vmatrix} \Sigma F_{XI} \\ \Sigma F_{YI} \\ \Sigma F_{ZI} \end{vmatrix} = \frac{d}{dt} \left(m \begin{vmatrix} U_{IBI} \\ V_{IBI} \\ W_{IBI} \end{vmatrix} \right) = \frac{dm}{dt} \begin{vmatrix} U_{IBI} \\ V_{IBI} \\ W_{IBI} \end{vmatrix} + m \frac{d}{dt} \begin{vmatrix} U_{IBI} \\ V_{IBI} \\ W_{IBI} \end{vmatrix} \quad (4.1.1.1)$$

where the mass times velocity term is the linear momentum. In many cases of practical interest, the mass of the body is constant and the first term on the right of the second equality is zero. Even for thrusting bodies which lose mass as on-board fuel is burned, the mass derivative can still often be safely ignored, particularly if partial compensation is provided by first adjusting the mass value and the center-of-gravity position at each time step in the numerical integration and, second, including the "thrust forces" in the external force summation on the left side of the equation. (Thrust is actually an internal force arising according to Newton's Third Law in reaction to the fuel mass ejected through the jet/rocket exhaust). If the mass derivative is ignored, Eq. (4.1.1.1) reduces to the familiar force = mass * acceleration form:

$$\begin{vmatrix} \Sigma F_{XI} \\ \Sigma F_{YI} \\ \Sigma F_{ZI} \end{vmatrix} = m \begin{vmatrix} A_{XIBI} \\ A_{YIBI} \\ A_{ZIBI} \end{vmatrix} \quad (4.1.1.2)$$

The mass represents a measure of the inertial resistance of the body to translational motion.

Note that just as an accelerometer measures components of inertial acceleration projected onto the axis of sensitivity of the instrument, forces (and moments) are more easily measured (projected) in body axes by internally mounted strain-gage balance systems. Internal balances mounted within the body are now used almost universally in wind tunnel tests. It is, therefore,

convenient to rewrite the inertial quantities in Eq. (4.1.1.2) in terms of body-axis projected measurements as follows:

$$\begin{vmatrix} \Sigma F_{XI} \\ \Sigma F_{YI} \\ \Sigma F_{ZI} \end{vmatrix} = [\text{TRNBI}]^{-1} \begin{vmatrix} \Sigma F_{XB} \\ \Sigma F_{YB} \\ \Sigma F_{ZB} \end{vmatrix} \quad (4.1.1.3)$$

and

$$\begin{vmatrix} AXIBI \\ AYIBI \\ AZIBI \end{vmatrix} = [\text{TRNBI}]^{-1} \begin{vmatrix} AXBBI \\ AYBBI \\ AZBBI \end{vmatrix} \quad (4.1.1.4)$$

so that Eq. (4.1.1.2) can be rewritten as:

$$[\text{TRNBI}]^{-1} \begin{vmatrix} \Sigma F_{XB} \\ \Sigma F_{YB} \\ \Sigma F_{ZB} \end{vmatrix} = m [\text{TRNBI}]^{-1} \begin{vmatrix} AXBBI \\ AYBBI \\ AZBBI \end{vmatrix} \quad (4.1.1.5)$$

or:

$$\begin{vmatrix} \Sigma F_{XB} \\ \Sigma F_{YB} \\ \Sigma F_{ZB} \end{vmatrix} = m \begin{vmatrix} AXBBI \\ AYBBI \\ AZBBI \end{vmatrix} \quad (4.1.1.6)$$

Note that Eq. (4.1.1.6) is still a fundamentally inertial relationship [like Eq. (4.1.1.2)], but it is now expressed in terms of projected body-axis state variables.

Although the forces are now more easily related to measured components in Eq. (4.1.1.6), the intent of a motion simulation is to solve for accelerations which can be integrated for velocities and, ultimately, positions. The integral of the projected components of an acceleration involves cross/coupling terms just as does the derivative of a projection. It is desirable, therefore, to redefine the acceleration in Eq. (4.1.1.6) in terms of components that can be integrated directly. A relation between the true projected acceleration and a direct derivative of the projected velocity can be developed from the projected velocity relation:

$$\begin{vmatrix} UBBI \\ VBBI \\ WBBI \end{vmatrix} = [\text{TRNBI}] \begin{vmatrix} UIBI \\ VIBI \\ WIBI \end{vmatrix} \quad (4.1.1.7)$$

Taking derivatives of both sides by the chain rule:

$$\frac{d}{dt} \begin{vmatrix} UBBI \\ VBBI \\ WBBI \end{vmatrix} = \frac{d}{dt} [\text{TRNBI}] \begin{vmatrix} UIBI \\ VIBI \\ WIBI \end{vmatrix} + [\text{TRNBI}] \frac{d}{dt} \begin{vmatrix} UIBI \\ VIBI \\ WIBI \end{vmatrix} \quad (4.1.1.8)$$

and using Eq. (1.4.6):

$$\begin{vmatrix} DUBBI \\ DVBBI \\ DWBBI \end{vmatrix} = -[\tilde{\omega} BBI] [TRNBI] \begin{vmatrix} UIBI \\ VIBI \\ WIBI \end{vmatrix} + [TRNBI] \begin{vmatrix} AXIBI \\ AYIBI \\ AZIBI \end{vmatrix} \quad (4.1.1.9)$$

or:

$$\begin{vmatrix} DUBBI \\ DVBBI \\ DWBBI \end{vmatrix} = -[\tilde{\omega} BBI] \begin{vmatrix} UBBI \\ VBBI \\ WBBI \end{vmatrix} + \begin{vmatrix} AXBBI \\ AYBBI \\ AZBBI \end{vmatrix} \quad (4.1.1.10)$$

Substituting Eq. (4.1.10) into Eq. (4.1.1.6) and solving for the derivative of the projected velocity results in the form of the translational equations used in most numerical motion simulations:

$$\begin{vmatrix} DUBBI \\ DVBBI \\ DWBBI \end{vmatrix} = \frac{1}{m} \begin{vmatrix} FXB \\ FYB \\ FZB \end{vmatrix} - [\tilde{\omega} BBI] \begin{vmatrix} UBBI \\ VBBI \\ WBBI \end{vmatrix} \quad (4.1.1.11)$$

where the summation on the force vector has been dropped to indicate that no external reaction forces are applied to the body for unrestrained, free-fall simulations. Equation (4.1.1.11) is sometimes referred to as the "Euler form" of the linear equations of motion.

Equation (4.1.1.11) represents the form of the translational free-fall equations used in AEDC wind tunnel and off-line simulations. The projected velocity derivatives (sometimes misleadingly referred to as "linear accelerations") are computed from the measured forces and integrated numerically to determine body-axis velocities at the next point in the trajectory. Also at each time step the body-axis velocity components resulting from each integration are transformed to inertial axes (by the inverse of Eq. (4.1.1.7)) and themselves loaded to the integrator to determine the position of the body axes at the next time step.

The Eq. (4.1.1.11) form of the acceleration terms is also used in the AEDC free-drop data extraction program to compute the applied forces which cause a given motion based on accelerations and velocities obtained by differentiating camera-measured reduced position data. For instrumented drop models, a relationship between the common numerical acceleration term in Eq. (4.1.1.11) and reduced accelerometer readings transferred to the cg of an instrumented model can be obtained by substituting accelerometer-measured and gravity terms into Eq. (4.1.1.10):

$$\begin{vmatrix} DUBBI \\ DVBBI \\ DWBBI \end{vmatrix} = -[\tilde{\omega} BBI] \begin{vmatrix} UBBI \\ VBBI \\ WBBI \end{vmatrix} + \begin{vmatrix} AXMBBI \\ AYMBBI \\ AZMBBI \end{vmatrix} + [TRNTE] \begin{vmatrix} 0.0 \\ 0.0 \\ GG \end{vmatrix} \quad (4.1.1.12)$$

4.1.2 Translational Equations for Restricted Motion

Translational equations become more complicated for cases involving physical restraint of the motion. For restrained cases, some fixture attached to the store body must be "held" in some manner by a mechanism attached to the aircraft. Common restraints include ball-in-socket pivot

mechanisms and rails which force translational motion of the fixture. If the store has more than one fixture (such as forward and aft rail hangers), it becomes extremely difficult to determine the reaction forces imposed at both fixtures simultaneously. It is possible, however, to represent the combined resultant of the reactions at the two fixtures by an equivalent system involving a combined reaction force at one of the fixtures (usually the aft fixture) and an associated equivalent reaction moment at that fixture. The aft fixture equivalent reaction moment includes a contribution representative of the reaction force at the forward fixture (which is not determined explicitly) times its moment arm relative to the aft fixture point. Restricted motion requires that the translational motion and the rotational motion of the store must be interrelated. Restricted motion is, therefore, often simulated numerically by solving the restricted rotational equations of motion to determine the basic store motion and then performing an inverse solution of the translational equations only to determine the resultant reaction force at the aft fixture necessary to allow that motion. Restricted translational equations are developed in this section.

Another coordinate reference system will be introduced for restrained motion equation derivation. The hook-hanger-pivot system will be denoted by the letter "H" and will be assumed to be located at some fixed transfer distance relative to the body-axis origin and will be assumed never to be rotated relative to body axes (Fig. 11). The motion of the store body axes can then be determined to be a combination of the motion of the hook axes relative to inertial space and the motion of the body about the hook point. Beginning with the relationship between the inertial positions of inertial, body, and hook axes:

$$\begin{vmatrix} XIBI \\ YIBI \\ ZIBI \end{vmatrix} = \begin{vmatrix} XIHI \\ YIHI \\ ZIHI \end{vmatrix} + \begin{vmatrix} XIBH \\ YIBH \\ ZIBH \end{vmatrix} \quad (4.1.2.1)$$

where:

$$\begin{vmatrix} XIBH \\ YIBH \\ ZIBH \end{vmatrix} = [TRNBI]^{-1} \begin{vmatrix} XBBH \\ YBBH \\ ZBBH \end{vmatrix} \quad (4.1.2.2)$$

Taking derivatives of both sides using the chain rule to get inertial velocity:

$$\frac{d}{dt} \begin{vmatrix} XIBI \\ YIBI \\ ZIBI \end{vmatrix} = \frac{d}{dt} \begin{vmatrix} XIHI \\ YIHI \\ ZIHI \end{vmatrix} + \frac{d}{dt} [TRNBI]^{-1} \begin{vmatrix} XBBH \\ YBBH \\ ZBBH \end{vmatrix} + [TRNBI]^{-1} \frac{d}{dt} \begin{vmatrix} XBBH \\ YBBH \\ ZBBH \end{vmatrix} \quad (4.1.2.3)$$

or (noting that the derivative of the fixed transfer distance is zero):

$$\begin{vmatrix} UIBI \\ VIBI \\ WIBI \end{vmatrix} = \begin{vmatrix} UIHI \\ VIHI \\ WIHI \end{vmatrix} + [TRNBI]^{-1} [\tilde{\omega} BBI] \begin{vmatrix} XBBH \\ YBBH \\ ZBBH \end{vmatrix} \quad (4.1.2.4)$$

Projecting to body-axis components by [TRNBI] :

$$\begin{vmatrix} \text{UBBI} \\ \text{VBBI} \\ \text{WBBI} \end{vmatrix} = \begin{vmatrix} \text{UBHI} \\ \text{VBHI} \\ \text{WBHI} \end{vmatrix} + [\tilde{\omega} \text{BBI}] \begin{vmatrix} \text{XBBH} \\ \text{YBBH} \\ \text{ZBBH} \end{vmatrix} \quad (4.1.2.5)$$

Equation (4.1.2.5) provides the interconnect between hook velocities and body velocities. A similar relation for accelerations can be developed by taking a second derivative of Eq. (4.1.2.4):

$$\begin{aligned} \frac{d}{dt} \begin{vmatrix} \text{UIBI} \\ \text{VIBI} \\ \text{WIBI} \end{vmatrix} &= \frac{d}{dt} \begin{vmatrix} \text{UIHI} \\ \text{VIHI} \\ \text{WIHI} \end{vmatrix} + \frac{d}{dt} [\text{TRNBI}]^{-1} [\tilde{\omega} \text{BBI}] \begin{vmatrix} \text{XBBH} \\ \text{YBBH} \\ \text{ZBBH} \end{vmatrix} + [\text{TRNBI}]^{-1} \frac{d}{dt} [\tilde{\omega} \text{BBI}] \begin{vmatrix} \text{XBBH} \\ \text{YBBH} \\ \text{ZBBH} \end{vmatrix} \\ &+ [\text{TRNBI}]^{-1} [\tilde{\omega} \text{BBI}] \frac{d}{dt} \begin{vmatrix} \text{XBBH} \\ \text{YBBH} \\ \text{ZBBH} \end{vmatrix} \end{aligned} \quad (4.1.2.6)$$

or:

$$\begin{vmatrix} \text{AXIBI} \\ \text{AYIBI} \\ \text{AZIBI} \end{vmatrix} = \begin{vmatrix} \text{AXIHI} \\ \text{AYIHI} \\ \text{AZIHI} \end{vmatrix} + [\text{TRNBI}]^{-1} [\tilde{\omega} \text{BBI}] [\tilde{\omega} \text{BBI}] \begin{vmatrix} \text{XBBH} \\ \text{YBBH} \\ \text{ZBBH} \end{vmatrix} + [\text{TRNBI}]^{-1} [\text{D}\tilde{\omega} \text{BBI}] \begin{vmatrix} \text{XBBH} \\ \text{YBBH} \\ \text{ZBBH} \end{vmatrix} \quad (4.1.2.7)$$

Project to body axis components by [TRNBI]:

$$\begin{vmatrix} \text{AXBBI} \\ \text{AYBBI} \\ \text{AZBBI} \end{vmatrix} = \begin{vmatrix} \text{AXBHI} \\ \text{AYBHI} \\ \text{AZBHI} \end{vmatrix} + [\tilde{\omega} \text{BBI}] [\tilde{\omega} \text{BBI}] \begin{vmatrix} \text{XBBH} \\ \text{YBBH} \\ \text{ZBBH} \end{vmatrix} + [\text{D}\tilde{\omega} \text{BBI}] \begin{vmatrix} \text{XBBH} \\ \text{YBBH} \\ \text{ZBBH} \end{vmatrix} \quad (4.1.2.8)$$

This relation provides the interconnect between hook accelerations and body accelerations.

In an actual numerical motion simulation for restricted motion, the rotational accelerations are determined from a solution of the rotational equations (which will be developed in the next section), the hook accelerations are determined by the prescribed motion of the aircraft (to which the hook is attached) as described in Section 4.3, and the rotational velocities are determined by integrating the rotational accelerations. As noted at the beginning of this section, the translational motion of the store must be geometrically related to its rotational motion when the store is constrained. That relationship has now been defined by Eq. (4.1.2.8). Once Eq. (4.1.2.8) is solved for the body-axis accelerations, the reaction forces at the point of constraint can be determined based on extending Eq. (4.1.1.6) (the free-body form of Newton's translational law) to include reaction force terms:

$$\begin{vmatrix} \Sigma F_{XB} \\ \Sigma F_{YB} \\ \Sigma F_{ZB} \end{vmatrix} = \begin{vmatrix} F_{XB} \\ F_{YB} \\ F_{ZB} \end{vmatrix} + \begin{vmatrix} R_{XB} \\ R_{YB} \\ R_{ZB} \end{vmatrix} = m \begin{vmatrix} \text{AXBBI} \\ \text{AYBBI} \\ \text{AZBBI} \end{vmatrix} \quad (4.1.2.9)$$

The relationship between the body-axis projected acceleration and the derivative of the body-axis projected velocity (Eq. 4.1.1.10) can also be used in conjunction with Eq. (4.1.2.8) to determine the parameters normally integrated to determine the body-projected velocities at each time step:

$$\begin{vmatrix} DUBBI \\ DVBBI \\ DWBBI \end{vmatrix} = \begin{vmatrix} AXBHI \\ AYBHI \\ AZBHI \end{vmatrix} + [\tilde{\omega} BBI] [\tilde{\omega} BBI] \begin{vmatrix} XBBH \\ YBBH \\ ZBBH \end{vmatrix} + [D\tilde{\omega} BBI] \begin{vmatrix} XBBH \\ YBBH \\ ZBBH \end{vmatrix} - [\tilde{\omega} BBI] \begin{vmatrix} UBBI \\ VBBI \\ WBBI \end{vmatrix} \quad (4.1.2.10)$$

The integrated values of the body velocities are then converted to inertial projections and passed to the integrator to determine the inertial positions at each time step, just as in free-body simulations.

Sometimes it is convenient to rewrite Eq. (4.1.2.10) in terms of the derivatives of the projected body-axis components of the hook velocity vector {DUBHI} instead of the hook acceleration {AXBHI}. The projected hook velocity derivative is developed much the same as the projected body velocity derivative in Eq. (4.1.1.10). Beginning with:

$$\begin{vmatrix} UBHI \\ VBHI \\ WBHI \end{vmatrix} = [TRNBI] \begin{vmatrix} UIHI \\ VIHI \\ WIHI \end{vmatrix} \quad (4.1.2.11)$$

and taking derivatives of both sides by the chain rule:

$$\begin{vmatrix} DUBHI \\ DVBIHI \\ DWBHI \end{vmatrix} = -[\tilde{\omega} BBI] \begin{vmatrix} UBHI \\ VBHI \\ WBHI \end{vmatrix} + \begin{vmatrix} AXBHI \\ AYBHI \\ AZBHI \end{vmatrix} \quad (4.1.2.12)$$

Substituting Eqs. (4.1.2.12) and (4.1.2.5) into Eq. (4.1.2.10) yields:

$$\begin{vmatrix} DUBBI \\ DVBBI \\ DWBBI \end{vmatrix} = \begin{vmatrix} DUBHI \\ DVBIHI \\ DWBHI \end{vmatrix} + [D\tilde{\omega} BBI] \begin{vmatrix} XBBH \\ YBBH \\ ZBBH \end{vmatrix} \quad (4.1.2.13)$$

Both the Eq. (4.1.2.10) form and the Eq. (4.1.2.13) form of the projected body-axis velocity derivative are used in AEDC simulations.

4.2 ROTATIONAL EQUATIONS OF MOTION

Just as it was shown in Section 4.1 that the forces on the body are related to the linear momentum of the body, it will be shown in this section that the moments of the forces on the body are related to its angular momentum. Before proceeding with the important rotational equations for unrestricted and restricted motions in Sections 4.2.1 and 4.2.2, a brief introductory section will be presented to define some of the basic rotational terms and the most general form of the inertial rotational motion equations.

The angular momentum of a body about a point is simply the sum of the moments of the linear momentum of each point in the body, i.e., the linear momentum of each point in the body crossed with its moment arm to the point of interest. However, whereas the entire body could be treated as a point mass for the derivation of the linear equations of motion in Sections 4.1.1 and 4.1.2, the integrated sum of the linear momentum of each infinitesimal element of the store must be considered for the rotational equations because each mass element in the body has a different moment arm to the point of interest. It has repeatedly been stressed throughout this document that physical quantities are fundamentally inertial in nature. This results in some particular complications in the definition of rotational terms, because often the point about which the moments are resolved (usually the store center of gravity or hook pivot point) is not inertially fixed. As a result, three separate derivations of the rotational equations of motion will be presented. First, the equations for rotation of a rigid body about an inertially fixed point O will be developed and presented in this section. The rotational equations for a free-falling body about its center of gravity B, will then be presented in Section 4.2.1. Finally, the rotational equations for the body about an arbitrarily moving hook point will be developed in Section 4.2.2.

Figure 12 illustrates an arbitrary point p with mass Δm within a rigid body and the position vectors from p to the center of gravity B, the hook pivot point H, and an inertially fixed point O. The inertial components of the angular momentum of p about inertial point O are formed from the cross product of the inertial moment arm vector from p to O and the inertial components of the linear momentum of particle p relative to the inertial origin:

$$\begin{vmatrix} \Delta HXIOI \\ \Delta HYIOI \\ \Delta HZIOI \end{vmatrix} = \begin{vmatrix} XI_{IpO} \\ YI_{IpO} \\ ZI_{IpO} \end{vmatrix} \times \Delta m \begin{vmatrix} UI_{IpI} \\ VI_{IpI} \\ WI_{IpI} \end{vmatrix} \quad (4.2.0.1)$$

where $\{XI_{IpO}\}$ is the inertial position of point "p" relative to the fixed point and the term on the right of the cross-product operator is the linear momentum of the differential mass at point p. The angular momentum of the entire store about the fixed point is obtained by summing the contributions of all the individual masses:

$$\begin{vmatrix} HXIOI \\ HYIOI \\ HZIOI \end{vmatrix} = \sum \begin{vmatrix} XI_{IpO} \\ YI_{IpO} \\ ZI_{IpO} \end{vmatrix} \times \Delta m \begin{vmatrix} UI_{IpI} \\ VI_{IpI} \\ WI_{IpI} \end{vmatrix} \quad (4.2.0.2)$$

If derivatives are taken of both sides by the chain rule:

$$\begin{vmatrix} DHXIOI \\ DHYIOI \\ DHZIOI \end{vmatrix} = \sum \begin{vmatrix} UI_{IpO} \\ VI_{IpO} \\ WI_{IpO} \end{vmatrix} \times \Delta m \begin{vmatrix} UI_{IpI} \\ VI_{IpI} \\ WI_{IpI} \end{vmatrix} + \sum \begin{vmatrix} XI_{IpO} \\ YI_{IpO} \\ ZI_{IpO} \end{vmatrix} \times \frac{d}{dt} \left(\Delta m \begin{vmatrix} UI_{IpI} \\ VI_{IpI} \\ WI_{IpI} \end{vmatrix} \right) \quad (4.2.0.3)$$

Note that $\{UI_{IpI}\} = \{UI_{IpO}\}$ because point O is inertially fixed. The first term on the right of Eq. (4.2.0.3) is, therefore, the cross product of a vector with itself (with a Δm factor thrown in) and is zero by vector identity ($\{A\} \times \{A\} = 0$). The remaining term on the right can be recognized to be the sum of the infinitesimal forces on each particle in the body crossed with the moment arms

from each particle to point O. Rewriting Eq. (4.2.0.3) using Eq. (4.1.0.2) and assuming the differential mass does not vary:

$$\begin{vmatrix} DHXIOI \\ DHYIOI \\ DHZIOI \end{vmatrix} = \Sigma \begin{vmatrix} XIPO \\ YIPO \\ ZIPO \end{vmatrix} X \Delta m \begin{vmatrix} AXIpI \\ AYIpI \\ AZIpI \end{vmatrix} = \Sigma \begin{vmatrix} XIPO \\ YIPO \\ ZIPO \end{vmatrix} X \begin{vmatrix} \Delta FXI \\ \Delta FYI \\ \Delta FZI \end{vmatrix} \quad (4.2.0.3)$$

The cross product on the right represents the vector sum of the moments about O of the forces acting on all particles of the body. However, since the internal forces induced by one particle within the body on another are canceled by the equal and opposite force induced by the second particle on the first (Newton's Third Law), only the moments of forces external to the body remain:

$$\begin{vmatrix} DHXIOI \\ DHYIOI \\ DHZIOI \end{vmatrix} = \Sigma \begin{vmatrix} XIPO \\ YIPO \\ ZIPO \end{vmatrix} X \begin{vmatrix} \Delta FXI \\ \Delta FYI \\ \Delta FZI \end{vmatrix} = \Sigma \begin{vmatrix} MXI \\ MYI \\ MZI \end{vmatrix} \text{ about O} \quad (4.2.0.4)$$

Equation (4.2.0.4) represents the most fundamental form of Newton's rotational law of motion. Note that a minor exception to the usual extended nomenclature system has been made for the moment term; the subscript "about O" has been used in place of a more formal name (such as "MXIOI") to be in keeping with common aerodynamic practice.

The classic form of Eq. (4.2.0.4) is not easily applicable to store separation problems because the store moments are usually resolved about the store center of gravity or hook points rather than about an inertially fixed point. Alternate expressions for rotational equations involving angular momentums and moments of forces about the mass center or hook point are developed in Sections 4.2.1 and 4.2.2, respectively. It will be demonstrated in Section 4.2.1 that the rotational equations involving properties about the mass center will result in an expression remarkably similar to Eq. (4.2.0.4). The rotational equations about the hook point in Section 4.2.2, however, will introduce additional terms which are sometimes overlooked in the developments available in the literature for rotational equations involving motion constraints.

4.2.1 Rotational Equations for Unrestricted Motion

The rotational equations can also be written in terms of the angular momentum of the body about the mass center or body axis system origin B. This form of the rotational equations is the most useful form for free-falling stores. Referring again to Fig. 12, the inertial components of the angular momentum of p about point B are formed from the cross product of the inertial moment arm vector from p to B and the inertial components of the linear momentum of particle p relative to the inertial origin:

$$\begin{vmatrix} \Delta HXIBI \\ \Delta HYIBI \\ \Delta HZIBI \end{vmatrix} = \begin{vmatrix} XIpB \\ YIpB \\ ZIpB \end{vmatrix} X \Delta m \begin{vmatrix} UIpI \\ VIpI \\ WIpI \end{vmatrix} \quad (4.2.1.1)$$

where $\{X_{IpB}\}$ is the inertial position of point "p" relative to the center of mass and the term on the right of the cross-product operator is the linear momentum of the differential mass at point p. The angular momentum of the entire store about the mass center is obtained by summing the contributions of all individual masses:

$$\begin{vmatrix} HXIBI \\ HYIBI \\ HZIBI \end{vmatrix} = \Sigma \begin{vmatrix} X_{IpB} \\ Y_{IpB} \\ Z_{IpB} \end{vmatrix} X \Delta m \begin{vmatrix} UIpI \\ VIpI \\ WIpI \end{vmatrix} \quad (4.2.1.2)$$

If derivatives are taken of both sides (and the mass derivative is again assumed to be zero):

$$\begin{vmatrix} DHXIBI \\ DHYIBI \\ DHZIBI \end{vmatrix} = \Sigma \begin{vmatrix} X_{IpB} \\ Y_{IpB} \\ Z_{IpB} \end{vmatrix} X \Delta m \begin{vmatrix} AXIpI \\ AYIpI \\ AZIpI \end{vmatrix} + \Sigma \begin{vmatrix} UIpB \\ VIpB \\ WIpB \end{vmatrix} X \Delta m \begin{vmatrix} UIpI \\ VIpI \\ WIpI \end{vmatrix} \quad (4.2.1.3)$$

Equation (4.2.1.3) can be rewritten by expanding the last vector as:

$$\begin{vmatrix} DHXIBI \\ DHYIBI \\ DHZIBI \end{vmatrix} = \Sigma \begin{vmatrix} X_{IpB} \\ Y_{IpB} \\ Z_{IpB} \end{vmatrix} X \Delta m \begin{vmatrix} AXIpI \\ AYIpI \\ AZIpI \end{vmatrix} + \Sigma \begin{vmatrix} UIpB \\ VIpB \\ WIpB \end{vmatrix} X \Delta m \left(\begin{vmatrix} UIBI \\ VIBI \\ WIBI \end{vmatrix} + \begin{vmatrix} UIpB \\ VIpB \\ WIpB \end{vmatrix} \right) \quad (4.2.1.4)$$

or:

$$\begin{aligned} \begin{vmatrix} DHXIBI \\ DHYIBI \\ DHZIBI \end{vmatrix} &= \Sigma \begin{vmatrix} X_{IpB} \\ Y_{IpB} \\ Z_{IpB} \end{vmatrix} X \Delta m \begin{vmatrix} AXIpI \\ AYIpI \\ AZIpI \end{vmatrix} + \Sigma \begin{vmatrix} UIpB \\ VIpB \\ WIpB \end{vmatrix} X \Delta m \begin{vmatrix} UIBI \\ VIBI \\ WIBI \end{vmatrix} \\ &\quad + \Sigma \begin{vmatrix} UIpB \\ VIpB \\ WIpB \end{vmatrix} X \Delta m \begin{vmatrix} UIpB \\ VIpB \\ WIpB \end{vmatrix} \end{aligned} \quad (4.2.1.5)$$

The last cross product of Eq. (4.2.1.5) is zero by vector identity of a vector crossed with itself. The middle cross product can also be shown to be zero after the manipulation which follows. Beginning with the middle cross product and using the vector identity, $\{A\} \times \{B\} = -\{B\} \times \{A\}$:

$$\Sigma \begin{vmatrix} UIpB \\ VIpB \\ WIpB \end{vmatrix} X \Delta m \begin{vmatrix} UIBI \\ VIBI \\ WIBI \end{vmatrix} = - \begin{vmatrix} UIBI \\ VIBI \\ WIBI \end{vmatrix} X \Sigma \Delta m \begin{vmatrix} UIpB \\ VIpB \\ WIpB \end{vmatrix} = - \begin{vmatrix} UIBI \\ VIBI \\ WIBI \end{vmatrix} X \frac{d}{dt} \Sigma \Delta m \begin{vmatrix} X_{IpB} \\ Y_{IpB} \\ Z_{IpB} \end{vmatrix} \quad (4.2.1.6)$$

By definition of the mass center, the sum of the mass moments about point B is zero, so that:

$$\Sigma \begin{vmatrix} UIpB \\ VIpB \\ WIpB \end{vmatrix} X \Delta m \begin{vmatrix} UIBI \\ VIBI \\ WIBI \end{vmatrix} = - \begin{vmatrix} UIBI \\ VIBI \\ WIBI \end{vmatrix} X \frac{d}{dt} \Sigma \Delta m \begin{vmatrix} X_{IpB} \\ Y_{IpB} \\ Z_{IpB} \end{vmatrix} = - \begin{vmatrix} UIBI \\ VIBI \\ WIBI \end{vmatrix} X \begin{vmatrix} 0 \\ 0 \\ 0 \end{vmatrix} = \begin{vmatrix} 0 \\ 0 \\ 0 \end{vmatrix} \quad (4.2.1.7)$$

Equation (4.2.1.5) can, therefore, be rewritten as:

$$\begin{vmatrix} DHXIBI \\ DHYIBI \\ DHZIBI \end{vmatrix} = \Sigma \begin{vmatrix} XI_{IpB} \\ YI_{IpB} \\ ZI_{IpB} \end{vmatrix} X \Delta m \begin{vmatrix} AXI_{IpI} \\ AYI_{IpI} \\ AZI_{IpI} \end{vmatrix} = \Sigma \begin{vmatrix} XI_{IpB} \\ YI_{IpB} \\ YI_{IpB} \end{vmatrix} X \begin{vmatrix} \Delta FXI \\ \Delta FYI \\ \Delta FZI \end{vmatrix} \quad (4.2.1.8)$$

The term on the right is the vector sum of the moments about B of the forces acting on all particles of the body. Again, internal forces cancel and only moments of forces external to the body remain:

$$\begin{vmatrix} DHXIBI \\ DHYIBI \\ DHZIBI \end{vmatrix} = \Sigma \begin{vmatrix} XI_{IpB} \\ YI_{IpB} \\ ZI_{IpB} \end{vmatrix} X \begin{vmatrix} \Delta FXI \\ \Delta FYI \\ \Delta FZI \end{vmatrix} = \begin{vmatrix} \Sigma MXI \\ \Sigma MYI \\ \Sigma MZI \end{vmatrix} \text{ about B} \quad (4.2.1.9)$$

Equation (4.2.1.9) is the basic form of Newton's rotational law developed about the non-inertially-fixed center of gravity point of the body. Note that Eq. (4.2.1.9) has the same Moment = time rate of change of angular momentum form as the rotational equations about an inertially fixed point previously presented in Eq. (4.2.0.5). It will be shown in Section 4.2.2 that the rotational equations only take this general form when the moments are taken about the mass center or an inertially fixed point. Additional terms will be necessary when the moments are taken about an arbitrary point in Section 4.2.2.

Motion simulations of rotational motion are basically generated by solving Newton's rotational law for the store angular accelerations which are then integrated over time to get angular velocities and the angular orientations of the body relative to inertial axes. To do this, it is convenient to rewrite the store rotational equations in terms of rotational velocities and rotational accelerations rather than cross products of the moment arms with the linear velocities and linear accelerations. A rather involved process is necessary to rewrite Eqs. (4.2.1.2) and (4.2.1.9) in terms of rotational velocities and accelerations. First, Eq. (4.2.1.2) for the angular momentum can be expanded as:

$$\begin{vmatrix} HXIBI \\ HYIBI \\ HZIBI \end{vmatrix} = \Sigma \begin{vmatrix} XI_{IpB} \\ YI_{IpB} \\ ZI_{IpB} \end{vmatrix} X \Delta m \left(\begin{vmatrix} UIBI \\ VIBI \\ WIBI \end{vmatrix} + \begin{vmatrix} UI_{IpB} \\ VI_{IpB} \\ WI_{IpB} \end{vmatrix} \right) \quad (4.2.1.10)$$

The inertial components of the linear velocities of each individual point in a rigid body relative to body axes are a simple function of the inertial rotation velocity:

$$\begin{vmatrix} UI_{IpB} \\ VI_{IpB} \\ WI_{IpB} \end{vmatrix} = [\tilde{\omega} IBI] \begin{vmatrix} XI_{IpB} \\ YI_{IpB} \\ ZI_{IpB} \end{vmatrix} \quad (4.2.1.11)$$

Equation (4.2.1.11) can be substituted into Eq. (4.2.1.10). In doing so, however, it will be convenient to express the velocity relations using the cross product forms rather than the skew-symmetric forms because cross products are already involved in Eq. (4.2.1.10):

$$\begin{vmatrix} \text{HXIBI} \\ \text{HYIBI} \\ \text{HZIBI} \end{vmatrix} = \Sigma \begin{vmatrix} \text{XI}_{\text{IpB}} \\ \text{YI}_{\text{IpB}} \\ \text{ZI}_{\text{IpB}} \end{vmatrix} \times \Delta m \left(\begin{vmatrix} \text{UIBI} \\ \text{VIBI} \\ \text{WIBI} \end{vmatrix} + \begin{vmatrix} \text{PIBI} \\ \text{QIBI} \\ \text{RIBI} \end{vmatrix} \times \begin{vmatrix} \text{XI}_{\text{IpB}} \\ \text{YI}_{\text{IpB}} \\ \text{ZI}_{\text{IpB}} \end{vmatrix} \right) \quad (4.2.1.12)$$

Several important simplifications of the rotational equations (including the elimination of some of the nested cross products) can be made by fully expanding the Eq. (4.2.1.12) form out to three separate scalar equations. Beginning by expanding the inner cross product:

$$\begin{vmatrix} \text{HXIBI} \\ \text{HYIBI} \\ \text{HZIBI} \end{vmatrix} = \Sigma \begin{vmatrix} \text{XI}_{\text{IpB}} \\ \text{YI}_{\text{IpB}} \\ \text{ZI}_{\text{IpB}} \end{vmatrix} \times \Delta m \begin{vmatrix} \text{UIBI} + \text{QIBI}^* \text{ZI}_{\text{IpB}} - \text{RIBI}^* \text{YI}_{\text{IpB}} \\ \text{VIBI} - \text{PIBI}^* \text{ZI}_{\text{IpB}} + \text{RIBI}^* \text{XI}_{\text{IpB}} \\ \text{WIBI} + \text{PIBI}^* \text{YI}_{\text{IpB}} - \text{QIBI}^* \text{XI}_{\text{IpB}} \end{vmatrix} \quad (4.2.1.13)$$

Expanding further:

$$\begin{aligned} \text{HXIBI} &= \Sigma [\text{YI}_{\text{IpB}}^* \{ \text{WIBI} + \text{PIBI}^* \text{YI}_{\text{IpB}} - \text{QIBI}^* \text{XI}_{\text{IpB}} \} \\ &\quad - \text{ZI}_{\text{IpB}}^* \{ \text{VIBI} - \text{PIBI}^* \text{ZI}_{\text{IpB}} + \text{RIBI}^* \text{XI}_{\text{IpB}} \}] \Delta m \\ \text{HYIBI} &= \Sigma [-\text{XI}_{\text{IpB}}^* \{ \text{WIBI} + \text{PIBI}^* \text{YI}_{\text{IpB}} - \text{QIBI}^* \text{XI}_{\text{IpB}} \} \\ &\quad + \text{ZI}_{\text{IpB}}^* \{ \text{UIBI} + \text{QIBI}^* \text{ZI}_{\text{IpB}} - \text{RIBI}^* \text{YI}_{\text{IpB}} \}] \Delta m \end{aligned} \quad (4.2.1.14)$$

$$\begin{aligned} \text{HZIBI} &= \Sigma [\text{XI}_{\text{IpB}}^* \{ \text{VIBI} - \text{PIBI}^* \text{ZI}_{\text{IpB}} + \text{RIBI}^* \text{XI}_{\text{IpB}} \} \\ &\quad - (\text{YI}_{\text{IpB}}^* \{ \text{UIBI} + \text{QIBI}^* \text{ZI}_{\text{IpB}} - \text{RIBI}^* \text{YI}_{\text{IpB}} \})] \Delta m \end{aligned}$$

Rearranging:

$$\begin{aligned} \text{HXIBI} &= + \text{PIBI}^* \Sigma [(\text{YI}_{\text{IpB}})^2 + (\text{ZI}_{\text{IpB}})^2] \Delta m \\ &\quad - \text{QIBI}^* \Sigma [(\text{XI}_{\text{IpB}})^* (\text{YI}_{\text{IpB}})] \Delta m \\ &\quad - \text{RIBI}^* \Sigma [(\text{XI}_{\text{IpB}})^* (\text{ZI}_{\text{IpB}})] \Delta m \\ &\quad + \Sigma \text{WIBI}^* (\text{YI}_{\text{IpB}}) \Delta m - \Sigma \text{VIBI}^* (\text{ZI}_{\text{IpB}}) \Delta m \\ \text{HYIBI} &= - \text{PIBI}^* \Sigma [(\text{YI}_{\text{IpB}})^* (\text{XI}_{\text{IpB}})] \Delta m \\ &\quad + \text{QIBI}^* \Sigma [(\text{XI}_{\text{IpB}})^2 + (\text{ZI}_{\text{IpB}})^2] \Delta m \\ &\quad - \text{RIBI}^* \Sigma [(\text{YI}_{\text{IpB}})^* (\text{ZI}_{\text{IpB}})] \Delta m \\ &\quad - \Sigma \text{WIBI}^* (\text{XI}_{\text{IpB}}) \Delta m + \Sigma \text{UIBI}^* (\text{ZI}_{\text{IpB}}) \Delta m \end{aligned} \quad (4.2.1.15)$$

$$\begin{aligned} \text{HZIBI} &= - \text{PIBI}^* \Sigma [(\text{ZI}_{\text{IpB}})^* (\text{XI}_{\text{IpB}})] \Delta m \\ &\quad - \text{QIBI}^* \Sigma [(\text{ZI}_{\text{IpB}})^* (\text{YI}_{\text{IpB}})] \Delta m \\ &\quad + \text{RIBI}^* \Sigma [(\text{XI}_{\text{IpB}})^2 + (\text{YI}_{\text{IpB}})^2] \Delta m \\ &\quad - \Sigma \text{VIBI}^* (\text{XI}_{\text{IpB}}) \Delta m + \Sigma \text{UIBI}^* (\text{YI}_{\text{IpB}}) \Delta m \end{aligned}$$

The summations of the discrete mass elements in Eqs. (4.2.1.15) can now be replaced with integrals. Note first that:

$$\int \text{XI}_{\text{IpB}} \, dm = \int \text{YI}_{\text{IpB}} \, dm = \int \text{ZI}_{\text{IpB}} \, dm = 0.0 \quad (4.2.1.16)$$

since the body axis origin is at the mass center (by definition, the integrated sum of the mass moments about the mass center is zero). Equation (4.2.1.15) can then be rewritten as:

$$\begin{aligned}
 \text{HXIBI} &= + \text{PIBI}^* \int [(\text{YIpB})^2 + (\text{ZIpB})^2] dm \\
 &\quad - \text{QIBI}^* \int [(\text{XIpB})(\text{YIpB})] dm \\
 &\quad - \text{RIBI}^* \int [(\text{XIpB})(\text{ZIpB})] dm \\
 \text{HYIBI} &= - \text{PIBI}^* \int [(\text{YIpB})(\text{XIpB})] dm \\
 &\quad + \text{QIBI}^* \int [(\text{XIpB})^2 + (\text{ZIpB})^2] dm \\
 &\quad - \text{RIBI}^* \int [(\text{YIpB})(\text{ZIpB})] dm \\
 \text{HZIBI} &= - \text{PIBI}^* \int [(\text{ZIpB})(\text{XIpB})] dm \\
 &\quad - \text{QIBI}^* \int [(\text{ZIpB})(\text{YIpB})] dm \\
 &\quad + \text{RIBI}^* \int [(\text{XIpB})^2 + (\text{YIpB})^2] dm
 \end{aligned} \tag{4.2.1.17}$$

Equations (4.2.1.17) represent the angular momentum about the body axis origin expressed in terms of rotation velocities. The three mass integrals in each of Eqs. (4.2.1.17) represent important physical properties of the store and are referred to as moments and products of inertia. The inertias represent a measure of the inertial resistance of the body to rotational motion and are the rotational analogy of the mass term in the linear equations of motion [Eq. (4.1.1.2)]. The inertias represent the distribution of the mass within the body. The individual mass distribution integrals are:

Moments of Inertia	Products of Inertia
$I_{xxIB} = \int (\text{YIpB}^2 + \text{ZIpB}^2) dm$	$I_{xyIB} = I_{yxIB} = \int \text{XIpB}^* \text{YIpB} dm$
$I_{yyIB} = \int (\text{XIpB}^2 + \text{ZIpB}^2) dm$	$I_{xzIB} = I_{zxIB} = \int \text{XIpB}^* \text{ZIpB} dm$
$I_{zzIB} = \int (\text{XIpB}^2 + \text{YIpB}^2) dm$	$I_{yzIB} = I_{zyIB} = \int \text{YIpB}^* \text{ZIpB} dm$

(4.2.1.18)

where the $\{\text{XIpB}\}$ vector denotes the inertial components of the position of each individual infinitesimal mass element, "p", within the body relative to the body-axis origin. The inertias can be expressed in matrix (or tensor) form as:

$$[\mathbf{I}]_{IB} = \begin{bmatrix} I_{IB}(1,1) & I_{IB}(1,2) & I_{IB}(1,3) \\ I_{IB}(2,1) & I_{IB}(2,2) & I_{IB}(2,3) \\ I_{IB}(3,1) & I_{IB}(3,2) & I_{IB}(3,3) \end{bmatrix} = \begin{bmatrix} I_{xxIB} & -I_{xyIB} & -I_{xzIB} \\ -I_{yxIB} & I_{yyIB} & -I_{yzIB} \\ -I_{zxIB} & -I_{zyIB} & I_{zzIB} \end{bmatrix} \tag{4.2.1.19}$$

Another way for expressing the inertia terms is in an alternate vector equation form which is useful in some applications (as will be shown later). First position vector of each mass element $\text{RIPB} = \{\text{XIpB}, \text{YIpB}, \text{ZIpB}\}$ is defined, then the inertia matrix can be written as:

$$\begin{aligned}
 [\mathbf{I}]_{IB} &= \int \left(\text{RIPB}^2 \begin{bmatrix} 1 & 0 & 0 \\ 0 & 1 & 0 \\ 0 & 0 & 1 \end{bmatrix} - \{\text{RIPB}\} \{\text{RIPB}\}^T \right) dm \\
 &= \int \left(\text{RIPB}^2 \begin{bmatrix} 1 & 0 & 0 \\ 0 & 1 & 0 \\ 0 & 0 & 1 \end{bmatrix} - \begin{vmatrix} \text{XIpB} \\ \text{YIpB} \\ \text{ZIpB} \end{vmatrix} \begin{bmatrix} \text{XIpB} & \text{YIpB} & \text{ZIpB} \end{bmatrix} \right) dm
 \end{aligned} \tag{4.2.1.20}$$

where $RIP^2 = XIpB^2 + YIpB^2 + ZIpB^2$. An examination of Eq. (4.2.1.20) will reveal that each element corresponds to one of the expressions of Eq. (4.2.1.19).

Using the inertial tensor, the angular momentum equations (Eq. (4.2.1.17)) can be expanded into matrix form as:

$$\begin{vmatrix} HXIBI \\ HYIBI \\ HZIBI \end{vmatrix} = [I]_{IB} \begin{vmatrix} PIBI \\ QIBI \\ RIBI \end{vmatrix} \quad (4.2.1.21)$$

Finally, replacing the angular momentum as originally developed in Eq. (4.2.1.9) with the angular momentum defined in terms of angular velocities from Eq. (4.2.1.21), the rotational equations of motion for the free-falling body can be written as:

$$\begin{vmatrix} \Sigma MXI \\ \Sigma MYI \\ \Sigma MZI \end{vmatrix}_{\text{about B}} = \frac{d}{dt} \left\{ [I]_{IB} \begin{vmatrix} PIBI \\ QIBI \\ RIBI \end{vmatrix} \right\} = \frac{d}{dt} [I]_{IB} \begin{vmatrix} PIBI \\ QIBI \\ RIBI \end{vmatrix} + [I]_{IB} \begin{vmatrix} \alpha XIBI \\ \alpha YIBI \\ \alpha ZIBI \end{vmatrix} \quad (4.2.1.22)$$

Even after all this manipulation, however, the rotational equations are not yet in the final form most convenient for numerical simulation. In the Eq. (4.2.1.22) form, the rotational equations are virtually unmanageable because at each time step of the trajectory, as the body axes rotate relative to the inertial axes, the inertia integrals of Eq. (4.2.1.18) have to be re-evaluated. Implementation of the rotational equations is greatly simplified by projecting the terms in Eq. (4.2.1.22) into body-fixed axes. In body-axis form, the inertia components for a rigid body (without time-dependent mass changes) are constants which need only be evaluated once per trajectory. Body axis inertias can be obtained by re-expressing Eqs. (4.2.1.22) as incremental mass moments about the body axes:

Moments of Inertia	Products of Inertia
$I_{xxBB} = \int (YBpB^2 + ZBpB^2) dm$	$I_{xyBB} = I_{yxBB} = XBpB * YBpB dm$
$I_{yyBB} = \int (XBpB^2 + ZBpB^2) dm$	$I_{xzBB} = I_{zxBB} = XBpB * ZBpB dm$
$I_{zzBB} = \int (XBpB^2 + YBpB^2) dm$	$I_{yzBB} = I_{zyBB} = YBpB * ZBpB dm$

(4.2.1.23)

although it should be pointed out that the expressions of Eq. (4.2.1.23) are rarely (if ever) used in actual practice to determine the inertias of a true store. Instead, experimental inertia measurements obtained using the actual flight hardware and some form of torsional balance are usually necessary because of the extreme difficulty in evaluating the mass integrals for all the various components of a typical store. In most cases, the body-axis inertias are constant inputs that are provided to the engineers responsible for motion simulations from separate organizations responsible for aircraft/store mass properties. A note of caution is in order at this point - in many aircraft and store manufacturing companies, mass properties engineers use a body-fixed axis system in which the XB and ZB axes are rotated so that XB points aft and ZB points up relative to the store. In such cases a sign change on the provided I_{xyBB} and I_{yzBB} terms must be accomplished before the values are used in the motion simulations.

Expressions are needed to relate each inertial term in Eq. (4.2.1.22) to a corresponding body-axis term so that the equation can be expressed in body axis projections:

$$\begin{vmatrix} \Sigma MXI \\ \Sigma MYI \\ \Sigma MZI \end{vmatrix}_{\text{about B}} = [\text{TRNBI}]^{-1} \begin{vmatrix} \Sigma MXB \\ \Sigma MYB \\ \Sigma MZB \end{vmatrix}_{\text{about B}} \quad (4.2.1.24)$$

$$\begin{vmatrix} PIBI \\ QIBI \\ RIBI \end{vmatrix} = [\text{TRNBI}]^{-1} \begin{vmatrix} PBBI \\ QBBI \\ RBBI \end{vmatrix} \quad (4.2.1.25)$$

$$\begin{vmatrix} HXIBI \\ HYIBI \\ HZIBI \end{vmatrix} = [\text{TRNBI}]^{-1} \begin{vmatrix} HXBBI \\ HYBBI \\ HZBBI \end{vmatrix} \quad (4.2.1.26)$$

The expression for projecting the inertia matrix in Eq. (4.2.1.22) from inertial components to body components involves a "conjugate" transformation similar to the alternate rotational transformations outlined in Section 1.5. The inertia transform is developed in the next several equations.

First, beginning with Eq. (4.2.1.20), but rewriting the 3 by 3 identity matrix as [1] to avoid confusion with the inertia matrix [I]:

$$[I]_{IB} = \int (RIPB^2 [1] - \{RIPB\} \{RIPB\}^T) dm \quad (4.2.1.27)$$

Note that

$$\{RIPB\} = [\text{TRNBI}]^T \{RBpB\}, \{RIPB\}^T = \{RBpB\}^T [\text{TRNBI}] \quad (4.2.1.28)$$

and

$$RIPB^2 = RBpB^2 \quad (4.2.1.29)$$

since the magnitude of the position vector is constant irrespective of the axis directions in which its components are measured. Substituting Eqs. (4.2.1.28) and (4.2.1.29) into Eq. (4.2.1.27):

$$\begin{aligned} [I]_{IB} &= \int (RIPB^2 [1] - [\text{TRNBI}]^T \{RBpB\} \{RBpB\}^T [\text{TRNBI}]) dm \\ &= \int ([\text{TRNBI}]^T RBpB^2 [1] [\text{TRNBI}] - [\text{TRNBI}]^T \{RBpB\} \{RBpB\}^T [\text{TRNBI}]) dm \\ &= [\text{TRNBI}]^T \int (RBpB^2 [1] \{RBpB\} \{RBpB\}^T) dm [\text{TRNBI}] \\ &= [\text{TRNBI}]^T [I]_{BB} [\text{TRNBI}] = [\text{TRNBI}]^{-1} [I]_{BB} [\text{TRNBI}] \end{aligned} \quad (4.2.1.30)$$

If Eqs. (4.2.1.24) through (4.2.1.26) and Eqs. (4.2.1.30) are substituted into Eq. (4.2.1.22):

$$\begin{aligned} [\text{TRNBI}]^{-1} \begin{vmatrix} \Sigma MXB \\ \Sigma MYB \\ \Sigma MZB \end{vmatrix}_{\text{about B}} &= \frac{d}{dt} \left\{ [\text{TRNBI}]^{-1} [I]_{BB} [\text{TRNBI}] [\text{TRNBI}]^{-1} \begin{vmatrix} PBBI \\ QBBI \\ RBBI \end{vmatrix} \right\} \\ &= \frac{d}{dt} \left\{ [\text{TRNBI}]^{-1} [I]_{BB} \begin{vmatrix} PBBI \\ QBBI \\ RBBI \end{vmatrix} \right\} \end{aligned} \quad (4.2.1.31)$$

Note that Eq. (4.2.1.31) is still a fundamentally inertial relationship [like Eq. (4.2.1.22)] but it is now expressed in terms of projected body-axis state variables. Evaluating the derivative in Eq. (4.2.1.31) by the chain rule:

$$\begin{aligned} [\text{TRNBI}]^{-1} \begin{vmatrix} \Sigma MXB \\ \Sigma MYB \\ \Sigma MZB \end{vmatrix}_{\text{about B}} &= [\text{TRNBI}]^{-1} [\tilde{\omega} BBI] [I]_{BB} \begin{vmatrix} PBBI \\ QBBI \\ RBBI \end{vmatrix} \\ &+ [\text{TRNBI}]^{-1} \frac{d}{dt} [I]_{BB} \begin{vmatrix} PBBI \\ QBBI \\ RBBI \end{vmatrix} + [\text{TRNBI}]^{-1} [I]_{BB} \begin{vmatrix} DPBBI \\ DQBBI \\ DRBBI \end{vmatrix} \end{aligned} \quad (4.2.1.32)$$

In many cases of practical interest, the distribution of mass within the body is constant and the middle term on the right of the equality is zero. Even for thrusting bodies which lose mass as on-board fuel is burned (thus changing inertias), the inertia matrix derivative can still often be safely ignored, particularly if partial compensation for the missing terms is provided by adjusting the inertias at periodic time steps in the numerical integration. Multiplying through by $[\text{TRNBI}]$ and deleting the inertia derivative term:

$$\begin{vmatrix} \Sigma MXB \\ \Sigma MYB \\ \Sigma MZB \end{vmatrix}_{\text{about B}} = [\tilde{\omega} BBI] [I]_{BB} \begin{vmatrix} PBBI \\ QBBI \\ RBBI \end{vmatrix} + [I]_{BB} \begin{vmatrix} DPBBI \\ DQBBI \\ DRBBI \end{vmatrix} \quad (4.2.1.33)$$

From Eqs. (4.2.1.26) and (4.2.1.21), the product involving the angular velocity vector can be rewritten:

$$[I]_{BB} \begin{vmatrix} PBBI \\ QBBI \\ RBBI \end{vmatrix} = \begin{vmatrix} HXBBI \\ HYBBI \\ HZBBI \end{vmatrix} \quad (4.2.1.34)$$

Similarly:

$$[I]_{BB} \begin{vmatrix} DPBBI \\ DQBBI \\ DRBBI \end{vmatrix} = \begin{vmatrix} DHXBBI \\ DHYBBI \\ DHZBBI \end{vmatrix} \quad (4.2.1.35)$$

so that Eq. (4.2.1.33) can be rewritten using Eqs. (4.2.1.34) and (4.2.1.35) as:

$$\begin{vmatrix} \Sigma MXB \\ \Sigma MYB \\ \Sigma MZB \end{vmatrix}_{\text{about B}} = [\tilde{\omega} \text{BBI}] \begin{vmatrix} HXBBI \\ HYBBI \\ HZBBI \end{vmatrix} + \begin{vmatrix} DHXBBI \\ DHYBBI \\ DHZBBI \end{vmatrix} \quad (4.2.1.36)$$

which is sometimes referred to as the "Euler form" of the rotational equations of motion. Solving for {DHXBBI}:

$$\begin{aligned} \begin{vmatrix} DHXBBI \\ DHYBBI \\ DHZBBI \end{vmatrix} &= -[\tilde{\omega} \text{BBI}] [I]_{BB} \begin{vmatrix} PBBI \\ QBBI \\ RBBI \end{vmatrix} + \begin{vmatrix} MXB \\ MYB \\ MZB \end{vmatrix}_{\text{about B}} \\ &= -[\tilde{\omega} \text{BBI}] \begin{vmatrix} HXBBI \\ HYBBI \\ HZBBI \end{vmatrix} + \begin{vmatrix} MXB \\ MYB \\ MZB \end{vmatrix}_{\text{about B}} \end{aligned} \quad (4.2.1.37)$$

where the summation on the moment vector has been dropped to indicate that no external reaction moments are applied to the body for unrestrained, free-fall simulations. Finally, from Eq. (4.2.1.35):

$$\begin{vmatrix} DPBBI \\ DQBBI \\ DRBBI \end{vmatrix} = [I]_{BB}^{-1} \begin{vmatrix} DHXBBI \\ DHYBBI \\ DHZBBI \end{vmatrix} \quad (4.2.1.38)$$

The inverse inertia matrix in Eq. (4.2.1.38) must be evaluated using standard matrix inversion techniques. The inertia matrix is not orthogonal and, unlike the orthogonal transformation matrices, its inverse is not identical with its transpose.

Equations (4.2.1.37) substituted into Eq. (4.2.1.38) represent the final form of the rotational free-fall equations used in AEDC wind tunnel and off-line simulations. The projected angular velocity derivatives from Eq. (4.2.1.38) are computed from the measured moments at each time step and integrated numerically to determine the body-axis angular velocities at the next point in the trajectory.

Also, at each time step in the trajectory, the body-axis angular velocity components resulting from each integration must be transformed to a form which can be integrated to determine the angular orientation of the body axes relative to inertial axes. There are three fundamentally different ways in which this can be accomplished which are described in Section 4.2.3.

4.2.2 Rotational Equations for Restricted Motion

The rotational equations can also be written in terms of the angular momentum of the body about the origin of the hook axis system, H. It is convenient to calculate the angular momentum about the hook point and sum the moments about the hook point because the unknown pivot reac-

tion forces (which produce no moment at the pivot) are thus removed from the rotational equations. As a result, simultaneous solutions of coupled systems of equations may not be necessary for some specialized restricted-motion cases. (In most restricted cases, however, the actual implementation within a motion simulation of the constraints associated with some types of pivot and rail mechanisms often introduces additional levels of complication which necessitate simultaneous solution of multiple equations. Implementation of physical constraints for restricted motion will be described in later sections.) The current section will deal only with the development of the basic equations for motion about a moving hook point. Referring again to Fig. 12, the inertial components of the angular momentum of p about point H are formed from the cross product of the inertial moment arm vector from p to H and the inertial components of the linear momentum of particle p relative to the inertial origin:

$$\begin{vmatrix} \Delta H X I H I \\ \Delta H Y I H I \\ \Delta H Z I H I \end{vmatrix} = \begin{vmatrix} X I p H \\ Y I p H \\ Z I p H \end{vmatrix} \times \Delta m \begin{vmatrix} U I p I \\ V I p I \\ W I p I \end{vmatrix} \quad (4.2.2.1)$$

where $\{X I p H\}$ is the inertial position of point "p" relative to the hook point and the term on the right of the cross-product operator is the linear momentum of the differential mass at point p. The angular momentum of the entire store about the pivot is obtained by summing the contributions of all individual masses:

$$\begin{vmatrix} H X I H I \\ H Y I H I \\ H Z I H I \end{vmatrix} = \Sigma \begin{vmatrix} X I p H \\ Y I p H \\ Z I p H \end{vmatrix} \times \Delta m \begin{vmatrix} U I p I \\ V I p I \\ W I p I \end{vmatrix} \quad (4.2.2.2)$$

Equation (4.2.2.2) can be rewritten by expanding the $\{X I p H\}$ vector:

$$\begin{aligned} \begin{vmatrix} H X I H I \\ H Y I H I \\ H Z I H I \end{vmatrix} &= \Sigma \left(\begin{vmatrix} X I B H \\ Y I B H \\ Z I B H \end{vmatrix} + \begin{vmatrix} X I p B \\ Y I p B \\ Z I p B \end{vmatrix} \right) \times \Delta m \begin{vmatrix} U I p I \\ V I p I \\ W I p I \end{vmatrix} \\ &= \Sigma \begin{vmatrix} X I B H \\ Y I B H \\ Z I B H \end{vmatrix} \times \Delta m \begin{vmatrix} U I p I \\ V I p I \\ W I p I \end{vmatrix} + \Sigma \begin{vmatrix} X I p B \\ Y I p B \\ Z I p B \end{vmatrix} \times \Delta m \begin{vmatrix} U I p I \\ V I p I \\ W I p I \end{vmatrix} \end{aligned} \quad (4.2.2.3)$$

The term on the right is recognizable as the angular momentum about the body axis origin [Eq. (4.2.1.2)]:

$$\begin{vmatrix} H X I H I \\ H Y I H I \\ H Z I H I \end{vmatrix} = \Sigma \begin{vmatrix} X I B H \\ Y I B H \\ Z I B H \end{vmatrix} \times \Delta m \begin{vmatrix} U I p I \\ V I p I \\ W I p I \end{vmatrix} + \begin{vmatrix} H X I B I \\ H Y I B I \\ H Z I B I \end{vmatrix} \quad (4.2.2.4)$$

Note, however, by definition of the mass center that:

$$\Sigma \Delta m \begin{vmatrix} U I p I \\ V I p I \\ W I p I \end{vmatrix} = \Sigma \frac{d}{dt} \Delta m \begin{vmatrix} X I p I \\ Y I p I \\ Z I p I \end{vmatrix} = \frac{d}{dt} m \begin{vmatrix} X I p I \\ Y I p I \\ Z I p I \end{vmatrix} = m \begin{vmatrix} U I B I \\ V I B I \\ W I B I \end{vmatrix} \quad (4.2.2.5)$$

Substituting Eq. (4.2.2.5) into (4.2.2.4):

$$\begin{vmatrix} HXIGHI \\ HYIHI \\ HZIHI \end{vmatrix} = \begin{vmatrix} XIBH \\ YIBH \\ ZIBH \end{vmatrix} \times m \begin{vmatrix} UIBI \\ VIBI \\ WIBI \end{vmatrix} + \begin{vmatrix} HXIBI \\ HYIBI \\ HZIBI \end{vmatrix} \quad (4.2.2.6)$$

If derivatives are taken of both sides by the chain rule:

$$\begin{vmatrix} DHXIGHI \\ DHYIHI \\ DHZIHI \end{vmatrix} = \begin{vmatrix} XIBH \\ YIBH \\ ZIBH \end{vmatrix} \times m \begin{vmatrix} AXIBI \\ AYIBI \\ AZIBI \end{vmatrix} + \begin{vmatrix} UIBH \\ VIBH \\ WIBH \end{vmatrix} \times m \begin{vmatrix} UIBI \\ VIBI \\ WIBI \end{vmatrix} + \begin{vmatrix} DHXIBI \\ DHYIBI \\ DHZIBI \end{vmatrix} \quad (4.2.2.7)$$

Substituting in the relation between moments about the body axes and the angular momentum about body axes [Eq. (4.2.1.9)]:

$$\begin{vmatrix} DHXIGHI \\ DHYIHI \\ DHZIHI \end{vmatrix} = \begin{vmatrix} XIBH \\ YIBH \\ ZIBH \end{vmatrix} \times m \begin{vmatrix} AXIBI \\ AYIBI \\ AZIBI \end{vmatrix} + \begin{vmatrix} UIBH \\ VIBH \\ WIBH \end{vmatrix} \times m \begin{vmatrix} UIBI \\ VIBI \\ WIBI \end{vmatrix} + \begin{vmatrix} \Sigma MXI \\ \Sigma MYI \\ \Sigma MZI \end{vmatrix}_{\text{about B}} \quad (4.2.2.8)$$

or:

$$\begin{vmatrix} DHXIGHI \\ DHYIHI \\ DHZIHI \end{vmatrix} = \begin{vmatrix} XIBH \\ YIBH \\ ZIBH \end{vmatrix} \times \begin{vmatrix} FXI \\ FYI \\ FZI \end{vmatrix} + \begin{vmatrix} UIBH \\ VIBH \\ WIBH \end{vmatrix} \times m \begin{vmatrix} UIBI \\ VIBI \\ WIBI \end{vmatrix} + \begin{vmatrix} \Sigma MXI \\ \Sigma MYI \\ \Sigma MZI \end{vmatrix}_{\text{about B}} \quad (4.2.2.9)$$

But:

$$\begin{vmatrix} XIBH \\ YIBH \\ ZIBH \end{vmatrix} \times \begin{vmatrix} FXI \\ FYI \\ FZI \end{vmatrix} + \begin{vmatrix} \Sigma MXI \\ \Sigma MYI \\ \Sigma MZI \end{vmatrix}_{\text{about B}} = \begin{vmatrix} \Sigma MXI \\ \Sigma MYI \\ \Sigma MZI \end{vmatrix}_{\text{about H}} \quad (4.2.2.10)$$

so that Eq. (4.2.2.9) becomes:

$$\begin{vmatrix} \Sigma MXI \\ \Sigma MYI \\ \Sigma MZI \end{vmatrix}_{\text{about H}} = \begin{vmatrix} DHXIGHI \\ DHYIHI \\ DHZIHI \end{vmatrix} - \begin{vmatrix} UIBH \\ VIBH \\ WIBH \end{vmatrix} \times m \begin{vmatrix} UIBI \\ VIBI \\ WIBI \end{vmatrix} \quad (4.2.2.11)$$

Equation (4.2.2.11) can be slightly simplified by expanding the {UIBH} vector:

$$\begin{vmatrix} \Sigma MXI \\ \Sigma MYI \\ \Sigma MZI \end{vmatrix}_{\text{about H}} = \begin{vmatrix} DHXIGHI \\ DHYIHI \\ DHZIHI \end{vmatrix} - \left(\begin{vmatrix} UIBI \\ VIBI \\ WIBI \end{vmatrix} - \begin{vmatrix} UIHI \\ VIHI \\ WIHI \end{vmatrix} \right) \times m \begin{vmatrix} UIBI \\ VIBI \\ WIBI \end{vmatrix} \quad (4.2.2.11)$$

$$= \begin{vmatrix} DHXIGHI \\ DHYIHI \\ DHZIHI \end{vmatrix} - \begin{vmatrix} UIBI \\ VIBI \\ WIBI \end{vmatrix} \times m \begin{vmatrix} UIBI \\ VIBI \\ WIBI \end{vmatrix} + \begin{vmatrix} UIHI \\ VIHI \\ WIHI \end{vmatrix} \times m \begin{vmatrix} UIBI \\ VIBI \\ WIBI \end{vmatrix} \quad (4.2.2.12)$$

Using the vector property that a vector crossed with itself is zero:

$$\begin{vmatrix} \Sigma MXI \\ \Sigma MYI \\ \Sigma MZI \end{vmatrix}_{\text{about H}} = \begin{vmatrix} DHXIHI \\ DHYIHI \\ DHZIHI \end{vmatrix} + \begin{vmatrix} UIHI \\ VIHI \\ WIHI \end{vmatrix} \times m \begin{vmatrix} UIBI \\ VIBI \\ WIBI \end{vmatrix} \quad (4.2.2.13)$$

Equation (4.2.2.13) is the basic form of Newton's rotational law developed about a non-inertially-fixed hook point attached to the body. Note that Eq. (4.2.2.13) does not have the same form as the rotational equations about an inertially fixed point [Eq. (4.2.0.5)] or the store center of mass [Eq. (4.2.1.9)] because of the additional cross product term.

Motion simulations of rotational motion are basically generated by solving Newton's rotational law for the store angular accelerations which are then integrated over time to get angular velocities and the angular orientations of the body relative to inertial axes. To do this it is convenient to rewrite the store angular momentum in terms of rotational velocities and accelerations instead of cross products of linear velocities and accelerations with appropriate moment arms. Equation (4.2.2.2) for the angular momentum can be expanded as:

$$\begin{vmatrix} HXIHI \\ HYIHI \\ HZIHI \end{vmatrix} = \Sigma \left(\begin{vmatrix} XI_{IpB} \\ YI_{IpB} \\ ZI_{IpB} \end{vmatrix} + \begin{vmatrix} XIBH \\ YIBH \\ ZIBH \end{vmatrix} \right) \times \Delta m \left(\begin{vmatrix} UIHI \\ VIHI \\ WIHI \end{vmatrix} + \begin{vmatrix} UIBH \\ VIBH \\ WIBH \end{vmatrix} + \begin{vmatrix} UI_{IpB} \\ VI_{IpB} \\ WI_{IpB} \end{vmatrix} \right) \quad (4.2.2.14)$$

The components of the velocity of the body axes relative to hook axes were previously determined in body axis projection form in Eq. (4.1.2.4) but can be rewritten using Eq. (1.5.4) to be:

$$\begin{vmatrix} UIBH \\ VIBH \\ WIBH \end{vmatrix} = [\text{TRNBI}]^{-1} [\tilde{\omega} \text{IBI}] \begin{vmatrix} XBBH \\ YBBH \\ ZBBH \end{vmatrix} = [\text{TRNBI}]^{-1} [\text{TRNBI}] [\tilde{\omega} \text{IBI}] [\text{TRNBI}]^{-1} \begin{vmatrix} XBBH \\ YBBH \\ ZBBH \end{vmatrix}$$

$$= [\tilde{\omega} \text{IBI}] \begin{vmatrix} XIBH \\ YIBH \\ ZIBH \end{vmatrix} \quad (4.2.2.15)$$

Because hook axis and body axes are fixed relative to one another and are always parallel, almost identical expressions can be developed for the velocities of each individual point in the body relative to body axes:

$$\begin{vmatrix} UI_{IpB} \\ VI_{IpB} \\ WI_{IpB} \end{vmatrix} = [\tilde{\omega} \text{IBI}] \begin{vmatrix} XI_{IpB} \\ YI_{IpB} \\ ZI_{IpB} \end{vmatrix} \quad 4.2.2.16$$

Equations (4.2.2.15) and (4.2.2.16) can now be substituted into Eq. (4.2.2.14). In doing so, however, it will be convenient to express the velocity relations using the cross product forms rather than the skew-symmetric forms because cross products are already involved in Eq. (4.2.2.14):

$$\begin{vmatrix} HXIII \\ HYIII \\ HZIII \end{vmatrix} = \Sigma \left\{ \left(\begin{vmatrix} XIpB \\ YIpB \\ ZIpB \end{vmatrix} + \begin{vmatrix} XIBH \\ YIBH \\ ZIBH \end{vmatrix} \right) \times \Delta m \left(\begin{vmatrix} UIHI \\ VIHI \\ WIHI \end{vmatrix} + \begin{vmatrix} PIBI \\ QIBI \\ RIBI \end{vmatrix} \times \left(\begin{vmatrix} XIBH \\ YIBH \\ ZIBH \end{vmatrix} + \begin{vmatrix} XIpB \\ YIpB \\ ZIpB \end{vmatrix} \right) \right) \right\} \quad (4.2.2.17)$$

Several important simplifications of the rotational equations (including the elimination of some of the nested cross products) can be made by fully expanding the Eq. (4.2.2.17) form out to three separate scalar equations. Beginning by expanding the inner cross product:

$$\begin{vmatrix} HXIII \\ HYIII \\ HZIII \end{vmatrix} = \Sigma \left\{ \left(\begin{vmatrix} XIpB \\ YIpB \\ ZIpB \end{vmatrix} + \begin{vmatrix} XIBH \\ YIBH \\ ZIBH \end{vmatrix} \right) \times \Delta m \left| \begin{array}{l} UIHI + QIBI*(ZIpB + ZIBH) - RIBI*(YIpB + YIBH) \\ VIHI - PIBI*(ZIpB + ZIBH) + RIBI*(XIpB + XIBH) \\ WIHI + PIBI*(YIpB + YIBH) - QIBI*(XIpB + XIBH) \end{array} \right| \right\} \quad (4.2.2.18)$$

Expanding further:

$$HXIII = \Sigma [(YIpB + YIBH)*\{WIHI + PIBI*(YIpB + YIBH) - QIBI*(XIpB + XIBH)\} - (ZIpB + ZIBH)*\{VIHI - PIBI*(ZIpB + ZIBH) + RIBI*(XIpB + XIBH)\}] \Delta m$$

$$HYIII = \Sigma [-(XIpB + XIBH)*\{WIHI + PIBI*(YIpB + YIBH) - QIBI*(XIpB + XIBH)\} + (ZIpB + ZIBH)*\{UIHI + QIBI*(ZIpB + ZIBH) - RIBI*(YIpB + YIBH)\}] \Delta m$$

$$HZIII = \Sigma [(XIpB + XIBH)*\{VIHI - PIBI*(ZIpB + ZIBH) + RIBI*(XIpB + XIBH)\} - (YIpB + YIBH)*\{UIHI + QIBI*(ZIpB + ZIBH) - RIBI*(YIpB + YIBH)\}] \Delta m \quad (4.2.2.19)$$

Rearranging:

$$\begin{aligned} HXIII &= + PIBI*\Sigma [(YIpB + YIBH)^2 + (ZIpB + ZIBH)^2] \Delta m \\ &\quad - QIBI*\Sigma [(XIpB + XIBH)*(YIpB + YIBH)] \Delta m \\ &\quad - RIBI*\Sigma [(XIpB + XIBH)*(ZIpB + ZIBH)] \Delta m \\ &\quad + \Sigma WIHI*(YIpB + YIBH) \Delta m - \Sigma VIHI*(ZIpB + ZIBH) \Delta m \end{aligned}$$

$$\begin{aligned} HYIII &= - PIBI*\Sigma [(YIpB + YIBH)*(XIpB + XIBH)] \Delta m \quad (4.2.2.20) \\ &\quad - QIBI*\Sigma [(XIpB + XIBH)^2*(ZIpB + ZIBH)^2] \Delta m \\ &\quad - RIBI*\Sigma [(YIpB + YIBH)*(ZIpB + ZIBH)] \Delta m \\ &\quad - \Sigma WIHI*(XIpB + XIBH) \Delta m + \Sigma UIHI*(ZIpB + ZIBH) \Delta m \end{aligned}$$

$$\begin{aligned} HZIII &= - PIBI*\Sigma [(ZIpB + ZIBH)*(XIpB + XIBH)] \Delta m \\ &\quad - QIBI*\Sigma [(ZIpB + ZIBH)*(YIpB + YIBH)] \Delta m \\ &\quad + RIBI*\Sigma [(XIpB + XIBH)^2 + (YIpB + YIBH)^2] \Delta m \\ &\quad + \Sigma VIHI*(XIpB + XIBH) \Delta m - \Sigma UIHI*(YIpB + YIBH) \Delta m \end{aligned}$$

The summations of the discrete mass elements in Eqs. (4.2.2.20) can now be replaced with integrals. Note first that:

$$\int X_{IpB} dm = \int Y_{IpB} dm = \int Z_{IpB} dm = 0.0 \quad (4.2.2.21)$$

by virtue of the fact that the body axis origin is at the mass center (by definition the integrated sum of the mass moments about the mass center is zero). Equations (4.2.2.21) can then be rewritten as:

$$\begin{aligned} HX_{IHI} &= + PIBI^* \int [(Y_{IpB} + YIBH)^2 + (Z_{IpB} + ZIBH)^2] dm \\ &- QIBI^* \int [X_{IpB} + XIBH]^* (Y_{IpB} + YIBH) dm \\ &- RIBI^* \int [(X_{IpB} + XIBH)^* (Z_{IpB} + ZIBH)] dm \\ &+ WIHI^* YIBH^* m - VIHI^* ZIBH^* m \end{aligned}$$

$$\begin{aligned} HY_{IHI} &= - PIBI^* \int [(Y_{IpB} + YIBH)^* (X_{IpB} + XIBH)] dm \\ &+ QIBI^* \int [(X_{IpB} + XIBH)^2 + (Z_{IpB} + ZIBH)^2] dm \\ &- RIBI^* \int [(Y_{IpB} + YIBH)^* (Z_{IpB} + ZIBH)] dm \\ &- WIHI^* XIBH^* m + UIHI^* ZIBH^* m \end{aligned} \quad (4.2.2.22)$$

$$\begin{aligned} HZ_{IHI} &= - PIBI^* \int [(Z_{IpB} + ZIBH)^* (X_{IpB} + XIBH)] dm \\ &- QIBI^* \int [(Z_{IpB} + ZIBH)^* (Y_{IpB} + YIBH)] dm \\ &+ RIBI^* \int [(X_{IpB} + XIBH)^2 + (Y_{IpB} + YIBH)^2] dm \\ &+ VIHI^* XIBH^* m - UIHI^* YIBH^* m \end{aligned}$$

Noting that $\{X_{IpH}\} = \{X_{IpB}\} + \{XIBH\}$, Eqs. (4.2.2.22) can also be written as:

$$\begin{aligned} HX_{IHI} &= + PIBI^* \int [(Y_{IpH})^2 + (Z_{IpH})^2] dm \\ &- QIBI^* \int [(X_{IpH})^* (Y_{IpH})] dm \\ &- RIBI^* \int [(X_{IpH})^* (Z_{IpH})] dm \\ &+ WIHI^* YIBH^* m - VIHI^* ZIBH^* m \end{aligned}$$

$$\begin{aligned} HY_{IHI} &= - PIBI^* \int [(Y_{IpH})^* (X_{IpH})] dm \\ &+ QIBI^* \int [(X_{IpH})^2 + (Z_{IpH})^2] dm \\ &- RIBI^* \int [(Y_{IpH})^* (Z_{IpH})] dm \\ &- WIHI^* XIBH^* m + UIHI^* ZIBH^* m \end{aligned} \quad (4.2.2.23)$$

$$\begin{aligned} HZ_{IHI} &= - PIBI^* \int [(Z_{IpH})^* (X_{IpH})] dm \\ &- QIBI^* \int [(Z_{IpH})^* (Y_{IpH})] dm \\ &+ RIBI^* \int [(X_{IpH})^2 + (Y_{IpH})^2] dm \\ &+ VIHI^* XIBH^* m - UIHI^* YIBH^* m \end{aligned}$$

Equations (4.2.2.22) or (4.2.2.23) represent the angular momentum about the hook axis origin expressed in terms of rotational velocities. The three mass integrals in each of Eqs. (4.2.2.22) [or Eq. (4.2.2.23)] represent important physical properties of the store and are referred to as moments and products of inertia. The inertias represent a measure of the inertial resistance of the body to rotational motion and are the rotational analogy of the mass term in the linear equations of motion. The inertias represent the distribution of the mass within the body (in this case relative to the pivot point of rotation). The individual mass distribution integrals are:

Moments of Inertia $I_{xxIH} = \int (YIpH^2 + ZIpH^2) dm$ $I_{yyIH} = \int (XIpH^2 + ZIpH^2) dm$ $I_{zzIH} = \int (XIpH^2 + YIpH^2) dm$	Products of Inertia $I_{xyIH} = I_{yxIH} = \int XIpH * YIpH dm$ $I_{xzIH} = I_{zxIH} = \int XIpH * ZIpH dm$ $I_{yzIH} = I_{zyIH} = \int YIpH * ZIpH dm$
---	---

(4.2.2.24)

where the $\{XIpH\}$ vector denotes the inertial components of the position of each individual infinitesimal mass element "p" within the body relative to the hook-axis origin. The inertias can be expressed in matrix (or tensor) form as:

$$[I]_{IH} = \begin{bmatrix} I_{IH}(1,1) & I_{IH}(1,2) & I_{IH}(1,3) \\ I_{IH}(2,1) & I_{IH}(2,2) & I_{IH}(2,3) \\ I_{IH}(3,1) & I_{IH}(3,2) & I_{IH}(3,3) \end{bmatrix} = \begin{bmatrix} I_{xxIH} & -I_{xyIH} & -I_{xzIH} \\ -I_{yxIH} & I_{yyIH} & -I_{yzIH} \\ -I_{zxIH} & -I_{zyIH} & I_{zzIH} \end{bmatrix} \quad (4.2.2.25)$$

The inertias about the hook point are a derived term which change if the position of the pivot point relative to the body axis origin changes. It is desirable to derive the hook point inertias based on some transformation of inertias about the body axes because the body axis inertias can be considered to be a definable store mass property. Relationships between inertias about hook axes and about body axes can be determined by equating the integrals in Eq. (4.2.2.22) with the corresponding integrals in Eq. (4.2.2.23). For example:

$$\begin{aligned} I_{xxIH} &= \int [YIpH^2 + ZIpH^2] dm = \int [(YIpB + YIBH)^2 + (ZIpB + ZIBH)^2] dm \\ &= \int [YIpB^2 + 2*YIpB*YIBH + YIBH^2 + ZIpB^2 + 2*ZIpB*ZIBH + ZIBH^2] dm \end{aligned} \quad (4.2.2.26)$$

which can be simplified using the relations of Eq. (4.2.2.21) to:

$$\begin{aligned} I_{xxIH} &= \int [YIpB^2 + YIBH^2 + ZIpB^2 + ZIBH^2] dm \\ &= \int [YIpB^2 + ZIpB^2] dm + [YIBH^2 + ZIBH^2] dm \\ &= \int [YIpB^2 + ZIpB^2] dm + [YIBH^2 + ZIBH^2] *m \\ &= I_{xxIB} + [YIBH^2 + ZIBH^2] *m \end{aligned} \quad (4.2.2.27)$$

Similar inertia transfer equations can be developed for the other terms in the inertia tensor:

$$\begin{aligned} I_{xxIH} &= I_{xxIB} + m(YIBH^2 + ZIBH^2) \\ I_{yyIH} &= I_{yyIB} + m(XIBH^2 + ZIBH^2) \\ I_{zzIH} &= I_{zzIB} + m(XIBH^2 + YIBH^2) \\ I_{xyIH} &= I_{xyIB} + m(XIBH * YIBH) \\ I_{xzIH} &= I_{xzIB} + m(XIBH * ZIBH) \\ I_{yzIH} &= I_{yzIB} + m(YIBH * ZIBH) \end{aligned} \quad (4.2.2.28)$$

Collectively, Eqs. (4.2.2.28) are known as the "parallel-axis theorem" for inertia transfers (a consequence of the fact that the body and hook axes are parallel so that the $\{PIBI\}$ vector can be equated with the $\{PIHI\}$ vector).

Using the inertial tensor, the angular momentum equations [Eq. (4.2.2.22)] can be written in matrix form as:

$$\begin{aligned} \begin{vmatrix} HXIGH \\ HYIHI \\ HZIHI \end{vmatrix} &= [I]_{IH} \begin{vmatrix} PIBI \\ QIBI \\ RIBI \end{vmatrix} + \begin{vmatrix} WIHI*YIBH*m - VIHI*ZIBH*m \\ -WIHI*XIBH*m + UIHI*ZIBH*m \\ VIHI*XIBH*m - UIHI*YIBH*m \end{vmatrix} \\ &= [I]_{IH} \begin{vmatrix} PIBI \\ QIBI \\ RIBI \end{vmatrix} + m \begin{vmatrix} XIBH \\ YIBH \\ ZIBH \end{vmatrix} \times \begin{vmatrix} UIHI \\ VIHI \\ WIHI \end{vmatrix} \end{aligned} \quad (4.2.2.29)$$

or:

$$\begin{aligned} \begin{vmatrix} HXIGH \\ HYIHI \\ HZIHI \end{vmatrix} &= \begin{vmatrix} HXIHH \\ HYIHH \\ HZIHH \end{vmatrix} + m \begin{vmatrix} XIBH \\ YIBH \\ ZIBH \end{vmatrix} \times \begin{vmatrix} UIHI \\ VIHI \\ WIHI \end{vmatrix} \end{aligned} \quad (4.2.2.30)$$

where:

$$\begin{vmatrix} HXIHH \\ HYIHH \\ HZIHH \end{vmatrix} = [I]_{IH} \begin{vmatrix} PIBI \\ QIBI \\ RIBI \end{vmatrix} \quad (4.2.2.31)$$

The {HXIGH} vector in Eq. (4.2.2.29) represents the "absolute" angular momentum of the body relative to inertial axes. The {HXIHH} portion of the absolute vector represents the "relative" momentum with respect to the hook axes and represents the terms that would arise if the linear momentums of the point masses with respect to the hook point were used instead of linear momentums relative to inertial axes in the original expression for moments of linear momentum [Eq. (4.2.2.2)]. The cross product term in Eq. (4.2.2.30) represents the "correction" to the relative angular momentum to account for the hook point not being inertially fixed. The "relative" component of Eq. (4.2.2.30) is specifically identified because it will appear later in the actual implementation of the rotational equations.

Replacing the angular momentum defined in terms of cross products of linear velocities as developed in Eq.(4.2.2.13) with the angular momentum defined in terms of angular velocities as developed in Eq. (4.2.2.29), the rotational equations of motion for the body pivoting about the hook point can be written as:

$$\begin{aligned} \begin{vmatrix} \Sigma MXI \\ \Sigma MYI \\ \Sigma MZI \end{vmatrix} \text{ about } H &= \frac{d}{dt} \left\{ [I]_{IH} \begin{vmatrix} PIBI \\ QIBI \\ RIBI \end{vmatrix} + m \begin{vmatrix} XIBH \\ YIBH \\ ZIBH \end{vmatrix} \times \begin{vmatrix} UIHI \\ VIHI \\ WIHI \end{vmatrix} \right\} + \begin{vmatrix} UIHI \\ VIHI \\ WIHI \end{vmatrix} \times m \begin{vmatrix} UIBI \\ VIBI \\ WIBI \end{vmatrix} \end{aligned} \quad (4.2.2.32)$$

Equation (4.2.2.32) can be simplified by expanding out the {XIBH} vector and evaluating the derivative of the cross product term:

$$\begin{aligned}
\begin{vmatrix} \Sigma MXI \\ \Sigma MYI \\ \Sigma MZI \end{vmatrix}_{\text{about H}} &= \frac{d}{dt} \left\{ [I]_{IH} \begin{vmatrix} PIBI \\ QIBI \\ RIBI \end{vmatrix} \right\} + \frac{d}{dt} \left\{ m \left(\begin{vmatrix} XIBI \\ YIBI \\ ZIBI \end{vmatrix} - \begin{vmatrix} XIHI \\ YIHI \\ ZIHI \end{vmatrix} \right) \times \begin{vmatrix} UIHI \\ VIHI \\ WIHI \end{vmatrix} \right\} \\
&\quad + \begin{vmatrix} UIHI \\ VIHI \\ WIHI \end{vmatrix} \times m \begin{vmatrix} UIBI \\ VIBI \\ WIBI \end{vmatrix} \\
&= \frac{d}{dt} \left\{ [I]_{IH} \begin{vmatrix} PIBI \\ QIBI \\ RIBI \end{vmatrix} \right\} + \frac{d}{dt} \left\{ m \left(\begin{vmatrix} XIBI \\ YIBI \\ ZIBI \end{vmatrix} - \begin{vmatrix} XIHI \\ YIHI \\ ZIHI \end{vmatrix} \right) \right\} \times \begin{vmatrix} UIHI \\ VIHI \\ WIHI \end{vmatrix} \\
&\quad + m \begin{vmatrix} XIBH \\ YIBH \\ ZIBH \end{vmatrix} \times \frac{d}{dt} \begin{vmatrix} UIHI \\ VIHI \\ WIHI \end{vmatrix} + \begin{vmatrix} UIHI \\ VIHI \\ WIHI \end{vmatrix} \times m \begin{vmatrix} UIBI \\ VIBI \\ WIBI \end{vmatrix} \\
&= \frac{d}{dt} \left\{ [I]_{IH} \begin{vmatrix} PIBI \\ QIBI \\ RIBI \end{vmatrix} \right\} + m \left(\begin{vmatrix} UIBI \\ VIBI \\ WIBI \end{vmatrix} - \begin{vmatrix} UIHI \\ VIHI \\ WIHI \end{vmatrix} \right) \times \begin{vmatrix} UIHI \\ VIHI \\ WIHI \end{vmatrix} \quad (4.2.2.33) \\
&\quad + m \begin{vmatrix} XIBH \\ YIBH \\ ZIBH \end{vmatrix} \times \begin{vmatrix} AXIHI \\ AYIHI \\ AZIHI \end{vmatrix} + \begin{vmatrix} UIHI \\ VIHI \\ WIHI \end{vmatrix} \times m \begin{vmatrix} UIBI \\ VIBI \\ WIBI \end{vmatrix} \\
&= \frac{d}{dt} \left\{ [I]_{IH} \begin{vmatrix} PIBI \\ QIBI \\ RIBI \end{vmatrix} \right\} + m \begin{vmatrix} UIBI \\ VIBI \\ WIBI \end{vmatrix} \times \begin{vmatrix} UIHI \\ VIHI \\ WIHI \end{vmatrix} - m \begin{vmatrix} UIHI \\ VIHI \\ WIHI \end{vmatrix} \times \begin{vmatrix} UIHI \\ VIHI \\ WIHI \end{vmatrix} \\
&\quad + m \begin{vmatrix} XIBH \\ YIBH \\ ZIBH \end{vmatrix} \times \begin{vmatrix} AXIHI \\ AYIHI \\ AZIHI \end{vmatrix} + \begin{vmatrix} UIHI \\ VIHI \\ WIHI \end{vmatrix} \times m \begin{vmatrix} UIBI \\ VIBI \\ WIBI \end{vmatrix}
\end{aligned}$$

By vector identities; $\{A\} \times \{B\} = -\{B\} \times \{A\}$ and $\{A\} \times \{A\} = 0$, Eq. (4.2.2.33) reduces to:

$$\begin{aligned}
\begin{vmatrix} \Sigma MXI \\ \Sigma MYI \\ \Sigma MZI \end{vmatrix}_{\text{about H}} &= \frac{d}{dt} \left\{ [I]_{IH} \begin{vmatrix} PIBI \\ QIBI \\ RIBI \end{vmatrix} \right\} + m \begin{vmatrix} XIBH \\ YIBH \\ ZIBH \end{vmatrix} \times \begin{vmatrix} AXIHI \\ AYIHI \\ AZIHI \end{vmatrix} \quad (4.2.2.34)
\end{aligned}$$

which is the final inertial form of the rotational equations of motion about the hook point. Before proceeding with application of Eq. (4.2.2.34) to restricted rotational problems in body axis projection form, it should be noted that the unrestricted rotational equations which were earlier presented in Section 4.2.1 are obtained simply by setting the $\{XIBH\}$ vector to zero in Eqs. (4.2.2.34) and (4.2.2.28), which results in the expression previously presented as Eq. (4.2.1.22).

Equation (4.2.2.34) represents the full inertial form of the rotational equations of motion. In this form, however, the rotational equations are virtually unmanageable because at each time step of the trajectory, as the body and hook axes rotate relative to the inertial axes, the inertia integrals of Eq. (4.2.2.24) have to be re-evaluated. Implementation of the rotational equations is greatly simplified by projecting the terms in Eq. (4.2.2.34) into the fixed body or hook axis systems. In body-axis or hook-axis forms the inertia components for a rigid body (without time-dependent mass changes) are constants which need only be evaluated once per trajectory.

Normally measured or computed inertias about the store body axes defined according to the relations of Eq. (4.2.1.23) are provided for the simulation. In most cases, the body-axis inertias are constant inputs that are provided to the engineers responsible for motion simulations from the personnel responsible for determining store mass properties. Again, the caution mentioned in the previous section should be repeated - mass properties engineers often use a body-fixed axis system in which the XB and ZB axes are rotated so that they point in opposite directions from the axes normally used in motion simulations. In such cases, a sign change on the provided I_{xyBB} and I_{yzBB} terms must be accomplished before the values are used in the motion simulations. The motion simulation engineers must also transfer the inertias from the body-axis origin to the hook axis origin for implementation in the restricted rotational equations. The body axis coordinates of the inertias about the hook axis pivot point are obtained by applying the Parallel-Axis Theorem to the body-axis inertia components:

$$\begin{aligned} I_{xxBH} &= I_{xxBB} + m(YBBH^2 + ZBBH^2) \\ I_{yyBH} &= I_{yyBB} + m(XBBH^2 + ZBBH^2) \\ I_{zzBH} &= I_{zzBB} + m(XBBH^2 + YBBH^2) \\ I_{xyBH} &= I_{xyBB} + m(XBBH * YBBH) \\ I_{xzBH} &= I_{xzBB} + m(XBBH * ZBBH) \\ I_{yzBH} &= I_{yzBB} + m(YBBH * ZBBH) \end{aligned} \quad (4.2.2.35)$$

Projection relations for transforming inertial quantities to the body axis measurement directions were previously presented in Eqs. (4.2.1.24) through (4.2.1.26) and Eq. (4.2.1.30) for each of the terms in the inertial rotational equations. Analogous transformations are used to project each term in Eq. (4.2.2.34). After the substitutions, Eq. (4.2.2.34) can be written in terms of body-axis properties:

$$\begin{aligned} \begin{vmatrix} \Sigma MXI \\ \Sigma MYI \\ \Sigma MZI \end{vmatrix}_{\text{about } H} &= \frac{d}{dt} \left\{ [I]_{IH} \begin{vmatrix} PIBI \\ QIBI \\ RIBI \end{vmatrix} \right\} + m \begin{vmatrix} XIBH \\ YIBH \\ ZIBH \end{vmatrix} \times \begin{vmatrix} AXIHI \\ AYIHI \\ AZIHI \end{vmatrix} \\ &= [\text{TRNBI}]^{-1} \begin{vmatrix} \Sigma MXB \\ \Sigma MYB \\ \Sigma MZB \end{vmatrix}_{\text{about } H} = \frac{d}{dt} \left\{ [\text{TRNBI}]^{-1} [I]_{BH} [\text{TRNBI}] [\text{TRNBI}]^{-1} \begin{vmatrix} PBBI \\ QBBI \\ RBBI \end{vmatrix} \right\} \\ &\quad + m [\text{TRNBI}]^{-1} \begin{vmatrix} XBBH \\ YBBH \\ ZBBH \end{vmatrix} \times [\text{TRNBI}]^{-1} \begin{vmatrix} AXBHI \\ AYBHI \\ AZBHI \end{vmatrix} \\ &= \frac{d}{dt} [\text{TRNBI}]^{-1} [I]_{BH} \begin{vmatrix} PBBI \\ QBBI \\ RBBI \end{vmatrix} + m [\text{TRNBI}]^{-1} \left(\begin{vmatrix} XBBH \\ YBBH \\ ZBBH \end{vmatrix} \times \begin{vmatrix} AXBHI \\ AYBHI \\ AZBHI \end{vmatrix} \right) \end{aligned} \quad (4.2.2.36)$$

Note that Eq. (4.2.2.36) is still a fundamentally inertial relationship [like Eq. (4.2.2.34)], but it is now expressed in terms of projected body-axis state variables. Evaluating the derivative in Eq. (4.2.2.36) by the chain rule:

$$\begin{aligned}
 [\text{TRNBI}]^{-1} \begin{vmatrix} \Sigma MXB \\ \Sigma MYB \\ \Sigma MZB \end{vmatrix}_{\text{about H}} &= [\text{TRNBI}]^{-1} [\tilde{\omega} \text{ BBI}] [\text{I}]_{BH} \begin{vmatrix} \text{PBBI} \\ \text{QBBI} \\ \text{RBBI} \end{vmatrix} \\
 &+ [\text{TRNBI}]^{-1} \frac{d}{dt} [\text{I}]_{BH} \begin{vmatrix} \text{PBBI} \\ \text{QBBI} \\ \text{RBBI} \end{vmatrix} + [\text{TRNBI}]^{-1} [\text{I}]_{BH} \begin{vmatrix} \text{DPBBI} \\ \text{DQBBI} \\ \text{DRBBI} \end{vmatrix} \quad (4.2.2.37) \\
 &+ m [\text{TRNBI}]^{-1} \left(\begin{vmatrix} \text{XBBH} \\ \text{YBBH} \\ \text{ZBBH} \end{vmatrix} \times \begin{vmatrix} \text{AXBHI} \\ \text{AYBHI} \\ \text{AZBHI} \end{vmatrix} \right)
 \end{aligned}$$

Multiplying through by $[\text{TRNBI}]$ and deleting the inertia derivative term:

$$\begin{aligned}
 \begin{vmatrix} \Sigma MXB \\ \Sigma MYB \\ \Sigma MZB \end{vmatrix}_{\text{about H}} &= [\tilde{\omega} \text{ BBI}] [\text{I}]_{BH} \begin{vmatrix} \text{PBBI} \\ \text{QBBI} \\ \text{RBBI} \end{vmatrix} + [\text{I}]_{BH} \begin{vmatrix} \text{DPBBI} \\ \text{DQBBI} \\ \text{DRBBI} \end{vmatrix} \quad (4.2.2.38) \\
 &+ m \begin{vmatrix} \text{XBBH} \\ \text{YBBH} \\ \text{ZBBH} \end{vmatrix} \times \begin{vmatrix} \text{AXBHI} \\ \text{AYBHI} \\ \text{AZBHI} \end{vmatrix}
 \end{aligned}$$

Part of the first term in Eq. (4.2.2.38) can be recognized as the body axis projections of the relative momentum from Eq. (4.2.2.31):

$$\begin{vmatrix} \text{HXBHH} \\ \text{HYBHH} \\ \text{HZBHH} \end{vmatrix} = [\text{I}]_{BH} \begin{vmatrix} \text{PBBI} \\ \text{QBBI} \\ \text{RBBI} \end{vmatrix} \quad (4.2.2.39)$$

so that:

$$\begin{vmatrix} \Sigma MXB \\ \Sigma MYB \\ \Sigma MZB \end{vmatrix}_{\text{about H}} = [\tilde{\omega} \text{ BBI}] \begin{vmatrix} \text{HXBHH} \\ \text{HYBHH} \\ \text{HZBHH} \end{vmatrix} + [\text{I}]_{BH} \begin{vmatrix} \text{DPBBI} \\ \text{DQBBI} \\ \text{DRBBI} \end{vmatrix} + m \begin{vmatrix} \text{XBBH} \\ \text{YBBH} \\ \text{ZBBH} \end{vmatrix} \times \begin{vmatrix} \text{AXBHI} \\ \text{AYBHI} \\ \text{AZBHI} \end{vmatrix} \quad (4.2.2.40)$$

The sum of the moments about the hook point are:

$$\begin{aligned}
 \begin{vmatrix} \Sigma MXB \\ \Sigma MYB \\ \Sigma MZB \end{vmatrix}_{\text{about H}} &= \begin{vmatrix} \text{MXB} \\ \text{MYB} \\ \text{MZB} \end{vmatrix}_{\text{about B}} + \begin{vmatrix} \text{XBBH} \\ \text{YBBH} \\ \text{ZBBH} \end{vmatrix} \times \begin{vmatrix} \text{FXB} \\ \text{FYB} \\ \text{FZB} \end{vmatrix} + \begin{vmatrix} \text{RLB} \\ \text{RMB} \\ \text{RNB} \end{vmatrix} \quad (4.2.2.41) \\
 &= \begin{vmatrix} \text{MXB} \\ \text{MYB} \\ \text{MZB} \end{vmatrix}_{\text{about B}} + \begin{vmatrix} \text{YBBH*FZB} - \text{ZBBH*FYB} \\ \text{ZBBH*FXB} - \text{XBBH*FZB} \\ \text{XBBH*FYB} - \text{YBBH*FXB} \end{vmatrix} + \begin{vmatrix} \text{RLB} \\ \text{RMB} \\ \text{RNB} \end{vmatrix}
 \end{aligned}$$

Inserting Eqs. (4.2.2.41) into Eq. (4.2.2.40) and solving for {DPBBI}:

$$\begin{vmatrix} DPBBI \\ DQBBI \\ DRBBI \end{vmatrix} = [I]_{BH}^{-1} \left\{ -[\tilde{\omega} BBI] \begin{vmatrix} HXBHH \\ HYBHH \\ HZBHH \end{vmatrix} + \begin{vmatrix} MXB \\ MYB \\ MZB \end{vmatrix} \text{ about B} + \begin{vmatrix} XBBH \\ YBBH \\ ZBBH \end{vmatrix} \times \begin{vmatrix} FXB \\ FYB \\ FZB \end{vmatrix} \right. \\ \left. + \begin{vmatrix} RLB \\ RMB \\ RNB \end{vmatrix} - m \begin{vmatrix} XBBH \\ YBBH \\ ZBBH \end{vmatrix} \times \begin{vmatrix} AXBHI \\ AYBHI \\ AZBHI \end{vmatrix} \right\} \quad (4.2.2.42)$$

Equation (4.2.2.42) represents the form of the restricted rotational equations used in AEDC wind tunnel and off-line simulations. The projected angular velocity derivatives are computed from the measured forces and moments and the calculated reaction moments (Section 4.3) and integrated numerically to determine body-axis angular velocities at the next point in the trajectory. Angular orientations are determined the same way as they are determined for free-fall simulations and will be discussed in the next section.

The key to restricted rotational simulations is the development of constraint equations to determine the reaction moment vector, {RXB} as a function of time, for Eq. (4.2.2.42) which causes the desired motion. Equation (4.2.2.42) can be solved only if the reaction moments are determined beforehand or if a system of equations coupling both Eq. (4.2.2.42) and the necessary constraint equations is solved simultaneously. Unfortunately, as will be shown in Section 4.3, the development of the constraint equations can be extremely complicated [more so even than the derivation of Eq. (4.2.2.42)].

Because of the complexity of the constraint equations and because the corresponding systems of simultaneous equations can be ill-posed or ill-conditioned, it is important that internal consistency checks be implemented to ensure a reasonable simulation has been obtained. An easy and important check as to whether the constraint equations and rotational equations have been properly implemented is to simply take the results of the constrained solution (the calculated reaction forces and moments along with the {DPBBI} vector) and see if the angular velocity derivatives can be reproduced using the unconstrained rotational equations. The approach is to extend the unconstrained rotational equations [Eqs. (4.2.1.38)] to include the reaction moments and forces at the pivot point in the summation of the moments about the body-axis origin point:

$$[I]_{BB} \begin{vmatrix} DPBBI \\ DQBBI \\ DRBBI \end{vmatrix} = -[\tilde{\omega} BBI] \begin{vmatrix} HXBBI \\ HYBBI \\ HZBBI \end{vmatrix} + \begin{vmatrix} MXB \\ MYB \\ MZB \end{vmatrix} \text{ about B} + \begin{vmatrix} RLB \\ RMB \\ RNB \end{vmatrix} - \begin{vmatrix} XBBH \\ YBBH \\ ZBBH \end{vmatrix} \times \begin{vmatrix} RXB \\ RYB \\ RZB \end{vmatrix} \quad (4.2.2.43)$$

where {RLB, RMB, RNB} is the reaction moment vector determined from the constrained rotational equations in conjunction with Eq. (4.2.2.42) and {RXB, RYB, RZB} is the reaction force vector determined from Eq. (4.1.2.9). Given the reaction force and moment vectors from the constrained rotational equations, the {DPBBI} vector computed from Eq. (4.2.2.43) should be

identical to the vector originally determined by Eq. (4.2.2.42) (within numerical accuracy). Generally speaking, the difference between the {DPBBI} vector magnitude as computed by Eqs. (4.2.2.42) and (4.2.2.43) should be less than 0.05 percent - larger differences may be indicative of improperly posed constraint conditions. The importance of internal consistency checks of this nature is stressed because of the complexity of constraint modeling which will be discussed in Section 4.3.

4.2.3 Angular Orientations and Their Derivatives

The angular orientation of one coordinate system relative to another is a surprisingly complicated property which is difficult to define numerically. In fact, whole fields of advanced mathematics (some involving complex matrices and "three-dimensional" complex numbers) have been developed just to quantify the orientation problem. Some indication of the fundamental complexity of the property of orientation in comparison to most of the other physical motion properties can be obtained just by noting that angular orientation cannot be represented by a three-element vector of orthogonal components (as can linear positions or angular and linear velocities and accelerations). This fact can be illustrated by noting how orientations have been modeled thus far in the current document. Orientation has been represented in previous sections using 3 by 3 transformation matrices (which may be considered to be "three" related vectors) and by three sequential rotation angles (which have been shown to be non-orthogonal because yaw-pitch-roll sequences produce different orientations from pitch-yaw-roll sequences). It has also been demonstrated in previous sections that velocity vectors can be obtained by integrating acceleration vectors and that linear position vectors can be obtained by integrating velocity vectors. It is not possible, however, to integrate the angular velocity vector to get an angular orientation vector because there is no such thing as an angular orientation vector. The fundamental issues addressed in this section, then, involve how angular orientations are expressed in a numerical simulation and how orientations are updated in time in a numerical simulation.

The discussion of rotational orientation parameters begins with an analysis based on the fundamental principles of calculus of what is meant by the "derivative" of a rotating vector. The equivalence between the 3 by 3 transformation matrix form for specifying orientation as developed previously in Section 1.4 and the "direction cosine" approach to defining orientations is then developed in Section 4.2.3.2. The formulas for the derivatives of the transformation matrices [which were earlier presented without proof in Eqs. (1.4.5) and (1.4.6)] will then be derived in Section 4.2.3.3. The formulas for the derivatives of the three sequential modified Euler rotation angles are presented in Section 4.2.3.4. Finally, the four-parameter forms for defining orientations and their derivatives are developed in Section 4.2.3.5.

4.2.3.1 Derivatives of Rotating Vectors

It is, perhaps, most instructive to study the derivatives of angular orientation terms by first developing a more fundamental study of just what is meant by the "derivative" of a vector - especially when it is measured in a rotating reference frame. Most of the following vector-derivative discussion is adapted from Ref. 3.

Vectors have both magnitude and direction and, therefore, the time rate of change of a vector must include both a change in magnitude component and a change in direction component. The major difficulty arises when the reference coordinate system relative to which the direction of the vector is defined is itself rotating so that the directions of the reference axes are also varying with time. If $\{x\}$ is an arbitrary vector which varies in time, then, when drawn at successive times, the tip of the vector traces out a space curve sometimes referred to as a "hodograph" as shown in Fig. 13. In store separation, for example, the hodograph of the $\{\text{XIBI}\}$ vector represents the path of the center of gravity of the store during the trajectory - the so-called "locus of the cg." The time derivative of the vector is obtained from the Fundamental Theorem of Calculus:

$$\frac{d\{\bar{x}\}}{dt} = \lim_{\Delta t \rightarrow 0} \frac{\{\bar{x}(t + \Delta t)\} - \{\bar{x}(t)\}}{\Delta t} \lim_{\Delta t \rightarrow 0} \frac{\{\Delta \bar{x}\}}{\Delta t} \quad (4.2.3.1.1)$$

Thus, the derivative of the vector is simply the velocity of its endpoint along the hodograph as illustrated in Fig 13. Now suppose that the components of a kinematic vector such as $\{\text{XIBI}\}$ are measured relative to an inertially fixed system so that:

$$\{\text{XIBI}\} = \bar{i}_I \text{ XIBI} + \bar{j}_I \text{ YIBI} + \bar{k}_I \text{ ZIBI} \quad (4.2.3.1.2)$$

The special nomenclature has been temporarily extended in Eq. (4.2.3.1.2) to include unit vectors for the directions of the measurement axes where \bar{i}_I , \bar{j}_I , and \bar{k}_I are unit vectors in the inertial X, Y, and Z directions, respective

$$\begin{aligned} \frac{d\{\text{XIBI}\}}{dt} &= \{\text{UIBI}\} = \frac{d(\bar{i}_I \text{ XIBI} + \bar{j}_I \text{ YIBI} + \bar{k}_I \text{ ZIBI})}{dt} \\ &= \bar{i}_I \frac{d\text{XIBI}}{dt} + \bar{j}_I \frac{d\text{YIBI}}{dt} + \text{XIBI} \frac{d\bar{i}_I}{dt} + \text{YIBI} \frac{d\bar{j}_I}{dt} + \text{ZIBI} \frac{d\bar{k}_I}{dt} \end{aligned} \quad (4.2.3.1.3)$$

The first three terms on the right of Eq. (4.2.3.1.3) represent the change in magnitude of the vector relative to the measurement system whereas the last three terms on the right represent the change in direction of the measurement system. (In this case the measurement system is the inertial system). Because the inertial axis system is (by definition) non-rotating, the inertial unit vectors do not change direction with time and Eq. (4.2.3.1.3) reduces to:

$$\{\text{UIBI}\} \bar{i} \frac{d\text{XIBI}}{dt} + \bar{j} \frac{d\text{YIBI}}{dt} + \bar{k} \frac{d\text{ZIBI}}{dt} \quad (4.2.3.14)$$

It is helpful to note that the unit vectors in Eq. (4.2.3.1.3) must also obey Eq. (4.2.3.1.1) - the tip of each inertial unit vector does not move in space and, therefore, the endpoint of the inertial vector marks only a single degenerate point in space rather than a full hodograph curve and the velocities along the hodographs are zero.

Now consider what happens when the measurement directions are not inertially fixed but are, instead, rotating relative to the inertial system. A position vector expressed in terms of com-

ponents measured in an axis system fixed within the rotating body, for instance, may be represented in the expanded nomenclature as:

$$\{XBBI\} = \dot{i}_B X BBI + \dot{j}_B Y BBI + \dot{k}_B Z BBI \quad (4.2.3.1.5)$$

with \dot{i}_B , \dot{j}_B , and \dot{k}_B being unit vectors in the body axis directions. The derivative can again be written using the chain rule:

$$\begin{aligned} \{UBBI\} &= \frac{d\dot{i}_B X BBI + \dot{j}_B Y BBI + \dot{k}_B Z BBI}{dt} \\ &= \dot{i}_B \frac{dX BBI}{dt} + \dot{j}_B \frac{dY BBI}{dt} + \dot{k}_B \frac{dZ BBI}{dt} + X BBI \frac{d\dot{i}_B}{dt} + Y BBI \frac{d\dot{j}_B}{dt} + Z BBI \frac{d\dot{k}_B}{dt} \end{aligned} \quad (4.2.3.1.6)$$

The first three terms to the right of the equality in Eq. (4.2.3.1.6) again represent the change in magnitude of the vector relative to the measurement system (which is the body axis system in this case) and the last three terms on the right represent the change in direction of the measurement system. Unlike the inertial component case, however, the derivatives of the body axis unit vectors are not zero, i.e., the body measurement system is changing direction. Figure 14 illustrates a body with a body-fixed axis system rotating with an angular velocity $\bar{\omega}$ about an axis through the body. The vector velocities for the body-fixed unit vectors are also illustrated. Recalling that the derivative of a vector is the velocity of its tip along the hodograph, it can be seen that the hodographs of the \dot{i}_B , \dot{j}_B , and \dot{k}_B unit vectors are circles centered on the rotation axis. (The hodograph of the \dot{i}_B vector is illustrated in Fig. 14). From simple geometry considerations the linear velocity of the tip of each inertial unit vector is simply the cross product of the rotational velocity vector with that unit vector:

$$\frac{d\dot{i}_B}{dt} = \{\bar{\omega} BBI\} X \dot{i}_B ; \quad \frac{d\dot{j}_B}{dt} = \{\bar{\omega} BBI\} X \dot{j}_B ; \quad \frac{d\dot{k}_B}{dt} = \{\bar{\omega} BBI\} X \dot{k}_B \quad (4.2.3.1.7)$$

Substituting Eqs. (4.2.3.1.7) into (4.2.3.1.6):

$$\begin{aligned} \{UBBI\} &= \dot{i}_B \frac{dX BBI}{dt} + \dot{j}_B \frac{dY BBI}{dt} + \dot{k}_B \frac{dZ BBI}{dt} \\ &\quad + X BBI \{\bar{\omega} BBI\} X \dot{i}_B + Y BBI \{\bar{\omega} BBI\} X \dot{j}_B + Z BBI \{\bar{\omega} BBI\} X \dot{k}_B \\ &= \dot{i}_B \frac{dX BBI}{dt} + \dot{j}_B \frac{dY BBI}{dt} + \dot{k}_B \frac{dZ BBI}{dt} \\ &\quad + (\bar{\omega} BBI X X BBI) \dot{i}_B + (\bar{\omega} BBI X Y BBI) \dot{j}_B + (\bar{\omega} BBI X Z BBI) \dot{k}_B \end{aligned} \quad (4.2.3.1.8)$$

or (in full vector form without using the expanded unit vectors):

$$\begin{vmatrix} \text{UBBI} \\ \text{VBBI} \\ \text{WBBI} \end{vmatrix} = \begin{vmatrix} \text{PBBI} \\ \text{QBBI} \\ \text{RBBI} \end{vmatrix} \times \begin{vmatrix} \text{XBBI} \\ \text{YBBI} \\ \text{ZBBI} \end{vmatrix} + \begin{vmatrix} \text{DXBBI} \\ \text{DYBBI} \\ \text{DZBBI} \end{vmatrix} \quad (4.2.3.1.9)$$

Equation (4.2.3.1.9) was previously developed as Eq. (1.4.8) using the formulas for derivatives of transformation matrices.

Equations such as Eq. (4.2.3.1.9) are often written in "substantial" derivative form in which the rotating frame components of the absolute derivative of a vector are represented by a combination of the direct derivative of the terms which were measured within the rotating frame coupled with the vector cross-product of the rotational velocity vector with the rotating terms.

$$\begin{aligned} \delta\{\text{vector}\} &= \frac{d}{dt}\{\text{vector components in rotating frame}\} \\ &+ \bar{\omega} \times \{\text{vector components in rotating frame}\} \end{aligned} \quad (4.2.3.1.10)$$

where the δ operator denotes the rotating frame components of the absolute derivative of a rotating frame vector. The Eq. (4.2.3.1.10) form of vector differentiation is often referred to as the "Theorem of Coriolis" in honor of a French military engineer who served with Napoleon and who noted that Napoleon's long-range cannons were missing their targets because the " $\bar{\omega} \times$ " components associated with the rotational velocity of the earth had not been included in the cannon range calculations.

Substantial derivatives have been avoided in the current document because it is often difficult to determine which portions of the original vector should be included in the rotating cross product portion of a substantial derivative (and what sign should be used) and the mathematics fall out directly as a result of the chain rule when the equations are written using the skew-symmetric matrix derivative formulas (which will be more fully developed in Section 4.2.3.3). Indeed, the author has noted several instances in published literature where motion equations have been incorrectly derived because terms measured relative to inertial axes had been inadvertently included in the rotational cross-product portion of a substantial derivative. One of the prime advantages of the current nomenclature is that such errors are easily noted and avoided because the "names" of the terms do not match up in the nomenclature system. Before presenting the actual formal derivation of the skew-symmetric formulas for the derivatives of transformation matrices, some additional background information showing the equivalence of the rotational transformation matrix form for specifying angular orientation with the direction cosine matrix form will be demonstrated in the next section.

4.2.3.2 Direction Cosines and Redundancy

The 3 by 3 rotational transformation matrices resulting from three sequential rotations of a body have already been developed in Section 1.3. A completely unrelated approach for specifying orientation matrices based on the components of pre-rotation and post-rotation unit vectors will be developed in this section. It will be shown that the resultant 3 by 3 matrices from this sec-

ond approach are identical to the matrices formed by the sequential rotations, but an increased understanding of the meaning of the 3 by 3 transformation can be gained because of the alternate point of view. Again, the rotational matrix describing the orientation of body axes relative to inertial axes will be used as an example.

Using rotational projection matrices, it has already been demonstrated that the body axis unit vectors can be interpreted as the projection of the inertial axis unit vectors into the body directions:

$$\begin{vmatrix} \bar{i}_B \\ \bar{j}_B \\ \bar{k}_B \end{vmatrix} = [\text{TRNBI}] \begin{vmatrix} \bar{i}_I \\ \bar{j}_I \\ \bar{k}_I \end{vmatrix} \quad (4.2.3.2.1)$$

It is also possible to mathematically write the projection of one vector onto another using the dot or inner product of the two vectors. The dot product is defined as the product of the magnitude of the two vectors with the cosine of the angle between them:

$$(\{\bar{A}\} \bullet \{\bar{B}\}) = (\text{mag } A) (\text{mag } B) \cos(\text{angle}(\bar{A}, \bar{B})) \quad (4.2.3.2.2)$$

Note that the dot product is a scalar and not a vector. Using dot products, Eq. (4.2.3.2.1) can be rewritten as:

$$\begin{vmatrix} \bar{i}_B \\ \bar{j}_B \\ \bar{k}_B \end{vmatrix} = \begin{vmatrix} (\bar{i}_B \bullet \bar{i}_I) \bar{i}_I + (\bar{i}_B \bullet \bar{j}_I) \bar{j}_I + (\bar{i}_B \bullet \bar{k}_I) \bar{k}_I \\ (\bar{j}_B \bullet \bar{i}_I) \bar{i}_I + (\bar{j}_B \bullet \bar{j}_I) \bar{j}_I + (\bar{j}_B \bullet \bar{k}_I) \bar{k}_I \\ (\bar{k}_B \bullet \bar{i}_I) \bar{i}_I + (\bar{k}_B \bullet \bar{j}_I) \bar{j}_I + (\bar{k}_B \bullet \bar{k}_I) \bar{k}_I \end{vmatrix} = \begin{bmatrix} (\bar{i}_B \bullet \bar{i}_I) & (\bar{i}_B \bullet \bar{j}_I) & (\bar{i}_B \bullet \bar{k}_I) \\ (\bar{j}_B \bullet \bar{i}_I) & (\bar{j}_B \bullet \bar{j}_I) & (\bar{j}_B \bullet \bar{k}_I) \\ (\bar{k}_B \bullet \bar{i}_I) & (\bar{k}_B \bullet \bar{j}_I) & (\bar{k}_B \bullet \bar{k}_I) \end{bmatrix} \begin{vmatrix} \bar{i}_I \\ \bar{j}_I \\ \bar{k}_I \end{vmatrix} \quad (4.2.3.2.3)$$

Because the unit vectors each have unit magnitude, each dot product [according to Eq. (4.2.3.2.2)] is simply the cosine of the angle between the respective unit vectors (hence the terminology of direction "cosine" matrices):

$$\begin{aligned} \begin{vmatrix} \bar{i}_B \\ \bar{j}_B \\ \bar{k}_B \end{vmatrix} &= \begin{bmatrix} \cos(\text{angle}(\bar{i}_B, \bar{i}_I)) & \cos(\text{angle}(\bar{i}_B, \bar{j}_I)) & \cos(\text{angle}(\bar{i}_B, \bar{k}_I)) \\ \cos(\text{angle}(\bar{j}_B, \bar{i}_I)) & \cos(\text{angle}(\bar{j}_B, \bar{j}_I)) & \cos(\text{angle}(\bar{j}_B, \bar{k}_I)) \\ \cos(\text{angle}(\bar{k}_B, \bar{i}_I)) & \cos(\text{angle}(\bar{k}_B, \bar{j}_I)) & \cos(\text{angle}(\bar{k}_B, \bar{k}_I)) \end{bmatrix} \begin{vmatrix} \bar{i}_I \\ \bar{j}_I \\ \bar{k}_I \end{vmatrix} \\ &= \begin{bmatrix} \text{TRNBI}(1,1) & \text{TRNBI}(1,2) & \text{TRNBI}(1,3) \\ \text{TRNBI}(2,1) & \text{TRNBI}(2,2) & \text{TRNBI}(2,3) \\ \text{TRNBI}(3,1) & \text{TRNBI}(3,2) & \text{TRNBI}(3,3) \end{bmatrix} \begin{vmatrix} \bar{i}_I \\ \bar{j}_I \\ \bar{k}_I \end{vmatrix} \end{aligned} \quad (4.2.3.2.4)$$

If a shorthand system is used to assign numbers 1, 2, and 3 to the unit vector directions \bar{i} , \bar{j} , and \bar{k} , the first subscript of each element in TRNBI represents a body-axis vector direction, the second subscript represents an inertial axis direction, and each of the nine elements represents the cosine of the angle between the two specified directions. For example, the term TRNBI(3,1) represents the cosine of the angle between the body-axis z direction and the inertial axis x direction.

The property of rotation matrices presented earlier in Section 1.3 that the matrix inverse is identical to its transpose can now be vividly demonstrated. The direction cosine matrix for inertial axes relative to body axes is:

$$\begin{vmatrix} \bar{i}_I \\ \bar{j}_I \\ \bar{k}_I \end{vmatrix} = \begin{bmatrix} \cos(\text{angle}(\bar{i}_I, \bar{i}_B)) & \cos(\text{angle}(\bar{i}_I, \bar{j}_B)) & \cos(\text{angle}(\bar{i}_I, \bar{k}_B)) \\ \cos(\text{angle}(\bar{j}_I, \bar{i}_B)) & \cos(\text{angle}(\bar{j}_I, \bar{j}_B)) & \cos(\text{angle}(\bar{j}_I, \bar{k}_B)) \\ \cos(\text{angle}(\bar{k}_I, \bar{i}_B)) & \cos(\text{angle}(\bar{k}_I, \bar{j}_B)) & \cos(\text{angle}(\bar{k}_I, \bar{k}_B)) \end{bmatrix} \begin{vmatrix} \bar{i}_B \\ \bar{j}_B \\ \bar{k}_B \end{vmatrix}$$

$$= [\text{TRNIB}] \begin{vmatrix} \bar{i}_B \\ \bar{j}_B \\ \bar{k}_B \end{vmatrix} \quad (4.2.3.2.5)$$

Noting that the cosines of the angles between the body and inertial unit vectors are identical to the cosines of the angles between inertial and body vectors and comparing the terms in the matrix of Eq. (4.2.3.2.4) with those in Eq. (4.2.3.2.5) discloses that:

$$\text{TRNIB} = \text{TRNBI}^{-1} = \text{TRNBIT} \quad (4.2.3.2.6)$$

Before leaving the subject of the direction cosine matrix, the issue of redundancy must be addressed. It has already been noted that the nine elements of the direction cosine transformation matrix can be determined from three sequential modified Euler angles. It follows, therefore, that rotation must be basically a "three-parameter" property and at least six of the nine terms in the transformation matrix must (in some manner) be redundant. Generally, three different formulations of equations can be developed to define the redundancies, and (because of the different needs of different simulation applications) all three forms will be presented here. The first set of redundancy equations is based on the orthogonality condition that the sums of the squares of the elements in each row or column of a rotation matrix must add up to unity:

$$\begin{aligned} \text{TRNBI}(m,1)^2 + \text{TRNBI}(m,2)^2 + \text{TRNBI}(m,3)^2 &= 1 \\ \text{TRNBI}(1,n)^2 + \text{TRNBI}(2,n)^2 + \text{TRNBI}(3,n)^2 &= 1 \end{aligned} \quad (4.2.3.2.7)$$

where m and n are the row and column counters, respectively, of the rotation matrix. The second set of redundancy equations can be developed from the requirement that the matrix inverse is equal to the matrix transpose. Writing:

$$[\text{TRNBI}] [\text{TRNBI}]^{-1} = [\text{TRNBI}] [\text{TRNBI}]^T = [1] \quad (4.2.3.2.8)$$

where [1] is the identity matrix:

$$\begin{bmatrix} \text{TRNBI}(1,1) & \text{TRNBI}(1,2) & \text{TRNBI}(1,3) \\ \text{TRNBI}(2,1) & \text{TRNBI}(2,2) & \text{TRNBI}(2,3) \\ \text{TRNBI}(3,1) & \text{TRNBI}(3,2) & \text{TRNBI}(3,3) \end{bmatrix} \begin{bmatrix} \text{TRNBI}(1,1) & \text{TRNBI}(2,1) & \text{TRNBI}(3,1) \\ \text{TRNBI}(1,2) & \text{TRNBI}(2,2) & \text{TRNBI}(3,2) \\ \text{TRNBI}(1,3) & \text{TRNBI}(2,3) & \text{TRNBI}(3,3) \end{bmatrix}$$

$$= \begin{bmatrix} 1 & 0 & 0 \\ 0 & 1 & 0 \\ 0 & 0 & 1 \end{bmatrix} \quad (4.2.3.2.9)$$

Multiplication of the m^{th} row of [TRNBI] with the n^{th} column of $[\text{TRNBI}]^T$ where $m = n$ results in three redundancy conditions:

$$\begin{aligned} \text{TRNBI}(1,1)^2 + \text{TRNBI}(1,2)^2 + \text{TRNBI}(1,3)^2 &= 1 \\ \text{TRNBI}(2,1)^2 + \text{TRNBI}(2,2)^2 + \text{TRNBI}(2,3)^2 &= 1 \\ \text{TRNBI}(3,1)^2 + \text{TRNBI}(3,2)^2 + \text{TRNBI}(3,3)^2 &= 1 \end{aligned} \quad (4.2.3.2.10)$$

Multiplication of the m^{th} row of [TRNBI] with the n^{th} column of $[\text{TRNBI}]^T$ (or the n^{th} row times the m^{th} column) where m is not equal to n results in three more redundancy conditions:

$$\begin{aligned} \text{TRNBI}(1,1)*\text{TRNBI}(2,1) + \text{TRNBI}(1,2)*\text{TRNBI}(2,2) + \text{TRNBI}(1,3)*\text{TRNBI}(2,3) &= 0 \\ \text{TRNBI}(1,1)*\text{TRNBI}(3,1) + \text{TRNBI}(1,2)*\text{TRNBI}(3,2) + \text{TRNBI}(1,3)*\text{TRNBI}(3,3) &= 0 \\ \text{TRNBI}(2,1)*\text{TRNBI}(3,1) + \text{TRNBI}(2,2)*\text{TRNBI}(3,2) + \text{TRNBI}(2,3)*\text{TRNBI}(3,3) &= 0 \end{aligned} \quad (4.2.3.2.11)$$

This gives six redundancy relations among the nine elements of the direction cosine matrix. An alternate form of the same six redundancy relations can be derived by exchanging the order of the matrix multiplication in Eq. (4.2.3.2.8) to the form:

$$[\text{TRNBI}]^{-1} [\text{TRNBI}] = [\text{TRNBI}]^T [\text{TRNBI}] = [1] \quad (4.2.3.2.12)$$

which results in the following six equivalent relations:

$$\begin{aligned} \text{TRNBI}(1,1)^2 + \text{TRNBI}(2,1)^2 + \text{TRNBI}(3,1)^2 &= 1 \\ \text{TRNBI}(1,2)^2 + \text{TRNBI}(2,2)^2 + \text{TRNBI}(3,2)^2 &= 1 \\ \text{TRNBI}(1,3)^2 + \text{TRNBI}(2,3)^2 + \text{TRNBI}(3,3)^2 &= 1 \\ \text{TRNBI}(1,1)*\text{TRNBI}(1,2) + \text{TRNBI}(2,1)*\text{TRNBI}(2,2) + \text{TRNBI}(3,1)*\text{TRNBI}(3,2) &= 0 \\ \text{TRNBI}(1,1)*\text{TRNBI}(1,3) + \text{TRNBI}(2,1)*\text{TRNBI}(2,3) + \text{TRNBI}(3,1)*\text{TRNBI}(3,3) &= 0 \\ \text{TRNBI}(1,2)*\text{TRNBI}(1,3) + \text{TRNBI}(2,2)*\text{TRNBI}(2,3) + \text{TRNBI}(3,2)*\text{TRNBI}(3,3) &= 0 \end{aligned} \quad (4.2.3.2.13)$$

The twelve redundancy expressions of Eqs. (4.2.3.2.10) through (4.2.3.2.13) can also be developed using an alternate derivation. First, the \bar{i} , \bar{j} , and \bar{k} unit vectors must be orthogonal to one another in both the body and inertial systems. This orthogonality can be expressed in terms of dot products as:

$$\begin{array}{llll} \bar{i}_I \bullet \bar{i}_I = 1 & \bar{i}_I \bullet \bar{j}_I = 0 & \bar{i}_B \bullet \bar{i}_B = 1 & \bar{i}_B \bullet \bar{j}_B = 0 \\ \bar{j}_I \bullet \bar{j}_I = 1 & \bar{j}_I \bullet \bar{i}_I = 0 & \bar{j}_B \bullet \bar{j}_B = 1 & \bar{j}_B \bullet \bar{i}_B = 0 \\ \bar{k}_I \bullet \bar{k}_I = 1 & \bar{k}_I \bullet \bar{i}_I = 0 & \bar{k}_B \bullet \bar{k}_B = 1 & \bar{k}_B \bullet \bar{i}_B = 0 \end{array} \quad (4.2.3.2.14)$$

If the relations of Eq. (4.2.3.2.4) are used to expand out the six inertial dot products in the first two columns of Eq. (4.2.3.2.14) in terms of body-axis unit vectors and the six body dot products in the remaining two columns in terms of inertial-axis unit vectors, the twelve redundancy relations of Eqs. (4.2.3.2.10) through (4.2.3.2.13) result. The third set of redundancy equations also arises from the fact that the three unit vectors must be orthogonal to one another. For this formula-

lation, however, that orthogonality is expressed in terms of the cross-product relations between the inertial and body unit vectors:

$$\begin{aligned} \bar{i}_I \times \bar{j}_I &= \bar{k}_I \\ \bar{i}_B \times \bar{j}_B &= \bar{k}_B \\ \bar{j}_I \times \bar{k}_I &= \bar{i}_I \\ \bar{j}_B \times \bar{k}_B &= \bar{i}_B \\ \bar{k}_I \times \bar{i}_I &= \bar{j}_I \\ \bar{k}_B \times \bar{i}_B &= \bar{j}_B \end{aligned} \quad (4.2.3.2.15)$$

Again the relations of Eq. (4.2.3.2.4) are used to expand out the inertial cross products in terms of body-axis unit vectors and the body cross products in terms of inertial-axis unit vectors. Expanding $\bar{i}_B \times \bar{j}_B = \bar{k}_B$, for example:

$$\begin{aligned} &(\text{TRNBI}(3,1) \bar{i}_I + \text{TRNBI}(3,2) \bar{j}_I + \text{TRNBI}(3,3) \bar{k}_I) \\ &= (\text{TRNBI}(1,1) \bar{i}_I + \text{TRNBI}(1,2) \bar{j}_I + \text{TRNBI}(1,3) \bar{k}_I) \\ &\quad \times (\text{TRNBI}(2,1) \bar{i}_I + \text{TRNBI}(2,2) \bar{j}_I + \text{TRNBI}(2,3) \bar{k}_I) \end{aligned} \quad (4.2.3.2.16)$$

Evaluating the cross product in Eq. (4.2.3.2.16) and equating the coefficients results in three redundancy relations:

$$\begin{aligned} \text{TRNBI}(3,1) &= \text{TRNBI}(1,2) * \text{TRNBI}(2,3) - \text{TRNBI}(1,3) * \text{TRNBI}(2,2) \\ \text{TRNBI}(3,2) &= \text{TRNBI}(1,3) * \text{TRNBI}(2,1) - \text{TRNBI}(1,1) * \text{TRNBI}(2,3) \\ \text{TRNBI}(3,3) &= \text{TRNBI}(1,1) * \text{TRNBI}(2,2) - \text{TRNBI}(1,2) * \text{TRNBI}(2,1) \end{aligned} \quad (4.2.3.2.17)$$

Six more redundancy relations can be derived by looking at the other cross-product relations of Eq. (4.2.3.2.15):

$$\begin{aligned} \text{TRNBI}(1,1) &= \text{TRNBI}(2,2) * \text{TRNBI}(3,3) - \text{TRNBI}(2,3) * \text{TRNBI}(3,2) \\ \text{TRNBI}(1,2) &= \text{TRNBI}(2,3) * \text{TRNBI}(3,1) - \text{TRNBI}(2,1) * \text{TRNBI}(3,3) \\ \text{TRNBI}(1,3) &= \text{TRNBI}(2,1) * \text{TRNBI}(3,2) - \text{TRNBI}(2,2) * \text{TRNBI}(3,1) \\ \text{TRNBI}(2,1) &= \text{TRNBI}(1,3) * \text{TRNBI}(3,2) - \text{TRNBI}(1,2) * \text{TRNBI}(3,3) \\ \text{TRNBI}(2,2) &= \text{TRNBI}(1,1) * \text{TRNBI}(3,3) - \text{TRNBI}(1,3) * \text{TRNBI}(3,1) \\ \text{TRNBI}(2,3) &= \text{TRNBI}(1,2) * \text{TRNBI}(3,1) - \text{TRNBI}(1,1) * \text{TRNBI}(3,2) \end{aligned} \quad (4.2.3.2.18)$$

Each of the three formulations of the redundancy equations presented here is equally valid, and the selection of which form to use depends entirely on which terms are available in the simulation.

One of the more common attempted usages of the redundancy conditions is to reduce numerical errors in transformation matrix terms which occur because of the limited precision of modern digital computers and which are often augmented because the direction cosine terms are repeatedly updated in time in a numerical simulation. There are, however, very real dangers associated with such attempts. The potential dangers of both non-use and overdependence on the redundancy conditions will be illustrated here by an example from the field of computer-graphic animation, which also makes extensive use of continuously updated transformation matrices.

In early three-dimensional graphics programs, rotation of a body on the computer screen was accomplished by pre-multiplying the original geometry coordinates of the body by a rota-

tional projection matrix to define "global" geometry coordinates which were then projected to the graphics display space. The appearance of a constant roll rotation of an object on the graphics screen, for example, could be obtained by defining new rolled geometry coordinates at each display update:

$$\begin{aligned} \begin{vmatrix} X_g \\ Y_g \\ Z_g \end{vmatrix}_n &= [\text{TRNx}(\Delta\phi)] \begin{vmatrix} X_g \\ Y_g \\ Z_g \end{vmatrix}_{n-1} = [\text{TRNx}(\Delta\phi)] [\text{TRNx}(\Delta\phi)] \begin{vmatrix} X_g \\ Y_g \\ Z_g \end{vmatrix}_{n-2} \quad (4.2.3.2.19) \\ &= [\text{TRNx}(\Delta\phi)] \dots [\text{TRNx}(\Delta\phi)] \begin{vmatrix} X_g \\ Y_g \\ Z_g \end{vmatrix}_0 = [\text{TRNx}(\Delta\phi)]^n \begin{vmatrix} X_g \\ Y_g \\ Z_g \end{vmatrix}_0 \end{aligned}$$

where n is a display update counter and $\Delta\phi$ is the change in body roll angle for each display update. Unfortunately, at each of the repeated thousands of multiplications by the roll transformation, numerical precision errors associated with the evaluation of the sine and cosine trig functions mount up. Eventually, because of cumulative precision errors, the cumulative transformation matrix $[\text{TRNx}(\Delta\phi)]^n$ becomes non-orthogonal and the body becomes grossly distorted and skewed on the graphics screen. The same kinds of errors also occur in numerical trajectory simulations when the terms in the $[\text{TRNBI}]$ matrix are repeatedly updated over a large number of time steps.

One way to avoid the numerical distortion of a transformation matrix is to periodically "orthogonalize" the matrix using either the redundancy relations or using a more rigorous matrix orthogonalization technique such as the classical Gram-Schmidt procedure. Orthogonalization prevents the gross distortion of the rotational transformation but may still allow angular "drift" or "precession" of the rotating body with time. Consider again the case of a body continuously rotating in roll. After a large number of updates, the cumulative transform will no longer have exactly the form of a pure roll rotation as presented in Eq. (1.3.6); instead, random numerical error terms will appear:

$$[\text{TRNx}] = \begin{bmatrix} 1 & 0 & 0 \\ 0 & \epsilon(2,2) + \cos(n\Delta\phi) & \epsilon(2,3) + \sin(n\Delta\phi) \\ 0 & \epsilon(3,2) - \sin(n\Delta\phi) & \epsilon(3,3) + \cos(n\Delta\phi) \end{bmatrix} \quad (4.2.3.2.20)$$

where the ϵ terms are the independent cumulative errors which result from continuously updating the direction cosine terms. Now suppose that the redundancy condition of Eq. (2.3.2.7) (the sum of the squares of the terms in the row should equal unity) is not satisfied for the second row because of the numerical update errors. Redundancy Eq. (2.3.2.7) can be used to adjust terms in the second row of the matrix until unity magnitude is achieved. One way this condition can be applied is to replace the zero-value $\text{TRNx}(2,1)$ term with a value of $\text{SQRT}(1 - \epsilon(2,2)^2 - \epsilon(2,3)^2)$. This replacement, however, means that the transformation is no longer representative of a pure roll rotation because the $\text{TRN}(2,1)$ term can be non-zero only if some yaw or pitch occurs. This is the source of the numerical "drift" which occurs when the transformation is continuously

updated and orthogonalized. Drift occurs no matter what order the redundancy conditions are applied in, and drift angles can change magnitude and direction if the redundancy conditions are applied in different orders. Although angular drift can be minimized by using an optimal procedure such as Gram-Schmidt orthogonalization, after thousands of updates the roll axis of the body will have drifted to large pitch and yaw angles on the graphics screen. Drift can be avoided only by avoiding use of repeatedly updated transformation matrices in specifying orientations. In graphics, continuously updated viewing rotations are avoided by using an alternate system in which the point the observer is looking from and the point the observer is looking at are specified instead (the appearance of a viewing rotation is achieved by moving the point being looked from along a circular path about the object being viewed). In trajectory simulations, numerical drift is avoided by either limiting the number of allowed transformation updates (limiting the time span of the simulation) or by using another method such as outlined in Section 4.2.3.5 for specifying rotations.

4.2.3.3 Derivatives of Rotational Transformation Matrices

One method for describing the angular orientation of one coordinate system relative to another is through the specification of the direction cosine transformation matrix relating the two systems. Often the transformation matrix is selected as the primary quantity for defining store body orientations relative to inertial axes during a trajectory simulation and, therefore, a method must be developed to update the transformation at each time step of the simulation. The transformation matrix is updated in time by computing the derivative transformation matrix at each time step and performing a numerical time integration of each of the terms in the original transformation using the computed derivatives to determine the updated terms in the transformation matrix for the next time step. The formulas for computing the derivatives of both transformation matrices and inverse transformation matrices were previously presented without proof in Eqs. (1.4.5) and (1.4.6). Many of the equations which have been developed up to this point in other sections have used those transformation derivative formulas. The actual derivation of the formulas will now be presented in this section using the specific case of the [TRNBI] matrix as an example.

It is convenient to begin with the relation between the body axis unit vectors and inertial axis unit vectors:

$$\begin{vmatrix} \bar{i}_B \\ \bar{j}_B \\ \bar{k}_B \end{vmatrix} = [\text{TRNBI}] \begin{vmatrix} \bar{i}_I \\ \bar{j}_I \\ \bar{k}_I \end{vmatrix} \quad (4.2.3.3.1)$$

If derivatives are taken of both sides by the chain rule to get the rate of change of the body axis unit vectors:

$$\frac{d}{dt} \begin{vmatrix} \bar{i}_B \\ \bar{j}_B \\ \bar{k}_B \end{vmatrix} = \frac{d}{dt} [\text{TRNBI}] \begin{vmatrix} \bar{i}_I \\ \bar{j}_I \\ \bar{k}_I \end{vmatrix} + [\text{TRNBI}] \frac{d}{dt} \begin{vmatrix} \bar{i}_I \\ \bar{j}_I \\ \bar{k}_I \end{vmatrix} \quad (4.2.3.3.2)$$

Note again that the inertial unit vectors do not change either magnitude or direction with time (their inertial derivatives are zero) so that Eq. (4.2.3.3.2) reduces to:

$$\begin{aligned} \frac{d}{dt} \begin{vmatrix} \bar{i}_B \\ \bar{j}_B \\ \bar{k}_B \end{vmatrix} &= \frac{d}{dt} [\text{TRNBI}] \begin{vmatrix} \bar{i}_I \\ \bar{j}_I \\ \bar{k}_I \end{vmatrix} = [\text{DTRNBI}] \begin{vmatrix} \bar{i}_I \\ \bar{j}_I \\ \bar{k}_I \end{vmatrix} \\ &= \boxed{\begin{matrix} \text{DTRNBI}(1,1) & \text{DTRNBI}(1,2) & \text{DTRNBI}(1,3) \\ \text{DTRNBI}(2,1) & \text{DTRNBI}(2,2) & \text{DTRNBI}(2,3) \\ \text{DTRNBI}(3,1) & \text{DTRNBI}(3,2) & \text{DTRNBI}(3,3) \end{matrix}} \begin{vmatrix} \bar{i}_I \\ \bar{j}_I \\ \bar{k}_I \end{vmatrix} \end{aligned} \quad (4.2.3.3.3)$$

It was demonstrated in Section 4.2.3.1 that although the body axis unit vectors do not change in magnitude as the body rotates, they do change in direction. The velocities of the tips of the unit vectors along the hodographs were previously developed as Eqs. (4.2.3.1.7). The cross products from Eq. (4.2.3.1.7) can be evaluated in determinant form as:

$$\begin{aligned} \frac{d\bar{i}_B}{dt} = \bar{\omega} \text{BBI} X \bar{i}_B &= \begin{vmatrix} \bar{i}_B & \bar{j}_B & \bar{k}_B \\ \text{PBBI} & \text{QBBI} & \text{RBBI} \\ 1 & 0 & 0 \end{vmatrix} = \text{RBBI} \bar{j}_B - \text{QBBI} \bar{k}_B \\ \frac{d\bar{j}_B}{dt} = \bar{\omega} \text{BBI} X \bar{j}_B &= \begin{vmatrix} \bar{i}_B & \bar{j}_B & \bar{k}_B \\ \text{PBBI} & \text{QBBI} & \text{RBBI} \\ 0 & 1 & 0 \end{vmatrix} = \text{PBBI} \bar{k}_B - \text{RBBI} \bar{i}_B \quad (4.2.3.3.4) \\ \frac{d\bar{k}_B}{dt} = \bar{\omega} \text{BBI} X \bar{k}_B &= \begin{vmatrix} \bar{i}_B & \bar{j}_B & \bar{k}_B \\ \text{PBBI} & \text{QBBI} & \text{RBBI} \\ 0 & 0 & 1 \end{vmatrix} = \text{QBBI} \bar{i}_B - \text{PBBI} \bar{j}_B \end{aligned}$$

Equations (4.2.3.3.4), (4.2.3.3.1), and (4.2.3.3.3) can now be combined to give expressions for the terms in the derivative transformation matrix. For instance, equating the $d\bar{i}_B/dt$ equation from Eq. (4.2.3.3.3) with the $d\bar{i}_B/dt$ equation from Eq. (4.2.3.3.4):

$$\frac{d\bar{i}_B}{dt} = \text{DTRNBI}(1,1)\bar{i}_I + \text{DTRNBI}(1,2)\bar{j}_I + \text{DTRNBI}(1,3)\bar{k}_I = \text{RBBI} \bar{j}_B - \text{QBBI} \bar{k}_B \quad (4.2.3.3.5)$$

Next, substituting Eq. (4.2.3.3.1) in for the body axis unit vectors:

$$\begin{aligned} &\text{DTRNBI}(1,1)\bar{i}_I + \text{DTRNBI}(1,2)\bar{j}_I + \text{DTRNBI}(1,3)\bar{k}_I \\ &= \text{RBBI} (\text{TRNBI}(2,1)\bar{i}_I + \text{TRNBI}(2,2)\bar{j}_I + \text{TRNBI}(2,3)\bar{k}_I) \\ &\quad - \text{QBBI} (\text{TRNBI}(3,1)\bar{i}_I + \text{TRNBI}(3,2)\bar{j}_I + \text{TRNBI}(3,3)\bar{k}_I) \end{aligned} \quad (4.2.3.3.6)$$

Similar expressions can be developed for the $d\bar{j}_B/dt$ and $d\bar{k}_B/dt$ expressions from Eqs. (4.2.3.3.4) and (4.2.3.3.3):

$$\begin{aligned}
& \text{DTRNBI}(2,1)\bar{i}_I + \text{DTRNBI}(2,2)\bar{j}_I + \text{DTRNBI}(2,3)\bar{k}_I \\
&= \text{PBBI}(\text{TRNBI}(3,1)\bar{i}_I + \text{TRNBI}(3,2)\bar{j}_I + \text{TRNBI}(3,3)\bar{k}_I) \\
&\quad - \text{RBBI}(\text{TRNBI}(1,1)\bar{i}_I + \text{TRNBI}(1,2)\bar{j}_I + \text{TRNBI}(1,3)\bar{k}_I)
\end{aligned} \tag{4.2.3.3.7}$$

$$\begin{aligned}
& \text{DTRNBI}(3,1)\bar{i}_I + \text{DTRNBI}(3,2)\bar{j}_I + \text{DTRNBI}(3,3)\bar{k}_I \\
&= \text{QBBI}(\text{TRNBI}(1,1)\bar{i}_I + \text{TRNBI}(1,2)\bar{j}_I + \text{TRNBI}(1,3)\bar{k}_I) \\
&\quad - \text{PBBI}(\text{TRNBI}(2,1)\bar{i}_I + \text{TRNBI}(2,2)\bar{j}_I + \text{TRNBI}(2,3)\bar{k}_I)
\end{aligned} \tag{4.2.3.3.8}$$

Equating vector components in Eqs. (4.2.3.3.6) through (4.2.3.3.8) results in the following nine expressions for the elements of the derivative transformation matrix:

$$\begin{aligned}
\text{DTRNBI}(1,1) &= \text{RBBI}^*\text{TRNBI}(2,1) - \text{QBBI}^*\text{TRNBI}(3,1) \\
\text{DTRNBI}(1,2) &= \text{RBBI}^*\text{TRNBI}(2,2) - \text{QBBI}^*\text{TRNBI}(3,2) \\
\text{DTRNBI}(1,3) &= \text{RBBI}^*\text{TRNBI}(2,3) - \text{QBBI}^*\text{TRNBI}(3,3) \\
\text{DTRNBI}(2,1) &= \text{PBBI}^*\text{TRNBI}(3,1) - \text{RBBI}^*\text{TRNBI}(1,1) \\
\text{DTRNBI}(2,2) &= \text{PBBI}^*\text{TRNBI}(3,2) - \text{RBBI}^*\text{TRNBI}(1,2) \\
\text{DTRNBI}(2,3) &= \text{PBBI}^*\text{TRNBI}(3,3) - \text{RBBI}^*\text{TRNBI}(1,3) \\
\text{DTRNBI}(3,1) &= \text{QBBI}^*\text{TRNBI}(1,1) - \text{PBBI}^*\text{TRNBI}(2,1) \\
\text{DTRNBI}(3,2) &= \text{QBBI}^*\text{TRNBI}(1,2) - \text{PBBI}^*\text{TRNBI}(2,2) \\
\text{DTRNBI}(3,3) &= \text{QBBI}^*\text{TRNBI}(1,3) - \text{PBBI}^*\text{TRNBI}(2,3)
\end{aligned} \tag{4.2.3.3.9}$$

Which, when written in matrix form, becomes the desired expression from Eq. (1.4.6):

$$[\text{DTRNBI}] = -[\tilde{\omega} \text{ BBI}] [\text{TRNBI}] \tag{4.2.3.3.10}$$

The Eq. (1.4.5) form for the derivative of $[\text{TRNBI}]^{-1}$ is obtained by a virtually identical process beginning with Eq. (4.2.3.3.1) rearranged to express the inertial unit vectors in terms of body vectors:

$$\left| \begin{array}{c} \bar{i}_I \\ \bar{j}_I \\ \bar{k}_I \end{array} \right| = [\text{TRNBI}]^{-1} \left| \begin{array}{c} \bar{i}_B \\ \bar{j}_B \\ \bar{k}_B \end{array} \right| \tag{4.2.3.3.11}$$

and then proceeding with the exact steps used in the development of Eqs. (4.2.3.3.2) through (4.2.3.3.10).

If the 3 by 3 transformation matrix is used to define store orientations in a simulation and it is necessary to update the store orientation in time, the nine terms in the transformation derivative from Eqs. (4.2.3.3.10) are evaluated at each time step and each of the nine terms is then integrated in time to compute the $[\text{TRNBI}]$ matrix at the new time step. There are, however, two shortcomings associated with this method for updating the orientations in numerical simulations.

First, nine separate orientation parameters must be integrated at each time step with associated large computing time. Second, after the integrations, numerical errors introduced in the integration process may cause the new [TRNBI] matrix to be slightly non-orthogonal. Compromise approaches are possible in which only a subset of the nine terms is actually integrated and the remaining terms are determined from the redundancy conditions. Such compromises may, however, introduce numerical drift biases in the computed orientations after repeated thousands of orientation updates, as outlined at the end of Section 4.2.3.2.

Equation (4.2.3.3.10) defines how the derivative transformation matrix is determined when the angular velocities are known. For some applications (such as extraction of motion properties from flight or scaled drop model data), the inverse problem of determination of angular velocities given the derivative transformation must be solved. Beginning with Eq. (4.2.3.3.10) and post-multiplying both sides by [TRNBI]^T:

$$[DTRNBI][TRNBI]^T = -[\tilde{\omega} BBI] \quad (4.2.3.3.12)$$

$$\begin{bmatrix} DTRNBI(1,1) & DTRNBI(1,2) & DTRNBI(1,3) \\ DTRNBI(2,1) & DTRNBI(2,2) & DTRNBI(2,3) \\ DTRNBI(3,1) & DTRNBI(3,2) & DTRNBI(3,3) \end{bmatrix} \begin{bmatrix} TRNBI(1,1) & TRNBI(2,1) & TRNBI(3,1) \\ TRNBI(1,2) & TRNBI(2,2) & TRNBI(3,2) \\ TRNBI(1,3) & TRNBI(2,3) & TRNBI(3,3) \end{bmatrix} = \begin{bmatrix} 0 & RBBI & -QBBI \\ -RBBI & 0 & PBBI \\ QBBI & -PBBI & 0 \end{bmatrix} \quad (4.2.3.3.13)$$

Expanding out and equating terms:

$$\begin{aligned} PBBI &= DTRNBI(2,1)TRNBI(3,1) + DTRNBI(2,2)TRNBI(3,2) \\ &\quad + DTRNBI(2,3)TRNBI(3,3) \\ -PBBI &= DTRNBI(3,1)TRNBI(2,1) + DTRNBI(3,2)TRNBI(2,2) \\ &\quad + DTRNBI(3,3)TRNBI(2,3) \\ QBBI &= DTRNBI(3,1)TRNBI(1,1) + DTRNBI(3,2)TRNBI(1,2) \\ &\quad + DTRNBI(3,3)TRNBI(1,3) \\ -QBBI &= DTRNBI(1,1)TRNBI(3,1) + DTRNBI(1,2)TRNBI(3,2) \\ &\quad + DTRNBI(1,3)TRNBI(3,3) \\ RBBI &= DTRNBI(1,1)TRNBI(2,1) + DTRNBI(1,2)TRNBI(2,2) \\ &\quad + DTRNBI(1,3)TRNBI(2,3) \\ -RBBI &= DTRNBI(2,1)TRNBI(1,1) + DTRNBI(2,2)TRNBI(1,2) \\ &\quad + DTRNBI(2,3)TRNBI(1,3) \end{aligned} \quad (4.2.3.3.14)$$

Note that there are two expressions for each angular velocity component. This is a consequence of the redundancy of the direction cosine matrix form. The equivalence of the two expressions for any one of the angular velocity components may be shown by using the redundancy relations of Eqs. (4.2.3.2.17) and (4.2.3.2.18).

4.2.3.4 Derivatives of the Modified Euler Angles

A second method for describing the angular orientation of one coordinate system relative to another is through the specification of the three modified Euler angles (yaw-pitch-roll sequence) relating the two systems. This representation was previously described in Section 1.3. The orientations of the store in time for trajectory simulations can then be updated by computing the derivatives of the three modified Euler angles at each time step and integrating the original angles using those derivatives to determine new modified Euler angles for the orientation at each new time step.

As developed in Eq. (1.3.7), a rotational projection transformation matrix can be considered to be formed by three sequential yaw-pitch-roll Euler rotations. For the orientation of body axes relative to inertial axes these may be written as:

$$[\text{TRNBI}] = [\text{TRNx}(\phi_{\text{BI}})] [\text{TRNy}(\theta_{\text{BI}})] [\text{TRNz}(\psi_{\text{BI}})] \quad (4.2.3.4.1)$$

where the three orthogonal rotations are defined by Eqs. (1.3.3), (1.3.5), and (1.3.6). If the body is rotated to a new orientation with new angles ($\psi_{\text{BI}} + \Delta\psi_{\text{BI}}$, $\theta_{\text{BI}} + \Delta\theta_{\text{BI}}$, $\phi_{\text{BI}} + \Delta\phi_{\text{BI}}$) over an infinitesimal time step Δt , then, in the limit, the time rate of change of the orientation can be represented by:

$$\begin{vmatrix} \text{PBBI} \\ \text{QBBI} \\ \text{RBBI} \end{vmatrix} = \lim_{\Delta t \rightarrow 0} \left\{ \begin{vmatrix} \Delta\phi_{\text{BI}} \\ 0 \\ 0 \end{vmatrix} + [\text{TRNx}(\phi_{\text{BI}})] \begin{vmatrix} 0 \\ \Delta\theta_{\text{BI}} \\ 0 \end{vmatrix} + [\text{TRNx}(\phi_{\text{BI}})] [\text{TRNy}(\theta_{\text{BI}})] \begin{vmatrix} 0 \\ 0 \\ \Delta\psi_{\text{BI}} \end{vmatrix} \right\} \quad (4.2.3.4.2)$$

Note that in the limit for infinitesimal rotations, the rotation derivatives can be represented by a vector even though the sequence of the rotations creating $[\text{TRNBI}]$ in Eq. (4.2.3.4.1) is vitally important and the ψ_{BI} , θ_{BI} , and ϕ_{BI} terms are not themselves components of a vector. Replacing limits with derivatives and defining $D\psi_{\text{BI}} = d\psi_{\text{BI}}/dt$, $D\theta_{\text{BI}} = d\theta_{\text{BI}}/dt$, and $D\phi_{\text{BI}} = d\phi_{\text{BI}}/dt$:

$$\begin{vmatrix} \text{PBBI} \\ \text{QBBI} \\ \text{RBBI} \end{vmatrix} = \begin{vmatrix} D\phi_{\text{BI}} \\ 0 \\ 0 \end{vmatrix} + [\text{TRNx}(\phi_{\text{BI}})] \begin{vmatrix} 0 \\ D\theta_{\text{BI}} \\ 0 \end{vmatrix} + [\text{TRNx}(\phi_{\text{BI}})] [\text{TRNy}(\theta_{\text{BI}})] \begin{vmatrix} 0 \\ 0 \\ D\psi_{\text{BI}} \end{vmatrix} \quad (4.2.3.4.3)$$

The three equations of (4.2.3.4.3) can be expanded and then rewritten using a single matrix:

$$\begin{vmatrix} \text{PBBI} \\ \text{QBBI} \\ \text{RBBI} \end{vmatrix} = \begin{bmatrix} 1 & 0 & -\sin\theta_{\text{BI}} \\ 0 & \cos\phi_{\text{BI}} & \cos\theta_{\text{BI}}\sin\phi_{\text{BI}} \\ 0 & -\sin\phi_{\text{BI}} & \cos\theta_{\text{BI}}\cos\phi_{\text{BI}} \end{bmatrix} \begin{vmatrix} D\phi_{\text{BI}} \\ D\theta_{\text{BI}} \\ D\psi_{\text{BI}} \end{vmatrix} \quad (4.2.3.4.4)$$

The matrix in Eq. (4.2.3.4.4) is not an orthogonal rotational transformation, so that an explicit solution for the modified Euler angle derivatives must be obtained by direct matrix inversion:

$$\begin{array}{c}
 \left| \begin{array}{c} D\phi_{BI} \\ D\theta_{BI} \\ D\Psi_{BI} \end{array} \right| = (1/\cos\theta_{BI}) \left[\begin{array}{ccc} \cos\theta_{BI} & \sin\theta_{BI}\sin\phi_{BI} & \sin\theta_{BI}\cos\phi_{BI} \\ 0 & \cos\theta_{BI}\cos\phi_{BI} & -\cos\theta_{BI}\sin\phi_{BI} \\ 0 & \sin\phi_{BI} & \cos\phi_{BI} \end{array} \right] \left| \begin{array}{c} PBBI \\ QBBI \\ RBBI \end{array} \right| \\
 \tan\theta_{BI} (QBBI \sin\phi_{BI} + RBBI \cos\phi_{BI}) + PBBI \\
 = QBBI \cos\phi_{BI} - RBBI \sin\phi_{BI} \\
 \sec\theta_{BI} (QBBI \sin\phi_{BI} + RBBI \cos\phi_{BI})
 \end{array} \quad (4.2.3.4.5)$$

Care must be taken in Eq. (4.2.3.4.5) to ensure proper units since the angles are usually specified in degrees and the angular velocities in radians per second.

In a numerical trajectory simulation, Eqs. (4.2.3.4.5) can be used to determine the modified Euler angle derivatives at each time step based on the angular velocity terms. The Euler angle derivatives can then be integrated to determine the modified Euler angles for the new store orientation at the next time step. Unfortunately, direct computation of the modified Euler angles by integration of the Euler rates is often not desirable because the $(1/\cos\theta_{BI}) = \sec\theta_{BI}$ term in Eq. (4.2.3.4.5) is not defined for pitch angles which are odd multiples of $\pi/2$ radians and the resulting numerical instabilities can cause the simulation to "blow up." In addition, elaborate quadrant check algorithms must be implemented to enforce the range limitations on the modified Euler angles as noted in Eq. (1.3.9). For instance, if a pitch angle of $\theta_B = -89$ deg at one time step is integrated to a value of -91.5 deg [which is outside the +90 to -90 range on pitch angle in Eq. (1.3.9)], then a quadrant check algorithm must reset the new pitch angle to -88.5 deg and shift both Ψ_{BI} and ϕ_{BI} by 180 deg. For these reasons, modified Euler angle derivatives are almost never used in practical simulations.

4.2.3.5 Four-Parameter Forms (Euler Parameters, Quaternions, and Cayley-Klein Parameters)

Thus far, the store orientation and the time rate of change of the store orientation have been modeled using the nine terms in the direction cosine transformation matrix in Section 4.2.3.3 and using the three modified Euler angles in Section 4.2.3.4. The transformation matrix form was shown to have some numerical difficulty in maintaining orthogonality and also shown to require computation and integration of nine separate terms. The three modified Euler angles were shown to be entirely adequate for defining orientation, but their derivatives are undefined at pitch angles which are multiples of 90 deg. Obviously, if three parameters do not provide quite enough information to quantify the time rate of change of orientation and nine parameters provide unnecessary redundant information, four-parameter systems may represent the "best" compromise.

Three different four-parameter systems (Euler parameters, Quaternions, and Cayley-Klein parameters) have been proposed and, indeed, whole new branches of mathematics have been developed to support the quaternion and Cayley-Klein derivations. In the final analysis, however, the three approaches are equivalent - so much so that the term "quaternion" in common practice is applied to any of the four-parameter systems, not just to that particular system proposed by Hamilton. Quaternion approaches have advantages over the direction cosine terms in internal tra-

jectory computations because only four parameters are required to define the orientation rather than the nine terms in the direction cosine matrix and because numerical truncation errors in a digital computer simulation can be minimized while at the same time the size of the integration time step can be maximized. Quaternion approaches have advantages over the modified Euler angles because the quaternions are rigorously defined and do not "blow up" or reverse signs at angles where modified Euler angles and their derivatives may become undefined, switch signs, or shift by 180 deg. For these reasons quaternion approaches are often preferred in equation-of-motion simulations and are also used in the programs which have been developed at the AEDC for extracting motion and aerodynamic properties from free-flight film data and stores with telemetry capability. The direction cosine transformation matrix approach is still used in most of the wind tunnel trajectory generation software at the AEDC, but it should be noted that limitations of the physical support sting hardware used in captive trajectory testing usually causes termination of wind tunnel trajectory simulations before large angles can be reached or before numerical errors in the direction cosine terms can grow, thus reducing the value of the advantages offered by quaternion approaches.

The first four-parameter system was developed by Euler (ca. 1776) (Refs. 4 and 5). Euler's development was based entirely on physical principles noted from rotational trigonometry studies. Euler's derivation is entirely geometric in nature and does not require the introduction of new fields of mathematics. The Euler approach results in four "Euler parameters" to describe the rotational orientation of one coordinate system relative to another. The second four-parameter approach refers to a high-order three-dimensional "quaternion" mathematics developed by W. R. Hamilton (ca. 1843) (Refs. 6, 7, and 8) for describing rotational motion. The quaternion can be idealized as a sort of three-dimensional complex number with a real (or "scalar") part and three orthogonal imaginary parts. The values of the scalar and imaginary coefficients of the quaternion are identical to the values of the four Euler parameters. An excellent overview of quaternion algebra is available in Ref. 9 for readers with interests in that area. The third four-parameter approach is that developed by Cayley and Klein (Ref. 10) originally for gyroscopic and guidance analyses (and the study of tops). The Cayley-Klein approach models rotations using a two-by-two matrix of complex terms. The elements of the matrix (the Cayley-Klein parameters) turn out to be complex combinations of the same four numerical values making up the Euler parameters and the real and imaginary quaternion coefficients. The development of the four rotational parameters as will be presented in this section will generally follow the more-intuitive physical approach of Euler and is largely patterned after the treatment in Ref. 11 with a few math corrections and conversions to the present nomenclature. Each of the three different approaches to the four-parameter system has its advantages, however. Throughout most of the following sections the terms "Euler parameter," "quaternion," and "Cayley-Klein parameter" will be taken as synonymous, although the former is actually four separate numbers, the second is a single "three-dimensional" number, and the third is a complex four-element matrix.

Central to the development of all four-parameter approaches is a theorem proposed by Euler which states that any physical rotation of one coordinate frame relative to another can be represented by an equivalent single rotation through some finite angle, δ_e , about a specially selected axis. In other words, regardless of the history of rotations in any sequence of yaw, pitch, and roll, the final orientation of the body can be represented by one single rotation (through an angle

called "the" Euler angle) about a special axis which is called the "Euler axis." The reader should be warned again that the sequential yaw, pitch, and roll angles are sometimes misleadingly called "Euler" angles in common aerodynamic practice. Actually the three sequential angles are more properly called "modified Euler angles" and the term "the" Euler angle is reserved for the single equivalent angle. The Euler axis may be arbitrarily oriented with respect to the body-axis directions, and its direction, as well as the magnitude of the Euler angle, may vary as a function of time in the simulation. The four parameters in each of the four-parameter systems (as might be guessed) are related to the magnitude of the single Euler rotation and three terms defining the orientation of the Euler axis.

The proof of the Euler Theorem is based on a recognition of some of the fundamental properties of rotations. Proof of the theorem will, therefore, be presented before proceeding with the derivation of the Euler parameters. Euler's premise is that if an arbitrary rotation sequence (say from the "I" axes to the "B" axes) can truly be represented by a single rotation about one axis, then it follows that the components of a vector along that axis must be the same in both the I and B measurement systems. One way to prove the Euler Theorem is to simply prove that such a vector exists. As a first step, notice that the relationship between the inertial and body components of an arbitrary vector from point 1 to point 2 can be given by:

$$\begin{vmatrix} XB21 \\ YB21 \\ ZB21 \end{vmatrix} = [TRNBI] \begin{vmatrix} XI21 \\ YI21 \\ ZI21 \end{vmatrix} \quad (4.2.3.5.0.1)$$

If $\{XI21\}$ is subtracted from both sides:

$$\begin{vmatrix} XB21 \\ YB21 \\ ZB21 \end{vmatrix} - \begin{vmatrix} XI21 \\ YI21 \\ ZI21 \end{vmatrix} = [TRNBI] \begin{vmatrix} XI21 \\ YI21 \\ ZI21 \end{vmatrix} - \begin{vmatrix} XI21 \\ YI21 \\ ZI21 \end{vmatrix} = [[TRNBI] - [1]] \begin{vmatrix} XI21 \\ YI21 \\ ZI21 \end{vmatrix} \quad (4.2.3.5.0.2)$$

where [1] is the identity matrix. If an arbitrary vector is chosen so that the body and inertial components of the vector are identical, then Eq. (4.2.3.5.0.2) reduces to:

$$\begin{vmatrix} 0 \\ 0 \\ 0 \end{vmatrix} = [[TRNBI] - [1]] \begin{vmatrix} XI21 \\ YI21 \\ ZI21 \end{vmatrix} \quad (4.2.3.5.0.3)$$

The proof of the Euler Theorem requires that Eq. (4.2.3.5.0.3) have a unique solution. Such a solution exists only if the determinant of the matrix is zero:

$$\begin{vmatrix} TRNBI(1,1) - 1 & TRNBI(1,2) & TRNBI(1,3) \\ TRNBI(2,1) & TRNBI(2,2) - 1 & TRNBI(2,3) \\ TRNBI(3,1) & TRNBI(3,2) & TRNBI(3,3) - 1 \end{vmatrix} = 0 \quad (4.2.3.5.0.4)$$

where Eq. (4.2.3.5.0.4) is called the "characteristic form" or "Eigen form" of the equation. Expanding the determinant gives:

$$\begin{aligned}
 & [\text{TRNBI}(1,1)\text{TRNBI}(2,2)\text{TRNBI}(3,3) + \text{TRNBI}(1,2)\text{TRNBI}(2,3)\text{TRNBI}(3,1) \\
 & + \text{TRNBI}(2,1)\text{TRNBI}(3,2)\text{TRNBI}(1,3) - \text{TRNBI}(3,1)\text{TRNBI}(1,3)\text{TRNBI}(2,2) \\
 & - \text{TRNBI}(2,1)\text{TRNBI}(1,2)\text{TRNBI}(3,3) + \text{TRNBI}(3,2)\text{TRNBI}(2,3)\text{TRNBI}(1,1) - 1] \\
 & + [\text{TRNBI}(1,1) - \text{TRNBI}(2,2)\text{TRNBI}(3,3) + \text{TRNBI}(2,3)\text{TRNBI}(3,2) \\
 & + \text{TRNBI}(2,2) - \text{TRNBI}(1,1)\text{TRNBI}(3,3) + \text{TRNBI}(1,3)\text{TRNBI}(3,1) \\
 & + \text{TRNBI}(3,3) - \text{TRNBI}(1,1)\text{TRNBI}(2,2) + \text{TRNBI}(2,1)\text{TRNBI}(1,2)] = 0
 \end{aligned} \tag{4.2.3.5.0.5}$$

All terms in the second square brackets of Eq. (4.2.3.5.0.5) vanish as a result of the redundancy conditions of Eq. (4.2.3.2.18). Proof that all the terms in the first bracket also disappear is based on first demonstrating another fundamental property of rotational transformation matrices - that the determinant of a rotation matrix is unity. Proof of this corollary property can be accomplished in a few simple steps. First, recall that:

$$[\text{TRNBI}] [\text{TRNBI}]^T = [1] \tag{4.2.3.5.0.6}$$

for an orthogonal matrix. If determinants are taken of both sides, it is noted that the determinant of the identity matrix is 1.

$$|[\text{TRNBI}]| |[\text{TRNBI}]^T| = 1 \tag{4.2.3.5.0.7}$$

where a property of determinants that the determinant of a matrix product is equal to the product of the matrix determinants is used. Another property of determinants is that the value of a determinant does not change if the rows and columns of the matrix are interchanged. Using this property, Eq. (4.2.3.5.0.7) can be rewritten as:

$$|[\text{TRNBI}]|^2 = 1 \tag{4.2.3.5.0.8}$$

Expansion of the determinant in Eq. (4.2.3.5.0.8) will indicate that the first bracket in Eq. (4.2.3.5.0.5) also reduces to zero, thereby proving the Euler Theorem.

Armed with proof of Euler's Theorem, the classical Euler-parameter form of the four-parameter system will be developed in Section 4.2.3.5.1. Equations for transforming the four-parameter systems to the direction cosine matrix and modified Euler angle forms are then described in Sections 4.2.3.5.2 through 4.2.3.5.4, and the time derivatives of the four parameters for use in updating store orientations in motion simulations are developed in Section 4.2.3.5.5.

4.2.3.5.1 Derivation of Euler Parameter Form

A temporary auxiliary axis system designated by "e" will be used in the derivation of the four-parameter model. The Xe axis will be taken to be aligned with the Euler axis. Directions for

the Ye and Ze axes will be specified shortly. The orientation of the Euler Xe axis relative to the inertial axes will be identified by the inertial coordinates of a unit vector along the Euler axis:

$$\bar{i}_e = \bar{l}\bar{i}_I + m\bar{j}_I + n\bar{k}_I = \cos \alpha \bar{i}_I + \cos \beta \bar{j}_I + \cos \gamma \bar{k}_I \quad (4.2.3.5.1.1)$$

where \bar{i}_I , \bar{j}_I , and \bar{k}_I are the inertial unit vectors and where the l , m , and n or α , β , and γ terms are the direction cosines or direction angles, respectively, for the Euler Xe axis and vary in time as the direction of the Euler axis varies in time. The terms l , m , and n , (or, alternately α , β , and γ) and the single equivalent Euler rotation angle, δ_e , are the four fundamental quantities from which the four Euler parameters or quaternions will be determined. The goal of the remaining derivation is to express the orientation of the store in terms of these parameters and to develop methods for updating the orientations through time integration and converting to the Euler angle or direction cosine transformation matrix forms.

The rotation process begins with the body axes aligned with inertial axes as shown in Fig. 15. The figure illustrates the orientation of an Euler axis at a particular time instant in a trajectory. The store can be rotated about this Euler axis from its initial (coincident with inertial axes) orientation to its true time-dependent orientation. The axes are shown before the Euler rotation is applied and, for clarity, the inertial and body axes are shown with no relative translational offsets in the illustration (i.e., they have a common origin so that $\{XIBI\} = \{0\}$). Because the body and inertial directions are initially aligned before the rotation is applied, an expression virtually identical to that defined in Eq. (4.2.3.5.1.1) for the inertial components of the Euler axis unit vector can be developed for the body axis components of the vector:

$$\bar{i}_e = l\bar{i}_I + m\bar{j}_I + n\bar{k}_I = l\bar{i}_B + m\bar{j}_B + n\bar{k}_B \quad (4.2.3.5.1.2)$$

It is also extremely important to note that the body-axis components of the Euler unit vector do not change, even after rotation of the body about the Euler axis (only points not on the Euler axis are moved by the Euler rotation).

When a rigid body is rotated about an Euler axis, an arbitrary point, p, within the body which has initial inertial pre-rotation position coordinates of $p_i = p_{initial} = \{X_{Ip_i}I, Y_{Ip_i}I, Z_{Ip_i}I\}$ is moved to a new position $p_f = p_{final} = \{X_{Ip_f}I, Y_{Ip_f}I, Z_{Ip_f}I\}$. The movement of a point in the body due to the Euler rotation can be represented by the vector $\{p_{final} - p_{initial}\}$ which can be determined directly from the geometry of Fig. 15. Beginning first with the inertial pre-rotation position vector for arbitrary point p which may be expressed using extended unit vector notation as:

$$\{p_i\} = X_{Ip_i}I \bar{i}_I + Y_{Ip_i}I \bar{j}_I + Z_{Ip_i}I \bar{k}_I = X_{Bp_i}B \bar{i}_B + Y_{Bp_i}B \bar{j}_B + Z_{Bp_i}B \bar{k}_B \quad (4.2.3.5.1.3)$$

where it is noted that the inertial and body directions are initially aligned before the rotation is applied and where it is also noted that the body-axis components of point p are the same before and after the Euler rotation ($\{X_{Bp_i}B\} = \{X_{Bp_f}B\} = \{X_{Bp}B\}$) because both the body axes and point p rotate with the body. Note that point p traces out a portion of the arc of a circle as it is rotated from position p_i to p_f . The vector from the inertial origin to the point on the Euler axis at the cen-

ter of the circle of rotation for point p (which is denoted by lower case "e" in the figure and is not to be confused with the "earth" axes of Fig. 1) can be obtained by forming the scalar inner product of unit vector \hat{i}_e [Eq. (4.2.3.5.1.2)] with the position vector for point p [Eq. (4.2.3.5.1.3)] to determine the projection of the $\{XI_{IpI}\}$ vector onto the Euler axis:

$$\begin{aligned} X_{eeI} \hat{i}_e &= (l \hat{i}_I + m \hat{j}_I + n \hat{k}_I) \cdot (XI_{IpI} \hat{i}_I + YI_{IpI} \hat{j}_I + ZI_{IpI} \hat{k}_I) \\ &= (l XI_{IpI} + m YI_{IpI} + n ZI_{IpI}) \hat{i}_e \end{aligned} \quad (4.2.3.5.1.4)$$

which can be expressed in inertial coordinates by using Eq. (4.2.3.5.1.2) as:

$$\begin{aligned} X_{eeI} \hat{i}_e &= XI_{eI} \hat{i}_I + YI_{eI} \hat{j}_I + ZI_{eI} \hat{k}_I \\ &= (l XI_{IpI} + m YI_{IpI} + n ZI_{IpI}) (\hat{l}_I + m \hat{j}_I + n \hat{k}_I) \end{aligned} \quad (4.2.3.5.1.5)$$

The displacement of the arbitrary point from its initial to its final position as the body is rotated about the Euler axis takes place within a plane normal to the Euler axis at point e. Figure 16 shows a view of that plane looking down the Euler axis. The displacement of the arbitrary point $\{p_{final} - p_{initial}\}$ consists of two components, one in the direction of the vector from e to p_i and one normal to both that direction and the Euler axis direction, \hat{i}_e . These two directions will be used to define the axis directions for the Y_e and Z_e temporary axes which will have unit vectors \hat{j}_e and \hat{k}_e , respectively. The displacement component for point p in the Y_e direction as a result of the Euler rotation, δ_e , is apparent from the figure:

$$Y_{ep_{final}} \hat{j}_e = (Y_{epf} - Y_{epi}) \hat{j}_e = -Y_{epi} (1 - \cos \delta_e) \hat{j}_e \quad (4.2.3.5.1.6)$$

An expression for Y_{epi} is needed to evaluate Eq. (4.2.3.5.1.6). Such an expression can be developed in terms of the inertial-axis positions of point p_i and point e from the geometry of Figs. 15 and 16. First note that:

$$\begin{vmatrix} X_{epi} \\ Y_{epi} \\ Z_{epi} \end{vmatrix} = \begin{vmatrix} 0.0 \\ Y_{epi} \\ 0.0 \end{vmatrix} = \begin{vmatrix} X_{IpI} \\ Y_{IpI} \\ Z_{IpI} \end{vmatrix} - \begin{vmatrix} XI_{eI} \\ YI_{eI} \\ ZI_{eI} \end{vmatrix} \quad (4.2.3.5.1.7)$$

Each term in Eq. (4.2.3.5.1.7) can be projected into inertial axes so that the expressions developed above for the inertial coordinates of point e and point p can be used. It follows from Eq. (4.2.3.5.1.7) that:

$$\begin{vmatrix} XI_{IpI} \\ YI_{IpI} \\ ZI_{IpI} \end{vmatrix} = \begin{vmatrix} XI_{IpI} \\ YI_{IpI} \\ ZI_{IpI} \end{vmatrix} - \begin{vmatrix} XI_{eI} \\ YI_{eI} \\ ZI_{eI} \end{vmatrix} \quad (4.2.3.5.1.8)$$

noting that the $\{XI_{IpI}\}$ vector from Eq. (4.2.3.5.1.8) is the same as the Y_{epi} component in Eq. (4.2.3.5.1.7) because the X_{epi} and Z_{epi} terms are zero. Substituting into Eq. (4.2.3.5.1.6) results in:

$$\begin{aligned} Y_{ep_{final}} \hat{j}_e &= (Y_{epf} - Y_{epi}) \hat{j}_e = ((XI_{eI} - XI_{IpI}) \hat{i}_I + (YI_{eI} - YI_{IpI}) \hat{j}_I \\ &\quad + (ZI_{eI} - ZI_{IpI}) \hat{k}_I) (1 - \cos \delta_e) \end{aligned} \quad (4.2.3.5.1.9)$$

where it should be noted that Euler axis unit vectors are used on the left and inertial axis vectors are used on the right. Substituting Eqs. (4.2.3.5.1.5) and (4.2.3.5.1.3) into Eq. (4.2.3.5.1.9):

$$\begin{aligned}
 \text{Yepfpi} \bar{j}_e &= (\text{Yefpe} - \text{Yepie}) \bar{j}_e \\
 &= ((lXIp_iI + mYIp_iI + nZIp_iI) l \bar{i}_I - XIp_iI \bar{i}_I \\
 &\quad + (lXIp_iI + mYIp_iI + nZIp_iI) m \bar{j}_I - YIp_iI \bar{j}_I \\
 &\quad + (lXIp_iI + mYIp_iI + nZIp_iI) n \bar{k}_I - ZIp_iI \bar{k}_I) (1 - \cos \delta_e) \\
 &= ((l^2XIp_iI + lmYIp_iI + lnZIp_iI - XIp_iI) \bar{i}_I \\
 &\quad + (lmXIp_iI + m^2YIp_iI + mnZIp_iI - YIp_iI) \bar{j}_I \\
 &\quad + (lnXIp_iI + mnYIp_iI + n^2ZIp_iI - ZIp_iI) \bar{k}_I) (1 - \cos \delta_e)
 \end{aligned} \tag{4.2.3.5.1.10}$$

Equation (4.2.3.5.1.10) describes the change in position in the \bar{j}_e direction of an arbitrary point which has been rotated about the Euler axis. Even though it defines the Y_e component of the displacement, the expression is developed using terms that are coordinatized in the inertial directions. It is now necessary to develop a similar expression for the Z_e component of the displacement of the arbitrary point. From Fig. 16, it is easy to see that the magnitude of the Z_e displacement is:

$$\text{Zepfpi} \bar{k}_e = (\text{Zefpe} - \text{Zepie}) \bar{k}_e = (\text{Yepie}) \sin \delta_e \bar{k}_e \tag{4.2.3.5.1.11}$$

Just as it was important, however, to eliminate the unit vectors of the temporary Euler axis system and express the relation of Eq. (4.2.3.5.1.10) using inertial axis components only, it will be important to replace the \bar{k}_e vector in Eq. (4.2.3.5.1.11) with an equivalent expression using inertial terms. The Z_e direction is normal to the X_e - Y_e plane which implies that it is normal to the plane containing the X_{leI} unit vector [Eq. (4.2.3.5.1.5)] and the XIp_iI vector [Eq. (4.2.3.5.1.3)]. The unit vector direction is, therefore, given by the normalized cross product of the two vectors:

$$\begin{aligned}
 \bar{k}_e &= \frac{\{X_{leI}\} \times \{XIp_iI\}}{\text{mag}(\{X_{leI}\} \times \{XIp_iI\})} \\
 &= \frac{X_{eeI}}{(X_{eeI})(\text{Yepie})} (\bar{i}_I + m\bar{j}_I + n\bar{k}_I) \times (XIp_iI \bar{i}_I + YIp_iI \bar{j}_I + ZIp_iI \bar{k}_I) \\
 &= \frac{1}{(\text{Yepie})} \left| \begin{array}{ccc} \bar{i}_I & \bar{j}_I & \bar{k}_I \\ l & m & n \\ XIp_iI & YIp_iI & ZIp_iI \end{array} \right|
 \end{aligned} \tag{4.2.3.5.1.12}$$

where it is noted in the second equality that the magnitude of a vector cross product is equal to the product of the magnitude of the first vector with the magnitude of that part of the second vector which is perpendicular to the first. Combining Eqs. (4.2.3.5.1.11) and (4.2.3.5.1.12) yields:

$$\begin{aligned} Zep_{fpI} \bar{k}_e &= (Zep_{fe} - Zep_{pe}) \bar{k}_e = \frac{(Yep_{je} \sin \delta_e)}{Yep_{pe}} \begin{vmatrix} \bar{i}_I & \bar{j}_I & \bar{k}_I \\ l & m & n \\ XI_{pi}I & YI_{pi}I & ZI_{pi}I \end{vmatrix} \\ &= ((mZI_{pi}I - nYI_{pi}I)\bar{i}_I + (nXI_{pi}I - lZI_{pi}I)\bar{j}_I + (lYI_{pi}I - mXI_{pi}I)\bar{k}_I) \sin \delta_e \quad (4.2.3.5.1.13) \end{aligned}$$

The final position of point p can be obtained as the sum of the initial position of point p plus the change in position in the \bar{j}_e direction from Eq. (4.2.3.5.1.10) plus the change in position in the \bar{k}_e direction from Eq. (4.2.3.5.1.13):

$$\begin{aligned} XI_{pfI} &= XI_{pi}I + (l^2XI_{pi}I + lmYI_{pi}I + lnZI_{pi}I - XI_{pi}I)(1 - \cos \delta_e) \\ &\quad + (mZI_{pi}I - nYI_{pi}I) \sin \delta_e \\ YI_{pfI} &= YI_{pi}I + (lmXI_{pi}I + m^2YI_{pi}I + mnZI_{pi}I - YI_{pi}I)(1 - \cos \delta_e) \\ &\quad + (nXI_{pi}I - lZI_{pi}I) \sin \delta_e \\ ZI_{pfI} &= ZI_{pi}I + (lnXI_{pi}I + mnYI_{pi}I + n^2ZI_{pi}I - ZI_{pi}I)(1 - \cos \delta_e) \\ &\quad + (lYI_{pi}I - mXI_{pi}I) \sin \delta_e \quad (4.2.3.5.1.14) \end{aligned}$$

Recalling from Eq. (4.2.3.5.1.3) that $\{XI_{pi}\}_{\text{initial}} = \{XB_{pI}\}$ because the body and inertial axes are coincident before the rotation, Eq. (4.2.3.5.1.14) can be written in matrix form as:

$$\begin{vmatrix} XI_{pi} \\ YI_{pi} \\ ZI_{pi} \end{vmatrix} = \begin{bmatrix} \cos \delta_e + l^2(1-\cos \delta_e) & lm(1-\cos \delta_e) - nsin \delta_e & ln(1-\cos \delta_e) + msin \delta_e \\ lm(1-\cos \delta_e) + nsin \delta_e & \cos \delta_e + m^2(1-\cos \delta_e) & mn(1-\cos \delta_e) - lsin \delta_e \\ ln(1-\cos \delta_e) - msin \delta_e & mn(1-\cos \delta_e) + lsin \delta_e & \cos \delta_e + n^2(1-\cos \delta_e) \end{bmatrix} \begin{vmatrix} XB_{pI} \\ YB_{pI} \\ ZB_{pI} \end{vmatrix} \quad (4.2.3.5.1.15)$$

where the subscript f is omitted from the left side of the equation. Obviously, the matrix in Eq. (4.2.3.5.1.15) must be an alternate way to express the transformation $[TRNIB] = [TRNBI]^T = [TRNBI]^{-1}$ using l , m , n , and δ_e rather than Ψ_{BI} , θ_{BI} , and ϕ_{BI} . Transposing the matrix in Eq. (4.2.3.5.1.15) and equating to the sequential orthogonal rotation matrix from Eq. (1.3.8) results in:

$$\begin{aligned} [TRNBI] &= [TRN(\Psi_{BI}, \theta_{BI}, \phi_{BI})] = \begin{bmatrix} TRNBI(1,1) & TRNBI(1,2) & TRNBI(1,3) \\ TRNBI(2,1) & TRNBI(2,2) & TRNBI(2,3) \\ TRNBI(3,1) & TRNBI(3,2) & TRNBI(3,3) \end{bmatrix} \\ &= \begin{bmatrix} \cos \theta \cos \Psi & \cos \theta \sin \Psi & -\sin \theta \\ \sin \phi \sin \theta \cos \Psi - \cos \phi \sin \Psi & \sin \phi \sin \theta \sin \Psi + \cos \phi \cos \Psi & \sin \phi \cos \theta \\ \cos \phi \sin \theta \cos \Psi + \sin \phi \sin \Psi & \cos \phi \sin \theta \sin \Psi - \sin \phi \cos \Psi & \cos \phi \cos \theta \end{bmatrix} \\ &= \begin{bmatrix} \cos \delta_e + l^2(1-\cos \delta_e) & lm(1-\cos \delta_e) + nsin \delta_e & ln(1-\cos \delta_e) - msin \delta_e \\ lm(1-\cos \delta_e) - nsin \delta_e & \cos \delta_e + m^2(1-\cos \delta_e) & mn(1-\cos \delta_e) + lsin \delta_e \\ ln(1-\cos \delta_e) + msin \delta_e & mn(1-\cos \delta_e) - lsin \delta_e & \cos \delta_e + n^2(1-\cos \delta_e) \end{bmatrix} \quad (4.2.3.5.1.16) \end{aligned}$$

where the BI subscripts have been left off for clarity. Inspection of Eqs. (4.2.3.5.1.16) at this point can be somewhat disheartening because it seems that after the long series of manipulations the terms in the TRNBI matrix are still just as complicated as the original pitch-yaw-roll form. Both formulations are made up of many combinations of transcendental trigonometric functions (especially when it is realized that the l , m , and n terms for the Euler axis unit vector are also trig cosine functions of the direction angles between the Euler axis and each of the three inertial axis directions). Fortunately, however, a simple variable substitution can be used which will eliminate the trig functions entirely from the four-parameter form of the rotational transformation and which will also lead to a much simpler form of the [TRNBI] matrix. The substitute variables are four "Euler parameters" which replace the l , m , n , and δ_e terms according to the relations:

$$\begin{aligned} E0BI &= \cos(\delta_e/2), E1BI = l\sin(\delta_e/2), E2BI = m\sin(\delta_e/2), E3BI = n\sin(\delta_e/2) \\ \text{or} \\ E0BI &= \cos(\delta_e/2), E1BI = \cos\alpha \sin(\delta_e/2), E2BI = \cos\beta \sin(\delta_e/2), E3BI = \cos\gamma \sin(\delta_e/2) \end{aligned} \quad (4.2.3.5.1.17)$$

Note that the four Euler parameters all have values in the range -1 to +1. Using the Euler parameters, [TRNBI] can be rewritten (after repeated application of the trig "half-angle" formulas) as:

$$\begin{aligned} [\text{TRNBI}] &= \begin{bmatrix} \text{TRNBI}(1,1) & \text{TRNBI}(1,2) & \text{TRNBI}(1,3) \\ \text{TRNBI}(2,1) & \text{TRNBI}(2,2) & \text{TRNBI}(2,3) \\ \text{TRNBI}(3,1) & \text{TRNBI}(3,2) & \text{TRNBI}(3,3) \end{bmatrix} \\ &= \begin{bmatrix} E1^2 + E0^2 - E2^2 - E3^2 & 2(E1*E2 + E3*E0) & 2(E1*E3 - E2*E0) \\ 2(E1*E2 - E3*E0) & E2^2 + E0^2 - E1^2 - E3^2 & 2(E2*E3 + E1*E0) \\ 2(E1*E3 + E2*E0) & 2(E2*E3 - E1*E0) & E3^2 + E0^2 - E1^2 - E2^2 \end{bmatrix} \end{aligned} \quad (4.2.3.5.1.18)$$

where again the BI subscripts have been omitted for clarity. Note that the Eq. (4.2.3.5.1.18) form of the transformation matrix includes only simple algebraic functions with no transcendental trig functions.

The actual mathematical process of moving from the form of Eq. (4.2.3.5.1.16) to the form of Eq. (4.2.3.5.1.18) is rather tedious, but the reverse equivalence of the two forms can be demonstrated in a rather straightforward manner. For example, beginning with the TRNBI(1,1) term from Eq. (4.2.3.5.1.18) and inserting the Euler parameter definitions from Eq. (4.2.3.5.1.17):

$$\begin{aligned} \text{TRNBI}(1,1) &= E1BI^2 + E0BI^2 - E2BI^2 - E3BI^2 \\ &= l^2 \sin^2(\delta_e/2) + \cos^2(\delta_e/2) - m^2 \sin^2(\delta_e/2) - n^2 \sin^2(\delta_e/2) \end{aligned} \quad (4.2.3.5.1.19)$$

This can be expanded using the trigonometric "half-angle" formulas and the relation that $l^2 + m^2 + n^2 = 1$ for the Euler axis direction cosines (since \vec{i}_e is a unit vector):

$$\begin{aligned}
\text{TRNBI}(1,1) &= \\
l^2(1 - \cos \delta_e)/2 + (1 + \cos \delta_e)/2 - m^2(1 - \cos \delta_e)/2 - n^2(1 - \cos \delta_e)/2 \\
&= (1 + \cos \delta_e)/2 + 2l^2(1 - \cos \delta_e)/2 - (l^2 + m^2 + n^2)(1 - \cos \delta_e)/2 \\
&= 1/2 + 1/2\cos \delta_e + l^2(1 - \cos \delta_e) - 1/2 + 1/2\cos \delta_e \\
&= l^2(1 - \cos \delta_e) + \cos \delta_e
\end{aligned} \tag{4.2.3.5.1.20}$$

which matches the TRNBI(1,1) term from Eq. (4.2.3.5.16). It may also be instructive to show the equivalence for one of the off-diagonal terms:

$$\begin{aligned}
\text{TRNBI}(1,3) &= 2(E1BI * E3BI - E2BI * E0BI) \\
&= 2(l \sin(\delta_e/2) n \sin(\delta_e/2) - m \sin(\delta_e/2) \cos(\delta_e/2))
\end{aligned} \tag{4.2.3.5.1.21}$$

Again using the trig half-angle formulas:

$$\begin{aligned}
\text{TRNBI}(1,3) &= 2(l \sqrt{(1 - \cos \delta_e)/2} n \sqrt{(1 - \cos \delta_e)/2}) \\
&\quad - m \sqrt{(1 - \cos \delta_e)/2} \sqrt{(1 + \cos \delta_e)/2}) \\
&= 2(l n \sqrt{(1 - \cos \delta_e)/2}^2 - m \sqrt{((1 - \cos \delta_e)/2)((1 + \cos \delta_e)/2)}) \\
&= 2(l n (1 - \cos \delta_e)/2) - 2m \sqrt{(1 - \cos^2(\delta_e)/4)} \\
&= l n (1 - \cos \delta_e) - 2m \sqrt{\sin^2(\delta_e/4)} \\
&= l n (1 - \cos \delta_e) - m \sin \delta_e
\end{aligned} \tag{4.2.3.5.1.22}$$

which agrees with the TRNBI(1,3) term from Eq. (4.2.3.5.16).

It should be pointed out that only recently have attempts been made to standardize the names for the four Euler parameters. In various texts they have been named E1 through E4 (in a scrambled order from the E0 through E3 names used herein), or Q1 through Q4, or L0 through L3, or even a, b, c, d. The nomenclature used in the current text follows the suggestion made in American National Standard ANSI/AIAA R-004-1992 (Ref. 12) recently proposed by the American Institute of Aeronautics and Astronautics for the American National Standards Institute.

Since there are four Euler parameters and it has already been demonstrated that orientations can be uniquely defined by only three sequential modified Euler rotation angles, it follows that there must be a redundancy relationship which interrelates the Euler parameters. That relationship is based on orthogonality:

$$E0BI^2 + E1BI^2 + E2BI^2 + E3BI^2 = 1 \tag{4.2.3.5.1.23}$$

Equation (4.2.3.5.1.19) can be proved by inserting the Euler parameter definitions from Eq. (4.2.3.5.1.17):

$$\begin{aligned}
\cos^2(\delta_e/2) + l^2 \sin^2(\delta_e/2) + m^2 \sin^2(\delta_e/2) + n^2 \sin^2(\delta_e/2) &= 1 \\
\cos^2(\delta_e/2) + (l^2 + m^2 + n^2) \sin^2(\delta_e/2) &= 1 \\
\cos^2(\delta_e/2) + \sin^2(\delta_e/2) &= 1
\end{aligned} \tag{4.2.3.5.1.24}$$

where use is again made of the fact that the magnitude of the Euler unit vector is one.

Using Eq. (4.2.3.5.1.23), the matrix of Eq. (4.2.3.5.1.18) can be written in an alternate form which is sometimes also encountered in the literature:

$$[\text{TRNBI}] = \begin{bmatrix} 2(E1^2 + E0^2) - 1 & 2(E1*E2 + E3*E0) & 2(E1*E3 - E2*E0) \\ 2(E1*E2 - E3*E0) & 2(E2^2 + E0^2) - 1 & 2(E2*E3 + E1*E0) \\ 2(E1*E3 + E2*E0) & 2(E2*E3 - E1*E0) & 2(E3^2 + E0^2) - 1 \end{bmatrix} \quad (4.2.3.5.1.25)$$

Although the derivation of the four-parameter form of the rotation matrix has been rather long and tedious, the actual use of the four parameters in a simulation is simple. They are generally used as intermediate variables for calculation purposes only. Initial angular orientations are still normally input to the simulation by three input modified Euler angles which are converted to the four parameter form internally. Similarly, the time-dependent angular orientations from the simulation are normally converted from the four parameter form to modified Euler angles before being output because most analysts have a better understanding and interpretation of vehicle orientation in the sequential rotation angle form. Thus, although several pages of the derivation of the Euler parameter form have been presented, only the final form of Eq. (4.2.3.5.1.25) or Eq. (4.3.2.1.18) and the conversion equations of modified Euler angles to and from Euler parameters developed in the next several sections are needed to actually use them.

4.2.3.5.2 Computing Euler Parameters Given [TRNBI]

Thus far, the definitions for the Euler parameters (Eq. 4.2.3.5.1.17) and the [TRNBI] matrix [Eq. (4.2.3.5.1.18)] have been presented for cases where l , m , n , and δ_e are known. Such definitions are of little practical use, however, because the terms are rarely available *a priori*. Of more practical interest is the computation of Euler parameters when the terms of the [TRNBI] matrix itself are known. The needed relations can be developed from the four equations of Eqs. (4.2.3.5.1.18) and (4.2.3.5.1.19) in a rather straightforward manner although some difficulties arise because the Euler parameters are not necessarily uniquely determined by specifying [TRNBI]. Similar uniqueness issues also occur, of course, when the three sequential rotational angles are extracted from [TRNBI] using the relations of Eqs. (1.3.9) and (1.3.12) which is why the angles are mapped into the specified ranges in the definitions. For the Euler single equivalent rotation transformation, identical transformation matrices are created for (a) rotation about the positive Euler axis, X_e , by a positive angle δ_e ; (b) rotation about the negative Euler axis, $-X_e$, through a (negative) angle $-\delta_e$; (c) rotation about the positive X_e axis through the angle $-(2\pi - \delta_e)$; and (d) rotation about the negative X_e axis through the angle $+(2\pi - \delta_e)$. The first two rotations are described by identical values of $E0BI$, $E1BI$, $E2BI$, and $E3BI$, while the final two rotations have the same magnitudes of the four Euler parameters with opposite signs.

The relations for the Euler parameters as a function of the terms in the direction cosine transformation matrix are derived simply by taking ratios of appropriate terms in Eq. (4.2.3.5.1.18). First, adding the main diagonal elements (the "trace" of the matrix):

$$\begin{aligned}
& E1BI^2 + E0BI^2 - E2BI^2 - E3BI^2 + E2BI^2 + E0BI^2 - E1BI^2 - E3BI^2 + E3BI^2 + E0BI^2 - E1BI^2 - E2BI^2 \\
& = TRNBI(1,1) + TRNBI(2,2) + TRNBI(3,3) \\
& = -E1BI^2 + 3 E0BI^2 - E2BI^2 - E3BI^2 = -(E0BI^2 + E1BI^2 + E2BI^2 + E3BI^2) + 4 E0BI^2
\end{aligned} \tag{4.2.3.5.2.1}$$

which, using the orthogonality condition [Eq. (4.2.3.5.1.22)] can be rearranged as:

$$E0BI = (1/2) \sqrt{(1 + TRNBI(1,1) + TRNBI(2,2) + TRNBI(3,3))} \tag{4.2.3.5.2.2}$$

The expressions for the other three Euler parameters are obtained by subtracting the symmetric off-diagonal terms of Eq. (4.2.3.5.1.18) from one another. For example:

$$\begin{aligned}
& 2(E2BI * E3BI + E1BI * E0BI) - 2(E2BI * E3BI - E1BI * E0BI) = TRNBI(2,3) - TRNBI(3,2) \\
& = 4E1BI * E0BI
\end{aligned} \tag{4.2.3.5.2.3}$$

and similarly for the other two off-diagonal pairs. Rearranging:

$$\begin{aligned}
E1BI &= (TRNBI(2,3) - TRNBI(3,2)) / (4 E0BI) \\
E2BI &= (TRNBI(3,1) - TRNBI(1,3)) / (4 E0BI) \\
E3BI &= (TRNBI(1,2) - TRNBI(2,1)) / (4 E0BI)
\end{aligned} \tag{4.2.3.5.2.4}$$

The sign of $E0BI$ is not determined from Eq. (4.2.3.5.2.2), but if a positive sign is always assumed by convention, then the correct signs for $E1BI$, $E2BI$, and $E3BI$ are automatic from Eq. (4.2.3.5.2.4).

4.2.3.5.3 Computing Sequential Yaw-Pitch-Roll Angles Given Euler Parameters

The relationships for translating Euler parameters to sequential yaw-pitch-roll modified Euler angles are easily obtained by straightforward applications of Eqs. (1.3.9) or (1.3.12) using the terms of Eqs. (4.2.3.5.1.18) or (4.2.3.5.1.21).

$$\begin{aligned}
\Psi_{BI} &= \tan^{-1} \{ TRNBI(1,2) / TRNBI(1,1) \} \\
&= \tan^{-1} \{ 2(E1BI * E2BI + E3BI * E0BI) / (E1BI^2 + E0BI^2 - E2BI^2 - E3BI^2) \} \\
&= \tan^{-1} \{ 2(E1BI * E2BI + E3BI * E0BI) / (2(E1BI^2 + E0BI^2) - 1) \}
\end{aligned}$$

where $-180 < \Psi_{BI} < 180$

$$\theta_{BI} = \sin^{-1} \{ -TRNBI(1,3) \} = \sin^{-1} \{ -2(E1BI * E3BI - E2BI * E0BI) \}$$

where $-90 < \theta_{BI} < 90$

$$\begin{aligned}
\phi_{BI} &= \tan^{-1} \{ TRNBI(2,3) / TRNBI(3,3) \} \\
&= \tan^{-1} \{ 2(E2BI * E3BI + E1BI * E0BI) / (E3BI^2 + E0BI^2 - E1BI^2 - E2BI^2) \} \\
&= \tan^{-1} \{ 2(E2BI * E3BI + E1BI * E0BI) / (2(E3BI^2 + E0BI^2) - 1) \}
\end{aligned}$$

where $-180 < \phi_{BI} < 180$

$$(4.2.3.5.3.1)$$

4.2.3.5.4 Computing Euler Parameters Given Sequential Yaw-Pitch-Roll Angles

The Euler parameters can be determined from the yaw-pitch-roll sequence modified Euler angles by substituting the matrix terms from Eq. (4.2.3.5.1.16) into Eqs. (4.2.3.5.2.2) and (4.2.3.5.2.4).

$$\begin{aligned} E0BI = & (1/2) \text{SQRT}(1 + \cos \theta_{BI} \cos \psi_{BI} + \sin \phi_{BI} \sin \theta_{BI} \sin \psi_{BI} + \cos \phi_{BI} \cos \psi_{BI} \\ & + \cos \phi_{BI} \cos \theta_{BI}) \end{aligned}$$

$$E1BI = (\sin \phi_{BI} \cos \theta_{BI} - \cos \phi_{BI} \sin \theta_{BI} \sin \psi_{BI} + \sin \phi_{BI} \cos \psi_{BI}) / (4 E0BI)$$

$$E2BI = (\cos \phi_{BI} \sin \theta_{BI} \cos \psi_{BI} + \sin \phi_{BI} \sin \psi_{BI} + \sin \theta_{BI}) / (4 E0BI)$$

$$E3BI = (\cos \theta_{BI} \sin \psi_{BI} - \sin \phi_{BI} \sin \theta_{BI} \cos \psi_{BI} + \cos \phi_{BI} \sin \psi_{BI}) / (4 E0BI) \quad (4.2.3.5.4.1)$$

The form of Eq. (4.2.3.5.4.1) has apparent singularities in the E1BI, E2BI, and E3BI equations for E0BI = 0.0. These can be eliminated by rearranging Eqs. (4.2.3.5.4.1) by repeated and extensive use of the trigonometry half-angle formulas:

$$E0BI = \cos(\phi_{BI}/2)\cos(\theta_{BI}/2)\cos(\psi_{BI}/2) + \sin(\phi_{BI}/2)\sin(\theta_{BI}/2)\sin(\psi_{BI}/2)$$

$$E1BI = -\cos(\phi_{BI}/2)\sin(\theta_{BI}/2)\sin(\psi_{BI}/2) + \sin(\phi_{BI}/2)\cos(\theta_{BI}/2)\cos(\psi_{BI}/2)$$

$$E2BI = \cos(\phi_{BI}/2)\sin(\theta_{BI}/2)\cos(\psi_{BI}/2) + \sin(\phi_{BI}/2)\cos(\theta_{BI}/2)\sin(\psi_{BI}/2)$$

$$E3BI = \cos(\phi_{BI}/2)\cos(\theta_{BI}/2)\sin(\psi_{BI}/2) - \sin(\phi_{BI}/2)\sin(\theta_{BI}/2)\cos(\psi_{BI}/2) \quad (4.2.3.5.4.2)$$

Once again the actual mathematical process of moving from the form of Eq. (4.2.3.5.4.1) is quite tedious, but the reverse equivalence of the two forms can be demonstrated in a rather straightforward manner. For example, beginning with the first expression of Eq. (4.2.3.5.4.2) and substituting in the "half-angle" formulas:

$$\begin{aligned} E0BI = & \sqrt{\frac{(1 + \cos \phi_{BI})}{2}} \sqrt{\frac{(1 + \cos \theta_{BI})}{2}} \sqrt{\frac{(1 + \cos \psi_{BI})}{2}} + \sqrt{\frac{(1 - \cos \phi_{BI})}{2}} \sqrt{\frac{(1 - \cos \theta_{BI})}{2}} \sqrt{\frac{(1 - \cos \psi_{BI})}{2}} \\ = & \sqrt{\frac{(1 + \cos \phi_{BI})(1 + \cos \theta_{BI})(1 + \cos \psi_{BI})}{8}} + \sqrt{\frac{(1 - \cos \phi_{BI})(1 - \cos \theta_{BI})(1 - \cos \psi_{BI})}{8}} \end{aligned} \quad (4.2.3.5.4.3)$$

Now square both sides:

$$\begin{aligned}
 E0BI^2 &= \frac{(1+\cos\phi_{BI})(1+\cos\theta_{BI})(1+\cos\psi_{BI})}{8} + \frac{(1-\cos\phi_{BI})(1-\cos\theta_{BI})(1-\cos\psi_{BI})}{8} \\
 &\quad + 2 \sqrt{\frac{(1+\cos\phi_{BI})(1+\cos\theta_{BI})(1+\cos\psi_{BI})}{8}} \sqrt{\frac{(1-\cos\phi_{BI})(1-\cos\theta_{BI})(1-\cos\psi_{BI})}{8}} \\
 &= [1 + \cos\theta_{BI} + \cos\phi_{BI} + \cos\phi_{BI}\cos\theta_{BI} + \cos\psi_{BI} + \cos\theta_{BI}\cos\psi_{BI} + \cos\phi_{BI}\cos\psi_{BI} \\
 &\quad + \cos\phi_{BI}\cos\theta_{BI}\cos\psi_{BI}] / 8 \\
 &\quad + [1 - \cos\theta_{BI} - \cos\phi_{BI} + \cos\phi_{BI}\cos\theta_{BI} - \cos\psi_{BI} + \cos\theta_{BI}\cos\psi_{BI} + \cos\phi_{BI}\cos\psi_{BI} \\
 &\quad - \cos\phi_{BI}\cos\theta_{BI}\cos\psi_{BI}] / 8 \\
 &\quad + 2 \sqrt{[(1 - \cos^2\phi_{BI})(1 - \cos^2\theta_{BI})(1 - \cos^2\psi_{BI})] / 64} \\
 &= [2 + 2\cos\phi_{BI}\cos\theta_{BI} + 2\cos\theta_{BI}\cos\psi_{BI} + 2\cos\phi_{BI}\cos\psi_{BI}] / 8 \\
 &\quad + 2 \sqrt{[(\sin^2\phi_{BI})(\sin^2\theta_{BI})(\sin^2\psi_{BI})] / 64} \\
 &= [1 + \cos\phi_{BI}\cos\theta_{BI} + \cos\theta_{BI}\cos\psi_{BI} + \cos\phi_{BI}\cos\psi_{BI}] / 4 \\
 &\quad + [\sin\phi_{BI}\sin\theta_{BI}\sin\psi_{BI}] / 4 \tag{4.2.3.5.4.4}
 \end{aligned}$$

Finally, taking the square root of both sides:

$$\begin{aligned}
 E0BI &= (1/2) \text{SQRT}(1 + \cos\phi_{BI}\cos\theta_{BI} + \cos\phi_{BI}\cos\psi_{BI} + \cos\phi_{BI}\cos\theta_{BI} \\
 &\quad + \sin\phi_{BI}\sin\theta_{BI}\sin\psi_{BI}) \tag{4.2.3.5.4.5}
 \end{aligned}$$

which agrees with Eq. (4.2.3.5.4.1).

4.2.3.5.5 Euler Parameter Derivatives

The time derivatives of the Euler parameters are obtained simply by differentiating the expressions for the Euler parameters from Eqs. (4.2.3.5.2.2) and (4.2.3.5.2.4). First, it is convenient to rewrite the equations as:

$$\begin{aligned}
 4 E0BI^2 &= 1 + TRNBI(1,1) + TRNBI(2,2) + TRNBI(3,3) \\
 4 E0BI E1BI &= TRNBI(2,3) - TRNBI(3,2) \\
 4 E0BI E2BI &= TRNBI(3,1) - TRNBI(1,3) \\
 4 E0BI E3BI &= TRNBI(1,2) - TRNBI(2,1) \tag{4.2.3.5.5.1}
 \end{aligned}$$

Now take derivatives of each equation by the chain rule:

$$\begin{aligned} 8 E0BI DE0BI &= DTRNBI(1,1) + DTRNBI(2,2) + DTRNBI(3,3) \\ 4 E0BI DE1BI + 4 DE0BI E1BI &= DTRNBI(2,3) - DTRNBI(3,2) \\ 4 E0BI DE2BI + 4 DE0BI E2BI &= DTRNBI(3,1) - DTRNBI(1,3) \\ 4 E0BI DE3BI + 4 DE0BI E3BI &= DTRNBI(1,2) - DTRNBI(2,1) \end{aligned} \quad (4.2.3.5.5.2)$$

Next, replacing the derivative transformation matrix elements on the right side of Eqs. (4.2.3.5.5.2) with the relations of Eq. (4.2.3.3.9):

$$\begin{aligned} 8 E0BI DE0BI &= RBBI * TRNBI(2,1) - QBBI * TRNBI(3,1) + PBBI * TRNBI(3,2) \\ &\quad - RBBI * TRNBI(1,2) + QBBI * TRNBI(1,3) - PBBI * TRNBI(2,3) \\ 4 E0BI DE1BI + 4 DE0BI E1BI &= PBBI * TRNBI(3,3) - RBBI * TRNBI(1,3) \\ &\quad - QBBI * TRNBI(1,2) + PBBI * TRNBI(2,2) \quad (4.2.3.5.5.3) \\ 4 E0BI DE2BI + 4 DE0BI E2BI &= QBBI * TRNBI(1,1) - PBBI * TRNBI(2,1) \\ &\quad - RBBI * TRNBI(2,3) + QBBI * TRNBI(3,3) \\ 4 E0BI DE3BI + 4 DE0BI E3BI &= RBBI * TRNBI(2,2) - QBBI * TRNBI(3,2) \\ &\quad - PBBI * TRNBI(3,1) + RBBI * TRNBI(1,1) \end{aligned}$$

The four expressions of Eq. (4.2.3.5.5.3) can now be rearranged to give:

$$\begin{aligned} DE0BI &= [PBBI(TRNBI(3,2) - TRNBI(2,3)) + QBBI(TRNBI(1,3) - TRNBI(3,1)) \\ &\quad + RBBI(TRNBI(2,1) - TRNBI(1,2))] / (8 E0BI) \\ DE1BI &= -(DE0BI E1BI) / E0BI + [PBBI(TRNBI(3,3) + TRNBI(2,2)) \\ &\quad - QBBI(TRNBI(1,2)) - RBBI(TRNBI(1,3))] / (4 E0BI) \\ DE2BI &= -(DE0BI E2BI) / E0BI + [-PBBI(TRNBI(2,1)) \\ &\quad + QBBI(TRNBI(1,1) + TRNBI(3,3)) - RBBI(TRNBI(2,3))] / (4 E0BI) \quad (4.2.3.5.5.4) \\ DE3BI &= -(DE0BI E3BI) / E0BI + [-PBBI(TRNBI(3,1)) \\ &\quad - QBBI(TRNBI(3,2)) + RBBI(TRNBI(1,1) + TRNBI(2,2))] / (4 E0BI) \end{aligned}$$

The TRNBI elements in Eq. (4.2.3.5.5.4) can now be replaced with the equivalent Euler parameter elements from Eq. (4.2.3.5.1.1.18):

$$\begin{aligned} DE0BI &= [PBBI(2(E2BI * E3BI - E1BI * E0BI) - 2(E2BI * E3BI + E1BI * E0BI)) \\ &\quad + QBBI(2(E1BI * E3BI - E2BI * E0BI) - 2(E1BI * E3BI + E2BI * E0BI)) \\ &\quad + RBBI(2(E1BI * E2BI - E3BI * E0BI) - 2(E1BI * E2BI + E3BI * E0BI))] / (8 E0BI) \end{aligned}$$

$$\begin{aligned}
DE1BI &= - (DE0BI E1BI)/E0BI \\
&\quad + [PBBI(E3BI^2 + E0BI^2 - E1BI^2 - E2BI^2 + E2BI^2 + E0BI^2 - E1BI^2 - E3BI^2) \\
&\quad - QBBI(2(E1BI*E2BI + E3BI*E0BI)) \\
&\quad - RBBI(2(E1BI*E3BI - E2BI*E0BI))]/(4 E0BI) \\
\\
DE2BI &= - (DE0BI E2BI)/E0BI \\
&\quad + [-PBBI(2(E1BI*E2BI - E3BI*E0BI)) \\
&\quad + QBBI(E1BI^2 + E0BI^2 - E2BI^2 - E3BI^2 + E3BI^2 + E0BI^2 - E1BI^2 - E2BI^2) \\
&\quad - RBBI(2(E2BI*E3BI + E1BI*E0BI))]/(4 E0BI) \\
\\
DE3BI &= - (DE0BI E3BI)/E0BI \\
&\quad + [-PBBI(2(E1BI*E3BI + E2BI*E0BI)) \\
&\quad - QBBI(2(E2BI*E3BI - E1BI*E0BI)) \\
&\quad + RBBI(E1BI^2 + E0BI^2 - E2BI^2 - E3BI^2 + E2BI^2 + E0BI^2 - E1BI^2 - E3BI^2)]/(4 E0BI)
\end{aligned} \tag{4.2.3.5.5.5}$$

Rearranging and substituting the DE0BI expression into the other three expressions:

$$\begin{aligned}
DE0BI &= [PBBI (-4 E1BI*E0BI) + QBBI (-4 E2BI*E0BI) + RBBI (-4 E3BI*E0BI)]/(8E0BI) \\
&= (-1/2) [PBBI E1BI + QBBI E2BI + RBBI E3BI] \\
\\
DE1BI &= (E1BI [PBBI E1BI + QBBI E2BI + RBBI E3BI]/(2 E0BI) \\
&\quad + [PBBI(2 E0BI^2 - 2 E1BI^2) \\
&\quad - QBBI(2(E1BI*E2BI + E3BI*E0BI)) \\
&\quad - RBBI(2(E1BI*E3BI - E2BI*E0BI))]/(4 E0BI) \\
&= [PBBI(2 E1BI^2 + 2 E0BI^2 - 2 E1BI^2) \\
&\quad + QBBI(2(E1BI*E2BI - E1BI*E2BI - E3BI*E0BI)) \\
&\quad + RBBI(2(E1BI*E3BI - E1BI*E3BI + E2BI*E0BI))]/(4 E0BI) \\
&= (-1/2) [-PBBI E0BI + QBBI E3BI - RBBI E2BI] \\
\\
DE2BI &= - (DE0BI E2BI)/E0BI \\
&\quad + [-PBBI(2(E1BI*E2BI - E3BI*E0BI)) \\
&\quad + QBBI(E1BI^2 + E0BI^2 - E2BI^2 - E3BI^2 + E3BI^2 + E0BI^2 - E1BI^2 - E2BI^2) \\
&\quad - RBBI(2(E2BI*E3BI + E1BI*E0BI))]/(4 E0BI) \\
&= (-1/2) [-PBBI E3BI - QBBI E0BI + RBBI E1BI] \\
\\
DE3BI &= - (DE0BI E3BI)/E0BI \\
&\quad + [-PBBI(2(E1BI*E3BI + E2BI*E0BI)) \\
&\quad - QBBI(2(E2BI*E3BI - E1BI*E0BI)) \\
&\quad + RBBI(E1BI^2 + E0BI^2 - E2BI^2 - E3BI^2 + E2BI^2 + E0BI^2 - E1BI^2 - E3BI^2)]/(4 E0BI) \\
&= (-1/2) [PBBI E2BI - QBBI E1BI - RBBI E0BI]
\end{aligned} \tag{4.2.3.5.5.6}$$

This can be written in matrix form as:

$$\begin{vmatrix} DE0BI \\ DE1BI \\ DE2BI \\ DE3BI \end{vmatrix} = (-1/2) \begin{bmatrix} 0 & PBBI & QBBI & RBBI \\ -PBBI & 0 & -RBBI & QBBI \\ -QBBI & RBBI & 0 & -PBBI \\ -RBBI & -QBBI & PBBI & 0 \end{bmatrix} \begin{vmatrix} E0BI \\ E1BI \\ E2BI \\ E3BI \end{vmatrix} \quad (4.2.3.5.5.7)$$

Note that the matrix in Eq. (4.2.3.5.5.7) is a 16-element form of a skew-symmetric matrix and is analogous to the 9-element form of Eq. (1.4.7). Note that because of the constant multiplier of (-1/2) in Eq. (4.2.3.5.5.7), the Euler parameter rates have rough magnitudes of about half or less of the magnitude of the largest body-axis angular rate (usually PBBI) considering that the Euler parameters on the right of the equation all have magnitudes of unity or less. This gives the four parameter methods an additional advantage over the 3 by 3 matrix and modified Euler angle forms when choosing integration time steps - time steps can be larger because the slopes of the terms being integrated are smaller.

In numerical trajectory simulations, Eq. (4.2.3.5.5.7) is used to determine the Euler parameter derivatives at each time step. These derivatives are then used in a numerical time integration to determine the Euler parameters for the body rotation at the next time step. Two procedures, based on the orthogonality redundancy relation of Eq. (4.2.3.5.1.19) can be used to remove any integration bias errors. If a numerical error term is defined as:

$$\epsilon = 1 - (E0BI^2 + E1BI^2 + E2BI^2 + E3BI^2), \quad (4.2.3.5.5.8)$$

it is desirable to minimize the sum of the squares of the error, ϵ^2 . The first procedure is to add a correction term to the right-hand side of Eq. (4.2.3.5.5.7) proportional to the negative of the gradient of the error with respect to each Euler parameter. For example, the correction term for the E1BI parameter would be:

$$\frac{-d\epsilon^2}{dE1BI} = \frac{-2\epsilon d\epsilon}{dE1BI} = -2\epsilon(-2E1BI) = 4\epsilon E1BI \quad (4.2.3.5.5.9)$$

Adding this term to the DE1BI drives E1BI in the proper direction to reduce ϵ . Similar terms can be developed for the other Euler parameters and Eq. (4.2.3.5.5.7) can be rewritten using them as:

$$\begin{vmatrix} DE0BI \\ DE1BI \\ DE2BI \\ DE3BI \end{vmatrix} = (-1/2) \begin{bmatrix} 0 & PBBI & QBBI & RBBI \\ -PBBI & 0 & -RBBI & QBBI \\ -QBBI & RBBI & 0 & -PBBI \\ -RBBI & -QBBI & PBBI & 0 \end{bmatrix} \begin{vmatrix} E0BI \\ E1BI \\ E2BI \\ E3BI \end{vmatrix} + \begin{vmatrix} keE0BI \\ keE1BI \\ keE2BI \\ keE3BI \end{vmatrix} \quad (4.2.3.5.5.10)$$

where the k factor can be used instead of the factor of 4 to accelerate convergence. The second method for minimizing integration errors is more simple but not quite as rigorous. For the second approach, the Euler parameter rates are first integrated to determine an initial estimation for the

new Euler parameters. A least-squares correction factor to account for integration errors is determined by:

$$EC = 1/SQRT(E0BI^2 + E1BI^2 + E2BI^2 + E3BI^2) \quad (4.2.3.5.5.11)$$

and the Euler parameters from the initial iteration are recomputed as:

$$\begin{vmatrix} E0BI \\ E1BI \\ E2BI \\ E3BI \end{vmatrix} = \begin{vmatrix} E0BI*EC \\ E1BI*EC \\ E2BI*EC \\ E3BI*EC \end{vmatrix} \quad (4.2.3.5.5.12)$$

This second approach is used more often in numerical simulations because it is easier to implement.

Equation (4.2.3.5.5.7) for the derivatives of the Euler parameters can also be rearranged for cases where the rotational velocity vector is considered to be the independent parameter rather than the Euler parameters:

$$\begin{vmatrix} DE0BI \\ DE1BI \\ DE2BI \\ DE3BI \end{vmatrix} = (-1/2) \begin{vmatrix} E1BI & E2BI & E3BI \\ -E0BI & E3BI & -E2BI \\ -E3BI & -E0BI & E1BI \\ E2BI & -E1BI & -E0BI \end{vmatrix} \begin{vmatrix} PBBI \\ QBBI \\ RBBI \end{vmatrix} \quad (4.2.3.5.5.13)$$

where a 4 by 3 matrix of the Euler parameters is used.

Equations (4.2.3.5.5.7) and (4.2.3.5.5.13) define how the Euler parameter derivatives are determined when the Euler parameters and the angular velocities are known. For some applications (such as extraction of motion properties from flight or scaled drop model data) the inverse problem of determination of angular velocities given the Euler parameters and their derivatives must be solved. The relations are developed by inserting the expressions for the direction cosines and their derivatives from Eq. (4.2.3.5.1.8) into the relations of Eq. (4.2.3.3.14). The expression for the body-axis roll rate, for example, is developed as:

$$\begin{aligned} PBBI &= DTRNBI(2,1)TRNBI(3,1) + DTRNBI(2,2)TRNBI(3,2) \\ &\quad + DTRNBI(2,3)TRNBI(3,3) \\ &= 2(E1BI DE2BI + DE1BI E2BI - E3BI DE0BI - DE3BI E0BI)2(E1BI E3BI + E2BI E0BI) \\ &\quad + 2(E0BI DE0BI + E2BI DE2BI - E1BI DE1BI - E3BI DE3BI)2(E2BI E3BI - E1BI E0BI) \\ &\quad + 2(E2BI DE3BI + DE2BI E3BI + E1BI DE0BI + DE1BI E0BI)(E3BI^2 + E0BI^2 - E1BI^2 - E2BI^2) \end{aligned} \quad (4.2.3.5.5.14)$$

Expanding out and temporarily dropping the BI subscripts for clarity:

$$\begin{aligned}
 \text{PBBI} &= 4 [E1^2 DE2 E3 + DE1 E1 E2 E3^2 - DE0 E1 E3 - E0 E1 DE3 E3 \\
 &\quad + E0 E1 DE2 E2 + E0 DE1 E2^2 - DE0 E0 E2 E3 - E0^2 E2 DE3 \\
 &\quad + DE0 E0 E2 E3 + DE2 E2^2 E3 - DE1 E1 E2 E3 - E2 DE3 E3^2 \\
 &\quad - DE0 E0^2 E1 - E0 E1 DE2 E2 + E0 DE1 E1^2 + E0 E1 DE3 E3] \\
 &+ 2 [E2 DE3 E3^2 + DE2 E3^3 + DE0 E1 E3^2 + E0 DE1 E3^2 \\
 &\quad + E0^2 E2 DE3 + E0^2 DE2 E3 + DE0 E0^2 E1 + E0^3 DE1 \\
 &\quad - E1^2 E2 DE3 - E1^2 DE2 E3 - DE0 E1^3 - E0 DE1 E1^2 - E2^3 DE3 \\
 &\quad - DE2 E2^2 E3 - DE0 E1 E2^2 - E0 DE1 E2^2] \\
 &= 2E1^2 DE2 E3 - 2DE0 E1 E3^2 + 2E0 DE1 E2^2 - 2E0^2 E2 DE3 + 2DE2 E2^2 E3 \\
 &\quad - 2E2 DE3 E3^2 - 2DE0 E0^2 E1 + 2E0 DE1 E1^2 + 2DE2 E3^3 + 2E0 DE1 E3^2 \\
 &\quad + 2E0^2 DE2 E3 + 2E0^3 DE1 - 2E1^2 E2 DE3 - 2DE0 E1^3 - 2E2^3 DE3 - 2E0 E1 E2^2 \\
 &= 2DE2 E3 (E1^2 + E2^2 + E3^2 + E0^2) - 2DE0 E1 (E1^2 + E2^2 + E3^2 + E0^2) \\
 &\quad + 2E0 DE1 (E1^2 + E2^2 + E3^2 + E0^2) - 2E2 DE3 (E1^2 + E2^2 + E3^2 + E0^2) \\
 &= 2DE2 E3 - 2DE0 E1 + 2E0 DE1 - 2E2 DE3
 \end{aligned}
 \tag{4.2.3.5.5.15}$$

Similar expressions can be developed for yaw and pitch rates resulting in the final expressions:

$$\begin{aligned}
 \text{PBBI} &= 2(-E1BI DE0BI + E0BI DE1BI + E3BI DE2BI - E2BI DE3BI) \\
 \text{QBBI} &= 2(-E2BI DE0BI - E3BI DE1BI + E0BI DE2BI + E1BI DE3BI) \\
 \text{RBBI} &= 2(-E3BI DE0BI + E2BI DE1BI - E1BI DE2BI + E0BI DE3BI)
 \end{aligned}
 \tag{4.2.3.5.5.16}$$

4.3 MATH MODELS OF PHYSICAL CONSTRAINTS FOR RESTRICTED MOTION (BOUNDARY CONDITIONS)

The translational and rotational equations of motion for restricted motion as developed in Sections 4.1.2 and 4.2.2 are completely general and arbitrary and should be adequate for any possible aircraft maneuver and physical restraint device. The equations are posed relative to an accelerating hook axis system and include unknown reaction forces and moments at the hook point. The motion equations should accurately model any type of restricted motion as long as two criteria are met. First, the accelerations and velocities of the hook point must be modeled correctly and, second, proper reaction forces and moments that emulate the actions of the physical rail and pivot constraint devices used to attach the store to the aircraft must be determined for each equation-of-motion evaluation. The equations modeling the motion of the hook point and the physical restraint devices used by a variety of current inventory aircraft are developed in this section. The constraint equations represent boundary condition equations which must be satisfied simultaneously with the basic motion equations. Equations modeling the motion of the hook point are derived in Sections 4.3.1, 4.3.2, and 4.3.9. Equations modeling a variety of physical restraint devices used on current inventory aircraft are developed in the remaining sections.

The equations modeling the accelerations, velocities, and flight path of an aircraft-fixed point (often corresponding to the installed store cg location for store separation studies), given an

idealized wings-level constant-load-factor aircraft pull-up or push-over maneuver, are first developed in Section 4.3.1. The accelerations of both a pivot point fixed with the aircraft but at an offset position from the point described in Section 4.3.1 and of a hook point free to move along a launch rail attached to the maneuvering aircraft are then developed in Section 4.3.2. The reaction moments needed to impose the "simple" idealized pivot motion constraint are determined in Section 4.3.3. Simultaneous reaction equation/motion equation models for rigorous pivot solutions representative of actual F-15, F-16, F-18, and F-22 pivot hardware are then developed in Sections 4.3.4, 4.3.5, and 4.3.6. The systems of equations for simulations of rail-launched missiles are developed in Section 4.3.7. The equations modeling cradle eject launchers which restrict the store to motion only in the plane of the ejector are developed in Section 4.3.8. Finally, extensions to the Section 4.3.1 aircraft maneuver model which allow completely arbitrary aircraft maneuvers during the release event are developed in Section 4.3.9.

4.3.1 Accelerations, Velocities, and Flight Path of a Wings-Level Constant Load Factor Aircraft Pitch-Plane Maneuver

A major difficulty involved in simulating separations from maneuvering aircraft (whether or not restrained motion is involved) is the necessity to simulate the dynamically changing flow-field environment which is experienced by the store as a result of the dynamic motion of the aircraft. Wings-level constant load factor pull-up or push-over maneuvers, however, represent a particular class of aircraft maneuvers which are well suited to wind tunnel simulations because the free-stream velocity and angle of attack of the aircraft are constant during this particular kind of maneuver and the aerodynamics of the separating store can be reasonably simulated using steady-state measurements of aircraft flow-field effects (see Section 6.0). Although capabilities to simulate store release during completely arbitrary aircraft motion are not available in wind tunnel simulations, most practical launch points in the flight envelopes of most current aircraft can be adequately represented by the constant load factor model. The equations used to model the accelerations of an aircraft undergoing an idealized constant load factor maneuver are, therefore, presented in this section. Note, however, that all motion equations developed in this document are completely rigorous and only the current section defining the aircraft motion needs to be modified to allow a completely general maneuver capability as outlined in Section 4.3.9.

The wings-level constant load factor push-over or pull-up maneuver can be idealized as a circular arc flight motion in a plane normal to the local earth horizontal. The rotation of the aircraft weight vector relative to the aircraft as it pitches during the circular flight maneuver is usually ignored in wind tunnel simulations, although it is possible to also include this effect in more rigorous simulations. The idealized maneuver is illustrated in Fig. 17. An axis system aligned with the current tangent to the aircraft flight path at each time step in the trajectory and designated by the letter "F" for flight axes will be used in this section to help define the aircraft maneuver. If a force balance is made at the bottom of the loop in Fig. 17 (where the gravity vector is truly directly opposite the lift vector):

$$m * AZFFI = -Lift + Weight \quad (4.3.1.1)$$

Dividing through by m and multiplying by a ratio of the earth gravitational acceleration with itself:

$$\frac{AZFFI}{mGG} = \frac{(Weight - Lift)}{mGG} GG = \frac{(Weight - Lift)}{Weight} GG = \frac{(1 - Nz) GG}{Weight} \quad (4.3.1.2)$$

where Nz is known as the normal load factor. Note that the load factor is one for an aircraft in non-maneuvering wings-level flight.

For store separation purposes, the flight axis origin is generally assumed to be coincident with the location of the store center of gravity when the store is installed at its carriage position on the aircraft. In more general applications, the aircraft acceleration defined in Eq. (4.3.1.2) would be defined at the aircraft center of gravity and would need to be transferred to the flight axis/installed store origin using equations similar to those developed in Eq. (3.0.8). (Such equations are developed in Section 4.3.9). For the idealized push-over/pull-up maneuver, however, accelerations of the aircraft cg and the flight-axis origin (installed store cg) will be assumed to be identical.

The entire maneuver is defined by simply specifying the load factor, Nz . All other motion parameters of the idealized circular flight path relative to inertial axes are then based on closed form solutions using the resulting acceleration. The flight axis components of the acceleration of the flight path relative to inertial axes are:

$$\begin{vmatrix} AXFFI \\ AYFFI \\ AZFFI \end{vmatrix} = \begin{vmatrix} 0.0 \\ 0.0 \\ (1-Nz) GG \end{vmatrix} \quad (4.3.1.3)$$

The idealized rotational velocity of the flight axes relative to inertial axes is (using a small-angle approximation):

$$\begin{vmatrix} PFFI \\ QFFI \\ RFFI \end{vmatrix} = \begin{vmatrix} 0.0 \\ -AZFFI/UIIW \\ 0.0 \end{vmatrix} \quad (4.3.1.4)$$

where $UIIW$ is the aircraft flight velocity relative to the wind mass at the instant of release. The radius of the idealized circular flight path is:

$$Rpar = AZFFI / QFFI \quad (4.3.1.5)$$

It should be noted that $Rpar$ generally has a very large magnitude (on the order of several miles) and that it is a negative quantity for $Nz > 1.0$

The angular orientation of the flight path relative to the inertial axes at a given time is:

$$\begin{aligned} \text{PSIFI} &= 0.0 \\ \text{THAFI} &= \text{QFFI} * \text{Time} * 57.2958 \\ \text{PHIFI} &= 0.0 \end{aligned} \quad (4.3.1.6)$$

from which [TRNFI] can be calculated according to:

$$[\text{TRNFI}] = [\text{TRNx}(\text{PHIFI})] [\text{TRNy}(\text{THAFI})] [\text{TRNz}(\text{PSIFI})] \quad (4.3.1.7)$$

From the geometry of the circle, the inertial components of the position of the flight axes relative to inertial axes at a given time are:

$$\begin{vmatrix} \text{XIFI} \\ \text{YIFI} \\ \text{ZIFI} \end{vmatrix} = \begin{vmatrix} -\text{UIIW} * \text{Time} - \text{Rpar} * \sin(\text{THAFI}) \\ 0.0 \\ \text{Rpar} (1 - \cos(\text{THAFI})) \end{vmatrix} \quad (4.3.1.8)$$

Because the circular arc flight path radius (Rpar) is often very large (several miles or more), the $\sin(\text{THAFI})$ and $(1 - \cos(\text{THAFI}))$ functions which multiply it in Eq. (4.3.1.8) should be performed in Double Precision in computer simulations. Note that when $\text{Nz} = 1.0$, Rpar goes to infinity and $\sin(\text{THAFI})$ goes to zero, so that Eq. (4.3.1.8) is undefined. For the $\text{Nz} = 1$ case, $\{\text{XIFI}, \text{YIFI}, \text{ZIFI}\} = \{0,0,0\}$ at all times (the flight axes and inertial axes are coincident).

The flight-axis components of the velocity of the flight axes relative to inertial axes for the idealized motion are:

$$\begin{vmatrix} \text{UIFI} \\ \text{VIFI} \\ \text{WIFI} \end{vmatrix} = \begin{vmatrix} -\text{UIIW} * (1 - \cos(\text{THAFI})) \\ 0.0 \\ -\text{UIIW} \sin(\text{THAFI}) \end{vmatrix} \quad (4.3.1.9)$$

For restricted pivot-motion simulations, the transfer distance between the flight axis origin (at which the maneuver acceleration is assumed to act) and the hook-axis origin is often ignored (an approximation in keeping with the built-in idealizations of the defined maneuver model). Since the hook-axis and flight-axis origins are not accelerating or translating relative to one another, the hook-axis acceleration components have sometimes been approximated by:

$$\begin{vmatrix} \text{AXBHI} \\ \text{AYBHI} \\ \text{AZBHI} \end{vmatrix} \approx [\text{TRNBF}] \begin{vmatrix} \text{AXFFI} \\ \text{AYFFI} \\ \text{AZFFI} \end{vmatrix} \quad (4.3.1.10)$$

$$\text{where } [\text{TRNBF}] = [\text{TRNBI}] [\text{TRNFI}]^{-1} \quad (4.3.1.11)$$

For more exact pivot-motion simulations and for all rail-launched missile simulations, Eq. (4.3.1.10) may not be fully adequate because of the significance of the cross and Coriolis acceleration terms associated with the motion of and offset position of the hook relative to the flight-axis origin. More exact equations are derived in the next section which allow movement of the hook relative to the aircraft and rotation of a fixed hook system with a maneuvering aircraft.

Many of the maneuver parameters as developed in this section are defined in terms of flight-axis projections. It turns out that restricted motion simulations from maneuvering aircraft are more easily implemented when certain maneuver parameters are expressed as pylon-axis mea-

surements. The pylon axis system is described at the beginning of the next section and the transformations for projecting the important flight-axis maneuver terms as developed in this section to pylon axes are provided in Eqs. (4.3.2.12) through (4.3.2.15) in the next section.

The idealized push-over or pull-up maneuver is truly representative of only wings-level aircraft flight conditions (the aircraft roll angle relative to the earth horizontal is zero). If the aircraft is rolled (banked) relative to the earth horizontal, the aircraft motion for any fixed ratio of lift to weight will represent steady-state turning motion while at the same time spiraling either upward or downward if the resolved vertical component of the aircraft aerodynamic and thrust forces in the earth axis system do not exactly balance the aircraft weight.

4.3.2 Accelerations of a Fixed or Moving Hook Axis System Attached to a Maneuvering Aircraft

A more general form of the motion of the hook-axis system is developed in this section. The derivation of the generalized hook-axis equations closely parallels the restricted translational equation derivation in Section 4.2. The hook acceleration equations will be developed in this section for the general case of a hook point moving along a rail. The special case of a fixed pivot point can then be treated by simply zeroing out downrail translational terms. Three more axis systems designated "P" (for pylon axis system), "C" (for carriage axis system), and "A" (for aircraft axis system) will be introduced to aid the derivation (although the carriage axes will not immediately be used). The pylon, carriage, and aircraft axes each share a common origin with the flight axis system at a position corresponding to the location of the store center of gravity when it is at its installed position on the aircraft. The trajectory axis origin points are fixed relative to the aircraft, however, rather than fixed with the moving store body as are the store body axes. Aircraft axes are obtained by rotating flight axes through the negative of the aircraft angle of sideslip, -Beta, and the angle of attack, Alpha, relative to the flight path which brings the aircraft axes into alignment with the reference axes of the aircraft. The pylon axes are then rotated in yaw and pitch (but not roll) relative to the aircraft axes through the carriage incidence angles, IY and IP, so that the XP axis is parallel to the store carriage orientation. Note that because the pylon axes are not rotated in roll, the pylon ZP direction is still "down" relative to the aircraft. Carriage axes also include the rotation through the carriage roll orientation, IR, so that when the store is at its carriage position, its body axes are coincident with the carriage axes.

$$\begin{aligned}
 \text{PSIAF} &= -\text{Beta} \\
 \text{THAAF} &= \text{Alpha} \\
 \text{PHIAF} &= 0.0 \\
 \\
 \text{PSIPA} &= \text{IY} \\
 \text{THAPA} &= \text{IP} \\
 \text{PHIPA} &= 0.0 \\
 \\
 \text{PSICP} &= 0.0 \\
 \text{THACP} &= 0.0 \\
 \text{PHICP} &= \text{IR} \\
 \\
 \text{PSICA} &= \text{IY} \\
 \text{THACA} &= \text{IP} \\
 \text{PHICA} &= \text{IR}
 \end{aligned} \tag{4.3.2.1}$$

The negative sign on Beta in the PSIAF term is needed because of a well-entrenched aerospace sign convention which defines positive PSI as a nose-right rotation and positive Beta as a nose-left rotation. The various trajectory axis systems are depicted in Fig. 18. An overview of the relationships between the various trajectory axes for pitch-plane-only rotations is presented in Fig. 19. Using the angles from Eq. (4.3.2.1), the following useful transformations may be derived:

$$\begin{aligned} [\text{TRNAF}] &= [\text{TRNx(PHIAF)}] [\text{TRNy(THAAF)}] [\text{TRNz(PSIAF)}] \\ [\text{TRNPA}] &= [\text{TRNx(PHIPA)}] [\text{TRNy(THAPA)}] [\text{TRNz(PSIPA)}] \\ [\text{TRNCA}] &= [\text{TRNx(PHICA)}] [\text{TRNy(THACA)}] [\text{TRNz(PSICA)}] \\ [\text{TRNCP}] &= [\text{TRNx(PHICP)}] [\text{TRNy(THACP)}] [\text{TRNz(PSICP)}] \end{aligned} \quad (4.3.2.2)$$

and

$$\begin{aligned} [\text{TRNPF}] &= [\text{TRNPA}] [\text{TRNAF}] \\ [\text{TRNCF}] &= [\text{TRNCA}] [\text{TRNAF}] \\ [\text{TRNAI}] &= [\text{TRNAF}] [\text{TRNFI}] \\ [\text{TRNPI}] &= [\text{TRNPF}] [\text{TRNFI}] \\ [\text{TRNCI}] &= [\text{TRNCF}] [\text{TRNFI}] \\ [\text{TRNBF}] &= [\text{TRNBI}] [\text{TRNFI}]^{-1} \\ [\text{TRNBA}] &= [\text{TRNBI}] [\text{TRNAI}]^{-1} \\ [\text{TRNBP}] &= [\text{TRNBI}] [\text{TRNPI}]^{-1} \\ [\text{TRNBC}] &= [\text{TRNBI}] [\text{TRNCI}]^{-1} \end{aligned} \quad (4.3.2.3)$$

where $[\text{TRNFI}]$ was defined by Eq. (4.3.1.7) for a constant N_z maneuver.

The motion of the hook axes as the hook translates down the rail parallel to the XP axis can be determined to be a combination of the motion of the pylon axes relative to inertial space and the motion of the hook point relative to the pylon axes. Beginning with the relationship between the inertial positions of inertial, hook, and pylon axes:

$$\begin{vmatrix} XIHI \\ YIHI \\ ZIHI \end{vmatrix} = \begin{vmatrix} XIPI \\ YIPI \\ ZIPI \end{vmatrix} + \begin{vmatrix} XIHP \\ YIHP \\ ZIHP \end{vmatrix} \quad (4.3.2.4)$$

where :

$$\begin{vmatrix} XIHP \\ YIHP \\ ZIHP \end{vmatrix} = [\text{TRNPI}]^{-1} \begin{vmatrix} XPHP \\ YPHP \\ ZPHP \end{vmatrix} \quad (4.3.2.5)$$

Taking derivatives of both sides using the chain rule to get inertial velocity:

$$\frac{d}{dt} \begin{vmatrix} XIHI \\ YIHI \\ ZIHI \end{vmatrix} = \frac{d}{dt} \begin{vmatrix} XIPI \\ YIPI \\ ZIPI \end{vmatrix} + \frac{d}{dt} [\text{TRNPI}]^{-1} \begin{vmatrix} XPHP \\ YPHP \\ ZPHP \end{vmatrix} + [\text{TRNPI}]^{-1} \frac{d}{dt} \begin{vmatrix} XPHP \\ YPHP \\ ZPHP \end{vmatrix} \quad (4.3.2.6)$$

or:

$$\begin{vmatrix} UIHI \\ VIHI \\ WIHI \end{vmatrix} = \begin{vmatrix} UIPI \\ VIPI \\ WIPI \end{vmatrix} + [TRNPI]^{-1} [\tilde{\omega} PPI] \begin{vmatrix} XPHP \\ YPHP \\ ZPHP \end{vmatrix} + [TRNPI]^{-1} \frac{d}{dt} \begin{vmatrix} XPHP \\ YPHP \\ ZPHP \end{vmatrix} \quad (4.3.2.7)$$

Projecting to pylon-axis components by [TRNPI] :

$$\begin{vmatrix} UPHI \\ VPHI \\ WPHI \end{vmatrix} = \begin{vmatrix} UPPI \\ VPPI \\ WPPI \end{vmatrix} + [\tilde{\omega} PPI] \begin{vmatrix} XPHP \\ YPHP \\ ZPHP \end{vmatrix} + \frac{d}{dt} \begin{vmatrix} XPHP \\ YPHP \\ ZPHP \end{vmatrix} \quad (4.3.2.8)$$

This relation provides the interconnect between pylon-axis velocities and hook velocities. A similar relation for accelerations can be developed by taking a second derivative of Eq. (4.3.2.7):

$$\begin{aligned} \frac{d}{dt} \begin{vmatrix} UIHI \\ VIHI \\ WIHI \end{vmatrix} &= \frac{d}{dt} \begin{vmatrix} UIPI \\ VIPI \\ WIPI \end{vmatrix} + \frac{d}{dt} [TRNPI]^{-1} [\tilde{\omega} PPI] \begin{vmatrix} XPHP \\ YPHP \\ ZPHP \end{vmatrix} + [TRNPI]^{-1} \frac{d}{dt} [\tilde{\omega} PPI] \begin{vmatrix} XPHP \\ YPHP \\ ZPHP \end{vmatrix} \\ &+ [TRNPI]^{-1} [\tilde{\omega} PPI] \frac{d}{dt} \begin{vmatrix} XPHP \\ YPHP \\ ZPHP \end{vmatrix} + \frac{d}{dt} [TRNPI]^{-1} \frac{d}{dt} \begin{vmatrix} XPHP \\ YPHP \\ ZPHP \end{vmatrix} + [TRNPI]^{-1} \frac{d^2}{dt^2} \begin{vmatrix} XPHP \\ YPHP \\ ZPHP \end{vmatrix} \end{aligned} \quad (4.3.2.9)$$

or:

$$\begin{aligned} \begin{vmatrix} AXIHI \\ AYIHI \\ AZIHI \end{vmatrix} &= \begin{vmatrix} AXIPI \\ AYIPI \\ AZIPI \end{vmatrix} + [TRNPI]^{-1} [\tilde{\omega} PPI] [\tilde{\omega} PPI] \begin{vmatrix} XPHP \\ YPHP \\ ZPHP \end{vmatrix} + [TRNPI]^{-1} [D\tilde{\omega} PPI] \begin{vmatrix} XPHP \\ YPHP \\ ZPHP \end{vmatrix} \\ &+ 2 * [TRNPI]^{-1} [\tilde{\omega} PPI] \begin{vmatrix} DXPHP \\ DYPHP \\ DZPHP \end{vmatrix} + [TRNPI]^{-1} \begin{vmatrix} DDXPHP \\ DDYPHP \\ DDZPHP \end{vmatrix} \end{aligned} \quad (4.3.2.10)$$

Project to pylon axis components by [TRNPI]:

$$\begin{aligned} \begin{vmatrix} AXPHI \\ AYPHI \\ AZPHI \end{vmatrix} &= \begin{vmatrix} AXPPI \\ AYPPI \\ AZPPI \end{vmatrix} + [\tilde{\omega} PPI] [\tilde{\omega} PPI] \begin{vmatrix} XPHP \\ YPHP \\ ZPHP \end{vmatrix} + [D\tilde{\omega} PPI] \begin{vmatrix} XPHP \\ YPHP \\ ZPHP \end{vmatrix} \\ &+ 2 * [\tilde{\omega} PPI] \begin{vmatrix} DXPHP \\ DYPHP \\ DZPHP \end{vmatrix} + \begin{vmatrix} DDXPHP \\ DDYPHP \\ DDZPHP \end{vmatrix} \end{aligned} \quad (4.3.2.11)$$

This relation provides the full interconnect between pylon-axis origin accelerations and hook accelerations. For a rail-motion simulation, the only remaining requirements are to determine expressions for and first and second derivatives of the position of the hook down the rail at each time step and to evaluate the skew-symmetric matrices. The first term is the reference acceleration of the pylon axis origin. The following term is the normal/centripetal acceleration. The next term is the tangential contribution. The term with the multiplier of 2 is the hook Coriolis acceleration. The double-dot term is the relative downrail acceleration. As can be seen, several of these terms were not included in Eq. (4.3.1.10).

Before proceeding to application of Eq. (4.3.2.11) to rail motion, a few comments about how the equation relates to the pivot acceleration for tank simulations are in order. For the pivoting tank case, the hook axes do not translate or accelerate relative to pylon axes which cancels out the last two terms in Eq. (4.3.2.11). For the idealized pull-up/push-over maneuvers normally simulated, the derivative skew-symmetric matrix will be shown in a subsequent paragraph to be a matrix of zeros, leaving only the first two terms to the right of the equality in Eq. (4.3.2.11). As an approximation, the effects of the transfer distance between hook and pylon axes could be neglected allowing the equating of hook-axis accelerations and the acceleration of the common origin of the pylon, flight, and aircraft axis systems as was done in Eq. (4.3.1.10). However, for a completely rigorous solution the acceleration terms associated with the aircraft rotations during the maneuver and the offsets from the aircraft maneuver center to the hook point must be included.

The remainder of this section is devoted to determining expressions for the various terms in the generalized acceleration equation [Eq. (4.3.2.11)]. The aircraft maneuver will be assumed to be the idealized pull-up/push-over described in Section 4.3.1, although the equations developed in this section are equally valid for any arbitrary maneuver provided the motion of the flight/pylon/aircraft axis origin is known (Section 4.3.9).

The first term to the right of the equality in Eq. (4.3.2.11) involves the pylon-axis components of the acceleration of the pylon axes. For the idealized maneuver these can be obtained from Eq. (4.3.1.3) by the relation (because pylon and flight axes have a common origin):

$$\begin{vmatrix} AXPPI \\ AYPPI \\ AZPPI \end{vmatrix} = [\text{TRNPF}] \begin{vmatrix} AXFFI \\ AYFFI \\ AZFFI \end{vmatrix} \quad (4.3.2.12)$$

The second term in Eq. (4.3.2.11) is the skew-symmetric matrix, $[\tilde{\omega} PPI]$, involving PPPI, QPPI, and RPPI. Again, noting that the pylon and flight origins are coincident (so that QPPI = QFFI), Eq. (4.3.1.4) can be used to form:

$$\begin{vmatrix} PPPI \\ QPPI \\ RPPI \end{vmatrix} = [\text{TRNPF}] \begin{vmatrix} PFFI \\ QFFI \\ RFFI \end{vmatrix} \quad (4.3.2.13)$$

so that:

$$[\tilde{\omega} PPI] = \begin{bmatrix} 0 & -RPPI & QPPI \\ RPPI & 0 & -PPPI \\ -QPPI & PPPI & 0 \end{bmatrix} \quad (4.3.2.14)$$

The time derivative of the skew-symmetric matrix, $[D\tilde{\omega} PPI]$, is formed of the derivatives of the terms in Eq. (4.3.2.13). For the idealized pull-up/push-over maneuver, all the terms are zero since both the {PFFI} vector and the transformation are time invariant:

$$[D\tilde{\omega} PPI] = [0] \quad (4.3.2.15)$$

The derivative skew-symmetric matrix would, of course, contain non-zero values for an arbitrary non-idealized aircraft maneuver. For arbitrary maneuvers, Eqs. (4.3.2.12), (4.3.2.13), and (4.3.2.15) would be replaced by appropriate relations from Section 4.3.9.

The final remaining terms in Eq. (4.3.2.11) are the {XPHP} vector and its derivatives (although the derivatives are unnecessary for the special case of a fixed pivot which does not move down a rail). The {XPHP} vector must be expanded out in terms of known quantities available from other portions of the simulation and actually has a somewhat complex derivation of its own. Beginning with the body axis components of the position of the hook axes relative to the body axes and projecting to inertial axes:

$$\begin{vmatrix} XIHB \\ YIHB \\ ZIHB \end{vmatrix} = [TRNBI]^{-1} \begin{vmatrix} XBHB \\ YBHB \\ ZBHB \end{vmatrix} \quad (4.3.2.16)$$

The inertial axis components of the position of the hook axes relative to inertial axes are then:

$$\begin{vmatrix} XIHI \\ YIHI \\ ZIHI \end{vmatrix} = \begin{vmatrix} XIHB \\ YIHB \\ ZIHB \end{vmatrix} + \begin{vmatrix} XIBI \\ YIBI \\ ZIBI \end{vmatrix} \quad (4.3.2.17)$$

The inertial axis components of the position of the hook axes relative to flight axes are then:

$$\begin{vmatrix} XIHF \\ YIHF \\ ZIHF \end{vmatrix} = \begin{vmatrix} XIHI \\ YIHI \\ ZIHI \end{vmatrix} - \begin{vmatrix} XIFI \\ YIFI \\ ZIFI \end{vmatrix} \quad (4.3.2.18)$$

Note that {XIHF} = {XIHP} because flight and pylon axes have a common origin. The full expression for {XPHP} can then be formed by combining Eqs. (4.3.2.16) through (4.3.2.18) and projecting into pylon axes:

$$\begin{vmatrix} XPHP \\ YPHP \\ ZPHP \end{vmatrix} = [TRNPI] \left\{ \begin{vmatrix} XIBI \\ YIBI \\ ZIBI \end{vmatrix} - \begin{vmatrix} XIFI \\ YIFI \\ ZIFI \end{vmatrix} + [TRNBI]^{-1} \begin{vmatrix} XBHB \\ YBHB \\ ZBHB \end{vmatrix} \right\} \quad (4.3.2.19)$$

Only the {XPHP} vector itself is needed if the pivot point is fixed relative to the aircraft. Also for a fixed hook, Eq. (4.3.2.19) need only be evaluated at the first time step to determine the hook position. The position equation must, however, be evaluated at each time step for a moving hook traveling down a rail or if the hook is attached to an aircraft undergoing an arbitrary maneuver.

ver for which [TRNPI] is not constant. If the hook translates down a rail, the distance the hook has moved must be calculated at each time step from the current value of {XPHP} minus the value at carriage. This hook travel distance is used to determine the point of release from the rail as will be described in Section 4.3.7.

If the hook is allowed to translate down a rail, the derivatives of the {XPHP} vector are also needed to evaluate Eq. (4.3.2.11). By the chain rule and noting that the derivative of the {XBHB} vector is zero:

$$\begin{aligned} \begin{vmatrix} DXPHP \\ DYPHP \\ DZPHP \end{vmatrix} &= -[\tilde{\omega} PPI] [TRNPI] \left\{ \begin{vmatrix} XIBI \\ YIBI \\ ZIBI \end{vmatrix} - \begin{vmatrix} XIFI \\ YIFI \\ ZIFI \end{vmatrix} + [TRNBI]^{-1} \begin{vmatrix} XBHB \\ YBHB \\ ZBHB \end{vmatrix} \right\} \\ &+ [TRNPI] \left\{ \begin{vmatrix} UIBI \\ VIBI \\ WIBI \end{vmatrix} - \begin{vmatrix} UIFI \\ VIFI \\ WIFI \end{vmatrix} + [TRNBI]^{-1} [\tilde{\omega} BBI] \begin{vmatrix} XBHB \\ YBHB \\ ZBHB \end{vmatrix} \right\} \\ &= -[\tilde{\omega} PPI] \begin{vmatrix} XPHP \\ YPHP \\ ZPHP \end{vmatrix} + \begin{vmatrix} UPHP \\ VPHP \\ WPHP \end{vmatrix} \end{aligned} \quad (4.3.2.20)$$

where {UPHP} is:

$$\begin{vmatrix} UPHP \\ VPHP \\ WPHP \end{vmatrix} = [TRNPI] \left\{ \begin{vmatrix} UIBI \\ VIBI \\ WIBI \end{vmatrix} - \begin{vmatrix} UIFI \\ VIFI \\ WIFI \end{vmatrix} + [TRNBI]^{-1} [\tilde{\omega} BBI] \begin{vmatrix} XBHB \\ YBHB \\ ZBHB \end{vmatrix} \right\} \quad (4.3.2.21)$$

Finally, as if Eq. (4.3.2.20) wasn't complex enough, its derivative is also needed for the hook relative acceleration term in Eq. (4.3.2.11):

$$\begin{aligned} \begin{vmatrix} DDXPHP \\ DDYPHP \\ DDZPHP \end{vmatrix} &= -[D\tilde{\omega} PPI] [TRNPI] \left\{ \begin{vmatrix} XIBI \\ YIBI \\ ZIBI \end{vmatrix} - \begin{vmatrix} XIFI \\ YIFI \\ ZIFI \end{vmatrix} + [TRNBI]^{-1} \begin{vmatrix} XBHB \\ YBHB \\ ZBHB \end{vmatrix} \right\} \\ &+ [\tilde{\omega} PPI] [\tilde{\omega} PPI] [TRNPI] \left\{ \begin{vmatrix} XIBI \\ YIBI \\ ZIBI \end{vmatrix} - \begin{vmatrix} XIFI \\ YIFI \\ ZIFI \end{vmatrix} + [TRNBI]^{-1} \begin{vmatrix} XBHB \\ YBHB \\ ZBHB \end{vmatrix} \right\} \\ &- [\tilde{\omega} PPI] [TRNPI] \left\{ \begin{vmatrix} UIBI \\ VIBI \\ WIBI \end{vmatrix} - \begin{vmatrix} UIFI \\ VIFI \\ WIFI \end{vmatrix} + [TRNBI]^{-1} [\tilde{\omega} BBI] \begin{vmatrix} XBHB \\ YBHB \\ ZBHB \end{vmatrix} \right\} \\ &- [\tilde{\omega} PPI] [TRNPI] \left\{ \begin{vmatrix} UIBI \\ VIBI \\ WIBI \end{vmatrix} - \begin{vmatrix} UIFI \\ VIFI \\ WIFI \end{vmatrix} + [TRNBI]^{-1} [\tilde{\omega} BBI] \begin{vmatrix} XBHB \\ YBHB \\ ZBHB \end{vmatrix} \right\} \end{aligned}$$

$$\begin{aligned}
 & + [\text{TRNPI}] \left\{ \begin{vmatrix} \text{AXIBI} \\ \text{AYIBI} \\ \text{AZIBI} \end{vmatrix} - \begin{vmatrix} \text{AXIFI} \\ \text{AYIFI} \\ \text{AZIFI} \end{vmatrix} \right. + [\text{TRNBI}]^{-1} [\tilde{\omega} \text{BBI}] [\tilde{\omega} \text{BBI}] \begin{vmatrix} \text{XBHB} \\ \text{YBHB} \\ \text{ZBHB} \end{vmatrix} \\
 & \left. + [\text{TRNBI}]^{-1} [\text{D}\tilde{\omega} \text{BBI}] \begin{vmatrix} \text{XBHB} \\ \text{YBHB} \\ \text{ZBHB} \end{vmatrix} \right\} \quad (4.3.2.22)
 \end{aligned}$$

It will be shown later in Section 4.3.7 that it is convenient in actual numerical simulations to re-express Eq. (4.3.2.22) in the following form:

$$\begin{aligned}
 & \left| \begin{array}{c} \text{DDXPHP} \\ \text{DDYPHP} \\ \text{DDZPHP} \end{array} \right| - [\text{TRNBP}]^{-1} \begin{vmatrix} \text{AXBBI} \\ \text{AYBBI} \\ \text{AZBBI} \end{vmatrix} - [\text{TRNBP}]^{-1} [\text{D}\tilde{\omega} \text{BBI}] \begin{vmatrix} \text{XBHB} \\ \text{YBHB} \\ \text{ZBHB} \end{vmatrix} \\
 & = - [\text{D}\tilde{\omega} \text{PPI}] \begin{vmatrix} \text{XPHP} \\ \text{YPHP} \\ \text{ZPHP} \end{vmatrix} - [\tilde{\omega} \text{PPI}] \begin{vmatrix} \text{DXPHP} \\ \text{DYPHP} \\ \text{DZPHP} \end{vmatrix} - [\tilde{\omega} \text{PPI}] \begin{vmatrix} \text{UPHP} \\ \text{VPHP} \\ \text{WPHP} \end{vmatrix} \quad (4.3.2.23) \\
 & + [\text{TRNBP}]^{-1} [\tilde{\omega} \text{BBI}] [\tilde{\omega} \text{BBI}] \begin{vmatrix} \text{XBHB} \\ \text{YBHB} \\ \text{ZBHB} \end{vmatrix} - \begin{vmatrix} \text{AXPPI} \\ \text{AYPPI} \\ \text{AZPPI} \end{vmatrix}
 \end{aligned}$$

At this point, Eqs. (4.3.12), (4.3.14), (4.3.15), (4.3.19), (4.3.20), and (4.3.22) can be substituted into Eq. (4.3.2.11) to define the total hook acceleration. At each time step in a numerical simulation for a downrail missile launch, every term in the expanded Eq. (4.3.2.11) is available except for the $\{\text{AXIBI}\}$ (or $\{\text{AXBBI}\}$) vector and the $[\text{D}\tilde{\omega} \text{BBI}]$ matrix which appear in the Eq. (4.3.2.22)/(4.3.2.23) contribution. A paradox arises over these terms, however, because the acceleration and angular velocity derivatives used in the calculation of the hook acceleration can only be determined by solving the body equations of motion, but the body equations of motion are posed assuming that the hook accelerations are known. As a result, it will be necessary to define additional constraint equations allowing a system of equations to be solved for the motion that simultaneously satisfies both the constraints and the basic store and hook motions. The full implementation of the downrail missile equations with constraints will be presented in Section 4.3.7. First, however, simpler cases involving fixed pivots which do not have relative acceleration components will be developed in Sections 4.3.3 through 4.3.6.

4.3.3 The Simple Pivot Rotational Constraint

The "simple" pivot is an idealization of a pivot mechanism which allows restricted yaw, pitch, and/or roll rotation about a fixed pivot point. The actual movements of the mechanism are not directly modeled - only the resulting motion restrictions are imposed. Although the simple pivot may not be rigorously representative of actual physical hardware, it is often adequate for engineering accuracy and can easily be implemented in a numerical simulation. The "simple" pivot model does not require simultaneous solution of a system of equations such as is necessary

for more rigorously defined models. The simple pivot concept is to solve the rotational equations for restricted motion [Eq. (4.2.2.42)] for the reaction moments that will cause specified values of the rotational velocity derivatives. Beginning with Eq. (4.2.2.42) and moving the reaction moments to the left side of the equation:

$$\begin{aligned} \left[\begin{array}{c} DPBBI \\ DQBBI \\ DRBBI \end{array} \right] - [I]_{BH}^{-1} \left[\begin{array}{c} RLB \\ RMB \\ RNB \end{array} \right] &= [I]_{BH}^{-1} \left\{ -[\tilde{\omega} BBI] \left[\begin{array}{c} HXBHH \\ HYBHH \\ HZBHH \end{array} \right] + \left[\begin{array}{c} MXB \\ MYB \\ MZB \end{array} \right] \text{ about B} \right. \\ &\quad \left. + \left[\begin{array}{c} XBBH \\ YBBH \\ ZBBH \end{array} \right] \times \left[\begin{array}{c} FXB \\ FYB \\ FZB \end{array} \right] - m \left[\begin{array}{c} XBBH \\ YBBH \\ ZBBH \end{array} \right] \times \left[\begin{array}{c} AXBHI \\ AYBHI \\ AZBHI \end{array} \right] \right\} \end{aligned} \quad (4.3.3.1)$$

Multiplying through by $[I]_{BH}$:

$$\begin{aligned} [I]_{BH} \left[\begin{array}{c} DPBBI \\ DQBBI \\ DRBBI \end{array} \right] - \left[\begin{array}{c} RLB \\ RMB \\ RNB \end{array} \right] &= \left[\begin{array}{c} DHXBHHO \\ DHYBHHO \\ DHZBHHO \end{array} \right] \\ = -[\tilde{\omega} BBI] [I]_{BH} \left[\begin{array}{c} PBBI \\ QBBI \\ RBBI \end{array} \right] &+ \left[\begin{array}{c} MXB \\ MYB \\ MZB \end{array} \right] \text{ about B} + \left[\begin{array}{c} XBBH \\ YBBH \\ ZBBH \end{array} \right] \times \left[\begin{array}{c} FXB \\ FYB \\ FZB \end{array} \right] \\ - m \left[\begin{array}{c} XBBH \\ YBBH \\ ZBBH \end{array} \right] \times \left[\begin{array}{c} AXBHI \\ AYBHI \\ AZBHI \end{array} \right] & \\ = -[\tilde{\omega} BBI] \left[\begin{array}{c} HXBHH \\ HYBHH \\ HZBHH \end{array} \right] &+ \left[\begin{array}{c} MXB \\ MYB \\ MZB \end{array} \right] \text{ about B} + \left[\begin{array}{c} XBBH \\ YBBH \\ ZBBH \end{array} \right] \times \left[\begin{array}{c} FXB \\ FYB \\ FZB \end{array} \right] \\ - m \left[\begin{array}{c} XBBH \\ YBBH \\ ZBBH \end{array} \right] \times \left[\begin{array}{c} AXBHI \\ AYBHI \\ AZBHI \end{array} \right] & \end{aligned} \quad (4.3.3.2)$$

$\{DHXBHHO\}$ is equivalent to the unconstrained momentum derivative about the pivot, as can be seen by setting the reaction moments to zero in Eq. (4.3.3.1). The unconstrained angular velocity derivatives are then:

$$\left[\begin{array}{c} DPBBIO \\ DQBBIO \\ DRBBIO \end{array} \right] = [I]_{BH}^{-1} \left[\begin{array}{c} DHXBHHO \\ DHYBHHO \\ DHZBHHO \end{array} \right] \quad (4.3.3.3)$$

The {DPBBI} vector represents the angular velocity derivatives that would exist if the constraint were not applied. However if a constraint is applied, then Eq. (4.3.3.2) is rewritten as:

$$\begin{vmatrix} DPBBI \\ DQBBI \\ DRBBI \end{vmatrix} = [I]BH^{-1} \begin{vmatrix} DHXBHHO \\ DHYBHHO \\ DHZBHHO \end{vmatrix} + [I]BH^{-1} \begin{vmatrix} RLB \\ RMB \\ RNB \end{vmatrix} \quad (4.3.3.4)$$

A desired value of the {DPBBI} vector can be obtained from the relation of Eq. (4.3.3.4) simply by solving for the reaction moments necessary to generate the desired angular velocity derivatives. Solving Eq. (4.3.3.4) for the necessary reaction moments:

$$\begin{vmatrix} RLB \\ RMB \\ RNB \end{vmatrix} = [I]BH \begin{vmatrix} DPBBI \\ DQBBI \\ DRBBI \end{vmatrix}_{\text{desired}} - \begin{vmatrix} DHXBHHO \\ DHYBHHO \\ DHZBHHO \end{vmatrix} \quad (4.3.3.5)$$

Implementation of the simple pivot in a numerical simulation requires that the unconstrained quantities be calculated according to Eqs. (4.3.3.2) and (4.3.3.3). Then the reaction moments for different constraints can be calculated from Eq. (4.3.3.5) by defining the desired rotational velocity derivative vector:

For completely unconstrained pivot motion:

$$\begin{vmatrix} DPBBI \\ DQBBI \\ DRBBI \end{vmatrix}_{\text{desired}} = \begin{vmatrix} DPBBI \\ DQBBIO \\ DRBBI \end{vmatrix} \quad (4.3.3.6)$$

which, when substituted into Eq. (4.3.3.5), results in the trivial solution that $RLB = RMB = RNB = 0.0$.

For pitch and yaw pivot motion with roll not allowed:

$$\begin{vmatrix} DPBBI \\ DQBBI \\ DRBBI \end{vmatrix}_{\text{desired}} = \begin{vmatrix} 0.0 \\ DQBBIO \\ DRBBI \end{vmatrix} \quad (4.3.3.7)$$

For pitch pivot motion with yaw and roll not allowed:

$$\begin{vmatrix} DPBBI \\ DQBBI \\ DRBBI \end{vmatrix}_{\text{desired}} = \begin{vmatrix} 0.0 \\ DQBBIO \\ 0.0 \end{vmatrix} \quad (4.3.3.8)$$

The reaction moments from Eq. (4.3.3.5) can then be used with the restricted rotational equations [Eq. (4.2.2.42)] to determine the angular velocity derivatives, which can, in turn, be used to determine the remaining store motion parameters.

It is also important in restricted simulations to model the conditions for release of the store from the constraint mechanism so that the simulation can transition to free-flight motion. Two conditions must be satisfied before simple pivot release simulations are allowed to switch to unrestricted motion. Restrained motion is arbitrarily imposed until the assembly pitches to a nose-down incidence angle relative to the aircraft greater than the design release angle of the mechanism. After satisfying the pitch criterion, calculated reaction forces at the pivot point are then tested. If reaction forces directed downward are required to maintain no vertical motion for the pivot point relative to the aircraft (indicated by a calculated RZP reaction force in the positive ZP direction) restrained motion continues. When upward directed forces are calculated (indicative of a force trying to pull the pivot point up), the simulation switches to full six-degree-of-freedom motion about the center of gravity of the assembly. The store pitch angles relative to pylon axes at each time step in the trajectory which are tested against the input design release angle are obtained from the relations of Eq. (1.3.9) as:

$$\text{THABP} = \sin^{-1} \{-\text{TRNBP}(1,3)\} \quad (4.3.3.9)$$

(assuming a yaw-pitch pivot sequence such as is used by many current aircraft pivot mechanisms).

The simple pivot represents a special restricted-motion case in which rotational and translational equations can be posed independently. However, the formulations specified by setting the conditions of Eqs. (4.3.3.7) or (4.3.3.8) are only an approximation which may not be fully consistent with true rotational rigid body dynamics. Actually, if any one of the rotational velocity derivatives is arbitrarily set to zero as in Eqs. (4.3.3.7) and (4.3.3.8), and if the store has any non-zero products of inertia about its pivot point, the full, unconstrained values of the rotational velocity derivatives in the other component directions would not be fully realized. In general, coupled systems of equations which must be solved simultaneously for the motion terms and the reaction forces and moments are necessary for fully consistent physical models. Also, the release criterion based on the RZP reaction forces may not represent a fully rigorous condition for switching to free motion, as will be described in Section 4.3.5 for the F-15 pivot assembly. For many engineering purposes, however, the "simple" model is quite accurate enough, and a somewhat simplified version of the "simple" pivot concept as presented in this section has been used for most wind tunnel pivot release simulations at the AEDC prior to the development of the more physically rigorous equations outlined in the next several sections.

4.3.4 True Pivot Rotational Constraint (F-16 Type)

Generalized constrained motion problems require the simultaneous solution of a coupled system of equations at each time step. The equations may be posed in several different ways, but it is generally convenient to fully expand out to a separate equation for each degree of freedom and each reaction force or moment component. The generalized constraint equations for the hook device used by the F-16 aircraft are developed in this section. Equations are developed to allow solution for twelve unknowns - three translational acceleration components of the store body {AXBBI, AYBBI, AZBBI}, three rotational acceleration components {DPBBI, DQBBI, DRBBI}, three reaction force components {RXB, RYB, RZB} and three reaction moment com-

ponents {RLB, RMB, RNB}. The equations could just as easily be posed in terms of any other consistent set of motion properties (for example, the equations could be written in terms of an unknown {DUBBI} vector instead of in terms of the {AXBBI} vector), but some advantages will be gained by using the selected motion quantities.

The basic translational and rotational equations of motion for the store have been previously developed in previous sections. This section's primary purpose is to derive the six additional constraint equations which model the restraint device and allow solution for the reaction forces and moments. The F-16 pivot device is depicted in Fig. 20. The F-16 hook consists of an upside-down "J" device attached to the store which is latched to a mating fitting which is fixed-mounted to the aircraft. The aircraft fitting is located between two parallel flat plates also fixed-mounted on the aircraft. Contact between the flat sides of the store hook and the plates to either side of it prevent out-of-plane motion of the hook. A small cylindrical shaft mounted normal to the flat sides of the store hook is machined as part of the hook. This shaft defines the pitch axis of the hook assembly. The two ends of this shaft fit into circular cutouts in the two side plates which are mounted to the aircraft. The pitch shaft is thus parallel to the lateral pylon axis, YP. The store is free to pitch about the axis defined by the pitch shaft. After pitching, the store assembly is then free to yaw about the new z-axis of the hook assembly (which is aligned with the ZB axis). The F-16 mechanism can thus be recognized as a pitch-yaw sequence device. The full range of motion of the hook device for which modeling equations must be developed is, therefore, a sequence of rotations beginning with unrestricted pitch about the YP axis followed by unrestricted yaw about the resulting new yaw axis of the hook with all subsequent roll rotational motion prevented. The roll restriction is enforced in the equations of motion by defining an intermediate axis system for which the y axis is aligned with the shaft pitch axis (YP), the z axis is aligned with the yaw axis (rotated in pitch relative to pylon axes), and the x axis is perpendicular to the z and y axes. This new axis system will be designated by the symbol "U" for "unyawed" axes because it represents an intermediate system for defining the pitch motion of the J-hook relative to pylon axes before the yaw motion of the store about the hook vertical axis is applied. The constraints can be written mathematically as:

$$\begin{aligned} \text{RMP} &= 0.0 \quad \text{free to pitch about the YP shaft axes} \\ \text{RNU} &= 0.0 \quad \text{free to yaw about pitched (unyawed) hook vertical axis} \\ \text{DPUUP} &= 0.0 \quad \text{restrained to no rotation about the mutually perpendicular axis} \end{aligned} \quad (4.3.4.1)$$

To be completely general and arbitrary it would be necessary to write a coupled two-body system of equations solving the motion of the J-hook about the pitch shaft axes simultaneously with the motion of the body axes relative to the vertical shaft of the J-hook. It is convenient, however, to solve the motion as a single body problem in terms of body-axis motion relative to hook axes by rewriting the Eq. (4.3.4.1) constraints in terms of quantities not directly involving the "unyawed" system. The $\text{RMP} = 0$ constraint, for instance, can be written out directly as projections of body axis terms:

$$\text{TRNBP}(1,2)*\text{RLB} + \text{TRNBP}(2,2)*\text{RMB} + \text{TRNBP}(3,2)*\text{RNB} = 0.0 \quad (4.3.4.2)$$

The RNU = 0 constraint can also be written easily by noting that the Z axes of unyawed and body axes are parallel so that RNU = RNB = 0.0. The development of a coupled single-body form for the third constraint of Eq. (4.3.4.1) involves an extremely complicated derivation, however, which will be carried out in the next twelve equations.

Beginning with the relations for the angular velocities for the unyawed axes relative to the pylon axes:

$$\begin{vmatrix} PUUP \\ QUUP \\ RUUP \end{vmatrix} = \begin{vmatrix} PUUI \\ QUUI \\ RUUI \end{vmatrix} - \begin{vmatrix} PUPI \\ QUPI \\ RUPI \end{vmatrix} = \begin{vmatrix} PUBI \\ QUBI \\ RUBI \end{vmatrix} + \begin{vmatrix} PUUB \\ QUUB \\ RUUB \end{vmatrix} - \begin{vmatrix} PUPI \\ QUPI \\ RUPI \end{vmatrix} \quad (4.3.4.3)$$

or:

$$\begin{vmatrix} PUUP \\ QUUP \\ RUUP \end{vmatrix} = [TRNBU]^T \begin{vmatrix} PBBI \\ QBBI \\ RBBI \end{vmatrix} + \begin{vmatrix} PUUB \\ QUUB \\ RUUB \end{vmatrix} - [TRNPU]^T \begin{vmatrix} PPPI \\ QPPI \\ RPPI \end{vmatrix} \quad (4.3.4.4)$$

Taking derivatives of both sides by the chain rule:

$$\begin{aligned} \frac{d}{dt} \begin{vmatrix} PUUP \\ QUUP \\ RUUP \end{vmatrix} &= \frac{d}{dt} [TRNBU]^T \begin{vmatrix} PBBI \\ QBBI \\ RBBI \end{vmatrix} + [TRNBU]^T \frac{d}{dt} \begin{vmatrix} PBBI \\ QBBI \\ RBBI \end{vmatrix} + \frac{d}{dt} \begin{vmatrix} PUUB \\ QUUB \\ RUUB \end{vmatrix} \\ &\quad - \frac{d}{dt} [TRNPU]^T \begin{vmatrix} PPPI \\ QPPI \\ RPPI \end{vmatrix} - [TRNPU]^T \frac{d}{dt} \begin{vmatrix} PPPI \\ QPPI \\ RPPI \end{vmatrix} \end{aligned} \quad (4.3.4.5)$$

or:

$$\begin{aligned} \begin{vmatrix} DPUUP \\ DQUUP \\ DRUUP \end{vmatrix} &= [TRNBU]^T [\tilde{\omega} BBU] \begin{vmatrix} PBBI \\ QBBI \\ RBBI \end{vmatrix} + [TRNBU]^T \begin{vmatrix} DPBBI \\ DQBBI \\ DRBBI \end{vmatrix} + \begin{vmatrix} DPUUB \\ DQUUB \\ DRUUB \end{vmatrix} \\ &\quad - [TRNPU]^T [\tilde{\omega} PPU] \begin{vmatrix} PPPI \\ QPPI \\ RPPI \end{vmatrix} - [TRNPU]^T \begin{vmatrix} DPPPI \\ DQPPI \\ DRPPI \end{vmatrix} \end{aligned} \quad (4.3.4.6)$$

Because only the constraint on DPUUP is of interest, it is convenient to rewrite Eq. (4.3.4.6) using cross-products instead of the skew-symmetric matrices:

$$\begin{aligned} \begin{vmatrix} DPUUP \\ DQUUP \\ DRUUP \end{vmatrix} &= [TRNBU]^T \left(\begin{pmatrix} PBBU \\ QBBU \\ RBBU \end{pmatrix} \times \begin{pmatrix} PBBI \\ QBBI \\ RBBI \end{pmatrix} \right) + [TRNBU]^T \begin{pmatrix} DPBBI \\ DQBBI \\ DRBBI \end{pmatrix} + \begin{pmatrix} DPUUB \\ DQUUB \\ DRUUB \end{pmatrix} \\ &\quad - [TRNPU]^T \left(\begin{pmatrix} PPPU \\ QPPU \\ RPPU \end{pmatrix} \times \begin{pmatrix} PPPI \\ QPPI \\ RPPI \end{pmatrix} \right) - [TRNPU]^T \begin{pmatrix} DPPPI \\ DQPPI \\ DRPPI \end{pmatrix} \end{aligned} \quad (4.3.4.7)$$

At this point $PBBU = QBBU = DPUUB = QRUUB = 0.0$ because the body is only allowed to yaw relative to the U axes, $PPPU = RPPU = 0.0$ because the unyawed axes are only allowed to pitch relative to pylon axes, and $DPUUP = 0.0$ for the desired constraint:

$$\begin{vmatrix} 0.0 \\ DQUUP \\ DRUUP \end{vmatrix} = [\text{TRNBU}]^T \begin{pmatrix} 0.0 & X & \begin{vmatrix} PBBI \\ QBBI \\ RBBI \end{vmatrix} \\ 0.0 & \begin{vmatrix} PPPI \\ QPPI \\ RPPI \end{vmatrix} \\ RBBU & \end{pmatrix} + [\text{TRNBU}]^T \begin{vmatrix} DPBBI \\ DQBBI \\ DRBBI \end{vmatrix} + \begin{vmatrix} 0.0 \\ 0.0 \\ DRUUB \end{vmatrix}$$

$$- [\text{TRNPU}]^T \begin{pmatrix} 0.0 & X & \begin{vmatrix} PPPI \\ QPPI \\ RPPI \end{vmatrix} \\ QSSU & \begin{vmatrix} PPU * RPPI \\ 0.0 \\ -QPPU * PPPI \end{vmatrix} \\ 0.0 & \end{pmatrix} - [\text{TRNPU}]^T \begin{vmatrix} DPPPI \\ DQPPI \\ DRPPI \end{vmatrix} \quad (4.3.4.8)$$

Expanding out the cross products:

$$\begin{vmatrix} 0.0 \\ DQUUP \\ DRUUP \end{vmatrix} = [\text{TRNBU}]^T \begin{pmatrix} -RBBU * QBBI \\ RBBU * PBBI \\ 0.0 \end{pmatrix} + [\text{TRNBU}]^T \begin{vmatrix} DPBBI \\ DQBBI \\ DRBBI \end{vmatrix} + \begin{vmatrix} 0.0 \\ 0.0 \\ DRUUB \end{vmatrix}$$

$$- [\text{TRNPU}]^T \begin{pmatrix} QPPU * RPPI \\ 0.0 \\ -QPPU * PPPI \end{pmatrix} - [\text{TRNPU}]^T \begin{vmatrix} DPPPI \\ DQPPI \\ DRPPI \end{vmatrix} \quad (4.3.4.9)$$

The x-component of vector Eq. (4.3.4.9) is the desired constraint equation. However, expressions for $RBBU$ and $QPPU$ at each time step must be developed before the equation can be evaluated. $RBBU$ can be developed beginning with the relation:

$$\begin{vmatrix} 0.0 \\ 0.0 \\ RBBU \end{vmatrix} = \begin{vmatrix} PBBI \\ QBBI \\ RBBI \end{vmatrix} - \begin{vmatrix} PBUI \\ QBUI \\ RBUI \end{vmatrix} = \begin{vmatrix} PBBI \\ QBBI \\ RBBI \end{vmatrix} - \begin{vmatrix} PBPI \\ QBPI \\ RBPI \end{vmatrix} - \begin{vmatrix} PBUP \\ QBUP \\ RBUP \end{vmatrix} \quad (4.3.4.10)$$

$$= \begin{vmatrix} PBBI \\ QBBI \\ RBBI \end{vmatrix} - [\text{TRNBP}] \begin{vmatrix} PPPI \\ QPPI \\ RPPI \end{vmatrix} - [\text{TRNBU}] \begin{vmatrix} PUUP \\ QUUP \\ RUUP \end{vmatrix}$$

Expanding out only the $RBBU$ term and noting that $PUUP = RUUS = 0.0$:

$$RBBU = RBBI - RBPI - \text{TRNBU}(3,2) * QUUP \quad (4.3.4.11)$$

But from Eq. (1.3.3), $\text{TRNBU}(3,2) = 0.0$ for a pure yaw rotation, so that:

$$RBBU = RBBI - RBPI \quad (4.3.4.12)$$

A similar derivation can be used to determine $QPPU$. Beginning with:

$$\begin{aligned}
 \begin{vmatrix} 0.0 \\ QPPU \\ 0.0 \end{vmatrix} &= \begin{vmatrix} PPPI \\ QPPI \\ RPPI \end{vmatrix} - \begin{vmatrix} PPUI \\ QPUI \\ RPUI \end{vmatrix} = \begin{vmatrix} PPPI \\ QPPI \\ RPPI \end{vmatrix} - \begin{vmatrix} PPBI \\ QPBI \\ RPBI \end{vmatrix} - \begin{vmatrix} PPUB \\ QPUB \\ RPUB \end{vmatrix} \\
 &= \begin{vmatrix} PPPI \\ QPPI \\ RPPI \end{vmatrix} - [TRNBP]^T \begin{vmatrix} PBBI \\ QBBI \\ RBBI \end{vmatrix} - [TRNPU] \begin{vmatrix} PUUB \\ QUUB \\ RUUB \end{vmatrix}
 \end{aligned} \tag{4.3.4.13}$$

Expanding out only the QPPU term and noting that PUUB = QUUB = 0.0:

$$QPPU = QPPI - QPBI - TRNPU(2,3) * RUUB \tag{4.3.4.14}$$

But from Eq. (1.3.5), TRNPU(2,3) = 0.0 for a pure pitch rotation, so that:

$$QPPU = QPPI - QPBI \tag{4.3.4.15}$$

This completes the derivation of the additional constraint equations.

Twelve linearly independent equations are necessary to determine the 12 independent variables at each time step. The first three of the necessary equations are the restricted translational equations of motion defined by Eq. (4.1.2.8). The double cross-product term in Eq. (4.1.2.8) is first evaluated (defining a temporary vector {OOXBBH} denoting Omega cross Omega cross r for the {XBBH} vector):

$$\begin{vmatrix} OOXBBH \\ OGYBBH \\ OOZBBH \end{vmatrix} = \begin{vmatrix} PBBI \\ QBBI \\ RBBI \end{vmatrix} \times \begin{vmatrix} PBBI \\ QBBI \\ RBBI \end{vmatrix} \times \begin{vmatrix} XBBH \\ YBBH \\ ZBBH \end{vmatrix} \tag{4.3.4.16}$$

Equations (4.1.2.8) are then written in terms of the unknowns and expanded into scalar form as:

$$\begin{aligned}
 \#1) \quad &- AXBBI + ZBBH * DQBBI - YBBH * DRBBI = - 00XBBH - AXBHI \\
 \#2) \quad &- AYBBI - ZBBH * DPBBI + XBBH * DRBBI = - 00YBBH - AYBHI \\
 \#3) \quad &- AZBBI + YBBH * DPBBI - XBBH * DQBBI = - 00ZBBH - AZBHI
 \end{aligned} \tag{4.3.4.17}$$

The next three equations are the restricted rotational equations of motion defined by Eq. (4.2.2.42). First, the body-axis components of the relative angular momentum about the hook axes are calculated directly from body-axis inertia terms:

$$\begin{vmatrix} HXBHH \\ HYBHH \\ HZBHH \end{vmatrix} = [I]_{BH} \begin{vmatrix} PBBI \\ QBBI \\ RBBI \end{vmatrix} \tag{4.3.4.18}$$

where the body-axis components of the inertia about the hook axes are computed from the parallel axis theorem:

$$\begin{aligned}
I_{xxBH} &= I_{xxBB} + m(YBBH^2 + ZBBH^2) \\
I_{yyBH} &= I_{yyBB} + m(XBBH^2 + ZBBH^2) \\
I_{zzBH} &= I_{zzBB} + m(XBBH^2 + YBBH^2) \\
I_{xyBH} &= I_{xyBB} + m(XBBH * YBBH) \\
I_{xzBH} &= I_{xzBB} + m(XBBH * ZBBH) \\
I_{yzBH} &= I_{yzBB} + m(YBBH * ZBBH)
\end{aligned} \tag{4.3.4.19}$$

Then Eq. (4.2.2.42) is expanded as:

$$\begin{aligned}
\#4) \quad &[I]_{BH}(1,1) * DPBBI + [I]_{BH}(1,2) * DQBBI + [I]_{BH}(1,3) * DRBBI - RLB \\
&= -QBBI * HZBHH + RBBI * HYBHH + MXB + YBBH * FZB - ZBBH * FYB \\
&\quad - m * YBBH * AZBHI + m * ZBBH * AYBHI \\
\#5) \quad &[I]_{BH}(2,1) * DPBBI + [I]_{BH}(2,2) * DQBBI + [I]_{BH}(2,3) * DRBBI - RMB \\
&= -RBBI * HXBHH + PBBI * HZBHH + MYB + ZBBH * FXB - XBBH * FZB \\
&\quad - m * ZBBH * AXBHI + m * XBBH * AZBHI \\
\#6) \quad &[I]_{BH}(3,1) * DPBBI + [I]_{BH}(3,2) * DQBBI + [I]_{BH}(3,3) * DRBBI - RNB \\
&= -PBBI * HYBHH + QBBI * HXBHH + MZB + XBBH * FYB - YBBH * FXB \\
&\quad - m * XBBH * AYBHI + m * YBBH * AXBHI
\end{aligned} \tag{4.3.4.20}$$

The next three equations come from the force balance on the body [Eq. (4.1.2.9)]. Rewriting:

$$\begin{aligned}
\#7) \quad &-AXBBI + RXB/m = -FXB/m \\
\#8) \quad &-AYBBI + RYB/m = -FYB/m \\
\#9) \quad &-AZBBI + RZB/m = -FZB/m
\end{aligned} \tag{4.3.4.21}$$

The final three equations arise from the constraints applied at the pivot point as developed in this section:

$$\begin{aligned}
\#10) \quad &TRNBP(1,2)*RLB + TRNBP(2,2)*RMB + TRNBP(3,2)*RNB = 0.0 \\
\#11) \quad &RNB = 0.0 \\
\#12) \quad &TRNBU(1,1)*DPBBI + TRNBU(2,1)*DQBBI + TRNBU(3,1)*DRBBI \\
&= TRNBU(1,1)*RBBU*QBBI - TRNBU(2,1)*RBBU*PBBI \\
&\quad + TRNPU(1,1) * QPPU * RPPI - TRNPU(3,1) * QPPU * PPPI \\
&\quad + TRNPU(1,1)*DPPPI + TRNPU(2,1)*DQPPI + TRNPU(3,1)*DRPPI
\end{aligned} \tag{4.3.4.22}$$

The {DPPPI} vector is zero for the idealized pitch plane maneuvers defined by constant load factors but could, of course, be non-zero for arbitrary non-idealized maneuvers. The RBBU and QPPU terms in the last equation are determined from Eqs. (4.3.4.11) and (4.3.4.14).

At each time step in the trajectory, the 12 equations are solved by a Gaussian Reduction with Columnal Pivoting algorithm for the 12 acceleration and reaction load terms. The store pitch-yaw-roll sequence pitch angle at each time step may then be extracted from the relations of Eq. (1.3.12) as:

$$NUBP = \tan^{-1} \{-TRNBP(1,3)/TRNBP(1,1)\} \tag{4.3.4.23}$$

This value is tested against the input design release angle (-11.0 deg for most F-16 installations) to determine when the first phase of motion is complete and it is time to begin testing the calculated reaction forces. After satisfying the pitch angle criteria, the calculated reaction forces are tested. First, the reaction forces from the 12-equation system are projected to pylon axes according to:

$$\begin{vmatrix} RXP \\ RYP \\ RZP \end{vmatrix} = [TRNBP]^T \begin{vmatrix} RXB \\ RYB \\ RZB \end{vmatrix} \quad (4.3.4.24)$$

If a physically impossible negative RZP reaction force (indicative of a force trying to pull up on the hook) is calculated, the simulation switches to the unrestrained equations of motion and the store is released.

Once the equations of motion are solved, the translational accelerations are rewritten as derivatives of the projected velocities using Eqs. (4.1.2.10) and the rotational and translational velocity derivatives are integrated over time to determine linear and angular projected velocities of the body axis system at the next time value. Once the updated orientation of the body relative to inertial axes is determined at each new time step (whether by integrating the derivative direction cosine matrix, or by integrating quaternion rates, or by integrating the derivatives of the modified Euler angles), the different projection matrices necessary to evaluate the system of equations at the next time step must be determined. The projection matrix for body axes relative to pylon axes at each time step is determined according to:

$$[TRNBP] = [TRNBI] [TRNPI]^T \quad (4.3.4.25)$$

where [TRNPI] comes from the aircraft maneuver. The pitch-yaw-roll sequence angles between body and pylon axes are then extracted from [TRNBP] according to the relations of Eqs. (1.3.12). The [TRNBU] matrix is determined by a rotation using Eq. (1.3.11) through the yaw angle ETABU = ETABP. And, finally, the [TRNPU] matrix is determined from:

$$[TRNPU] = [TRNBP]^T [TRNBU] \quad (4.3.4.26)$$

Before concluding the section on the modeling of the physical constraints of the F-16 pivot, it must be pointed out that the physical F-16 mechanism is not in itself sufficient to guarantee safe separation for the F-16 fuel tanks for which it is primarily intended. For certain situations a separating fuel tank might tend to over-rotate because of aerodynamic pitching moments. Under such circumstances it is possible that the tendency of the tank to pitch about its center of gravity might mean that the pivot assembly attached to the tail of the tank might move forward and upward toward the aircraft, resulting in a collision. To prevent this possibility, an aerodynamic mechanism consisting of horizontal fins attached to the rear of the tank is used in conjunction with the pivot mechanism. The tank tail fins are not intended to stabilize the tank, but are instead used to provide a strong vertically directed force at the rear of the tank during separation which positively disengages the pivot assembly after the design release angle is reached. The combined

mechanical/aerodynamic release mechanism of the F-16 will be contrasted with the much more complicated purely mechanical mechanism of the F-15 at the end of the next section.

4.3.5 True Pivot Rotational Constraint (F-15/F-18 Type)

The pivot constraint device used by the F-15 and F-18 (and which is being considered for the F-22 aircraft) features an offset roll axis. Allowing the store to roll about the offset axis during release has the favorable characteristic that structure in the aircraft is not required for supporting the pivot reaction rolling moments. Such roll freedom has the major disadvantages, however, that the mechanism is quite complex and motions near the aircraft are not as restricted, which can lead to separation problems. The primary pitch/yaw joint of the F-15 device is basically a ball-in-socket with an internal hook which fits into an open section in the ball. The hook is a complex mechanism and is difficult to visualize three-dimensionally, even with the help of simplified sketches such as those shown in Fig. 21.

The motion equations for F-15-type hook releases are developed as a coupled two-body system of equations because there are actually two structures comprising the store which move relative to one another. A new axis system designated the "R" or "roll" axis system (Fig. 22) is introduced for the F-15 hook equation derivation. The XR axis is parallel to body XB axes and is aligned with the offset roll joint. The ZR axis is in the plane containing the XR axis and the pitch/yaw hook point. The designation of "H" will be retained for the primary pitch-yaw hook axes about which the pitch and yaw motion occurs. A free-body diagram further detailing the relationships of the various axis systems is provided in Fig. 23. The structure between the pitch-yaw hook point and the roll axes will be referred to herein as the "roll structure" and will be treated as massless with no applied load. All aerodynamic and inertial load will be applied to the store "body structure" below the roll axes.

It is very important in restricted simulations to model the conditions correctly for release of the store from the constraint mechanism so that the simulation can properly transition to free-flight motion. Several conditions must be satisfied before the F-15 pivot release simulations are allowed to switch to unrestricted motion. The different phases of the release motion are illustrated in Fig. 24. Restrained pivot motion about the pitch/yaw pivot point is arbitrarily imposed until the assembly pitches to a nose-down incidence angle relative to the aircraft greater than the design release angle of the mechanism. Twenty-four equations in 24 unknowns are used to model the store motion during this first release phase. The release angle criterion is enforced by the internal hook of the socket mechanism which is designed not to allow translational motion of the ball out of the socket until a certain pitch angle is attained. A design release angle of -15 deg is being studied for both the F-18E/F and F-22 aircraft. Various angles from -15 to -26 deg have been simulated for the F-15. After satisfying the pitch criterion, the assembly enters a second phase of the release sequence in which the motion of the store forces the ball to remain engaged in the socket, even though the internal hook is no longer effective. The same 24 equations are used to model this phase. The calculated reaction forces at the pitch/yaw pivot point are tested to determine the point at which the assembly transitions to the third phase of motion. If the calculated reaction forces at the pivot point are directed downward, the socket assembly then must be applying reaction forces to the ball to prevent upward motion of the ball and the ball and socket

must, therefore, still be firmly engaged. At the instant upward directed forces are calculated (indicative of a force trying to pull the pivot point up), the simulation switches to the equations modeling the third phase of motion because the socket assembly physically cannot pull up on the ball when the internal hook is no longer engaged. During this third phase of the release, a revised set of motion equations which leaves the ball free to move vertically out of the socket is used to model the motion. The phase three equations introduce yet another unknown to the system (the vertical acceleration of the ball out of the socket), resulting in a system of 25 equations in 25 unknowns. During this third phase of the motion, the hook is not engaged within the cutout in the ball section, but its side bearing surfaces are still in contact with the internal sidewalls of the ball so that it still effectively restricts some of the store rotational motion. After the ball moves downward 0.3 in., the internal hook is no longer in contact with the internal surfaces of the ball joint and no rotational restraints at all are applied to the assembly for a fourth phase of motion covering the interval between 0.3 in. and 1 in. of vertical separation. Three of the 25 equations are replaced for this phase of the motion. After approximately 1 in. of downward motion, the ball is assumed to be pulled entirely out of the socket, and the simulation switches to the equations of motion for a free body during the fifth and final phase of the separation simulation.

At first, it may seem that a great amount of unnecessary effort has been expended to model each of the five phases of the pivot motion, particularly since two of the phases span only 1 in. of linear motion. In actuality, the restrictions applied during that first 1 in. of vertical motion as the ball is pulling out of the socket can make the difference between safe separation from the aircraft or recontact for certain important conditions. The restrictions during the pull-out phases can also make large differences in the reaction loads imparted to the aircraft structure because the largest reaction loads occur during that pull-out movement. Rigorous details of the ball/socket/internal hook modeling will be provided later in this section.

The motion of the store body axes can be modeled to be a combination of the motion of the pitch-yaw hook point relative to inertial space, the motion of the roll joint about the pitch-yaw hook point, and the motion of the body about the roll point. The first body treated in the two body problem will be the offset roll structure between the roll joint and the pitch-yaw joint. Following presentation of the roll structure equations, the equations for motion of the store body relative to the roll axes will be presented. The equations modeling the interconnection of the roll structure with the body structure will then be presented, followed by the equations modeling the constraints at the pitch/yaw point. Finally, the system of 24 equations for first two phases of the pivot release motion will be presented, followed by the revised systems of 25 equations for the third and fourth release phases.

Beginning with the relationship between the inertial positions of inertial, hook, and roll axes, the equations for the roll structure are developed in a manner analogous to the standard translational equations in Section 4.1.2:

$$\begin{vmatrix} XIRI \\ YIRI \\ ZIRI \end{vmatrix} = \begin{vmatrix} XIHI \\ YIHI \\ ZIHI \end{vmatrix} + \begin{vmatrix} XIRH \\ YIRH \\ ZIRH \end{vmatrix} \quad (4.3.5.1)$$

where:

$$\begin{vmatrix} XIRH \\ YIRH \\ ZIRH \end{vmatrix} = [TRNRI]^{-1} \begin{vmatrix} XRRH \\ YRRH \\ ZRRH \end{vmatrix} \quad (4.3.5.2)$$

Taking derivatives of both sides using the chain rule to get inertial velocity:

$$\frac{d}{dt} \begin{vmatrix} XIRI \\ YIRI \\ ZIRI \end{vmatrix} = \frac{d}{dt} \begin{vmatrix} XIHI \\ YIHI \\ ZIHI \end{vmatrix} + \frac{d}{dt} [TRNRI]^{-1} \begin{vmatrix} XRRH \\ YRRH \\ ZRRH \end{vmatrix} + [TRNRI]^{-1} \frac{d}{dt} \begin{vmatrix} XRRH \\ YRRH \\ ZRRH \end{vmatrix} \quad (4.3.5.3)$$

or (noting that the derivative of the fixed transfer distance is zero):

$$\begin{vmatrix} UIRI \\ VIRI \\ WIRI \end{vmatrix} = \begin{vmatrix} UIHI \\ VIHI \\ WIHI \end{vmatrix} + [TRNRI]^{-1} [\tilde{\omega} RRI] \begin{vmatrix} XRRH \\ YRRH \\ ZRRH \end{vmatrix} \quad (4.3.5.4)$$

Projecting to roll-axis components by [TRNRI] :

$$\begin{vmatrix} URRI \\ VRRI \\ WRRI \end{vmatrix} = \begin{vmatrix} URHI \\ VRHI \\ WRHI \end{vmatrix} + [\tilde{\omega} RRI] \begin{vmatrix} XRRH \\ YRRH \\ ZRRH \end{vmatrix} \quad (4.3.5.5)$$

Equation (4.3.5.5) provides the interconnect between pitch-yaw hook velocities and roll joint velocities. A similar relation for accelerations can be developed by taking a second derivative of Eq. (4.3.5.4):

$$\begin{aligned} \frac{d}{dt} \begin{vmatrix} UIRI \\ VIRI \\ WIRI \end{vmatrix} &= \frac{d}{dt} \begin{vmatrix} UIHI \\ VIHI \\ WIHI \end{vmatrix} + \frac{d}{dt} [TRNRI]^{-1} [\tilde{\omega} RRI] \begin{vmatrix} XRRH \\ YRRH \\ ZRRH \end{vmatrix} + [TRNRI]^{-1} \frac{d}{dt} [\tilde{\omega} RRI] \begin{vmatrix} XRRH \\ YRRH \\ ZRRH \end{vmatrix} \\ &\quad + [TRNRI]^{-1} [\tilde{\omega} RRI] \frac{d}{dt} \begin{vmatrix} XRRH \\ YRRH \\ ZRRH \end{vmatrix} \end{aligned} \quad (4.3.5.6)$$

or:

$$\begin{vmatrix} AXIRI \\ AYIRI \\ AZIRI \end{vmatrix} = \begin{vmatrix} AXIHI \\ AYIHI \\ AZIHI \end{vmatrix} + [TRNRI]^{-1} [\tilde{\omega} RRI] [\tilde{\omega} RRI] \begin{vmatrix} XRRH \\ YRRH \\ ZRRH \end{vmatrix} + [TRNRI]^{-1} [D\tilde{\omega} RRI] \begin{vmatrix} XRRH \\ YRRH \\ ZRRH \end{vmatrix} \quad (4.3.5.7)$$

Project to body-axis components by [TRNRI]:

$$\begin{vmatrix} AXRRI \\ AYRRI \\ AZRRI \end{vmatrix} = \begin{vmatrix} AXRHI \\ AYRHI \\ AZRHI \end{vmatrix} + [\tilde{\omega} RRI] [\tilde{\omega} RRI] \begin{vmatrix} XRRH \\ YRRH \\ ZRRH \end{vmatrix} + [D\tilde{\omega} RRI] \begin{vmatrix} XRRH \\ YRRH \\ ZRRH \end{vmatrix} \quad (4.3.5.8)$$

This relation provides the interconnect between pitch-yaw hook accelerations and roll joint accelerations.

A force balance on the roll structure requires:

$$\begin{vmatrix} \Sigma F_{XR} \\ \Sigma F_{YR} \\ \Sigma F_{ZR} \end{vmatrix} = \begin{vmatrix} -r_{XR} \\ -r_{YR} \\ -r_{ZR} \end{vmatrix} + \begin{vmatrix} RXR \\ RYR \\ RZR \end{vmatrix} = m_R \begin{vmatrix} AXRRI \\ AYRRI \\ AZRRI \end{vmatrix} \quad (4.3.5.9)$$

where the lower case "r" denotes an internal reaction force on the roll structure at the roll joint which is equal and opposite to the internal reaction force on the body structure at the roll joint. But the mass of the structure between the roll joint and the pitch-yaw joint is zero ($m_R = 0.0$), so that:

$$\begin{vmatrix} r_{XR} \\ r_{YR} \\ r_{ZR} \end{vmatrix} = \begin{vmatrix} RXR \\ RYR \\ RZR \end{vmatrix} \quad (4.3.5.10)$$

The relationship between projected acceleration and the derivative of projected velocity [analogous to Eq. (4.1.2.10)] can also be used in conjunction with Eq. (4.3.5.8) to determine the parameters normally integrated to determine the projected velocities at each time step:

$$\begin{vmatrix} DURRI \\ DVRRI \\ DWRRI \end{vmatrix} = \begin{vmatrix} AXRHI \\ AYRHI \\ AZRHI \end{vmatrix} + [\tilde{\omega} RRI] [\tilde{\omega} RRI] \begin{vmatrix} XRRH \\ YRRH \\ ZRRH \end{vmatrix} + [D\tilde{\omega} RRI] \begin{vmatrix} XRRH \\ YRRH \\ ZRRH \end{vmatrix} - [\tilde{\omega} RRI] \begin{vmatrix} URRI \\ VRRI \\ WRRI \end{vmatrix} \quad (4.3.5.11)$$

Having now developed expressions for the linear motion of the roll-joint axes relative to the pitch-yaw hook axes, an almost identical development will result in the following expressions for the linear motion of the body axes relative to the roll joint axes. The interconnect between roll joint velocities and body velocities is:

$$\begin{vmatrix} UBBI \\ VBBI \\ WBBI \end{vmatrix} = \begin{vmatrix} UBRI \\ VBRI \\ WBRI \end{vmatrix} + [\tilde{\omega} BBI] \begin{vmatrix} XBBR \\ YBBR \\ ZBBR \end{vmatrix} \quad (4.3.5.12)$$

The interconnect between roll joint accelerations and body accelerations is:

$$\begin{vmatrix} AXBBI \\ AYBBI \\ AZBBI \end{vmatrix} = \begin{vmatrix} AXBRI \\ AYBRI \\ AZBRI \end{vmatrix} + [\tilde{\omega} BBI] [\tilde{\omega} BBI] \begin{vmatrix} XBBR \\ YBBR \\ ZBBR \end{vmatrix} + [D\tilde{\omega} BBI] \begin{vmatrix} XBBR \\ YBBR \\ ZBBR \end{vmatrix} \quad (4.3.5.13)$$

A force balance on the body requires:

$$\begin{vmatrix} \Sigma F_{XB} \\ \Sigma F_{YB} \\ \Sigma F_{ZB} \end{vmatrix} = \begin{vmatrix} r_{XB} \\ r_{YB} \\ r_{ZB} \end{vmatrix} + \begin{vmatrix} F_{XB} \\ F_{YB} \\ F_{ZB} \end{vmatrix} = m_B \begin{vmatrix} A_{XBBI} \\ A_{YBBI} \\ A_{ZBBI} \end{vmatrix} \quad (4.3.5.14)$$

where the lower case "r" denotes an internal reaction force on the body at the roll joint which is equal and opposite to the internal reaction force on the roll structure at the roll joint and $m_B = m$ since all the mass is in the body structure.

The relationship between projected acceleration and the derivative of projected velocity [Eq. (4.1.2.10)] can also be used in conjunction with Eq. (4.3.5.13) to determine the parameters normally integrated to determine the projected velocities at each time step:

$$\begin{vmatrix} D_{UBBI} \\ D_{VBBI} \\ D_{WBBI} \end{vmatrix} = \begin{vmatrix} A_{XBRI} \\ A_{YBRI} \\ A_{ZBRI} \end{vmatrix} + [\tilde{\omega}_{BBI}] [\tilde{\omega}_{BBI}] \begin{vmatrix} X_{BBR} \\ Y_{BBR} \\ Z_{BBR} \end{vmatrix} + [D\tilde{\omega}_{BBI}] \begin{vmatrix} X_{BBH} \\ Y_{BBH} \\ Z_{BBH} \end{vmatrix} - [\tilde{\omega}_{BBI}] \begin{vmatrix} U_{BBI} \\ V_{BBI} \\ W_{BBI} \end{vmatrix} \quad (4.3.5.15)$$

The relation between the internal body-axis reaction forces of Eq. (4.3.5.14) and the internal roll-axis reaction forces of Eq. (4.3.5.9) is simply:

$$\begin{vmatrix} r_{XB} \\ r_{YB} \\ r_{ZB} \end{vmatrix} = [TRNBR] \begin{vmatrix} r_{XR} \\ r_{YR} \\ r_{ZR} \end{vmatrix} \quad (4.3.5.16)$$

A similar relation applies for reaction moments which will be needed for the rotational equations developed in the next several paragraphs:

$$\begin{vmatrix} r_{LB} \\ r_{MB} \\ r_{NB} \end{vmatrix} = [TRNMR] \begin{vmatrix} r_{LR} \\ r_{MR} \\ r_{NR} \end{vmatrix} \quad (4.3.5.17)$$

The rotational equations for the two-body problem are exactly analogous to the single-body equations developed in Section 4.2.2. The reader is referred to Section 4.2.2 for the full derivation of the equations. Only the application of the rotational equations to the two-body problem will be presented here. The rotational equations for the body about the roll axes are presented first, followed by the rotational equations of the roll axes about the pitch-yaw hook axes.

The body-axis components of the relative angular momentum about the roll joint axes are calculated directly from body-axis inertia terms:

$$\begin{vmatrix} H_{XBRR} \\ H_{YBRR} \\ H_{ZBRR} \end{vmatrix} = [I]_{BR} \begin{vmatrix} P_{BBI} \\ Q_{BBI} \\ R_{BBI} \end{vmatrix} \quad (4.3.5.18)$$

where the body-axis components of the inertia about the roll joint axes are computed from the parallel axis theorem:

$$\begin{aligned} I_{xxBR} &= I_{xxBB} + m(YBBR^2 + ZBBR^2) \\ I_{yyBR} &= I_{yyBB} + m(XBBR^2 + ZBBR^2) \\ I_{zzBR} &= I_{zzBB} + m(XBBR^2 + YBBR^2) \\ I_{xyBR} &= I_{xyBB} + m(XBBR * YBBR) \\ I_{xzBR} &= I_{xzBB} + m(XBBR * ZBBR) \\ I_{yzBR} &= I_{yzBB} + m(YBBR * ZBBR) \end{aligned} \quad (4.3.5.19)$$

The derivative of the relative angular momentum of the body structure is obtained from an expression analogous to Eq. (4.2.2.42):

$$\begin{aligned} [I]_{BR} \begin{vmatrix} DPBBI \\ DQBBI \\ DRBBI \end{vmatrix} &= -[\tilde{\omega} BBI] [I]_{BR} \begin{vmatrix} PBBI \\ QBBI \\ RBBI \end{vmatrix} + \begin{vmatrix} MXB \\ MYB \\ MZB \end{vmatrix} + \begin{vmatrix} rLB \\ rMB \\ rNB \end{vmatrix} + \begin{vmatrix} XBBR \\ YBBR \\ ZBBR \end{vmatrix} \times \begin{vmatrix} FXB \\ FYB \\ FZB \end{vmatrix} \\ &\quad - m \begin{vmatrix} XBBR \\ YBBR \\ ZBBR \end{vmatrix} \times \begin{vmatrix} AXBRI \\ AYBRI \\ AZBRI \end{vmatrix} \\ &= -[\tilde{\omega} BBI] \begin{vmatrix} HXBRR \\ HYBRR \\ HZBRR \end{vmatrix} + \begin{vmatrix} MXB \\ MYB \\ MZB \end{vmatrix} + \begin{vmatrix} rLB \\ rMB \\ rNB \end{vmatrix} + \begin{vmatrix} XBBR \\ YBBR \\ ZBBR \end{vmatrix} \times \begin{vmatrix} FXB \\ FYB \\ FZB \end{vmatrix} - m \begin{vmatrix} XBBR \\ YBBR \\ ZBBR \end{vmatrix} \times \begin{vmatrix} AXBRI \\ AYBRI \\ AZBRI \end{vmatrix} \end{aligned} \quad (4.3.5.20)$$

where the lower case "r" denotes internal reaction moments at the roll joint.

The rotational equations of motion for the structure between the pitch-yaw pivot and the roll axes are developed similarly but have some special properties because the structure is considered to be massless. The body-axis components of the relative angular momentum of the roll structure about the pitch-yaw hook axes are:

$$\begin{vmatrix} HXRHH \\ HYRHH \\ HZRHH \end{vmatrix} = [I]_{RH} \begin{vmatrix} PRRI \\ QRRI \\ RRRI \end{vmatrix} \quad (4.3.5.21)$$

But, since the structure is massless, it has zero inertia, so that:

$$\begin{vmatrix} HXRHH \\ HYRHH \\ HZRHH \end{vmatrix} = \begin{vmatrix} 0.0 \\ 0.0 \\ 0.0 \end{vmatrix} \quad (4.3.5.22)$$

The derivative of the projected relative angular momentum of the roll structure is obtained from an expression analogous to Eq. (4.2.2.42):

$$\begin{aligned}
 [I]_{RH} \begin{vmatrix} DPRRI \\ DQRRI \\ DRRRI \end{vmatrix} &= -[\tilde{\omega} RRI] [I]_{RH} \begin{vmatrix} PRRI \\ QRRI \\ RRRI \end{vmatrix} + \begin{vmatrix} -rLR \\ -rMR \\ -rNR \end{vmatrix} + \begin{vmatrix} RLR \\ RMR \\ RNR \end{vmatrix} + \begin{vmatrix} XRRH \\ YRRH \\ ZRRH \end{vmatrix} X \begin{vmatrix} -rXR \\ -rYR \\ -rZR \end{vmatrix} \\
 &\quad - m_R \begin{vmatrix} XRRH \\ YRRH \\ ZRRH \end{vmatrix} X \begin{vmatrix} AXRHI \\ AYRHI \\ AZRHI \end{vmatrix}
 \end{aligned} \tag{4.3.5.23}$$

However, if the roll structure is massless, then $[I]_{RH} = 0.0$ and $m_R = 0.0$, and the rotational equations for the roll structure reduce to:

$$\begin{vmatrix} 0.0 \\ 0.0 \\ 0.0 \end{vmatrix} = \begin{vmatrix} -rLR - rZR*YRRH + rYR*ZRRH + RLR \\ -rMR - rXR*ZRRH + rZR*XRRH + RMR \\ -rNR - rYR*XRRH + rXR*YRRH + RNR \end{vmatrix} \tag{4.3.5.24}$$

Note that the rotational velocity derivative vector drops out of the rotational equations because of the zero inertia matrix. As will be shown shortly, the rotations of the roll structure are fully proscribed through constraint relationships relative to the body rotations.

The fully generalized/fully expanded two-body equations for the first two phases of the pivot release simulation consist of 24 equations in 24 unknowns. The selected unknowns are: three translational acceleration components {AXBBI, AYBBI, AZBBI} of the body axes, three translational acceleration components {AXRRI, AYRRI, AZRRI} of the roll axes, three rotational acceleration components {DPBBI, DQBBI, DRBBI} of the body axes, three rotational acceleration components {DPRRI, DQRRI, DRRRI} of the roll axes, three internal reaction force components {rXB, rYB, rZB} at the roll joint, three external reaction force components {RXR, RYR, RZR} at the pitch-yaw hook point, three internal reaction moment components {rLB, rMB, rNB} at the roll joint, and three external reaction moment components {RLR, RMR, RNR} at the pitch-yaw hook point. Twenty-four linearly independent equations are necessary to determine the 24 independent variables. The first three of the necessary equations are the restricted translational equations of motion for the roll axes defined by Eq. (4.3.5.8). The double cross-product term in Eq. (4.3.5.8) is first evaluated and stored in temporary vector {OOXRRH} denoting Omega cross Omega cross r for the {XRRH} vector:

$$\begin{vmatrix} OOXRRH \\ OOVRRH \\ OOZRRH \end{vmatrix} = \begin{vmatrix} PRRI \\ QRRI \\ RRRI \end{vmatrix} X \begin{vmatrix} PRRI \\ QRRI \\ RRRI \end{vmatrix} X \begin{vmatrix} XRRH \\ YRRH \\ ZRRH \end{vmatrix} \tag{4.3.5.25}$$

Then Eqs. (4.3.5.8) are written in terms of the first six unknowns and expanded into scalar form as:

$$\begin{aligned}
 \#1) \quad & ZRRH * DQRRI - YRRH * DRRRI - AXRRI = -OOXRRH - AXRHI \\
 \#2) \quad & -ZRRH * DPRRI + XRRH * DRRRI - AYRRI = -OOYRRH - AYRHI \\
 \#3) \quad & YRRH * DPRRI - XRRH * DQRRI - AZRRI = -OOZRRH - AZRHI
 \end{aligned} \tag{4.3.5.26}$$

The next three equations are the restricted rotational equations of motion for the roll joint axes defined by Eq. (4.3.5.24). Rewriting in scalar form [using Eqs. (4.3.5.16) and (4.3.5.17)]:

$$\begin{aligned}
 \#4) & -\text{TRNBR}(1,1) * \text{rLB} - \text{TRNBR}(2,1) * \text{rMB} - \text{TRNBR}(3,1) * \text{rNB} \\
 & + (-\text{YRRH} * \text{TRNBR}(1,3) + \text{ZRRH} * \text{TRNBR}(1,2)) * \text{rXB} \\
 & + (-\text{YRRH} * \text{TRNBR}(2,3) + \text{ZRRH} * \text{TRNBR}(2,2)) * \text{rYB} \\
 & + (-\text{YRRH} * \text{TRNBR}(3,3) + \text{ZRRH} * \text{TRNBR}(3,2)) * \text{rZB} + \text{RLR} = 0.0 \\
 \#5) & -\text{TRNBR}(1,2) * \text{rLB} - \text{TRNBR}(2,2) * \text{rMB} - \text{TRNBR}(3,2) * \text{rNB} \\
 & + (-\text{ZRRH} * \text{TRNBR}(1,1) + \text{XRRH} * \text{TRNBR}(1,3)) * \text{rXB} \\
 & + (-\text{ZRRH} * \text{TRNBR}(2,1) + \text{XRRH} * \text{TRNBR}(2,3)) * \text{rYB} \\
 & + (-\text{ZRRH} * \text{TRNBR}(3,1) + \text{XRRH} * \text{TRNBR}(3,3)) * \text{rZB} + \text{RMR} = 0.0 \\
 \#6) & -\text{TRNBR}(1,3) * \text{rLB} - \text{TRNBR}(2,3) * \text{rMB} - \text{TRNBR}(3,3) * \text{rNB} \\
 & + (-\text{XRRH} * \text{TRNBR}(1,2) + \text{YRRH} * \text{TRNBR}(1,1)) * \text{rXB} \\
 & + (-\text{XRRH} * \text{TRNBR}(2,2) + \text{YRRH} * \text{TRNBR}(2,1)) * \text{rYB} \\
 & + (-\text{XRRH} * \text{TRNBR}(3,2) + \text{YRRH} * \text{TRNBR}(3,1)) * \text{rZB} + \text{RNR} = 0.0
 \end{aligned} \tag{4.3.5.27}$$

The next three of the necessary equations are the restricted translational equations of motion for the body axes defined by Eq. (4.3.5.13). The double cross-product term in Eq. (4.3.5.13) is first evaluated and stored in a temporary vector:

$$\begin{vmatrix} \text{OOXBBR} \\ \text{OOYBBR} \\ \text{OOZBBR} \end{vmatrix} = \begin{vmatrix} \text{PBBI} \\ \text{QBBI} \\ \text{RBBI} \end{vmatrix} \times \begin{vmatrix} \text{PBBI} \\ \text{QBBI} \\ \text{RBBI} \end{vmatrix} \times \begin{vmatrix} \text{XBBR} \\ \text{YBBR} \\ \text{ZBBR} \end{vmatrix} \tag{4.3.5.28}$$

Equations (4.3.5.13) are then written in terms of the unknowns and expanded into scalar form as:

$$\begin{aligned}
 \#7) & \text{TRNBR}(1,1) * \text{AXRRI} + \text{TRNBR}(1,2) * \text{AYRRI} + \text{TRNBR}(1,3) * \text{AZRRI} \\
 & - \text{AXBBI} + \text{ZBBR} * \text{DQBBI} - \text{YBBR} * \text{DRBBI} = -\text{OOXBBR} \\
 \#8) & \text{TRNBR}(2,1) * \text{AXRRI} + \text{TRNBR}(2,2) * \text{AYRRI} + \text{TRNBR}(2,3) * \text{AZRRI} \\
 & - \text{AYBBI} - \text{ZBBR} * \text{DPBBI} + \text{XBBR} * \text{DRBBI} = -\text{OOYBBR} \\
 \#9) & \text{TRNBR}(3,1) * \text{AXRRI} + \text{TRNBR}(3,2) * \text{AYRRI} + \text{TRNBR}(3,3) * \text{AZRRI} \\
 & - \text{AZBBI} + \text{YBBR} * \text{DPBBI} - \text{XBBR} * \text{DQBBI} = -\text{OOZBBR}
 \end{aligned} \tag{4.3.5.29}$$

The next three equations come from the force balance on the body [Eq. (4.3.5.14)]. Rewriting:

$$\begin{aligned}
 \#10) & -\text{AXBBI} + \text{rXB}/m = -\text{FXB}/m \\
 \#11) & -\text{AYBBI} + \text{rYB}/m = -\text{FYB}/m \\
 \#12) & -\text{AZBBI} + \text{rZB}/m = -\text{FZB}/m
 \end{aligned} \tag{4.3.5.30}$$

The next three equations come from the force balance on the roll structure [Eq. (4.3.5.10)]. Rewriting using Eq. (4.3.5.16):

$$\begin{aligned}
 \#13) & -\text{RXR} + \text{TRNBR}(1,1) * \text{rXB} + \text{TRNBR}(2,1) * \text{rYB} + \text{TRNBR}(3,1) * \text{rZB} = 0.0 \\
 \#14) & -\text{RYR} + \text{TRNBR}(1,2) * \text{rXB} + \text{TRNBR}(2,2) * \text{rYB} + \text{TRNBR}(3,2) * \text{rZB} = 0.0 \\
 \#15) & -\text{RZR} + \text{TRNBR}(1,3) * \text{rXB} + \text{TRNBR}(2,3) * \text{rYB} + \text{TRNBR}(3,3) * \text{rZB} = 0.0
 \end{aligned} \tag{4.3.5.31}$$

The next three equations are the restricted rotational equations of motion for the body axes. First, the body-axis components of the angular momentum about the roll axes are calculated directly from body-axis inertia terms using Eqs. (4.3.5.18) and (4.3.5.19). Then Eq. (4.3.5.20) is expanded in terms of the selected unknowns as:

$$\begin{aligned}
 \#16) \quad & [I]_{BR}(1,1) * DPBBI + [I]_{BR}(1,2) * DQBBI + [I]_{BR}(1,3) * DRBBI - rLB \\
 & + (YBBR * TRNBR(3,1) - ZBBR * TRNBR(2,1)) * m * AXRRI \\
 & + (YBBR * TRNBR(3,2) - ZBBR * TRNBR(2,2)) * m * AYRRI \\
 & + (YBBR * TRNBR(3,3) - ZBBR * TRNBR(2,3)) * m * AZRRI \\
 & = - QBBI * HZBRR + RBBI * HYBRR + MXB + YBBR * FZB - ZBBR * FYB \\
 \#17) \quad & [I]_{BR}(2,1) * DPBBI + [I]_{BR}(2,2) * DQBBI + [I]_{BR}(2,3) * DRBBI - rMB \\
 & + (ZBBR * TRNBR(1,1) - XBBR * TRNBR(3,1)) * m * AXRRI \quad (4.3.5.32) \\
 & + (ZBBR * TRNBR(1,2) - XBBR * TRNBR(3,2)) * m * AYRRI \\
 & + (ZBBR * TRNBR(1,3) - XBBR * TRNBR(3,3)) * m * AZRRI \\
 & = - RBBI * HXBRR + PBBI * HZBRR + MYB + ZBBR * FXB - XBBR * FZB \\
 \#18) \quad & [I]_{BR}(3,1) * DPBBI + [I]_{BR}(3,2) * DQBBI + [I]_{BR}(3,3) * DRBBI - rNB \\
 & + (XBBR * TRNBR(2,1) - YBBR * TRNBR(1,1)) * m * AXRRI \\
 & + (XBBR * TRNBR(2,2) - YBBR * TRNBR(1,2)) * m * AYRRI \\
 & + (XBBR * TRNBR(2,3) - YBBR * TRNBR(1,3)) * m * AZRRI \\
 & = - PBBI * HYBRR + QBBI * HXBRR + MZB + XBBR * FYB - YBBR * FXB
 \end{aligned}$$

Six more constraint equations are needed to allow solution for the 24 unknowns; three of those equations arise from the requirement that the yaw and pitch rates of the body match the yaw and pitch rates of the roll assembly at the roll joint. This requirement puts constraints on the internal reaction moments at the roll joint. The first internal constraint equation is trivial - the body axes are able to rotate freely (without resistance) about the roll axis. The internal reaction rolling moment is, therefore, zero:

$$rLB = 0.0 \quad (4.3.5.33)$$

The yaw/pitch internal constraints require the development of a relation between the rotational accelerations of the body and of the roll assembly between the roll axis and the pitch/yaw axis. Beginning with the relationship between body and roll axis rotational velocities:

$$\begin{vmatrix} PBBI - PBBR \\ QBBI - QBBR \\ RBBI - RBBR \end{vmatrix} = [TRNBR] \begin{vmatrix} PRRI \\ QRRI \\ RRRI \end{vmatrix} = \begin{vmatrix} PBRI \\ QBRI \\ RBRI \end{vmatrix} \quad (4.3.5.34)$$

Where {PBBR} represents the rotation of the body relative to the roll assembly. Taking derivatives of both sides by the chain rule:

$$\frac{d}{dt} \begin{vmatrix} PBBI \\ QBBI \\ RBBI \end{vmatrix} - \frac{d}{dt} \begin{vmatrix} PBBR \\ QBBR \\ RBBR \end{vmatrix} = \frac{d}{dt} [TRNBR] \begin{vmatrix} PRRI \\ QRRI \\ RRRI \end{vmatrix} + [TRNBR] \frac{d}{dt} \begin{vmatrix} PRRI \\ QRRI \\ RRRI \end{vmatrix} \quad (4.3.5.35)$$

or:

$$\begin{vmatrix} DPBBI \\ DQBBI \\ DRBBI \end{vmatrix} - \begin{vmatrix} DPBBR \\ DQBBR \\ DRBBR \end{vmatrix} = -[\tilde{\omega} BBR] [TRNBR] \begin{vmatrix} PRRI \\ QRRI \\ RRRRI \end{vmatrix} + [TRNBR] \begin{vmatrix} DPRRI \\ DQRRI \\ DRRRI \end{vmatrix} \quad (4.3.5.36)$$

Note that the last term in Eq. (4.3.5.36) represents the projection of the derivative of a projection and is not equivalent to the {DPBRI} vector. It is convenient to rewrite Eq. (4.3.5.36) using cross products instead of the skew-symmetric matrix:

$$\begin{vmatrix} DPBBI \\ DQBBI \\ DRBBI \end{vmatrix} - \begin{vmatrix} DPBBR \\ DQBBR \\ DRBBR \end{vmatrix} = - \begin{vmatrix} PBBR \\ QBBR \\ RBBR \end{vmatrix} \times \begin{vmatrix} PBRI \\ QBRI \\ RBRI \end{vmatrix} + [TRNBR] \begin{vmatrix} DPRRI \\ DQRRI \\ DRRRI \end{vmatrix} \quad (4.3.5.37)$$

The desired constraints are that no relative pitch or yaw rotational velocity exist between body and roll axes, so that:

$$QBBR = RBBR = DQBBR = DRBBR = 0.0 \quad (4.3.5.38)$$

Substituting Eq. (4.3.5.38) into Eq. (4.3.5.37):

$$\begin{vmatrix} DPBBI - DPBBR \\ DQBBI \\ DRBBI \end{vmatrix} = - \begin{vmatrix} PBBR \\ 0.0 \\ 0.0 \end{vmatrix} \times \begin{vmatrix} PBRI \\ QBRI \\ RBRI \end{vmatrix} + [TRNBR] \begin{vmatrix} DPRRI \\ DQRRI \\ DRRRI \end{vmatrix} \quad (4.3.5.39)$$

Expanding the cross product results in the final constraint equation:

$$\begin{vmatrix} DPBBI - DPBBR \\ DQBBI \\ DRBBI \end{vmatrix} = \begin{vmatrix} 0.0 \\ PBBR * RBRI \\ -PBBR * QBRI \end{vmatrix} + [TRNBR] \begin{vmatrix} DPRRI \\ DQRRI \\ DRRRI \end{vmatrix} \quad (4.3.5.40)$$

Note that the x component of vector Eq. (4.3.5.40) provides no useful information - one of the three necessary constraints was already defined by Eq. (4.3.5.33). The other two components of the vector equation provide the interrelation constraint between body and roll axis rotations. The PBBR term in Eq. (4.3.5.40) is evaluated from the relation of Eq. (4.3.5.34). The three internal constraints expanded out to scalar form are:

- #19) $rLB = 0.0$
- #20) $TRNBR(2,1)*DPRRI + TRNBR(2,2)*DQRRI + TRNBR(2,3)*DRRI - DQBBI = -(PBBI - PBRI) * RBRI$
- #21) $TRNBR(3,1)*DPRRI + TRNBR(3,2)*DQRRI + TRNBR(3,3)*DRRI - DRBBI = (PBBI - PBRI) * QBRI$

(4.3.5.41)

Where:

$$\begin{vmatrix} PBRI \\ QBRI \\ RBRI \end{vmatrix} = [TRNBR] \begin{vmatrix} PRRI \\ QRRI \\ RRRI \end{vmatrix} \quad (4.3.5.42)$$

The final three equations come from the pivot constraint at the pitch/yaw joint. The upper pivot of the F-15 assembly greatly differs mechanically from the F-16 type assembly described in Section 4.3.4 and is much more difficult to model. The primary pitch/yaw joint of the F-15 device as described earlier is basically a ball-in-socket with an internal hook which fits into an open section in the ball. The socket is fixed mounted into the lower surface of the aircraft wing or pylon. The internal hook is at the end of a vertical shaft which extends through the upper surface of the socket into the well. The vertical hook shaft defines the z axis of a new axis system (the shaft axis system designated by the character "S") which will be used to help describe hook motion. The internal hook (and therefore the ball fixture attached to the store which latches to the hook within the socket) is free to yaw about the shaft axis. In the F-15 aircraft the socket is often mounted flush with the lower surface of the pylon so that its internal hook is aligned with the ZP axis. In the F-22, the socket/hook assembly is normally pitched 5 deg relative to pylon axes: THASP = -THAPS = 5.0. The equations in this section are written using a specified orientation matrix [TRNPS] which defines the alignment of the shaft axes relative to pylon axes to allow for maximum flexibility. At its yawed position, the ball joint within the socket is free to pitch about the lateral axis of the yawed hook but the internal hook within the hollowed out section of the ball does not allow any other rotational components. In summary, the roll assembly is free to yaw about the shaft z-axis direction, is free to pitch about the resulting new internal hook pitch axis, and is restricted to allow no rotation about the remaining mutually perpendicular axis. The third component is enforced by defining the axis system for which the z axis is aligned with the shaft z axis, the y axis is rotated in yaw with the internal hook relative to shaft axes, and the x axis is perpendicular to the z and y axes. This new axis system will be designated by the symbol "U" for "unpitched" axes because it represents an intermediate system for defining the yaw motion of the hook relative to shaft axes before the pitch motion of the store about the internal hook is applied. The constraints can be written mathematically as:

$$\begin{aligned} RNS &= 0.0 \text{ free to yaw about shaft axes} \\ RMU &= 0.0 \text{ free to pitch about yawed (unpitched) bar axes} \\ DPUUS &= 0.0 \text{ restrained to no rotation about the mutually perpendicular axis} \end{aligned} \quad (4.3.5.43)$$

To be completely general and arbitrary it would be necessary to write a coupled two-body system of equations solving the yaw motion of the internal hook about the shaft axes simultaneously with the pitch motion of the roll assembly axes about the hook. It is convenient, however, to solve the pitch/yaw motion as a single body problem in terms of roll assembly motion relative to hook axes by rewriting the Eq. (4.3.5.43) constraints in terms of quantities not directly involving the "unpitched" system. The RNS = 0 constraint can be written out directly as projections of the unknown roll axis reaction force terms:

$$\text{TRNRS}(1,3)*\text{RLR} + \text{TRNRS}(2,3)*\text{RMR} + \text{TRNRS}(3,3)*\text{RNR} = 0.0 \quad (4.3.5.44)$$

The RMU = 0 constraint can also be written easily by noting that the y axes of unpitched and roll axes are parallel so that:

$$\text{RMU} = \text{RMR} = 0.0. \quad (4.3.5.45)$$

The development of a coupled single-body form for the third constraint of Eq. (4.3.5.43) involves an extremely complicated derivation, however, which will be carried out in the next twelve equations.

Beginning with the relations for the angular velocities for the unpitched axes relative to the yaw shaft:

$$\begin{vmatrix} \text{PUUS} \\ \text{QUUS} \\ \text{RUUS} \end{vmatrix} = \begin{vmatrix} \text{PUUI} \\ \text{QUUI} \\ \text{RUUI} \end{vmatrix} - \begin{vmatrix} \text{PUSI} \\ \text{QUSI} \\ \text{RUSI} \end{vmatrix} = \begin{vmatrix} \text{PURI} \\ \text{QURI} \\ \text{RURI} \end{vmatrix} + \begin{vmatrix} \text{PUUR} \\ \text{QUUR} \\ \text{RUUR} \end{vmatrix} - \begin{vmatrix} \text{PUSI} \\ \text{QUSI} \\ \text{RUSI} \end{vmatrix} \quad (4.3.5.46)$$

or:

$$\begin{vmatrix} \text{PUUS} \\ \text{QUUS} \\ \text{RUUS} \end{vmatrix} = [\text{TRNRU}]^T \begin{vmatrix} \text{PRRI} \\ \text{QRRI} \\ \text{RRRI} \end{vmatrix} + \begin{vmatrix} \text{PUUR} \\ \text{QUUR} \\ \text{RUUR} \end{vmatrix} - [\text{TRNSU}]^T \begin{vmatrix} \text{PSSI} \\ \text{QSSI} \\ \text{RSSI} \end{vmatrix} \quad (4.3.5.47)$$

where the angular velocity and angular velocity derivative components of the shaft axes are directly related to those of the pylon axes because pylon and shaft axes are both fixed relative to the aircraft ($\{\text{PSSI}\} = \{\text{PSPI}\}$):

$$\begin{vmatrix} \text{PSSI} \\ \text{QSSI} \\ \text{RSSI} \end{vmatrix} = [\text{TRNPS}]^T \begin{vmatrix} \text{PPPI} \\ \text{QPPI} \\ \text{RPPI} \end{vmatrix} \quad (4.3.5.48)$$

and

$$\begin{vmatrix} \text{DPSSI} \\ \text{DQSSI} \\ \text{DRSSI} \end{vmatrix} = [\text{TRNPS}]^T \begin{vmatrix} \text{DPPPI} \\ \text{DQPPI} \\ \text{DRPPI} \end{vmatrix} \quad (4.3.5.49)$$

The $\{\text{PPPI}\}$ and $\{\text{DPPPI}\}$ vectors are obtained from the aircraft maneuver model (Sections 4.3.1 or 4.3.9). The $[\text{TRNPS}]$ matrix comes from the geometry of the hook yaw shaft relative to pylon axes and is an input which depends on the mounting of the hook assembly. For most F-15 installations, the $[\text{TRNPS}]$ matrix is an identity; for the F-22, the $[\text{TRNPS}]$ matrix is created by a -5-deg pitch rotation using Eq. (1.3.8) [or Eq. (1.3.5)].

Taking derivatives of both sides by the chain rule:

$$\begin{aligned} \frac{d}{dt} \begin{vmatrix} PUUS \\ QUUS \\ RUUS \end{vmatrix} &= \frac{d}{dt} [TRNRU]^T \begin{vmatrix} PRRI \\ QRRI \\ RRRI \end{vmatrix} + [TRNRU]^T \frac{d}{dt} \begin{vmatrix} PRRI \\ QRRI \\ RRRI \end{vmatrix} + \frac{d}{dt} \begin{vmatrix} PUUR \\ QUUR \\ RUUR \end{vmatrix} \\ &\quad - \frac{d}{dt} [TRNSU]^T \begin{vmatrix} PSSI \\ QSSI \\ RSSI \end{vmatrix} - [TRNSU]^T \frac{d}{dt} \begin{vmatrix} PSSI \\ QSSI \\ RSSI \end{vmatrix} \end{aligned} \quad (4.3.5.50)$$

or:

$$\begin{aligned} \begin{vmatrix} DPUUS \\ DQUUS \\ DRUUS \end{vmatrix} &= [TRNRU]^T [\tilde{\omega} RRU] \begin{vmatrix} PRRI \\ QRRI \\ RRRI \end{vmatrix} + [TRNRU]^T \begin{vmatrix} DPRRI \\ DQRRI \\ DRRRI \end{vmatrix} + \begin{vmatrix} DPUUR \\ DQUUR \\ DRUUR \end{vmatrix} \\ &\quad - [TRNSU]^T [\tilde{\omega} SSU] \begin{vmatrix} PSSI \\ QSSI \\ RSSI \end{vmatrix} - [TRNSU]^T \begin{vmatrix} DPSSI \\ DQSSI \\ DRSSI \end{vmatrix} \end{aligned} \quad (4.3.5.51)$$

It is convenient to rewrite Eq. (4.3.5.51) using cross-products instead of the skew-symmetric matrices:

$$\begin{aligned} \begin{vmatrix} DPUUS \\ DQUUS \\ DRUUS \end{vmatrix} &= [TRNRU]^T \left(\begin{vmatrix} PRRU \\ QRRU \\ RRRU \end{vmatrix} \times \begin{vmatrix} PRRI \\ QRRI \\ RRRI \end{vmatrix} \right) + [TRNRU]^T \begin{vmatrix} DPRRI \\ DQRRI \\ DRRRI \end{vmatrix} + \begin{vmatrix} DPUUR \\ DQUUR \\ DRUUR \end{vmatrix} \\ &\quad - [TRNSU]^T \left(\begin{vmatrix} PSSU \\ QSSU \\ RSSU \end{vmatrix} \times \begin{vmatrix} PSSI \\ QSSI \\ RSSI \end{vmatrix} \right) - [TRNSU]^T \begin{vmatrix} DPSSI \\ DQSSI \\ DRSSI \end{vmatrix} \end{aligned} \quad (4.3.5.52)$$

At this point it can be recognized that $PRRU = RRRU = DPUUR = DRUUR = 0.0$ because the roll assembly is only allowed to pitch relative to the U axes, $PSSU = QSSU = 0.0$ because the unpitched axes are only allowed to yaw relative to shaft axes, and $DPUUS = 0.0$ for the desired constraint:

$$\begin{aligned} \begin{vmatrix} 0.0 \\ DQUUS \\ DRUUS \end{vmatrix} &= [TRNRU]^T \left(\begin{vmatrix} 0.0 \\ QRRU \\ 0.0 \end{vmatrix} \times \begin{vmatrix} PRRI \\ QRRI \\ RRRI \end{vmatrix} \right) + [TRNRU]^T \begin{vmatrix} DPRRI \\ DQRRI \\ DRRRI \end{vmatrix} + \begin{vmatrix} 0.0 \\ DQUUR \\ 0.0 \end{vmatrix} \\ &\quad - [TRNSU]^T \left(\begin{vmatrix} 0.0 \\ 0.0 \\ RSSU \end{vmatrix} \times \begin{vmatrix} PSSI \\ QSSI \\ RSSI \end{vmatrix} \right) - [TRNSU]^T \begin{vmatrix} DPSSI \\ DQSSI \\ DRSSI \end{vmatrix} \end{aligned} \quad (4.3.5.53)$$

Expanding out the cross products:

$$\begin{vmatrix} 0.0 \\ DQUUS \\ DRUSS \end{vmatrix} = [\text{TRNRUT}]^T \begin{vmatrix} QRRU * RRRI \\ 0.0 \\ -QRRU * PRRI \end{vmatrix} + [\text{TRNRU}]^T \begin{vmatrix} DPRRI \\ DQRRI \\ DRRRI \end{vmatrix} + \begin{vmatrix} 0.0 \\ DQUUR \\ 0.0 \end{vmatrix} \\ - [\text{TRNSU}]^T \begin{vmatrix} - RSSU * QSSI \\ RSSU * PSSI \\ 0.0 \end{vmatrix} - [\text{TRNSU}]^T \begin{vmatrix} DPSSI \\ DQSSI \\ DRSSI \end{vmatrix} \quad (4.3.5.54)$$

The x-component of vector Eq. (4.3.5.54) is the desired last constraint equation. However, expressions for QRRU and RSSU at each time step must be developed before the equation can be evaluated. QRRU can be developed beginning with the relation:

$$\begin{vmatrix} 0.0 \\ QRRU \\ 0.0 \end{vmatrix} = \begin{vmatrix} PRRI \\ QRRI \\ RRRI \end{vmatrix} - \begin{vmatrix} PRUI \\ QRUI \\ RRUI \end{vmatrix} = \begin{vmatrix} PRRI \\ QRRI \\ RRRI \end{vmatrix} - \begin{vmatrix} PRSI \\ QRSI \\ RRSI \end{vmatrix} - \begin{vmatrix} PRUS \\ QRUS \\ RRUS \end{vmatrix} \\ = \begin{vmatrix} PRRI \\ QRRI \\ RRRI \end{vmatrix} - [\text{TRNRS}] \begin{vmatrix} PSSI \\ QSSI \\ RSSI \end{vmatrix} - [\text{TRNRU}] \begin{vmatrix} PUUS \\ QUUS \\ RUUS \end{vmatrix} \quad (4.3.5.55)$$

Expanding out only the QRRU term and noting that PUUS = QUUS = 0.0:

$$QRRU = QRRI - QRSI - \text{TRNRU}(2,3) * RUUS \quad (4.3.5.56)$$

But from Eq. (1.3.5), TRNRU(2,3) = 0.0 for a pure pitch rotation, so that:

$$QRRU = QRRI - QRSI \quad (4.3.5.57)$$

A similar derivation can be used to determine RSSU. Beginning with:

$$\begin{vmatrix} 0.0 \\ 0.0 \\ RSSU \end{vmatrix} = \begin{vmatrix} PSSI \\ QSSI \\ RSSI \end{vmatrix} - \begin{vmatrix} PSUI \\ QSUI \\ RSUI \end{vmatrix} = \begin{vmatrix} PSSI \\ QSSI \\ RSSI \end{vmatrix} - \begin{vmatrix} PSRI \\ QSRI \\ RSRI \end{vmatrix} - \begin{vmatrix} PSUR \\ QSUR \\ RSUR \end{vmatrix} \\ = \begin{vmatrix} PSSI \\ QSSI \\ RSSI \end{vmatrix} - [\text{TRNRS}]^T \begin{vmatrix} PRRI \\ QRRI \\ RRRI \end{vmatrix} - [\text{TRNSU}] \begin{vmatrix} PUUR \\ QUUR \\ RUUR \end{vmatrix} \quad (4.3.5.58)$$

Expanding out only the RSSU term and noting that PUUR = RUUR = 0.0:

$$RSSU = RSSI - RSRI - \text{TRNSU}(3,2) * QUUR \quad (4.3.5.59)$$

But from Eq. (1.3.5), $\text{TRNSU}(3,2) = 0.0$ for a pure yaw rotation, so that:

$$\text{RSSU} = \text{RSSI} - \text{RSRI} \quad (4.3.5.60)$$

This completes the derivation of the additional constraint equations. The three pivot constraints expanded out to scalar form in terms of the selected system unknowns are:

$$\begin{aligned} \#22) \quad & \text{TRNRS}(1,3)*\text{RLR} + \text{TRNRS}(2,3)*\text{RMR} + \text{TRNRS}(3,3)*\text{RNR} = 0.0 \\ \#23) \quad & \text{RMR} = 0.0 \\ \#24) \quad & \text{TRNRU}(1,1)*\text{DPRRI} + \text{TRNRU}(2,1)*\text{DQRRI} + \text{TRNRU}(3,1)*\text{DRRRI} \\ & = -\text{TRNRU}(1,1)*\text{QRRU}*\text{RRRI} + \text{TRNRU}(3,1)*\text{QRRU}*\text{PRRI} \\ & - \text{TRNSU}(1,1) * \text{RSSU} * \text{QSSI} + \text{TRNSU}(2,1) * \text{RSSU} * \text{PSSI} \\ & + \text{TRNSU}(1,1)*\text{DPSSI} + \text{TRNSU}(2,1)*\text{DQSSI} + \text{TRNSU}(3,1)*\text{DRSSI} \end{aligned} \quad (4.3.5.61)$$

where the {DPSSI} vector is zero for the idealized pitch plane maneuvers defined by constant load factors but could, of course, be non-zero for arbitrary non-idealized maneuvers.

At this point the 24 equations necessary for modeling the first two phases of the release motion (while the pivot point is still firmly engaged in the socket) have been developed. At each time step in the trajectory, the 24 equations are solved by a Gaussian Reduction with Columnal Pivoting algorithm for the 24 acceleration and reaction load terms. The store pitch angle relative to the pylon axes at each new time step may then be extracted from the relations of Eq. (1.3.9) as:

$$\text{THABP} = \sin^{-1} \{-\text{TRNBP}(1,3)\} \quad (4.3.5.62)$$

This value is tested against the design release angle to determine when the store passes into the second phase of release motion. If the release angle criterion has been satisfied, then the calculated reaction forces must be tested to determine when the equations modeling the third phase of motion must be implemented. The calculated reaction forces from the 24-equation system can be projected into the shaft axis directions by:

$$\left| \begin{array}{c} \text{RXS} \\ \text{RYS} \\ \text{RZS} \end{array} \right| = [\text{TRNRS}]^T \left| \begin{array}{c} \text{RXR} \\ \text{RYR} \\ \text{RZR} \end{array} \right| \quad (4.3.5.63)$$

The calculated value of RZS is then tested to see when a physically impossible negative reaction is predicted. When this occurs, several of the equations in the original system of 24 equations must be replaced with equations which allow vertical translation of the ball joint out of the socket, and a revised solution using the new system must be obtained. The first three equations in the original system of equations which modeled translation of the roll hook axes relative to the pitch/yaw hook point [Eq. (4.3.5.26)] are the ones that need to be replaced. Formerly, the acceleration of the pitch/yaw hook point at the center of the ball joint attached to the store in Eq. (4.3.5.26) had been forced to match the acceleration of the corresponding point at the center of the receiving well which (because it is attached to the aircraft) was a known quantity defined by

the aircraft maneuver. The revised equations must treat the vertical component of the acceleration (in the shaft axis ZS direction) as an unknown which must be solved for based on certain constraints. A very small approximation is made to model the acceleration of the ball point - the shaft axis x and y components of the ball point are assumed to be identical to the XS and YS components of the acceleration of the receiving point on the well (i.e., the extremely small Coriolis effects during the 1 in. of motion of the ball out of the socket are ignored). The AZSHI component of the vertical acceleration of the ball out of the socket is then added as the 25th unknown. The necessary new 25th constraint equation is particularly simple - reaction force in the ZS direction must be zero.

The equations are implemented by first defining shaft axis components of the acceleration of the attachment point at the center of the socket:

$$\begin{vmatrix} AXSHI \\ AYSHI \\ AZSHI \end{vmatrix} = [TRNBS]^T \begin{vmatrix} AXBHI \\ AYBHI \\ AZBHI \end{vmatrix} \quad (4.3.5.64)$$

where the {AXBHI} vector is defined by the aircraft maneuver [Eq. (4.3.2.11) projected to body axes]. The roll-axis components of acceleration with the vertical component removed can be written as:

$$\begin{vmatrix} AXRHI1 \\ AYRHI1 \\ AZRHI1 \end{vmatrix} = [TRNRS] \begin{vmatrix} AXSHI \\ AYSHI \\ 0.0 \end{vmatrix} \quad (4.3.5.65)$$

Treating AZSHI as an unknown, the three equations of Eq. (4.3.5.26) can be rewritten as:

$$\begin{aligned} \#1) \quad & ZRRH * DQRRI - YRRH * DRRRI - AXRRI + TRNRS(1,3) * AZSHI \\ & = -OOXRRH - AXRHI1 \\ \#2) \quad & -ZRRH * DPRRI + XRRH * DRRRI - AYRRI + TRNRS(2,3) * AZSHI \\ & = -OOYRRH - AYRHI1 \\ \#3) \quad & YRRH * DPRRI - XRRH * DQRRI - AZRRI + TRNRS(3,3) * AZSHI \\ & = -OOZRRH - AZRHI1 \end{aligned} \quad (4.3.5.66)$$

The new 25th equation expanded in terms of the selected unknowns is:

$$\#25) \quad TRNRS(1,3) * RXR + TRNRS(2,3) * RYR + TRNRS(3,3) * RZR = 0.0 \quad 4.3.5.67$$

After the new system of 25 equations in 25 unknowns is solved, the total acceleration of the ball point allowing the ball point to move vertically relative to the socket can be written as:

$$\begin{vmatrix} AXRHI \\ AXRHI \\ AZRHI \end{vmatrix} = \begin{vmatrix} AXRHI1 \\ AXRHI1 \\ AZRHI1 \end{vmatrix} + [TRNRS] \begin{vmatrix} 0.0 \\ 0.0 \\ AZSHI \end{vmatrix} \quad (4.3.5.68)$$

The criteria for transition from the third phase of store motion to the fourth phase (or transition of the fourth phase to the fifth) are based on the vertical separation distance between the center of the socket and the center of the ball. The shaft-axis components of the position of the center of the socket relative to the pylon axis origin are:

$$\begin{vmatrix} XSHPCK \\ YSHPCK \\ ZSHPCK \end{vmatrix} = [TRNPS]^T \begin{vmatrix} XPHP \\ YPHP \\ ZPHP \end{vmatrix} \quad (4.3.5.69)$$

where {XPHP} is fixed for the socket point (which does not move relative to pylon axes) and is evaluated only at the first time step. The shaft axis components for the position of the moving hook point at the center of the ball are calculated at each time step using a similar relation but with the {XPHP} vector determined at every time step:

$$\begin{vmatrix} XSHP \\ YSHP \\ ZSHP \end{vmatrix} = [TRNPS]^T \begin{vmatrix} XPHP \\ YPHP \\ ZPHP \end{vmatrix} \quad (4.3.5.70)$$

The {XPHP} vectors used in the single evaluation of Eq. (4.3.5.69) at the carriage position and the evaluation of Eq. (4.3.5.70) at each time step are determined from the relation of Eq. (4.3.2.19). To evaluate Eq. (4.3.2.19), the {XBBH} vector is needed:

$$\begin{vmatrix} XBBH \\ YBBH \\ ZBBH \end{vmatrix} = \begin{vmatrix} XBBR \\ YBBR \\ ZBBR \end{vmatrix} + [TRNBR] \begin{vmatrix} XRRH \\ YRRH \\ ZRRH \end{vmatrix} \quad (4.3.5.71)$$

The distance the hook points have separated is obtained by subtracting {XSHPCK} from the value of {XSHP} at each time step. While the separation distance between the hook points is less than 0.3 in., the store is assumed to be in phase 3 motion with the internal hook still restricting some roll motion. While the separation distance is between 0.3 and 1.0 in., the internal hook is assumed to be disengaged and all rotational restraints at the pitch-yaw hook point are removed. Unrestricted rotational motion during phase 4 is implemented by replacing the rotational constraint equations at the pitch/yaw point [Eq. (4.3.5.61)] with zero moment restrictions. The new rotational restraint equations for the phase 4 system of 25 equations are:

- #22) RLR = 0.0
 - #23) RMR = 0.0
 - #24) RLN = 0.0
- (4.3.5.72)

This completes derivation of the original 24 by 24 system of equations for motion of the store about an aircraft fixed pivot point and the two 25 by 25 systems modeling the hook disengagement portion of the motion with and without internal rotational restraint at the pitch/yaw joint.

Once the appropriate 24 by 24 or 25 by 25 systems of equations are solved, the translational accelerations are rewritten as derivatives of the projected velocities using Eqs. (4.3.5.11) and

(4.3.5.15) and the rotational and translational velocity derivatives are integrated over time to determine linear and angular projected velocities. This integration is performed for both body-axis and roll-axis properties. Also at each time step, the velocities and angular transformations of the body axes relative to inertial axes and the angular transformations of the roll axes relative to inertial axes are integrated to determine the positions and orientations of the body axes and the orientations of the roll axes relative to inertial axes at the new time step. It is not necessary, however, to also integrate roll-axis velocities because roll-axes properties can be directly related to the body-axis properties. In fact, up to motion phase 4, it is not even necessary to directly determine the orientation of roll axes relative to inertial axes by integration of the rotational transformations at all because the upper joint is not allowed to roll and, therefore, all roll of the body relative to pylon axes must occur at the offset roll joint. Once the updated orientations of the body and roll joints relative to inertial axes are determined at each time step (whether by integrating the derivative direction cosine matrices, or by integrating quaternion rates, or by integrating the derivatives of the modified Euler angles), the different projection matrices necessary to evaluate the system of equations at the next time step must be determined. The projection matrix for body axes relative to pylon axes at each time step is determined according to:

$$[\text{TRNBP}] = [\text{TRNBI}] [\text{TRNPI}]^T \quad (4.3.5.73)$$

where $[\text{TRNPI}]$ comes from the aircraft maneuver. The projection for body axes relative to shaft axes is then:

$$[\text{TRNBS}] = [\text{TRNBP}] [\text{TRNPS}] \quad (4.3.5.74)$$

where $[\text{TRNPS}]$ may be an identity if the hook shaft is aligned perpendicularly to the lower surface of the pylon. The angles between body and shaft axes are then extracted from $[\text{TRNBS}]$ according to the relations of Eqs. (1.3.9). Up to phase 4 of the hook motion, the $[\text{TRNBR}]$ matrix may be determined by a rotation using Eq. (1.3.6) through the roll angle PHIBS. During phase 4, however, the total roll of the body relative to shaft axes does not all occur about the roll joint since the upper ball joint also allows some roll motion. For phase 4, the integrated rotational transformation for the roll joint must be used:

$$[\text{TRNRP}] = [\text{TRNRI}] [\text{TRNPI}]^T \quad (4.3.5.75)$$

so that:

$$[\text{TRNBR}] = [\text{TRNBP}] [\text{TRNRP}] \quad (4.3.5.76)$$

The $[\text{TRNRS}]$ matrix is then determined from:

$$[\text{TRNRS}] = [\text{TRNBR}]^T [\text{TRNBS}] \quad (4.3.5.77)$$

The $[\text{TRNRU}]$ matrix is determined by a rotation using Eq. (1.3.5) through the pitch angle THARS. And, finally, the $[\text{TRNSU}]$ matrix is determined from:

$$[\text{TRNSU}] = [\text{TRNRS}]^T [\text{TRNRU}] \quad (4.3.5.78)$$

This completes the derivation and implementation of the F-15-style pivot equations.

A numerical experiment has been conducted using a FORTRAN-coded form of the F-15 pivot mechanism equations to illustrate the relative importance of the five phases of the hook motion (Fig. 24) for which mathematical models were developed. The numerical experiment illustrates the extreme sensitivity of the reaction loads to idealizations in the physical description of the mechanism and serves to highlight concerns about the omission of such items as machine part manufacturing tolerances in the development of the equations. The numerical experiment also illustrates that the basic separation motion remains essentially unchanged, even with large differences in computed reaction loads. For the numerical experiment, analytical trajectories were generated for a fuel tank release configuration with various levels of sophistication in the mathematical model. The first case imposed free-body motion at the instant the vertical release force criterion ($RLS = 0$) was met (consistent with the "simple" pivot approximation of Section 4.3.3 or the F-16 pivot model as outlined in Section 4.3.4). In other words, the equations for the phase 3 and phase 4 motions illustrated in Fig. 24 were bypassed. The second case added the 1.0-in. travel release condition but skipped the phase 3 equations and implemented the phase 4 equations for the entire 1 in. of motion. The third case, in contrast, skipped the phase 4 equations but used the phase 3 conditions for the entire 1 in. of motion. The fourth and final case split the difference between case 2 and case 3 and implemented phase 3 constraints for the first 0.3 in. of motion and phase 4 constraints for the remaining 0.7 in.

The simulations for the numerical experiment were generated for an F-15 type installation (hook shaft aligned with the vertical pylon axis) for an empty 600-gal fuel tank at a transonic Mach number of 0.9 and at sea-level altitude. The selected release conditions involve low tank pitch inertia and large flight dynamic pressures and air loads which make the tank highly prone to over-rotation. Aerodynamic data were extracted from an F-22 tank test, although the source of the aero data is immaterial to the numerical experiment. Important motion parameters for the four cases are presented in plotted form in Fig. 25. The tank reaches its design release angle of -15 deg at about 0.095 sec into the trajectory as indicated in Fig. 25c. The vertical reaction forces remain positive, however, until the tank reaches a pitch angle of about -20 deg at about 0.115 sec into the trajectory, as shown in Fig. 25d.

Case number 1 releases at the point where RZS becomes zero as indicated by the 'square' symbols on the plots. Note in the comparison of hook positions (Fig. 25a), that the hook point immediately moves upward (in the negative ZP direction) upon release. The release point is clearly indicated by the sudden jump in the YPHP plot because the hook position equations were coded assuming that the roll structure is "spring-loaded" and returns immediately to its neutral, unrolled position at the instant of release. The ZPHP term for Case 1 shows penetration of the hook point into the wing structure to an extent of about 2 in. which is, of course, not a pleasant possibility. A physical explanation of this undesirable phenomenon can be realized by examining the reaction loads (Fig. 25d) on the body in terms of a free-body diagram at the instant of release. Such a free-body diagram at the instant the vertical reaction force goes to zero is provided in Fig. 26. Note from Figs. 26 and 25d that the axial reaction force is approximately 6,000 lb at the point where the vertical reaction force becomes zero. The large axial reaction is caused by the need to resist the tendency of the aft end of the tank to move forward as it tries to pitch about its center of

gravity under influence of the ejector and aerodynamic and inertial forces. The projected path of the hook point if not constrained by the release mechanism is indicated on the figure. It is actually the axial reaction force crossed with the moment arm from the pivot point to the cg rather than the vertical reaction force that prevents upward hook movement. Note that if the computations switch instantly to unrestrained motion at the instant RZS goes to zero, the 6,000 lb of axial reaction force also goes away. In the F-15 style mechanism, however, the ball has to move vertically out of the socket and the axial reaction force can still act during that motion. The axial reaction during that seemingly insignificant 1 in. of pull-out motion will be shown in cases 2, 3, and 4 to make the difference between safe release and recontact of the ball joint with the wing. Before continuing with a discussion of the F-15 style mechanism, a few comments about a similar problem with the F-16 mechanism are in order. The F-16 mechanism described in Section 4.3.4 does not have provision for forcing some vertical travel before removing the axial restraints and, therefore, has no physical mechanism for preventing upward hook motion into the wing. The F-16 fuel tanks do, however, have an aerodynamic method for preventing recontact. All F-16 fuel tanks are equipped with aft tail fins which (although they are not large enough to aerodynamically stabilize the tank) are sufficiently large to generate a downward lift force on the aft end of the tank during separation. This downward force on the tank aft end overcomes the inertial tendency of the hook point to move forward and upward as it tries to rotate about the cg and positively disengages the mechanism.

Cases 2, 3, and 4 each include the 1-in. vertical pull-out constraint and, as indicated in Fig 25a, do not show the undesirable upward hook motion. Note in the XPBP plot (Fig. 25b) that the tank cg position for all three cases moves slightly aft of the cg position of case 1. The added axial restraint does not allow the hook point to rotate forward as it pitches about the cg but, instead, forces the cg to rotate back as it pitches about the hook point. The actual internal restraints of the internal hook point in the ball joint are, however, extremely difficult to model rigorously because the mechanism has some built-in "slop." When the ball is fully engaged in the socket (before any vertical pull-out motion), the side bearing surfaces of the hook are in fairly firm contact with the sides of the cut-out section in the ball and internal roll is effectively prevented. When the ball is partially pulled out, the internal hook probably has little or no restraining surface contact. Cases 2, 3, and 4 model the pull-out motion with internal constraint, without constraint, and with a combination of constraint for the first 0.3 in. and no constraint for the remaining 0.7 in. It is up to engineering judgment as to which internal constraint model is most correct. The numerical experiment does, however, allow an objective comparison of the results of the different forms of modeling. Essentially, the separation motion of the large tank is relatively insensitive to choice of internal constraint model for the 1-in. motion; tolerance bands due to modeling of about 2 deg in the angular orientations for a 20-ft-long tank are indicated by Fig. 25c. The case 4 compromise constraint results in motion parameters midway between the fully free or fully constrained internal rotations. Reaction forces and moments, on the other hand, are significantly influenced by the choice of restraint models, as shown in Figs. 25d-e. The large variations in reaction forces can be a significant design issue for the structures in the aircraft wing necessary to support the loads imparted to it from the releasing store. The largest loads (indicated by the "open circle" symbols for full internal constraint) represent perhaps the most conservative design point. The other issue that should be addressed is the assumption in the modeling that the ball moves vertically out of the socket in the shaft-axis Z direction. Actually, once the ball moves a small amount out of the

socket it reaches a point where its spherical surface is in contact with only the lip of the socket and it is not restricted to only vertical motion. This may have some relieving effect on the reaction loads which have already been shown for the internal rotation constraint to be very sensitive to small nuances in the modeling.

4.3.6 Modified F-15 Hook without Offset Roll Joint

An alternate set of equations was developed to model a conceptual F-15-type pivot release mechanism but without the offset roll joint. Such a conceptual device was considered for the F-22 because it would restrain roll motion of the store. Although it is possible that the actual F-15 hook structure in its existing design may not support the roll reaction moments at the pivot point, the benefits of a roll-constrained pivot could be assessed using the conceptual pivot model. In addition, because the F-22 pivot had not been designed prior to early F-22 wind tunnel separation tests, the conceptual design was used on the first F-22 dynamic drop tests. Equations are developed to allow solution for twelve unknowns - three translational acceleration components of the store body {AXBBI, AYBBI, AZBBI}, three rotational acceleration components {DPBBI, DQBBI, DRBBI}, three reaction force components {RXB, RYB, RZB} and three reaction moment components {RLB, RMB, RNB}.

The basic translational and rotational equations of motion for the store about a single pivot point have already been developed in previous sections. The additional constraint equations which model the hook restraint device have already been developed in Section 4.3.5. The only difference between the equations of this section and those of Section 4.3.5 is the absence of the roll structure and the second half of the "two-body" equations. The reader is referred to Section 4.3.5 for the derivation and implementation of the hook restraint equation and Section 4.3.4 for the implementation of the single-body equations of motion.

Twelve linearly independent equations are necessary to determine the 12 independent variables at each time step. The first nine of the equations are exactly identical to the equations for the F-16-style hook as developed in Section 4.3.4. The first three of the necessary equations are the restricted translational equations of motion defined by Eq. (4.1.2.8). The double cross-product term in Eq. (4.1.2.8) is first evaluated (defining a temporary vector {OOXBBH} denoting Omega cross Omega cross r for the {XBBH} vector):

$$\begin{vmatrix} OOXBBH \\ OOYBBH \\ OOZBBH \end{vmatrix} = \begin{vmatrix} PBBI \\ QBBI \\ RBBI \end{vmatrix} X \begin{vmatrix} PBBI \\ QBBI \\ RBBI \end{vmatrix} X \begin{vmatrix} XBBH \\ YBBH \\ ZBBH \end{vmatrix} \quad (4.3.6.1)$$

Equations (4.1.2.8) are then written in terms of the unknowns and expanded into scalar form as:

$$\begin{aligned} \#1)- AXBBI + ZBBH * DQBBI - YBBH * DRBBI &= - OOXBBH - AXBHI \\ \#2)- AYBBI - ZBBH * DPBBI + XBBH * DRBBI &= - OOYBBH - AYBHI \\ \#3)- AZBBI + YBBH * DPBBI - XBBH * DQBBI &= - OOZBBH - AZBHI \end{aligned} \quad (4.3.6.2)$$

The next three equations are the restricted rotational equations of motion defined by Eq. (4.2.2.42). First, the body-axis components of the relative angular momentum about the hook axes are calculated directly from body-axis inertia terms:

$$\begin{vmatrix} \text{HXBHH} \\ \text{HYBHH} \\ \text{HZBHH} \end{vmatrix} = [\text{I}]_{\text{BH}} \begin{vmatrix} \text{PBBI} \\ \text{QBBI} \\ \text{RBBI} \end{vmatrix} \quad (4.3.6.3)$$

where the body-axis components of the inertia about the hook axes are computed from the parallel-axis theorem:

$$\begin{aligned} \text{I}_{xx\text{BH}} &= \text{I}_{xx\text{BB}} + m (\text{YBBH}^2 + \text{ZBBH}^2) \\ \text{I}_{yy\text{BH}} &= \text{I}_{yy\text{BB}} + m (\text{XBBH}^2 + \text{ZBBH}^2) \\ \text{I}_{zz\text{BH}} &= \text{I}_{zz\text{BB}} + m (\text{XBBH}^2 + \text{YBBH}^2) \\ \text{I}_{xy\text{BH}} &= \text{I}_{xy\text{BB}} + m (\text{XBBH} * \text{YBBH}) \\ \text{I}_{xz\text{BH}} &= \text{I}_{xz\text{BB}} + m (\text{XBBH} * \text{ZBBH}) \\ \text{I}_{yz\text{BH}} &= \text{I}_{yz\text{BB}} + m (\text{YBBH} * \text{ZBBH}) \end{aligned} \quad (4.3.6.4)$$

Then Eq. (4.2.2.42) is expanded as:

$$\begin{aligned} \#4) \quad &[\text{I}]_{\text{BH}}(1,1) * \text{DPBBI} + [\text{I}]_{\text{BH}}(1,2) * \text{DQBBI} + [\text{I}]_{\text{BH}}(1,3) * \text{DRBBI} - \text{RLB} \\ &= - \text{QBBI} * \text{HZBHH} + \text{RBBI} * \text{HYBHH} + \text{MXB} + \text{YBBH} * \text{FZB} - \text{ZBBH} * \text{FYB} \\ &\quad - m * \text{YBBH} * \text{AZBHI} + m * \text{ZBBH} * \text{AYBHI} \\ \#5) \quad &[\text{I}]_{\text{BH}}(2,1) * \text{DPBBI} + [\text{I}]_{\text{BH}}(2,2) * \text{DQBBI} + [\text{I}]_{\text{BH}}(2,3) * \text{DRBBI} - \text{RMB} \\ &= - \text{RBBI} * \text{HXBHH} + \text{PBBI} * \text{HZBHH} + \text{MYB} + \text{ZBBH} * \text{FXB} - \text{XBBH} * \text{FZB} \\ &\quad - m * \text{ZBBH} * \text{AXBHI} + m * \text{XBBH} * \text{AZBHI} \quad (4.3.6.5) \\ \#6) \quad &[\text{I}]_{\text{BH}}(3,1) * \text{DPBBI} + [\text{I}]_{\text{BH}}(3,2) * \text{DQBBI} + [\text{I}]_{\text{BH}}(3,3) * \text{DRBBI} - \text{RNB} \\ &= - \text{PBBI} * \text{HYBHH} + \text{QBBI} * \text{HXBHH} + \text{MZB} + \text{XBBH} * \text{FYB} - \text{YBBH} * \text{FXB} \\ &\quad - m * \text{XBBH} * \text{AYBHI} + m * \text{YBBH} * \text{AXBHI} \end{aligned}$$

The next three equations come from the force balance on the body [Eq. (4.1.2.9)]. Rewriting:

$$\begin{aligned} \#7) \quad &- \text{AXBBI} + \text{RXB}/m = - \text{FXB}/m \\ \#8) \quad &- \text{AYBBI} + \text{RYB}/m = - \text{FYB}/m \\ \#9) \quad &- \text{AZBBI} + \text{RZB}/m = - \text{FZB}/m \end{aligned} \quad (4.3.6.6)$$

The final three equations arise from the constraints applied at the pivot point and are exactly analogous to the pivot equations developed in Section 4.3.5, with the exception that the equations are defined as relations between the various intermediate pivot axes and the body axes rather than relations with the roll structure axes as in Eq. (4.3.5.60):

$$\begin{aligned} \#10) \quad &\text{TRNBS}(1,3)*\text{RLB} + \text{TRNBS}(2,3)*\text{RMB} + \text{TRNBS}(3,3)*\text{RNB} = 0.0 \\ \#11) \quad &\text{RMB} = 0.0 \\ \#12) \quad &\text{TRNBU}(1,1)*\text{DPBBI} + \text{TRNBU}(2,1)*\text{DQBBI} + \text{TRNBU}(3,1)*\text{DRBBI} \\ &= - \text{TRNBU}(1,1)*\text{QBBU}*\text{RBBI} + \text{TRNBU}(3,1)*\text{QBBU}*\text{PBBI} \\ &\quad - \text{TRNSU}(1,1) * \text{RSSU} * \text{QSSI} + \text{TRNSU}(2,1) * \text{RSSU} * \text{PSSI} \\ &\quad + \text{TRNSU}(1,1)*\text{DPSSI} + \text{TRNSU}(2,1)*\text{DQSSI} + \text{TRNSU}(3,1)*\text{DRSSI} \end{aligned} \quad (4.3.6.7)$$

The {DPSSI} vector is zero for the idealized pitch plane maneuvers defined by constant load factors but could, of course, be non-zero for arbitrary non-idealized maneuvers. The QBBU and RSSU terms in the last equation are determined from:

$$QBBU = QBBI - QBSI \quad (4.3.6.8)$$

and

$$RSSU = RSSI - RSBI \quad (4.3.6.9)$$

which are derived analogously to Eqs. (4.3.5.56) and (4.3.5.59) in the previous section.

At this point the 12 equations necessary for modeling the first two phases of the release motion (while the pivot point is still firmly engaged in the socket) have been developed. At each time step in the trajectory, the 12 equations are solved by a Gaussian Reduction with Columnal Pivoting algorithm for the 12 acceleration and reaction load terms. The store pitch angle relative to the pylon axes at each new time step may then be extracted from the relations of Eq. (1.3.9) as:

$$THABP = \sin^{-1} \{-TRNBP(1,3)\} \quad (4.3.6.10)$$

This value is tested against the design release angle to determine when the store passes into the second phase of release motion. If the release angle criterion has been satisfied, then the calculated reaction forces must be tested to determine when the equations modeling the third phase of motion must be implemented. The calculated reaction forces from the 12 equation system can be projected into the shaft-axis directions by:

$$\begin{vmatrix} RXS \\ RYS \\ RZS \end{vmatrix} = [TRNBS]^T \begin{vmatrix} RXB \\ RYB \\ RZB \end{vmatrix} \quad (4.3.6.11)$$

The calculated value of RZS is then tested to see when a physically impossible negative reaction force is predicted. When this occurs, several of the equations in the original system of 12 equations must be replaced with equations which allow vertical translation of the ball joint out of the socket, and a revised solution using the new system must be obtained. The first six equations in the original system of equations need to be replaced. Formerly, the acceleration of the pitch/yaw hook point at the center of the ball joint attached to the store in Eqs. (4.3.6.2) and (4.3.6.5) had been forced to match the acceleration of the corresponding point at the center of the receiving well which (because it is attached to the aircraft) was a known quantity defined by the aircraft maneuver. The revised equations must treat the vertical component of the acceleration (in the shaft-axis ZS direction) as an unknown which must be solved for, based on the constraints just as in Section 4.3.5. A very small approximation is made to model the acceleration of the ball point - the shaft-axis x and y components of the ball point are assumed to be identical to the XS and YS components of the acceleration of the receiving point on the well (i.e., the extremely small Coriolis effects during the 1 in. of motion of the ball out of the socket are ignored). The AZSHI component of the vertical acceleration of the ball out of the socket is then added as the 13th unknown. The necessary new 13th constraint equation is particularly simple: reaction force in the ZS direction must be zero.

The equations are implemented by first defining shaft-axis components of the acceleration of the attachment point at the center of the socket:

$$\begin{vmatrix} AXSHI \\ AYSHI \\ AZSHI \end{vmatrix} = [TRNBS]^T \begin{vmatrix} AXBHI \\ AYBHI \\ AZBHI \end{vmatrix} \quad (4.3.6.12)$$

where the {AXBHI} vector is defined by the aircraft maneuver [Eq. (4.3.2.11) projected to body axes]. The body-axis components of acceleration with the vertical component removed can be written as:

$$\begin{vmatrix} AXBHI1 \\ AYBHI1 \\ AZBHI1 \end{vmatrix} = [TRNBS] \begin{vmatrix} AXSHI \\ AYSHI \\ 0.0 \end{vmatrix} \quad (4.3.6.13)$$

Treating AZSHI as an unknown, the three equations of Eq. (4.3.6.2) can be rewritten as:

$$\begin{aligned} \#1) & - AXBBI + ZBBH * DQBBI - YBBH * DRBBI + TRNBS(1,3) * AZSHI \\ & = - OOXBBH - AXBHI1 \\ \#2) & - AYBBI - ZBBH * DPBBI + XBBH * DRBBI + TRNBS(2,3) * AZSHI \\ & = - OGYBBH - AYBHI1 \\ \#3) & - AZBBI + YBBH * DPBBI - XBBH * DQBBI + TRNBS(3,3) * AZSHI \\ & = - OOZBBH - AZBHI1 \end{aligned} \quad (4.3.6.14)$$

and Eq. (4.3.6.5) can be rewritten as:

$$\begin{aligned} \#4) & [I]BH(1,1) * DPBBI + [I]BH(1,2) * DQBBI + [I]BH(1,3) * DRBBI - RLB \\ & + (YBBH * TRNBS(3,3) - ZBBH * TRNBS(2,3)) * m * AZSHI \\ & = - QBBI * HZBHH + RBBI * HYBHH + MXB + YBBH * FZB - ZBBH * FYB \\ & - m * YBBH * AZBHI1 + m * ZBBH * AYBHI1 \\ \#5) & [I]BH(2,1) * DPBBI + [I]BH(2,2) * DQBBI + [I]BH(2,3) * DRBBI - RMB \\ & + (ZBBH * TRNBS(1,3) - XBBH * TRNBS(3,3)) * m * AZSHI \\ & = - RBBI * HXBHH + PBBI * HZBHH + MYB + ZBBH * FXB - XBBH * FZB \\ & - m * ZBBH * AXBHI1 + m * XBBH * AZBHI1 \\ \#6) & [I]BH(3,1) * DPBBI + [I]BH(3,2) * DQBBI + [I]BH(3,3) * DRBBI - RNB \\ & + (XBBH * TRNBS(2,3) - YBBH * TRNBS(1,3)) * m * AZSHI \\ & = - PBBI * HYBHH + QBBI * HXBHH + MZB + XBBH * FYB - YBBH * FXB \\ & - m * XBBH * AYBHI1 + m * YBBH * AXBHI1 \end{aligned} \quad (4.3.6.15)$$

The new 13th equation expanded in terms of the selected unknowns is:

$$\#13) TRNBS(1,3) * RXB + TRNBS(2,3) * RYB + TRNBS(3,3) * RZB = 0.0 \quad (4.3.6.16)$$

After the new system of 13 equations in 13 unknowns is solved, the total acceleration of the ball point allowing the ball point to move vertically relative to the socket can be written as:

$$\begin{vmatrix} AXBHI \\ AXBHI \\ AZBHI \end{vmatrix} = \begin{vmatrix} AXBHI_1 \\ AXBHI_1 \\ AZBHI_1 \end{vmatrix} + [TRNBS] \begin{vmatrix} 0.0 \\ 0.0 \\ AZSHI \end{vmatrix} \quad (4.3.6.17)$$

The criteria for transition from the third phase of store motion to the fourth phase (or transition of the fourth phase to the fifth) is based on the vertical separation distance between the center of the socket and the center of the ball. The shaft-axis components of the position of the center of the socket relative to the pylon-axis origin are:

$$\begin{vmatrix} XSHPCK \\ YSHPCK \\ ZSHPCK \end{vmatrix} = [TRNPS]^T \begin{vmatrix} XPHP \\ YPHP \\ ZPHP \end{vmatrix} \quad (4.3.6.18)$$

where {XPHP} is fixed for the socket point (which does not move relative to pylon axes) and is evaluated only at the first time step. The shaft-axis components for the position of the moving hook point at the center of the ball are calculated at each time step using a similar relation but with the {XPHP} vector determined at every time step from Eq. (4.3.2.19):

$$\begin{vmatrix} XSHP \\ YSHP \\ ZSHP \end{vmatrix} = [TRNPS]^T \begin{vmatrix} XPHP \\ YPHP \\ ZPHP \end{vmatrix} \quad (4.3.6.19)$$

The distance the hook points have separated is obtained by subtracting {XSHPCK} from the value of {XSHP} at each time step. While the separation distance between the hook points is less than 0.3 in., the store is assumed to be in phase 3 motion with the internal hook still restricting some roll motion. While the separation distance is between 0.3 and 1.0 in., the internal hook is assumed to be disengaged and all rotational restraints at the pitch-yaw hook point are removed. Unrestricted rotational motion during phase 4 is implemented by replacing the rotational constraint equations at the pitch/yaw point [Eq. (4.3.6.7)] with zero moment restrictions. The new rotational restraint equations for the phase 4 system of 13 equations are:

$$\begin{aligned} \#10) \quad RLB &= 0.0 \\ \#11) \quad RMB &= 0.0 \\ \#12) \quad RNB &= 0.0 \end{aligned} \quad (4.3.6.20)$$

This completes derivation of the original 12 by 12 system of equations for motion of the store about an aircraft fixed pivot point and the two 13 by 13 systems modeling the hook disengagement portion of the motion with and without rotational restraint at the hook point.

Once the appropriate 12 by 12 or 13 by 13 systems of equations are solved, the translational accelerations are rewritten as derivatives of the projected velocities using Eq. (4.1.2.10) and the rotational and translational velocity derivatives are integrated over time to determine linear and

angular projected velocities. Also at each time step, the velocities and angular transformations of the body axes are integrated to determine the positions and orientations of the body axes relative to inertial axes at the new time step. Once the updated orientation of the body relative to inertial axes is determined at each time step (whether by integrating the derivative direction cosine matrix, or by integrating quaternion rates, or by integrating the derivatives of the modified Euler angles), the different projection matrices necessary to evaluate the system of equations at the next time step must be determined. The projection matrix for body axes relative to pylon axes at each time step is determined according to:

$$[\text{TRNBP}] = [\text{TRNBI}] [\text{TRNPI}]^T \quad (4.3.6.21)$$

where $[\text{TRNPI}]$ comes from the aircraft maneuver. The projection for body axes relative to shaft axes is then:

$$[\text{TRNBS}] = [\text{TRNBP}] [\text{TRNPS}] \quad (4.3.6.22)$$

where $[\text{TRNPS}]$ may be an identity if the hook shaft is aligned perpendicularly to the lower surface of the pylon. The angles between body and shaft axes are then extracted from $[\text{TRNBS}]$ according to the relations of Eqs. (1.3.9). The $[\text{TRNBU}]$ matrix is determined by a rotation using Eq. (1.3.5) through the pitch angle THABS. And, finally, the $[\text{TRNSU}]$ matrix is determined from:

$$[\text{TRNSU}] = [\text{TRNBS}]^T [\text{TRNBU}] \quad (4.3.6.23)$$

4.3.7 Rail Constraints

The generalized constraint equations for launch rail devices are developed in this section. The equations are similar to those implemented for the F-16 hook in Section 4.3.4 but must be expanded to account for the fact that the hook point is free to accelerate down the rail and is not fixed with the aircraft as in pivot simulations. Equations are developed to allow solution for fifteen unknowns - the first twelve are the standard three translational acceleration components of the store body {AXBBI, AYBBI, AZBBI}, three rotational acceleration components {DPBBI, DQBBI, DRBBI}, three reaction force components {RXB, RYB, RZB} and three reaction moment components {RLB, RMB, RNB}; the additional three unknowns are the relative down-rail accelerations of the hook axes relative to the pylon-axis system {DDXPHP, DDYPHP, DDZPHP} outlined in Eq. (4.3.2.11).

The motion of a rail-launched missile is initially constrained by two or more rail hangers attached to the missile which slide along rails built into the launcher. Generally, the rail hangers of the missile have a cross-sectional "T" shape and slide within a "C" rail on the bottom of the launcher. Some rail hangers are of the "C" design and slide within grooves on the outside of the rail. The AMRAAM missile is equipped with both types of rail hardware, and details of its rail interface with the Modular Rail Launcher (which also supports rail launch of the AIM-9 Sidewinder missile) were, therefore, selected to be presented in Fig. 27 as a representative rail configuration. In the absence of rail structural flexing, the missile is constrained to translate-only

motion during that portion of the launch in which two or more of the rail hangers are in contact with the rail, after which it can possibly pivot slightly about the aft rail hanger during the extremely short time in which the aft hanger only is in contact with the rail. After the simulated aft missile rail hanger clears the rail, full 6-degree-of-freedom motion must then be allowed in the calculated trajectories. The constraints which must be modeled are, first, that the missile aft hook is fully free to translate along the rail with no resistance. This, of course, implies that rail friction or binding of the hook in the rail (which does sometimes occur during extreme aircraft maneuvers) are not modeled. The missile aft hook can also not have any acceleration (or velocity) components normal to the rail. During the time in which two or more of the missile rail hangers are attached to the rail, the missile rotational motion is constrained to match that of the launch aircraft. The rotational restraint is specified in terms of the angular derivatives of the body-axis orientation relative to the pylon axes because pylon axes are always in alignment with the launch rail. After the missile travels downrail a sufficient distance that all but one of the rail hangers is released, several types of rotational motion including pitch and/or yaw about the last hanger may be simulated. The constraints can be written mathematically as:

$$\begin{aligned} RXP = 0.0 & \quad \text{no resistance to downrail motion} \\ DDYPHP = 0.0 & \quad \text{no hook movement normal to rail} \\ DDZPHP = 0.0 & \end{aligned} \quad (4.3.7.1)$$

During the period of two-hook-on motion:

$$\begin{aligned} DPPBP = 0.0 & \quad \text{no rotation of missile body axes relative to the pylon} \\ DQPBP = 0.0 & \\ DRPBP = 0.0 & \end{aligned} \quad (4.3.7.2)$$

During the period of one-hook-on motion (if free to pitch and yaw):

$$\begin{aligned} DPPBP = 0.0 & \\ RMP = 0.0 & \\ RNP = 0.0 & \end{aligned} \quad (4.3.7.3)$$

or (if free to pitch only):

$$\begin{aligned} DPPBP = 0.0 & \\ RMP = 0.0 & \\ DRPBP = 0.0 & \end{aligned} \quad (4.3.7.4)$$

or (if free to yaw only):

$$\begin{aligned} DPPBP = 0.0 & \\ DQPBP = 0.0 & \\ RNP = 0.0 & \end{aligned} \quad (4.3.7.5)$$

The basic translational and rotational equations of motion for the store and for the accelerating hook have been previously developed in Sections 4.1.2, 4.2.2, and 4.3.2. It is necessary, however, to derive expressions for the rotational restraints for the rotations of the body axes relative to pylon axes. Beginning with the relations for the angular velocities of body and pylon axes:

$$\begin{vmatrix} PPBP \\ QPBP \\ RPBP \end{vmatrix} = \begin{vmatrix} PPBI \\ QPBI \\ RPBI \end{vmatrix} - \begin{vmatrix} PPPI \\ QPPI \\ PPPI \end{vmatrix} = [TRNBP]^T \begin{vmatrix} PBBI \\ QBBI \\ RBBI \end{vmatrix} - \begin{vmatrix} PPPI \\ QPPI \\ RPPI \end{vmatrix} \quad (4.3.7.6)$$

Taking derivatives of both sides by the chain rule:

$$\frac{d}{dt} \begin{vmatrix} PBP \\ QBP \\ RBP \end{vmatrix} = \frac{d}{dt} [TRNBP]^T \begin{vmatrix} PBBI \\ QBBI \\ RBBI \end{vmatrix} + [TRNBP]^T \frac{d}{dt} \begin{vmatrix} PBBI \\ QBBI \\ RBBI \end{vmatrix} - \frac{d}{dt} \begin{vmatrix} PPPI \\ QPPI \\ RPPI \end{vmatrix} \quad (4.3.7.7)$$

or:

$$\begin{aligned} \begin{vmatrix} DPPBP \\ DQPBP \\ DRPBP \end{vmatrix} &= [TRNBP]^T [\tilde{\omega}BBP] \begin{vmatrix} PBBI \\ QBBI \\ RBBI \end{vmatrix} + [TRNBP]^T \begin{vmatrix} DPBBI \\ DQBBI \\ DRBBI \end{vmatrix} - \begin{vmatrix} DPPPI \\ DQPPI \\ DRPPI \end{vmatrix} \\ &= \begin{vmatrix} XCROSS \\ YCROSS \\ ZCROSS \end{vmatrix} + [TRNBP]^T \begin{vmatrix} DPBBI \\ DQBBI \\ DRBBI \end{vmatrix} - \begin{vmatrix} DPPPI \\ DQPPI \\ DRPPI \end{vmatrix} \end{aligned} \quad (4.3.7.8)$$

where the {XCROSS} terms represent temporary variables to ease implementation of the equations in a computer code. The {DPPPI} vector is zero for the idealized pitch plane maneuvers defined by constant load factors but could, of course, be non-zero for arbitrary non-idealized maneuvers. The {PBP} vector used in the skew symmetric in Eq. (4.3.7.8) is obtained by projecting Eq. (4.3.7.6):

$$\begin{vmatrix} PBP \\ QBP \\ RBP \end{vmatrix} = [TRNBP] \begin{vmatrix} PPBP \\ QPBP \\ RPBP \end{vmatrix} \quad (4.3.7.9)$$

This completes the derivation of the additional constraint equations.

Fifteen linearly independent equations are necessary to determine the 15 independent variables at each time step. For the rail launch simulation, the first three of the necessary equations are the relations for the hook acceleration defined by Eq. (4.3.2.23). Equations (4.3.2.19), (4.3.2.20), and (4.3.2.21) are first evaluated for the {XPHP}, {DXPHP}, and {UPHP} vectors. The cross products in Eq. (4.3.2.23) of the pylon-axis rotational velocities and velocity derivatives from the aircraft maneuver with {XPHP}, {DXPHP}, and {UPHP} are then evaluated and stored in temporary variables {DDXPHP1}, {DDXPHP2}, and {DDXPHP3}. The double cross-product term in Eq. (4.3.2.23) is then evaluated and stored in temporary vector {OOXPHB}. Equations (4.3.2.23) can then be written in terms of the unknowns and expanded into scalar form as:

$$\begin{aligned} #1) \quad & DDXPHP - TRNBP(1,1)*AXBBI - TRNBP(2,1)*AYBBI - TRNBP(3,1)*AZBBI \\ & + (-TRNBP(2,1)*ZBBH + TRNBP(3,1)*YBBH)*DPBBI \\ & + (TRNBP(1,1)*ZBBH - TRNBP(3,1)*XBBH)*DQBBI \\ & + (-TRNBP(1,1)*YBBH + TRNBP(2,1)*XBBH)*DRBBI \\ & = -DDXPHP1 - DDXPHP2 - DDXPHP3 + OOXPHB - AXPPI \end{aligned}$$

- #2)
$$\begin{aligned} & \text{DDYPHP} - \text{TRNBP}(1,2)*\text{AXBBI} - \text{TRNBP}(2,2)*\text{AYBBI} - \text{TRNBP}(3,2)*\text{AZBBI} \\ & + (-\text{TRNBP}(2,2)*\text{ZBBH} + \text{TRNBP}(3,2)*\text{YBBH})*\text{DPBBI} \\ & + (\text{TRNBP}(1,2)*\text{ZBBH} - \text{TRNBP}(3,2)*\text{XBBH})*\text{DQBBI} \\ & + (-\text{TRNBP}(1,2)*\text{YBBH} + \text{TRNBP}(2,2)*\text{XBBH})*\text{DRBBI} \\ & = -\text{DDYPHP1} - \text{DDYPHP2} - \text{DDYPHP3} + \text{OOYPHB} - \text{AYPPI} \end{aligned} \quad (4.3.7.10)$$
- #3)
$$\begin{aligned} & \text{DDZPHP} - \text{TRNBP}(1,3)*\text{AXBBI} - \text{TRNBP}(2,3)*\text{AYBBI} - \text{TRNBP}(3,3)*\text{AZBBI} \\ & + (-\text{TRNBP}(2,3)*\text{ZBBH} + \text{TRNBP}(3,3)*\text{YBBH})*\text{DPBBI} \\ & + (\text{TRNBP}(1,3)*\text{ZBBH} - \text{TRNBP}(3,3)*\text{XBBH})*\text{DQBBI} \\ & + (-\text{TRNBP}(1,3)*\text{YBBH} + \text{TRNBP}(2,3)*\text{XBBH})*\text{DRBBI} \\ & = -\text{DDZPHP1} - \text{DDZPHP2} - \text{DDZPHP3} + \text{OOZPHB} - \text{AZPPI} \end{aligned}$$

The next three equations are the restricted rotational equations of motion defined by Eq. (4.2.2.42). First, the body-axis components of the relative angular momentum about the hook axes are calculated directly from body-axis inertia terms:

$$\begin{vmatrix} \text{HXBHH} \\ \text{HYBHH} \\ \text{HZBHH} \end{vmatrix} = [\mathbf{I}]_{\text{BH}} \begin{vmatrix} \text{PBBI} \\ \text{QBBI} \\ \text{RBBI} \end{vmatrix} \quad (4.3.7.11)$$

where the body-axis components of the inertia about the hook axes are computed from the parallel axis theorem:

$$\begin{aligned} \text{I}_{\text{XXBH}} &= \text{I}_{\text{XXBB}} + m(\text{YBBH}^2 + \text{ZBBH}^2) \\ \text{I}_{\text{YYBH}} &= \text{I}_{\text{YYBB}} + m(\text{XBBH}^2 + \text{ZBBH}^2) \\ \text{I}_{\text{ZZBH}} &= \text{I}_{\text{ZZBB}} + m(\text{XBBH}^2 + \text{YBBH}^2) \\ \text{I}_{\text{XYBH}} &= \text{I}_{\text{XYBB}} + m(\text{XBBH} * \text{YBBH}) \\ \text{I}_{\text{XZBH}} &= \text{I}_{\text{XZBB}} + m(\text{XBBH} * \text{ZBBH}) \\ \text{I}_{\text{YZBH}} &= \text{I}_{\text{YZBB}} + m(\text{YBBH} * \text{ZBBH}) \end{aligned} \quad (4.3.7.12)$$

In expanding Eq. (4.2.2.42), the acceleration of the moving hook which is specified by Eq. (4.3.2.11) must be included. First, Eq. (4.3.2.11) is rewritten as:

$$\{\text{AXPHI}\} = \{\text{AXPHI1}\} + \{\text{DDXPHP}\} \quad (4.3.7.13)$$

where $\{\text{AXPHI1}\}$ represents all the terms of Eq. (4.3.2.11) except the unknown $\{\text{DDXPHP}\}$ vector. Then Eq. (4.2.2.42) can be expanded as:

$$\begin{aligned} #4) \quad & [\mathbf{I}]_{\text{BH}}(1,1) * \text{DPBBI} + [\mathbf{I}]_{\text{BH}}(1,2) * \text{DQBBI} + [\mathbf{I}]_{\text{BH}}(1,3) * \text{DRBBI} - \text{RLB} \\ & + (\text{YBBH} * \text{TRNBP}(3,1) - \text{ZBBH} * \text{TRNBP}(2,1)) * m * \text{DDXPHP} \\ & + (\text{YBBH} * \text{TRNBP}(3,2) - \text{ZBBH} * \text{TRNBP}(2,2)) * m * \text{DDYPHP} \\ & + (\text{YBBH} * \text{TRNBP}(3,3) - \text{ZBBH} * \text{TRNBP}(2,3)) * m * \text{DDZPHP} \\ & = -\text{QBBI} * \text{HZBHH} + \text{RBBI} * \text{HYBHH} + \text{MXB} + \text{YBBH} * \text{FZB} - \text{ZBBH} * \text{FYB} \\ & - m * \text{YBBH} * \text{AZBHI1} + m * \text{ZBBH} * \text{AYBHI1} \end{aligned}$$

- #5) $[I]_{BH}(2,1) * DPBBI + [I]_{BH}(2,2) * DQBBI + [I]_{BH}(2,3) * DRBBI - RMB$
 $+ (ZBBH * TRNBP(1,1) - XBBH * TRNBP(3,1)) * m * DDXPHP$
 $+ (ZBBH * TRNBP(1,2) - XBBH * TRNBP(3,2)) * m * DDYPHP$
 $+ (ZBBH * TRNBP(1,3) - XBBH * TRNBP(3,3)) * m * DDZPHP$
 $= - RBBI * HXBHH + PBBI * HZBHH + MYB + ZBBH * FXB - XBBH * FZB$
 $- m * ZBBH * AXBHI1 + m * XBBH * AZBHI1$
- #6) $[I]_{BH}(3,1) * DPBBI + [I]_{BH}(3,2) * DQBBI + [I]_{BH}(3,3) * DRBBI - RNB$
 $+ (XBBH * TRNBP(2,1) - YBBH * TRNBP(1,1)) * m * DDXPHP$
 $+ (XBBH * TRNBP(2,2) - YBBH * TRNBP(1,2)) * m * DDYPHP$
 $+ (XBBH * TRNBP(2,3) - YBBH * TRNBP(1,3)) * m * DDZPHP$
 $= - PBBI * HYBHH + QBBI * HXBHH + MZB + XBBH * FYB - YBBH * FXB$
 $- m * XBBH * AYBHI1 + m * YBBH * AXBHI1$ (4.3.7.14)

The next three equations come from the force balance on the body [Eq. (4.1.2.9)]. Rewriting:

- #7) $- AXBBI + RXB/m = - FXB/m$
#8) $- AYBBI + RYB/m = - FYB/m$
#9) $- AZBBI + RZB/m = - FZB/m$ (4.3.7.15)

The next three equations represent the restricted rotational motion as derived earlier in this section. Four different options are available depending on the type of motion allowed. For completely restricted motion when two or more missile rail hangers are restricted by the rail, the equations [from Eq. (4.3.7.2)] are:

- #10) $TRNBP(1,1)*DPBBI + TRNBP(2,1)*DQBBI + TRNBP(3,1)*DRBBI$
 $= -XCROSS + DPPPI$
- #11) $TRNBP(1,2)*DPBBI + TRNBP(2,2)*DQBBI + TRNBP(3,2)*DRBBI$ (4.3.7.16)
 $= -YCROSS + DQPPI$
- #12) $TRNBP(1,3)*DPBBI + TRNBP(2,3)*DQBBI + TRNBP(3,3)*DRBBI$
 $= -ZCROSS + DRPPI$

For a missile allowed only to pitch during the short period when only one hanger is attached to the rail:

- #10) $TRNBP(1,1)*DPBBI + TRNBP(2,1)*DQBBI + TRNBP(3,1)*DRBBI$
 $= -XCROSS + DPPPI$
- #11) $TRNBP(1,2)*RLB + TRNBP(2,2)*RMB + TRNBP(3,2)*RNB = 0.0$ (4.3.7.17)
- #12) $TRNBP(1,3)*DPBBI + TRNBP(2,3)*DQBBI + TRNBP(3,3)*DRBBI$
 $= -ZCROSS + DRPPI$

For a missile allowed only to yaw during the short period when only one hanger is attached to the rail:

- $$\begin{aligned}
 \#10) \quad & \text{TRNBP}(1,1)*DPBBI + \text{TRNBP}(2,1)*DQBBI + \text{TRNBP}(3,1)*DRBBI \\
 & = -\text{XCROSS} + \text{DPPPI} \\
 \#11) \quad & \text{TRNBP}(1,2)*DPBBI + \text{TRNBP}(2,2)*DQBBI + \text{TRNBP}(3,2)*DRBBI \\
 & = -\text{YCROSS} + \text{DQPPPI} \\
 \#12) \quad & \text{TRNBP}(1,3)*RLB + \text{TRNBP}(2,3)*RMB + \text{TRNBP}(3,3)*RNB = 0.0
 \end{aligned} \tag{4.3.7.18}$$

For a missile allowed to both pitch and yaw during the short period when only one hanger is attached to the rail:

- $$\begin{aligned}
 \#10) \quad & \text{TRNBP}(1,1)*DPBBI + \text{TRNBP}(2,1)*DQBBI + \text{TRNBP}(3,1)*DRBBI \\
 & = -\text{XCROSS} + \text{DPPPI} \\
 \#11) \quad & \text{TRNBP}(1,2)*RLB + \text{TRNBP}(2,2)*RMB + \text{TRNBP}(3,2)*RNB = 0.0 \\
 \#12) \quad & \text{TRNBP}(1,3)*RLB + \text{TRNBP}(2,3)*RMB + \text{TRNBP}(3,3)*RNB = 0.0
 \end{aligned} \tag{4.3.7.19}$$

The last three equations arise from the constraints of no hook motion normal to the rail and no downrail reaction force:

- $$\begin{aligned}
 \#13) \quad & \text{TRNBP}(1,1)*RXB + \text{TRNBP}(2,1)*RYB + \text{TRNBP}(3,1)*RZB = 0.0 \\
 \#14) \quad & \text{DDYPHP} = 0.0 \\
 \#15) \quad & \text{DDZPHP} = 0.0
 \end{aligned} \tag{4.3.7.20}$$

At each time step in the trajectory, the 15 equations are solved by a Gaussian Reduction with Columnal Pivoting algorithm for the 15 acceleration and reaction load terms. The total hook acceleration is calculated from Eq. (4.3.7.13). The translational accelerations are rewritten as derivatives of the projected velocities using Eqs. (4.1.2.10), and the rotational and translational velocity derivatives are integrated over time to determine linear and angular projected velocities of the body-axis system.

Release conditions for rail launch simulations are particularly easy to incorporate. Two downrail travel distances are specified for the aft rail hanger of the store. The first distance is the distance from its carriage position that the aft hanger must travel during which at least one other hanger is attached to the rail. After the store translates this distance, the restraint equations are changed from translate-only restrictions [Eq. (4.3.7.16)] to translate and rotate about the aft hanger restrictions [Eqs. (4.3.7.17), (4.3.7.18), or (4.3.7.19)]. The second input distance is the downrail distance the aft hanger must travel before all missile hangers become free of the rail. At this point the simulation switches to the unrestrained motion equations. Aft hanger travel distances at each time step are obtained from :

$$\text{XHPCK} = \text{XPHP} + \text{XBBH} \tag{4.3.7.21}$$

where XPHP is obtained from Eq. (4.3.2.19) which is updated at each time step and where $\text{XBBH} = \text{XPBH}_0 = \text{XPPH}_0 = -\text{XPHP}_0$ because the body-axis origin and the pylon-axis origin are coincident at the instant of first motion. The hook travel distance from Eq. (4.3.7.21) is tested against the two input distances to determine the correct phase of the missile motion.

4.3.8 Cradle Launcher Restraint (Motion Restricted to Ejector Plane)

The generalized constraint equations for launchers in which the store is cradled in a yoke or on a pallet are developed in this section. The equations are applicable to the eject launchers used for air-to-air missiles on such aircraft as the F-15, F-18, and F-22. The F-15/F-18 missile eject launcher, for instance, is equipped with two ejector pistons fired by an explosive charge that impart an initial force to the missile to propel it away from the aircraft. The forward ejector piston is equipped with a crescent-shaped yoke which cradles the missile during the piston stroke. The yoke is designed to prevent missile yaw and roll motions during the piston stroke so that the piston force always acts through the missile centerline without imparting yaw or roll motions to the missile. The initial missile motion is thus constrained to the ejector plane. The AMRAAM Vertical Eject Launcher (AVEL) device used by the F-22 aircraft consists of a small pallet to which the missile is mounted which is, in turn, mounted to the roof of the main aircraft weapons bay using a system of linkages. When the linkages are operated, the missile and pallet are extended rapidly out of the bay and the missile is released from the pallet. Motion of the missile is therefore also constrained to remain in the ejector plane by the F-22 missile launcher. Equations are developed in this section to allow solution for twelve unknowns - the standard three translational acceleration components of the store body {AXBBI, AYBBI, AZBBI}, three rotational acceleration components {DPBBI, DQBBI, DRBBI}, three reaction force components {RXB, RYB, RZB} and three reaction moment components {RLB, RMB, RNB}. The equations for the ejector restraint are somewhat simpler than those previously developed for the other restraint devices because the moments can be taken about the store center of gravity rather than about an arbitrary hook point.

The constraints which must be modeled are, first, the translational constraint that the missile center of gravity have no components of acceleration normal to the plane of the ejectors. As was the case with the rail launcher constraints in the previous section, imposition of this constraint may be complicated for a maneuvering aircraft because the ejector plane moves with the aircraft. The rotational restraint is specified in terms of the angular derivatives of the body-axis orientation relative to the ejector plane so that no yaw or roll relative to ejector axes is allowed. A new axis system aligned with the ejector plane will be introduced for the development of ejector constraints. The new system will be designated "J" for "eJector" axes and will have its XJ axes aligned with the longitudinal axis of the store at its carriage position (coincident with the XP and XC axes) and its ZJ axis within the ejector plane of action. The carriage incidence angles, IY, IP, and IR, will again be needed as will a new angle, Ω_M , which defines the roll orientation of the ejector plane axes relative to the store body axis. Note that when the store is located at its carriage position, the store body axes and carriage axes are coincident so that PHIJC = Ω_M . The orientation transformations relating pylon, carriage, and ejector axes are:

$$\begin{aligned} \text{PSIJC} &= 0.0 \\ \text{THAJC} &= 0.0 \\ \text{PHIJC} &= \Omega_M \end{aligned} \quad (4.3.8.1)$$

Using the angles from Eq. (4.3.8.1) and the matrices previously defined in Eqs. (4.3.2.1) through (4.3.2.3), the following useful transformations may be derived:

$$\begin{aligned}
 [\text{TRNJC}] &= [\text{TRNx}(\text{PHIJC})] [\text{TRNy}(\text{THAJC})] [\text{TRNz}(\text{PSIJC})] \\
 [\text{TRNJP}] &= [\text{TRNJC}] [\text{TRNCP}] \\
 [\text{TRNJI}] &= [\text{TRNJP}] [\text{TRNPI}] \\
 [\text{TRNBJ}] &= [\text{TRNBI}] [\text{TRNJI}]^{-1}
 \end{aligned} \tag{4.3.8.2}$$

The ejector axes are illustrated in Fig. 28.

Twelve linearly independent equations are necessary to determine the 12 independent variables at each time step. The first three of the necessary equations are the translational equations of motion. The form developed in Eq. (4.1.2.9) is used. The equations are written in terms of the unknowns and expanded into scalar form as:

$$\begin{aligned}
 \#1) \quad \text{AXBBI} - \text{RXB}/m &= \text{FXB}/m \\
 \#2) \quad \text{AYBBI} - \text{RYB}/m &= \text{FYB}/m \\
 \#3) \quad \text{AZBBI} - \text{RZB}/m &= \text{FZB}/m
 \end{aligned} \tag{4.3.8.3}$$

The next three equations are the restricted rotational equations of motion defined by Eq. (4.2.2.43). The body-axis components of the angular momentum about the hook axes are calculated directly from body-axis inertia terms:

$$\left| \begin{array}{c} \text{HXBBI} \\ \text{HYBBI} \\ \text{HZBBI} \end{array} \right| = [\text{I}]_{\text{BB}} \left| \begin{array}{c} \text{PBBI} \\ \text{QBBI} \\ \text{RBBI} \end{array} \right| \tag{4.3.8.4}$$

Then Eq. (4.2.2.43) is expanded as:

$$\begin{aligned}
 \#4) \quad &[\text{I}]_{\text{BB}}(1,1) * \text{DPBBI} + [\text{I}]_{\text{BB}}(1,2) * \text{DQBBI} + [\text{I}]_{\text{BB}}(1,3) * \text{DRBBI} - \text{RLB} \\
 &= - \text{QBBI} * \text{HZBBI} + \text{RBBI} * \text{HYBBI} + \text{MXB} \\
 \#5) \quad &[\text{I}]_{\text{BB}}(2,1) * \text{DPBBI} + [\text{I}]_{\text{BB}}(2,2) * \text{DQBBI} + [\text{I}]_{\text{BB}}(2,3) * \text{DRBBI} - \text{RMB} \\
 &= - \text{RBBI} * \text{HXBBI} + \text{PBBI} * \text{HZBBI} + \text{MYB} \\
 \#6) \quad &[\text{I}]_{\text{BB}}(3,1) * \text{DPBBI} + [\text{I}]_{\text{BB}}(3,2) * \text{DQBBI} + [\text{I}]_{\text{BB}}(3,3) * \text{DRBBI} - \text{RNB} \\
 &= - \text{PBBI} * \text{HYBBI} + \text{QBBI} * \text{HXBBI} + \text{MZB}
 \end{aligned} \tag{4.3.8.5}$$

The next three equations come from the restraint that there is no acceleration of the body normal to the ejector plane. The constraint can be written as:

$$\begin{aligned}
 \text{RXJ} &= 0.0 \\
 \text{DDYJBJ} &= 0.0 \\
 \text{RZJ} &= 0.0
 \end{aligned} \tag{4.3.8.6}$$

where the RXJ and RZJ terms are defined by:

$$\left| \begin{array}{c} \text{RXJ} \\ \text{RYJ} \\ \text{RZJ} \end{array} \right| = [\text{TRNBJ}]^T \left| \begin{array}{c} \text{RXB} \\ \text{RYB} \\ \text{RZB} \end{array} \right| \tag{4.3.8.7}$$

The expression for DDYJBJ is somewhat more complicated but follows a derivation almost identical to that for the relative accelerations down a missile launch rail as developed in Eq. (4.3.2.22) in Section 4.3.2. First, the {XJBJ} vector must be expanded out in terms of known quantities available from other portions of the simulation and then its derivatives must be taken. Beginning with the inertial-axis components of the position of the body axes relative to flight axes:

$$\begin{vmatrix} XIBF \\ YIBF \\ ZIBF \end{vmatrix} = \begin{vmatrix} XIBI \\ YIBI \\ ZIBI \end{vmatrix} - \begin{vmatrix} XIFI \\ YIFI \\ ZIFI \end{vmatrix} \quad (4.3.8.8)$$

Note, however, that {XIBF} = {XIBJ} because flight and ejector axes have a common origin. The full expression for {XJBJ} can then be formed by projecting into ejector axes:

$$\begin{vmatrix} XJBJ \\ YJBJ \\ ZJBJ \end{vmatrix} = [\text{TRNJI}] \left\{ \begin{vmatrix} XIBI \\ YIBI \\ ZIBI \end{vmatrix} - \begin{vmatrix} XIFI \\ YIFI \\ ZIFI \end{vmatrix} \right\} \quad (4.3.8.9)$$

The derivatives of the {XJBJ} vector are now needed. By the chain rule:

$$\begin{aligned} \begin{vmatrix} DXJBJ \\ DYJBJ \\ DZJBJ \end{vmatrix} &= -[\tilde{\omega}_{JJI}] [\text{TRNJI}] \left\{ \begin{vmatrix} XIBI \\ YIBI \\ ZIBI \end{vmatrix} - \begin{vmatrix} XIFI \\ YIFI \\ ZIFI \end{vmatrix} \right\} \\ &\quad + [\text{TRNJI}] \left\{ \begin{vmatrix} UIBI \\ VIBI \\ WIBI \end{vmatrix} - \begin{vmatrix} UIFI \\ VIFI \\ WIFI \end{vmatrix} \right\} \\ &= -[\tilde{\omega}_{JJI}] \begin{vmatrix} XJBJ \\ YJBJ \\ ZJBJ \end{vmatrix} + \begin{vmatrix} UJBJ \\ VJBJ \\ WJBJ \end{vmatrix} \end{aligned} \quad (4.3.8.10)$$

where {UJBJ} is:

$$\begin{vmatrix} UJBJ \\ VJBJ \\ WJBJ \end{vmatrix} = [\text{TRNJI}] \left\{ \begin{vmatrix} UIBI \\ VIBI \\ WIBI \end{vmatrix} - \begin{vmatrix} UIFI \\ VIFI \\ WIFI \end{vmatrix} \right\} \quad (4.3.8.11)$$

Finally, the second derivative is needed:

$$\begin{aligned}
 \begin{vmatrix} DDXJBJ \\ DDYJBJ \\ DDZJBJ \end{vmatrix} &= -[D\tilde{\omega} JJI] [TRNJI] \left\{ \begin{vmatrix} XIBI \\ YIBI \\ ZIBI \end{vmatrix} - \begin{vmatrix} XIFI \\ YIFI \\ ZIFI \end{vmatrix} \right\} \\
 &+ [\tilde{\omega} JJI] [\tilde{\omega} JJI] [TRNJI] \left\{ \begin{vmatrix} XIBI \\ YIBI \\ ZIBI \end{vmatrix} - \begin{vmatrix} XIFI \\ YIFI \\ ZIFI \end{vmatrix} \right\} \\
 &- [\tilde{\omega} JJI] [TRNJI] \left\{ \begin{vmatrix} UIBI \\ VIBI \\ WIBI \end{vmatrix} - \begin{vmatrix} UIFI \\ VIFI \\ WIFI \end{vmatrix} \right\} - [\tilde{\omega} JJI] [TRNJI] \left\{ \begin{vmatrix} UIBI \\ VIBI \\ WIBI \end{vmatrix} - \begin{vmatrix} UIFI \\ VIFI \\ WIFI \end{vmatrix} \right\} \\
 &+ [TRNJI] \left\{ \begin{vmatrix} AXIBI \\ AYIBI \\ AZIBI \end{vmatrix} - \begin{vmatrix} AXIFI \\ AYIFI \\ AZIFI \end{vmatrix} \right\}
 \end{aligned} \tag{4.3.8.12}$$

It is convenient in actual numerical simulations to re-express Eq. (4.3.8.12) in the following form:

$$\begin{aligned}
 \begin{vmatrix} DDXJBJ \\ DDYJBJ \\ DDZJBJ \end{vmatrix} &- [TRNBJ]^{-1} \begin{vmatrix} AXBBI \\ AYBBI \\ AZBBI \end{vmatrix} \\
 &= -[D\tilde{\omega} JJI] \begin{vmatrix} XJBJ \\ YJBJ \\ ZJBJ \end{vmatrix} - [\tilde{\omega} JJI] \begin{vmatrix} DXJBJ \\ DYJBJ \\ DZJBJ \end{vmatrix} - [\tilde{\omega} JJI] \begin{vmatrix} UJBJ \\ VJBJ \\ WJBJ \end{vmatrix} - \begin{vmatrix} AXJJI \\ AYJJI \\ AZJJI \end{vmatrix}
 \end{aligned} \tag{4.3.8.13}$$

The terms in the skew symmetries and the ejector-axis acceleration term needed to evaluate Eq. (4.3.8.13) are obtained from:

$$\begin{vmatrix} PJJ \\ QJJI \\ RJJ \\ I \end{vmatrix} = [TRNJP] \begin{vmatrix} PPPI \\ QPPI \\ RPPI \end{vmatrix} = \begin{vmatrix} PJPI \\ QJPI \\ RJPI \end{vmatrix} \tag{4.3.8.14}$$

$$\begin{vmatrix} DPJJI \\ DQJJI \\ DRJJI \end{vmatrix} = [TRNJP] \begin{vmatrix} DPPPI \\ DQPPI \\ DRPPI \end{vmatrix} = \begin{vmatrix} DPJPI \\ DQJPI \\ DRJPI \end{vmatrix} \tag{4.3.8.15}$$

and

$$\begin{vmatrix} AXJJI \\ AYJJI \\ AZJJI \end{vmatrix} = [TRNJP] \begin{vmatrix} AXPPI \\ AYPPI \\ AZPPI \end{vmatrix} = \begin{vmatrix} AXJPI \\ AYJPI \\ AZJPI \end{vmatrix} \tag{4.3.8.16}$$

where it is noted that the origins of flight, pylon, and ejector axes are coincident and that the [TRNJP] matrix is time-invariant.

Using the relations of Eqs. (4.3.8.13) and (4.3.8.7), the relations of Eq. (4.3.8.6) can be expanded. First, the y-components of the three cross products on the right side of Eq. (4.3.8.13) are evaluated and stored in temporary variables ({DDYJBJ1}, {DDYJBJ2}, and {DDYJBJ3}), then the three constraints can be expanded in terms of the twelve unknowns as:

- #7) $\text{TRNBJ}(1,1)*\text{RXB} + \text{TRNBJ}(2,1)*\text{RYB} + \text{TRNBJ}(3,1)*\text{RZB} = 0.0$
- #8) $-\text{TRNBJ}(1,2)*\text{AXBBI} - \text{TRNBJ}(2,2)*\text{AYBBI} - \text{TRNBJ}(3,2)*\text{AZBBI}$
 $= -\text{DDYJBJ1} - \text{DDYJBJ2} - \text{DDYJBJ3} - \text{AYJJI}$
- #9) $\text{TRNBJ}(1,3)*\text{RXB} + \text{TRNBJ}(2,3)*\text{RYB} + \text{TRNBJ}(3,3)*\text{RZB} = 0.0$

The next three equations impose the ejector plane rotational constraints. The rotational constraints for a store free to pitch only in the ejector plane are:

$$\begin{aligned} \text{DPJBJ} &= 0.0 \\ \text{DRJBJ} &= 0.0 \\ \text{RMJ} &= 0.0 \end{aligned} \quad (4.3.8.18)$$

To impose the constraints, it is necessary to derive expressions for the rotational terms in Eq. (4.3.8.18). The derivation is virtually identical to that for motion restricted to the pylon pitch or yaw planes as developed for the rail launcher restrictions in Eq. (4.3.7.8) of Section 4.3.7. Beginning with the relations for the angular velocities of body and ejector axes:

$$\begin{vmatrix} \text{PBJJ} \\ \text{QBJJ} \\ \text{RBJJ} \end{vmatrix} = \begin{vmatrix} \text{PJBI} \\ \text{QJBI} \\ \text{RJBI} \end{vmatrix} - \begin{vmatrix} \text{PJPI} \\ \text{QJPI} \\ \text{PJPI} \end{vmatrix} = [\text{TRNBJ}]^T \begin{vmatrix} \text{PBBI} \\ \text{QBBI} \\ \text{RBBI} \end{vmatrix} - [\text{TRNJP}] \begin{vmatrix} \text{PPPI} \\ \text{QPPI} \\ \text{RPPI} \end{vmatrix} \quad (4.3.8.19)$$

Taking derivatives of both sides by the chain rule:

$$\begin{aligned} \frac{d}{dt} \begin{vmatrix} \text{PBJJ} \\ \text{QBJJ} \\ \text{RBJJ} \end{vmatrix} &= \frac{d}{dt} [\text{TRNBJ}]^T \begin{vmatrix} \text{PBBI} \\ \text{QBBI} \\ \text{RBBI} \end{vmatrix} + [\text{TRNBJ}]^T \frac{d}{dt} \begin{vmatrix} \text{PBBI} \\ \text{QBBI} \\ \text{RBBI} \end{vmatrix} - \frac{d}{dt} [\text{TRNJP}] \begin{vmatrix} \text{PPPI} \\ \text{QPPI} \\ \text{RPPI} \end{vmatrix} \\ &\quad + [\text{TRNJP}] \frac{d}{dt} \begin{vmatrix} \text{PPPI} \\ \text{QPPI} \\ \text{RPPI} \end{vmatrix} \end{aligned} \quad (4.3.8.20)$$

or (noting that the [TRNJP] matrix is time invariant):

$$\begin{aligned} \begin{vmatrix} \text{DPJBJ} \\ \text{DQJBJ} \\ \text{DRJBJ} \end{vmatrix} &= [\text{TRNBJ}]^T [\tilde{\omega}_{BBJ}] \begin{vmatrix} \text{PBBI} \\ \text{QBBI} \\ \text{RBBI} \end{vmatrix} + [\text{TRNBJ}]^T \begin{vmatrix} \text{DPBBI} \\ \text{DQBBI} \\ \text{DRBBI} \end{vmatrix} - [\text{TRNJP}] \begin{vmatrix} \text{DPPPI} \\ \text{DQPPI} \\ \text{DRPPI} \end{vmatrix} \\ &= \begin{vmatrix} \text{XCROSS} \\ \text{YCROSS} \\ \text{ZCROSS} \end{vmatrix} + [\text{TRNBJ}]^T \begin{vmatrix} \text{DPBBI} \\ \text{DQBBI} \\ \text{DRBBI} \end{vmatrix} - \begin{vmatrix} \text{DPJJI} \\ \text{DQJJI} \\ \text{DRJJI} \end{vmatrix} \end{aligned} \quad (4.3.8.21)$$

where the {XCROSS} terms represent temporary variables to ease implementation of the equations in a computer simulation. The {DPJJI} vector [defined by Eq. (4.3.8.15)] is zero for the idealized pitch plane maneuvers defined by constant load factors but could, of course, be non-zero for arbitrary non-idealized maneuvers. The {PBBJ} vector used in the skew symmetric in Eq. (4.3.8.21) is obtained by projecting Eq. (4.3.8.19):

$$\begin{vmatrix} PBBJ \\ QBBJ \\ RBBJ \end{vmatrix} = [TRNBJ] \begin{vmatrix} PJBJ \\ QJBJ \\ RJBJ \end{vmatrix} \quad (4.3.8.22)$$

The desired rotational constraint equations are obtained by combining Eqs. (4.3.8.22), (4.3.8.21), and (4.3.8.18):

- #10) $TRNBJ(1,1)*DPBBI + TRNBJ(2,1)*DQBBI + TRNBJ(3,1)*DRBBI = -XCROSS + DPJJI$ (4.3.8.23)
- #11) $TRNBJ(1,2)*RLB + TRNBJ(2,2)*RMB + TRNBJ(3,2)*RNB = 0.0$
- #12) $TRNBJ(1,3)*DPBBI + TRNBJ(2,3)*DQBBI + TRNBJ(3,3)*DRBBI = -ZCROSS + DRJJI$

At this point the 12 equations necessary for modeling the release motion have been developed. At each time step in the trajectory, the 12 equations are solved by a Gaussian Reduction with Columnal Pivoting algorithm for the 12 acceleration and reaction load terms.

Once the system of equations is solved, the translational accelerations are rewritten as derivatives of the projected velocities using Eq. (4.1.2.10) and the rotational and translational velocity derivatives are integrated over time to determine linear and angular projected velocities. Also at each time step, the velocities and angular transformations of the body axes are integrated to determine the positions and orientations of the body axes relative to inertial axes at the new time step.

Release conditions for ejector cradle-restrained motion simulations are dependent on the manner in which the ejector itself is modeled. Several different "idealized" ejector models are available within the AEDC simulations. In those models, the ejector forces may be represented by input curve fits of the ejector forces as a function of time or by curve fits of the ejector force as a function of ejector piston stroke. Cutoff of the ejector forces can be specified by either an input value of end-of-stroke time or an input value of end-of-stroke piston displacement. If cutoff is specified by end-of-stroke time, then the simulation simply switches from ejector-restrained motion to free motion when the specified time is reached. If the ejector cutoff is specified by an input maximum piston stroke, then the current piston stroke at each time instant must be calculated and tested against the cutoff value before releasing the ejector restrictions. The equations for calculating current piston stroke at each time step are provided in the next section.

4.3.8.1 Calculation of Ejector Piston Stroke

Several different "idealized" ejector models are available within the AEDC simulations. None of the models can be completely rigorous, however, because the actual mechanism of most

ejectors (explosive charges acting in pressure chambers on moving pistons) is extremely difficult to represent mathematically. In the available idealized models, ejector forces may be represented by input curve fits of the ejector forces as a function of time or by curve fits of the ejector forces as a function of ejector piston stroke. Cutoff of the ejector forces can be specified by either an input value of end-of-stroke time or an input value of end-of-stroke piston displacement. And, as noted in the previous section, cutoff of ejector cradle motion restrictions may also be keyed to a specified time or stroke value. The equations for calculating current piston stroke at each time step are provided in this section.

The calculation of piston stroke in the AEDC simulation package is basically accomplished in two phases and is performed in a stand-alone ejector module which is separate from the basic equation-of-motion modules. The first step in determining stroke distance is to combine the position of the compressed piston point on the aircraft relative to the origin of the flight/aircraft/pylon/ejector trajectory-axis systems (origin at the cg position of the active store when it is mounted at its carriage position) with the position of the trajectory-axis origin relative to the inertial-axis system (which changes as a result of the aircraft maneuver). This defines the inertial position of the point of application of the piston forces on the aircraft. The second step is to combine the position relative to the store body axes of the point on the store at which the piston force is applied with the position of the store body axes relative to inertial axes obtained from the store equations of motion at each time point in the simulation. This defines the inertial position of the point of application of the piston forces on the store. The stroke length is then the difference between the position of the aircraft load point and the store load point.

Options are available in the ejector simulation to model cases involving either an ejector mechanism fixed with the aircraft which pushes down on the store or an ejector fixed in the store that pushes up on the aircraft. A major idealization of the stroke calculation is that the point of piston force application on the store is assumed to be fixed with respect to the store and that the point of application of the piston force on the aircraft is fixed relative to the aircraft. In actuality, if the piston line-of-action is fixed-mounted in the store, then the piston contact point must be free to slide on a hardened surface of the aircraft. Likewise, if the piston unit is fixed-mounted in the aircraft, then the point of application of the force on the store must slide on the surface of the store. The removal of this idealization would have tremendous implications on the complexity of the model, since the tangential friction forces imparted to the store or aircraft at the piston contact points and the surface contours of the store or aircraft in the region of the contact points would also have to be included and the ejector force equations could not be kept in a separate ejector module but would have to be integrated into the store equation-of-motion package.

Forward and aft ejector pistons designated by the characters '1' and '2' may be simulated within the ejector package. The derivation that follows will be presented only for the forward ('1') ejector. The equations for the aft ejector (if the ejector unit is so equipped) are analogous. The points on the store at which the ejector pistons act are defined by the position vectors {XB1B} and {XB2B} which are defined from input quantities to the simulation.

The first phase in the calculation of the piston stroke is the determination of the inertial position of the aircraft-fixed contact point. Recall that when the store is mounted at its carriage

position on the aircraft, the store body axes are coincident with the carriage axes so that $[TRNBA]_{carriage} = [TRNCA]$ and $\{XB1B\} = \{XC1C\}$. The aircraft-axis components of the position of the piston contact point on the store are then:

$$\begin{vmatrix} XA1BO \\ YA1BO \\ ZA1BO \end{vmatrix} = [TRNCA] \begin{vmatrix} XB1B \\ YB1B \\ ZB1B \end{vmatrix} \quad (4.3.8.1.1)$$

Also the store body-axis origin is coincident with the flight-axis origin when the store is at its carriage position on the aircraft, so that:

$$\begin{vmatrix} XA1FO \\ YA1FO \\ ZA1FO \end{vmatrix} = \begin{vmatrix} XA1BO \\ YA1BO \\ ZA1BO \end{vmatrix} \quad (4.3.8.1.2)$$

Equation (4.3.8.1.2) defines the position of the contact point on the piston when the piston is compressed at its pre-launch position. This compressed piston contact position is fixed relative to the aircraft and moves with the aircraft during its flight maneuver. The inherent idealization evident in the previous equation is that the piston is assumed to stay in contact with the same point on the aircraft (that $\{XA1FO\}$ is constant). This assumption is certainly true if the ejector is mounted in the aircraft pushing down on the store. This assumption is also roughly true in the general case for a store-mounted ejector, but may not be fully valid if ejector forces are not large enough to dominate lateral aerodynamic forces which might move the store laterally, thus changing the point of application of the ejector on the aircraft or if the center of gravity of the store is offset laterally and rotation of the store about its cg changes the direction of the store-fixed ejector line of action. At subsequent times during the trajectory, the inertial-axis components of the position of the aircraft contact point relative to flight axes are dependent on the rotation of the aircraft during the maneuver and the translation of the flight-axis origin relative to the inertial origin resulting from the maneuver:

$$\begin{vmatrix} XI1FO \\ YI1FO \\ ZI1FO \end{vmatrix} = [TRNAI]^T \begin{vmatrix} XA1FO \\ YA1FO \\ ZA1FO \end{vmatrix} \quad (4.3.8.1.3)$$

and

$$\begin{vmatrix} XI1IO \\ YI1IO \\ ZI1IO \end{vmatrix} = \begin{vmatrix} XI1FO \\ YI1FO \\ ZI1FO \end{vmatrix} + \begin{vmatrix} XIFI \\ YIFI \\ ZIFI \end{vmatrix} \quad (4.3.8.1.4)$$

Equation (4.3.8.1.4) represents the inertial components as a function of time of the piston contact point on the aircraft.

The second step in the stroke calculation is to determine the position of the contact point on the store. The actual inertial components of the position of the contact point on the store relative

to the inertial axes are dependent on the translational and rotational movement of the store relative to inertial axes:

$$\begin{vmatrix} XI1B \\ YI1B \\ ZI1B \end{vmatrix} = [TRNBI]^T \begin{vmatrix} XB1B \\ YB1B \\ ZB1B \end{vmatrix} \quad (4.3.8.1.5)$$

from which:

$$\begin{vmatrix} XI1I \\ YI1I \\ ZI1I \end{vmatrix} = \begin{vmatrix} XI1B \\ YI1B \\ ZI1B \end{vmatrix} + \begin{vmatrix} XIBI \\ YIBI \\ ZIBI \end{vmatrix} \quad (4.3.8.1.6)$$

The inherent idealization evident in the previous equations is that the piston is assumed to stay in contact with the same point on the store (that is, $\{XB1B\}$ is constant). This assumption is certainly true if the ejector is mounted in the store pushing up on the aircraft. This assumption is also roughly true for an aircraft-mounted ejector, but may not be fully valid if ejector forces are not large enough to dominate lateral aerodynamic forces which might move the store laterally out of the ejector line of action, or if the center of gravity of the store is offset laterally and rotation of the store about its cg moves the specified contact point on the store out of the ejector line of action.

Finally the current stroke of the piston is computed as the inertial components of the current piston contact point on the store minus the components of the current position of the piston contact point on the aircraft:

$$\begin{vmatrix} XI1IO \\ YI1IO \\ ZI1IO \end{vmatrix} = \begin{vmatrix} XI1I \\ YI1I \\ ZI1I \end{vmatrix} - \begin{vmatrix} XI1O \\ YI1O \\ ZI1O \end{vmatrix} \quad (4.3.8.1.7)$$

Equation (4.3.8.1.7) represents the inertial-axis components of the idealized piston stroke. Of more interest is that component of the idealized stroke which is in the direction of the true ejector piston line-of-action. The orientation of the ejector line-of-action relative to the store body axes is fixed if the ejector unit is mounted within the store pushing up. On the other hand, the ejector line of action is constantly changing in direction relative to the store body during the trajectory if the ejector unit is mounted in the aircraft. The equations for the orientation of the ejector line of action for an aircraft-mounted ejector will be presented first, followed by the simpler equations for a store-fixed ejector.

The "J" for "eJector" axis system for motion restricted to an aircraft-fixed ejector plane was previously introduced in Section 4.3.8 in the derivation for the ejector cradle motion restriction. For that derivation, the J-axis system simply defined the plane of the ejectors based on the input roll orientation of the ejector plane relative to carriage axes according to Eq (4.3.8.2) (which is repeated below). The actual line of action of the ejector may be pitched relative to the carriage axes within the eJector axis XJ-ZJ plane. Defining symbol "L" to denote ejector Line-of-action

axes and using another input angle DTHAFE to denote the pitch angle of the ejector line of action within the ejector plane, the following angular orientation parameters can be developed in addition to those already previously defined in Eq. (4.3.8.1):

$$\begin{aligned} \text{PSIJC} &= 0.0 \\ \text{THAJC} &= 0.0 \\ \text{PHIJC} &= \Omega_M \end{aligned} \quad (4.3.8.1)$$

$$\begin{aligned} [\text{TRNJC}] &= [\text{TRNx}(\text{PHIJC})] [\text{TRNy}(\text{THAJC})] [\text{TRNz}(\text{PSIJC})] \\ [\text{TRNP}] &= [\text{TRNJC}] [\text{TRNCP}] \\ [\text{TRNJI}] &= [\text{TRNJP}] [\text{TRNPI}] \\ [\text{TRNBJ}] &= [\text{TRNBI}] [\text{TRNJI}]^{-1} \end{aligned} \quad (4.3.8.2)$$

$$\begin{aligned} \text{PSIJL} &= 0.0 \\ \text{THAJL} &= -\text{DTHAFE} \\ \text{PHI JL} &= 0.0 \\ [\text{TRN JL}] &= [\text{TRNx}(\text{PHI JL})] [\text{TRNy}(\text{THAJL})] [\text{TRNz}(\text{PSIJL})] \\ [\text{TRNLC}] &= [\text{TRN JL}]^{-1} [\text{TRNJC}] \end{aligned} \quad (4.3.8.1.8)$$

Note that the TRNLC matrix defining the orientation of the ejector line of action relative to aircraft-fixed carriage axes involves a roll-pitch sequence - rolling first from carriage axes to the ejector plane and then pitching to the ejector line of action. The orientation matrix for body axes relative to line-of-action axes at each time step and for line-of-action axes relative to inertial axes at all time steps can then be developed from:

$$\begin{aligned} [\text{TRNBL}] &= [\text{TRNBJ}] [\text{TRN JL}] \\ \text{and } [\text{TRNLI}] &= [\text{TRN JL}]^{-1} [\text{TRNJI}] \end{aligned} \quad (4.3.8.1.9)$$

where it is noted that the [TRNBL] terms are time-varying quantities and that the [TRNLI] matrix is time-invariant for an aircraft-fixed ejector.

A completely different set of expressions for [TRNBL] and [TRNLI] occur for a store-fixed ejector unit. First note that the store-fixed ejector plane is simply rolled within the body and that the ejector line of action is then pitched within the store-fixed ejector plane:

$$\begin{aligned} \text{PSIBJ} &= 0.0 \\ \text{THABJ} &= 0.0 \\ \text{PHIBJ} &= -\Omega_M \\ [\text{TRNBJ}] &= [\text{TRNx}(\text{PHIBJ})] [\text{TRNy}(\text{THABJ})] [\text{TRNz}(\text{PSIBJ})] \end{aligned} \quad (4.3.8.1.10)$$

$$\begin{aligned} \text{PSIJL} &= 0.0 \\ \text{THAJL} &= -\text{DTHAFE} \\ \text{PHI JL} &= 0.0 \\ [\text{TRN JL}] &= [\text{TRNx}(\text{PHI JL})] [\text{TRNy}(\text{THAJL})] [\text{TRNz}(\text{PSIJL})] \end{aligned} \quad (4.3.8.1.11)$$

Then the orientation matrix for body axes relative to line-of-action axes at all time steps and for line-of-action axes relative to inertial axes at each time step can then be developed from:

$$\begin{aligned} [\text{TRNBL}] &= [\text{TRNBJ}] [\text{TRNJI}] \\ \text{and } [\text{TRNLI}] &= [\text{TRNJI}]^{-1} [\text{TRNBL}] \end{aligned} \quad (4.3.8.1.12)$$

where it is noted that the [TRNBL] matrix is time-invariant and that the [TRNLI] terms are time-varying quantities for a store-fixed ejector .

Finally, now that [TRNLI] has been defined for both store-fixed and aircraft-fixed ejector units, the inertial components of stroke length can be projected into the ejector piston line-of-action directions as:

$$\begin{vmatrix} \text{XL11O} \\ \text{YL11O} \\ \text{ZL11O} \end{vmatrix} = [\text{TRNLI}] \begin{vmatrix} \text{XI11O} \\ \text{YI11O} \\ \text{ZI11O} \end{vmatrix} \quad (4.3.8.1.13)$$

Note that the idealized ejector equations do not rigorously force the XL11O and YL11O components in Eq. (4.3.8.1.13) to be zero, even though most ejector pistons only stroke in the ejector z direction. In the simulation, the calculated XL11O and YL11O values are ignored and ZL11O is used as the current ejector stroke for both force-versus-stroke curve-fit evaluations and end-of-stroke cutoff distance tests.

Regardless of whether ejector forces come from curve fits or table look-ups of force histories as a function of time or ejector stroke, the ejector line-of-action components of the computed ejector force at each time step must be rotated to body-axis components for the force summations on the body that will be used in the equation-of-motion evaluations. The body-axis components of the ejector force applied to the body by the forward ejector piston are given by:

$$\begin{vmatrix} \text{FEXB1} \\ \text{FEYB1} \\ \text{FEZB1} \end{vmatrix} = [\text{TRNBL}] \begin{vmatrix} 0.0 \\ 0.0 \\ \text{FEZL1} \end{vmatrix} \quad (4.3.8.1.14)$$

where FEZL1 comes from the ejector force curve fit or table look-up as a function of time or ejector stroke. Similarly, the ejector moment from the forward piston is given by:

$$\begin{vmatrix} \text{MEXB1} \\ \text{MEYB1} \\ \text{MEZB1} \end{vmatrix} = \begin{vmatrix} \text{XB1B} \\ \text{YB1B} \\ \text{ZB1B} \end{vmatrix} \times \begin{vmatrix} \text{FEXB1} \\ \text{FEYB1} \\ \text{FEZB1} \end{vmatrix} \quad (4.3.8.1.15)$$

The {FEXB1} and {FEXB2} contributions are summed with thrust forces, store aerodynamic forces, and store weight to compute the total external force vector {FXB} used in the equation-of-motion evaluation at each time step. Similarly, the ejector moment contributions are included in the total external moment vector {MXB}.

This completes the development of the stroke calculations for the idealized ejector models available as standard options in the AEDC simulation package. More rigorous models of actual ejector hardware require extensive modification to the simulation on a case-peculiar basis.

Before leaving the subject of ejector stroke length calculations, it should be pointed out that equations derived similarly to Eqs. (4.3.8.24) through (4.3.8.31) can be used to determine the distance from any fixed point on the store to any fixed point on the aircraft. The downrail motion of missile rail hangers formerly presented in Eq. (4.3.7.21), for instance, is just a trivial form of Eqs. (4.3.8.24) through (4.3.8.31) for the special case of hook motion restricted to the ZP direction. One common use of equations similar to Eqs. (4.3.8.24) through (4.3.8.31) is in the calculation of lanyard distances. Lanyards consist of cables or wires connecting a point on the store to a point on the aircraft and may serve several purposes. For some air-launched missiles such as the AMRAAM, the lanyard consists of a short cable which is severed when the missile travels a short distance from the ejector. When the missile flight control system senses breakage of the cable, the missile is assumed to be launched and the missile autopilot is activated. Lanyard cables are also often used for stores with spring-loaded deployable control surfaces such as the MK-20 store. Essentially, the deployable fin surfaces are depressed to their stowed position and the lanyard cable is tied around the aft end of the store to hold them in place until the store separates from the aircraft. At a supposedly safe distance from the aircraft, the store's lanyard cable breaks, releasing the pop-out fins. In numerical simulations, calculated lanyard lengths are often used to trigger switching to deployed-surface aerodynamic models or activation of autopilot models.

4.3.9 Accelerations, Velocities, and Flight Path of an Aircraft Undergoing an Arbitrary Non-Idealized Maneuver

Thus far, the aircraft maneuver has been limited to the constant load factor pitch-plane maneuvers described in Section 4.3.1. Implementation of arbitrary maneuvers into the equations of motion will be discussed in this section. The constant load factor maneuver can be reasonably simulated in wind tunnel testing because the aircraft angle of attack relative to the wind tunnel flow remains constant. The aircraft would, of course, be constantly changing its angles of attack and sideslip in a dynamic manner during an arbitrary maneuver. For this study, only the impacts of the arbitrary maneuver on the basic equations of motion will be discussed. Modeling of the dynamically changing aircraft flow environment during an arbitrary maneuver and its effects on the aerodynamic loads and resulting motion of the store will remain an item for future study. The basic premise for inclusion of an arbitrary maneuver capability into the store separation simulation is very simple: replace the equations developed in Section 4.3.1 for the idealized maneuver with a full simulation of arbitrary aircraft motion.

It is not this section's purpose to develop the full equations for an arbitrary aircraft motion simulation. Generally, it will be assumed that the aircraft motion transient is defined by some external simulation and provided as input to the store separation simulation. Aircraft motion simulations generally use the same forms of the equations of motion as defined in Sections 4.1.1 and 4.2.1 for the free-falling store. The only significant difference is that the aircraft motion is almost always defined relative to an inertial-axis system fixed relative to the earth and that simpler kine-

matics models can be used because the complicated restricted motion equations are not necessary. Aircraft motion simulations, provided by Lockheed Martin Tactical Aircraft Systems for the F-22 and Rockwell International for the B-1B, have been used along with the equations in this section to generate separation motions for stores during arbitrary F-22 and B-1 maneuvers.

The output from the aircraft motion simulation (which will be input to the store separation simulation) should consist of time histories of the basic motion parameters of the aircraft. The inertial-axis system for the aircraft simulation will be designated as the "I" or I-primed system. For many cases (including the F-22 and B-1 simulations), the vertical I' axis is coincident with earth gravitational acceleration vector. The y and z directions of the I' system may be somewhat arbitrary. Depending on the application, XI' may be aligned with true or magnetic North ("navigation" axes), with the original flight heading of the aircraft at store release (so-called "Earth" axes), or with the major direction of a flight test range. In many aircraft simulations the earth is approximated by a horizontal tangent plane and the earth's curvature is not included in the model. Also for store separation applications which are normally of small time duration, the Coriolis acceleration components associated with the cross-coupling of the rotational velocity of the earth with the relative translational velocity of the aircraft are often ignored. (Coriolis terms must be included in full ballistic trajectories for a store dropped from altitude and simulated all the way to the ground.) The aircraft motion variables are defined using an aircraft body-axis system which is analogous to the store body-axis system. The aircraft body axes will be designated by B'. The aircraft motion quantities which should be provided to the store separation simulation consist of the usual state variables: position {XI'B'T', YI'B'T', ZI'B'T'}, orientation {PSIB'T', THAB'T', PHIB'T'}, linear velocity {UB'B'T', VB'B'T', WB'B'T'}, rotational velocity {PB'B'T', QB'B'T', RB'B'T'}, linear velocity derivatives {DUB'B'T', DVB'B'T', DWB'B'T'}, rotational velocity derivatives {DPB'B'T', DQB'B'T', DRB'B'T'}, aircraft angles of attack and sideslip, altitude, and Mach number, all as a function of time. Time in the aircraft maneuver simulation will be designated as Time' in this section to avoid confusion with elapsed trajectory time (which is zero at first store motion) in the separation simulations. Generally, the aircraft motion quantities should be provided in tabular form which can be read right into the store separation simulation. Although it is still possible to calculate the translational and rotational velocities and velocity derivatives by properly differentiating the position and orientation terms (as is done in free-drop/flight data extraction programs), it is preferable to use the terms directly out of the aircraft simulation. If the aircraft simulation uses a true atmosphere model instead of a standard atmosphere model, the atmosphere model must also be provided. If the aircraft simulation uses an atmospheric winds model, then that model must also be provided for the store separation simulation.

Implementation of arbitrary aircraft motion into the store separation simulation requires primarily that the aircraft motion be redefined relative to the inertial-axis system which has been used to develop the store separation equations. In other words, the input aircraft motion quantities defined relative to the I' system which is earth-fixed must be transformed to quantities defined relative to the I system which has its origin at the cg of the active store at the instant of first motion and is translating at the aircraft flight velocity at that instant in the aircraft flight path direction at that instant. The transformation of the aircraft maneuver quantities is performed according to a multi-step process which will be outlined in the remainder of this section.

Step 1: Transform the input aircraft maneuver quantities to define the position and origin of the installed store cg (flight-, aircraft-, and pylon-axis origin) relative to the I' system.

The common origin of the aircraft-, flight-, and pylon-axis systems is assumed to be located at some fixed transfer distance relative to the aircraft body-axis origin (assuming that the cg-centered body axes for the aircraft can be considered not to move as fuel mass is burned during the short time of the separation trajectory). The motion of the aircraft-/flight-/pylon-axis origin can then be determined to be a combination of the motion of the aircraft body axes relative to aircraft inertial space and the motion of the installed store cg point relative to the aircraft cg point. Beginning with the relationship between the aircraft inertial positions of aircraft inertial, aircraft body, and the common origin of aircraft/flight/pylon axes:

$$\begin{vmatrix} XI'AI' \\ YI'AI' \\ ZI'AI' \end{vmatrix} = \begin{vmatrix} XI'B'T' \\ YI'B'T' \\ ZI'B'T' \end{vmatrix} + \begin{vmatrix} XI'AB' \\ YI'AB' \\ ZI'AB' \end{vmatrix} \quad (4.3.9.1)$$

where:

$$\begin{vmatrix} XI'AB' \\ YI'AB' \\ ZI'AB' \end{vmatrix} = [TRNB'T']^{-1} \begin{vmatrix} XB'AB' \\ YB'AB' \\ ZB'AB' \end{vmatrix} \quad (4.3.9.2)$$

Recall that for the constant Nz maneuvers of Section 4.3.1, the point at which the aircraft maneuver was defined was idealized to be coincident with the common origin of the aircraft, flight, and pylon axes - that idealization is removed in Eq. (4.3.9.1). Taking derivatives of both sides using the chain rule to get aircraft inertial velocity components of the aircraft, flight, and pylon trajectory-axis origin:

$$\frac{d}{dt} \begin{vmatrix} XI'AI' \\ YI'AI' \\ ZI'AI' \end{vmatrix} = \frac{d}{dt} \begin{vmatrix} XI'B'T' \\ YI'B'T' \\ ZI'B'T' \end{vmatrix} + \frac{d}{dt} [TRNB'T']^{-1} \begin{vmatrix} XB'AB' \\ YB'AB' \\ ZB'AB' \end{vmatrix} + [TRNB'T']^{-1} \frac{d}{dt} \begin{vmatrix} XB'AB' \\ YB'AB' \\ ZB'AB' \end{vmatrix} \quad (4.3.9.3)$$

or (noting that the derivative of the fixed transfer distance is zero):

$$\begin{vmatrix} UI'AI' \\ VI'AI' \\ WI'AI' \end{vmatrix} = \begin{vmatrix} UI'B'T' \\ VI'B'T' \\ WI'B'T' \end{vmatrix} + [TRNB'T']^{-1} [\tilde{\omega} B'B'T'] \begin{vmatrix} XB'AB' \\ YB'AB' \\ ZB'AB' \end{vmatrix} \quad (4.3.9.4)$$

Projecting to aircraft body-axis components by [TRNB'T']:

$$\begin{vmatrix} UB'AI' \\ VB'AI' \\ WB'AI' \end{vmatrix} = \begin{vmatrix} UB'B'T' \\ VB'B'T' \\ WB'B'T' \end{vmatrix} + [\tilde{\omega} B'B'T'] \begin{vmatrix} XB'AB' \\ YB'AB' \\ ZB'AB' \end{vmatrix} \quad (4.3.9.5)$$

A similar relation for accelerations can be developed by taking a second derivative of Eq. (4.3.9.4):

$$\begin{aligned} \frac{d}{dt} \begin{vmatrix} UI'AI' \\ VI'AI' \\ WI'AI' \end{vmatrix} &= \frac{d}{dt} \begin{vmatrix} UI'BI' \\ VI'BI' \\ WI'BI' \end{vmatrix} + \frac{d}{dt} [TRNB'T]^{-1} [\tilde{\omega}B'B'T] \begin{vmatrix} XB'AB' \\ YB'AB' \\ ZB'AB' \end{vmatrix} \\ &+ [TRNB'T]^{-1} \frac{d}{dt} [\tilde{\omega}B'B'T] \begin{vmatrix} XB'AB' \\ YB'AB' \\ ZB'AB' \end{vmatrix} + [TRNB'T]^{-1} [\tilde{\omega}B'B'T] \frac{d}{dt} \begin{vmatrix} XB'AB' \\ YB'AB' \\ ZB'AB' \end{vmatrix} \quad (4.3.9.6) \end{aligned}$$

or:

$$\begin{aligned} \begin{vmatrix} AXI'AI' \\ AYI'AI' \\ AZI'AI' \end{vmatrix} &= \begin{vmatrix} AXI'BT' \\ AYI'BT' \\ AZI'BT' \end{vmatrix} + [TRNB'T]^{-1} [\tilde{\omega}B'B'T] [\tilde{\omega}B'B'T] \begin{vmatrix} XB'AB' \\ YB'AB' \\ ZB'AB' \end{vmatrix} \\ &+ [TRNB'T]^{-1} [D\tilde{\omega}B'B'T] \begin{vmatrix} XB'AB' \\ YB'AB' \\ ZB'AB' \end{vmatrix} \quad (4.3.9.7) \end{aligned}$$

Project to body axis components by $[TRNB'T]$:

$$\begin{vmatrix} AXB'AI' \\ AYB'AI' \\ AZB'AI' \end{vmatrix} = \begin{vmatrix} AXB'BT' \\ AYB'BT' \\ AZB'BT' \end{vmatrix} + [\tilde{\omega}B'B'T] [\tilde{\omega}B'B'T] \begin{vmatrix} XB'AB' \\ YB'AB' \\ ZB'AB' \end{vmatrix} + [D\tilde{\omega}B'B'T] \begin{vmatrix} XB'AB' \\ XB'AB' \\ ZB'AB' \end{vmatrix} \quad (4.3.9.8)$$

This relation provides the interconnect between aircraft body-axis accelerations and the accelerations of the common origin of the flight, aircraft, and pylon trajectory-axis systems. The $\{AXB'BT'\}$ vector in Eq. (4.3.9.8) is obtained from the parameters provided from the external aircraft motion simulation using the relation:

$$\begin{vmatrix} AXB'B'I' \\ AYB'B'I' \\ AZB'B'I' \end{vmatrix} = \begin{vmatrix} DUB'B'I' \\ DV'B'B'I' \\ DWB'B'I' \end{vmatrix} + [\tilde{\omega}B'B'T] \begin{vmatrix} UB'B'I' \\ VB'B'I' \\ WB'B'I' \end{vmatrix} \quad (4.3.9.9)$$

which was formerly derived as Eq. (4.1.1.10).

Because the aircraft body (B') axis system and the aircraft store separation (A) axis system are parallel, the following relations are true:

$$\begin{aligned} PSIAI' &= PSIB'I' \\ THAAI' &= THAB'I' \\ PHIAI' &= PHIB'I' \\ PAAI' &= PB'B'I' \\ QAAI' &= QB'B'I' \\ RAAI' &= RB'B'I' \\ DPAAI' &= DPB'B'I' \\ DQAAI &= DQB'B'I' \\ DRAAI &= DRB'B'I' \end{aligned} \quad (4.3.9.10)$$

and Eqs. (4.3.9.5) and (4.3.9.8) can be rewritten as:

$$\begin{vmatrix} \text{UAAI}' \\ \text{VAAI}' \\ \text{WAAI}' \end{vmatrix} = \begin{vmatrix} \text{UB}'\text{B}'\text{T}' \\ \text{VB}'\text{B}'\text{T}' \\ \text{WB}'\text{B}'\text{T}' \end{vmatrix} + [\tilde{\omega}\text{B}'\text{B}'\text{T}'] \begin{vmatrix} \text{XB}'\text{AB}' \\ \text{YB}'\text{AB}' \\ \text{ZB}'\text{AB}' \end{vmatrix} \quad (4.3.9.11)$$

and

$$\begin{vmatrix} \text{AXAAI}' \\ \text{AYAAI}' \\ \text{AZAAI}' \end{vmatrix} = \begin{vmatrix} \text{AXB}'\text{B}'\text{T}' \\ \text{AYB}'\text{B}'\text{T}' \\ \text{AZB}'\text{B}'\text{T}' \end{vmatrix} + [\tilde{\omega}\text{B}'\text{B}'\text{T}'] [\tilde{\omega}\text{B}'\text{B}'\text{T}'] \begin{vmatrix} \text{XB}'\text{AB}' \\ \text{YB}'\text{AB}' \\ \text{ZB}'\text{AB}' \end{vmatrix} + [D\tilde{\omega}\text{B}'\text{B}'\text{T}'] \begin{vmatrix} \text{XB}'\text{AB}' \\ \text{XB}'\text{AB}' \\ \text{ZB}'\text{AB}' \end{vmatrix} \quad (4.3.9.12)$$

Step 2: Select the time in the supplied aircraft maneuver at which the store trajectory will start (Time'0).

Step 3: Interpolate certain aircraft state variables from Step 1 as a function of the selected release time to compute initial values for the store separation simulation.

The initial values will be designated by appending the suffix "0" to the end of the variable name. The interpolation should be performed using a high-order technique such as the Akima spline (Ref. 13) technique which has smooth derivatives in case linear and angular velocities and their derivatives are not provided from the aircraft motion simulation and have to be calculated from the provided positions and orientations. The following state variables need to be extracted at release time (Time'0) :

ALPHA0	XI'AI'0	PSIAI'0	UB'B'T'0
BETA0	YI'AI'0	THAAI'0	VB'B'T'0
ALTO	ZI'AI'0	PHIAI'0	WB'B'T'0

Recall that the store separation inertial axes are defined at the instant of store release and translate in the flight path direction at the instant of release at the aircraft velocity at the instant of release. The magnitude of the aircraft flight velocity at the instant of store release can then be calculated from:

$$U_{III}' = \sqrt{(\text{UB}'\text{B}'\text{T}'0^2 + \text{VB}'\text{B}'\text{T}'0^2 + \text{WB}'\text{B}'\text{T}'0^2)} \quad (4.3.9.13)$$

Equation (4.3.9.13) is written assuming that the air mass is not moving relative to the aircraft simulation inertial axes (i.e., no atmospheric winds). If winds were included in the aircraft simulation, then the velocities of the air mass relative to inertial axes would have to be removed from the aircraft velocities in Eq. (4.3.9.13) to get the velocity of the aircraft relative to the air mass (UIIW). Given the aircraft free-stream velocity and the altitude at launch, the aircraft Mach number at launch can be determined from the speed of sound obtained from standard atmospheric tables. If a non-standard atmosphere model was used in the aircraft simulation, other state variables from which Mach number can be calculated must be provided for the store simula-

tion. Note that the velocity of the aircraft as measured at the aircraft center of gravity is used in Eq. (4.3.9.14) to define the velocity of the store separation inertial axes relative to the inertial system used in the aircraft maneuver simulation. It should be pointed out that an alternate moving inertial system for store separation could be defined at the release instant, but using the velocity of the store carriage cg point on the aircraft (which is different from the aircraft cg velocity because of the rotation of the aircraft and the moment arms from store cg to aircraft cg). However, the alternate system leads to complications involving the definitions of the aircraft aerodynamic attack and sideslip angles [which are defined at the aircraft cg and are used subsequently in Eq. (4.3.9.15) below]. Also, one proposal for accounting for rotating aircraft aerodynamic effects is that computed aerodynamic increments in a swirling flow field be added to steady-state wind tunnel measurements at aircraft-referenced aerodynamic angles. Such a computational capability is more easily implemented if the initial aircraft velocity rather than the initial store velocity is used in the inertial-axis definition. The selected choice for the velocity of the inertial system leads to the rather unusual situation that the inertial axes are defined at the carriage cg of the active store but point in the direction of the time zero flight path of the aircraft cg and travel at the time zero aircraft cg velocity.

Step 4: Define a new inertial-axis system for the store separation simulations coincident with the aircraft flight path at the instant of release.

The orientation matrix for the aircraft axes relative to I' axes at the instant of release is:

$$[TRNAI'0] = [TRNx(PHIAI'0)] [TRNy(THAAI'0)] [TRNz(PSIAI'0)] \quad (4.3.9.14)$$

The orientation of the aircraft axes relative to the store separation inertial axes at the instant of release is:

$$[TRNAI0] = [TRNx(0.0)] [TRNy(ALPHA0)] [TRNz(-BETA0)] \quad (4.3.9.15)$$

Therefore the orientation of the store separation inertial axes relative to the aircraft-simulation inertial axes is:

$$[TRNII'] = [TRNAI0]^T [TRNAI'0] \quad (4.3.9.16)$$

Note that the orientation of the trajectory inertial axis system is fixed relative to the inertial system of the aircraft simulation since neither inertial system is allowed to rotate and the appended subscript can, therefore, be removed.

The heading, climb (-dive), and bank angles (PSIII', THAII', PHIII') of the store separation inertial flight path relative to the aircraft simulation inertial system can be extracted from the [TRNII'] matrix using the relations of Eq. (1.3.9), although heading is not important in most store separations.

Step 5: Redefine all aircraft motion parameters read in from the input tables relative to the store separation inertial axes.

These operations should be performed for every time value at which aircraft motion data are available. First, the aircraft simulation time is adjusted to map it to store separation time with time zero at first motion:

$$\text{Time}' = \text{Time} - \text{Time}'0 \quad (4.3.9.17)$$

The inertial components of the position of the aircraft axes relative to inertial axes are computed by projecting the I'-axis components of the change in position of aircraft axes relative to I' axes into I-axes components and then removing the offset term arising from the change in the store separation inertial axis position since first motion:

$$\begin{vmatrix} X_{IAI} \\ Y_{IAI} \\ Z_{IAI} \end{vmatrix} = [\text{TRNII}'] \left(\begin{vmatrix} X_{I'AI'} \\ Y_{I'AI'} \\ Z_{I'AI'} \end{vmatrix} - \begin{vmatrix} X_{I'AI'0} \\ Y_{I'AI'0} \\ Z_{I'AI'0} \end{vmatrix} - \begin{vmatrix} U_{III}' * \text{Time} \\ 0.0 \\ 0.0 \end{vmatrix} \right) \quad (4.3.9.18)$$

The orientation matrix for the aircraft axes at each time step relative to I' axes is:

$$[\text{TRNAI}'] = [\text{TRNx}(\text{PHIAI}')] [\text{TRNy}(\text{THAAI}')] [\text{TRNz}(\text{PSIAI}')] \quad (4.3.9.19)$$

The orientation matrix at each time step for the aircraft axes relative to trajectory inertial axes is:

$$[\text{TRNAI}] = [\text{TRNAI}'] [\text{TRNII}']^T \quad (4.3.9.20)$$

From which the modified Euler angles for the orientation of aircraft axes relative to inertial axes (PSIAI, THAAI, PHIAI) can be extracted at each time step using the relations of Eq. (1.3.9).

The aircraft-axis components of the velocity of aircraft axes relative to inertial axes are determined from the current velocity of the aircraft relative to I' axes minus the velocity of the store separation inertial axes relative to aircraft simulation inertial axes:

$$\begin{aligned} \begin{vmatrix} U_{AAI} \\ V_{AAI} \\ W_{AAI} \end{vmatrix} &= [\text{TRNAI}'] \begin{vmatrix} U_{I'AI} \\ V_{I'AI} \\ W_{I'AI} \end{vmatrix} = [\text{TRNAI}'] \left\{ \begin{vmatrix} U_{I'AI'} \\ V_{I'AI'} \\ W_{I'AI'} \end{vmatrix} - [\text{TRNII}']^T \begin{vmatrix} U_{III}' \\ 0.0' \\ 0.0 \end{vmatrix} \right\} \\ &= [\text{TRNAI}'] \left\{ [\text{TRNAI}']^T \begin{vmatrix} U_{AAI}' \\ V_{AAI}' \\ W_{AAI}' \end{vmatrix} - [\text{TRNAI}'0]^T \begin{vmatrix} U_{B'B'T'0} \\ V_{B'B'T'0} \\ W_{B'B'T'0} \end{vmatrix} \right\} \quad (4.3.9.21) \end{aligned}$$

Note that unlike the constant Nz maneuver, the {UAAI} vector is not necessarily zero at the instant of release because the initial velocity at the store and aircraft cg positions are not the same if the aircraft is rotating.

The aircraft rotational velocities relative to I axes and I' axes are identical because neither inertial axis system is rotating:

$$\begin{vmatrix} PAAI \\ QAAI \\ RAAI \end{vmatrix} = \begin{vmatrix} PAAI' \\ QAAI' \\ RAAI' \end{vmatrix} \quad (4.3.9.22)$$

Also because neither inertial axis system is accelerating:

$$\begin{vmatrix} AXAAI \\ AYAAI \\ AZAAI \end{vmatrix} = \begin{vmatrix} AXAAI' \\ AYAAI' \\ AZAAI' \end{vmatrix} \quad (4.3.9.23)$$

and:

$$\begin{vmatrix} DPAAI \\ DQAAI \\ DRAAI \end{vmatrix} = \begin{vmatrix} DPAAI' \\ DQAAI' \\ DRAAI' \end{vmatrix} \quad (4.3.9.24)$$

At this point all terms needed to define arbitrary motion of the aircraft trajectory axis origin relative to the store separation inertial axes have been defined. One last set of transformations is necessary to allow the arbitrary maneuver to be implemented into the store separation simulation. The simulation equations for the movement of the hook-axis system with a maneuvering aircraft as developed in Section 4.3.2 were generally written in terms of pylon-axis or flight-axis projections of the aircraft motion terms rather than aircraft-axis projections as developed in this section. However, noting that pylon and aircraft axes share a common origin and using the aircraft-to-pylon transformation matrix developed from the angles of Eq. (4.3.2.2), the arbitrary aircraft maneuver parameters can be rewritten as:

$$\begin{vmatrix} XIPI \\ YIPI \\ ZIPI \end{vmatrix} = \begin{vmatrix} XIAI \\ YIAI \\ ZIAI \end{vmatrix} = \begin{vmatrix} XIFI \\ YIFI \\ ZIFI \end{vmatrix} \quad (4.3.9.25)$$

$$\begin{vmatrix} UIFI \\ VIFI \\ WIFI \end{vmatrix} = \begin{vmatrix} UIPI \\ VIPI \\ WIPI \end{vmatrix} = [TRNAI]^T \begin{vmatrix} UAAI \\ VAAI \\ WAAI \end{vmatrix} \quad (4.3.9.26)$$

$$\begin{vmatrix} AXPPI \\ AYPPI \\ AZPPI \end{vmatrix} = [TRNPA] \begin{vmatrix} AXAAI \\ AYAAI \\ AZAAI \end{vmatrix} \quad (4.3.9.27)$$

$$[TRNPI] = [TRNPA] [TRNAI] \quad (4.3.9.28)$$

$$\begin{vmatrix} PPPI \\ QPPI \\ RPPI \end{vmatrix} = [TRNPA] \begin{vmatrix} PAAI \\ QAAI \\ RAAI \end{vmatrix} \quad (4.3.9.29)$$

$$\begin{vmatrix} DPPPI \\ DQPPI \\ DRPPI \end{vmatrix} = [TRNPA] \begin{vmatrix} DPAAI \\ DQAAI \\ DRAAI \end{vmatrix} \quad (4.3.9.30)$$

After each point in the input arbitrary aircraft trajectory has been transformed to the form of Eqs. (4.3.9.25) through (4.3.9.30) and stored as a new aircraft motion table, an interpolation routine (again Akima is preferred) can be used to retrieve the aircraft state variables required to evaluate the equations of Section 4.3.2 at each step in the store separation trajectory. (A smooth interpolation technique is required because the store separation time step may differ from the time step of the supplied aircraft maneuver simulation -- typically store separations are generated at extremely small time integration steps).

It should again be emphasized that this section has only addressed dynamic considerations involved in including arbitrary maneuvers in the equations of motion. Aerodynamic considerations associated with the store loads in a rapidly changing aircraft flow field will require more extensive study.

4.3.10 Strapdown Equations

The addition of an arbitrary aircraft maneuver capability into the store separation equations of motion introduces an added complication that there are now aircraft maneuver data available at negative time values describing what the aircraft was doing before the actual launch event. The equations for the store motion parameters which are required to keep the store "strapped down" to the aircraft prior to store launch are developed in this section. No actual time integration of the strapdown store motion properties is actually performed in the simulation (although the end result of such a solving of the store motion equations should be that the store stays with the aircraft during its maneuver). However, the strapdown equations can provide some important information about the design reaction loads which must be provided to keep the store attached to the aircraft before launch. In addition, inclusion of the store pre-launch motion information also allows more realistic graphics visualization of store motion relative to the aircraft.

At each before-launch time step in the aircraft maneuver simulation, the aircraft motion properties must first be transferred to the installed store center-of-gravity location according to the equations of Section 4.3.9. The store pre-launch motion characteristics can then be forced to match the motion variables of the carriage point on the aircraft according to the following relations.

Before launch the store cg position must translate with the aircraft, so that:

$$\begin{vmatrix} XIBI \\ YIBI \\ ZIBI \end{vmatrix} = \begin{vmatrix} XIFI \\ YIFI \\ ZIFI \end{vmatrix} \quad (4.3.10.1)$$

where the {XIFI} vector comes from the aircraft maneuver. Before launch the store must also rotate with the aircraft:

$$[\text{TRNBI}] = [\text{TRNCI}] \quad (4.3.10.2)$$

where $[\text{TRNCI}]$ also comes from the aircraft maneuver. Before launch the store translates with the aircraft velocity and (since the body-axis origin and the flight-axis origin are coincident before launch):

$$\begin{vmatrix} \text{UIBI} \\ \text{VIBI} \\ \text{WIBI} \end{vmatrix} = \begin{vmatrix} \text{UIFI} \\ \text{VIFI} \\ \text{WIFI} \end{vmatrix} \quad (4.3.10.3)$$

The body-axis components of the store velocity are obtained from Eq. (4.1.1.7). Before launch the store rotates with the aircraft angular velocity [see also initial condition Eq. (4.4.1.4)]:

$$\begin{vmatrix} \text{PBBI} \\ \text{QBBI} \\ \text{RBBI} \end{vmatrix} = [\text{TRNBP}] \begin{vmatrix} \text{PPPI} \\ \text{QPPI} \\ \text{RPPI} \end{vmatrix} = [\text{TRNBI}] [\text{TRNPI}]^T \begin{vmatrix} \text{PPPI} \\ \text{QPPI} \\ \text{RPPI} \end{vmatrix} \quad (4.3.10.4)$$

where both the $\{\text{PPPI}\}$ vector and the $[\text{TRNPI}]$ matrix come from the aircraft maneuver. Before launch the store accelerates with the aircraft and (since body and pylon axes have a common origin before launch):

$$\begin{vmatrix} \text{AXBBI} \\ \text{AYBBI} \\ \text{AZBBI} \end{vmatrix} = [\text{TRNBP}] \begin{vmatrix} \text{AXPPI} \\ \text{AYPPI} \\ \text{AZPPI} \end{vmatrix} \quad (4.3.10.5)$$

from which the $\{\text{DUBBI}\}$ vector can be obtained using Eq. (4.1.1.10). Finally, the angular velocity derivatives of the store must match those of the aircraft. Taking derivatives of Eq. (4.3.10.4):

$$\begin{vmatrix} \text{DPBBI} \\ \text{DQBBI} \\ \text{DRBBI} \end{vmatrix} = \frac{d}{dt} [\text{TRNBP}] \begin{vmatrix} \text{PPPI} \\ \text{QPPI} \\ \text{RPPI} \end{vmatrix} + [\text{TRNBP}] \begin{vmatrix} \text{DPPPI} \\ \text{DQPPI} \\ \text{DRPPI} \end{vmatrix} \quad (4.3.10.6)$$

But $[\text{TRNBP}]$ is constant before launch and Eq. (4.3.10.6) reduces to:

$$\begin{vmatrix} \text{DPBBI} \\ \text{DQBBI} \\ \text{DRBBI} \end{vmatrix} = [\text{TRNBP}] \begin{vmatrix} \text{DPPPI} \\ \text{DQPPI} \\ \text{DRPPI} \end{vmatrix} \quad (4.3.10.7)$$

Having now defined the major state variables of the body axes, the motion properties of the hook point (provided the $\{\text{XBBH}\}$ vector is defined) can be determined from Eqs. (4.1.2.10), (4.1.2.5), and (4.1.2.12).

This completes the definition of the strapdown kinematic properties. It is also possible as part of the strapdown section, however, to estimate the reaction loads required to enforce the

strapdown velocities and accelerations. Given the store acceleration from Eq. (4.3.10.5) and using the translational equations of motion from Eq. (4.1.1.6):

$$\begin{vmatrix} \Sigma F_{XB} \\ \Sigma F_{YB} \\ \Sigma F_{ZB} \end{vmatrix} = \begin{vmatrix} RXB \\ RYB \\ RZB \end{vmatrix} + \begin{vmatrix} FXB \\ FYB \\ FZB \end{vmatrix} = m \begin{vmatrix} AXBBI \\ AYBBI \\ AZBBI \end{vmatrix} \quad (4.3.10.8)$$

Before launch, however, the $\{FXB\}$ vector in Eq. (4.3.10.8) is made up of only an aerodynamic contribution and a store weight contribution (thrust and ejector forces are zero). Equation (4.3.10.8) can, therefore, be rewritten as:

$$\begin{aligned} \begin{vmatrix} RXB \\ RYB \\ RZB \end{vmatrix} + \begin{vmatrix} FXB_{AERO} \\ FYB_{AERO} \\ FZB_{AERO} \end{vmatrix} &= m \begin{vmatrix} AXBBI \\ AYBBI \\ AZBBI \end{vmatrix} - \begin{vmatrix} WXB \\ WYB \\ WZB \end{vmatrix} = m \begin{vmatrix} AXBBI \\ AYBBI \\ AZBBI \end{vmatrix} - [TRNBI] \begin{vmatrix} WXI \\ WYI \\ WZI \end{vmatrix} \\ &= m \begin{vmatrix} AXBBI \\ AYBBI \\ AZBBI \end{vmatrix} - [TRNBI] [TRNIE] \begin{vmatrix} 0.0 \\ 0.0 \\ WT \end{vmatrix} \end{aligned} \quad (4.3.10.9)$$

Equation (4.3.10.9) can be solved for the reaction loads required to keep the store attached to the aircraft as long as the aerodynamic loads on the store can be determined. Of course, for a store-separation motion simulation it is not necessary to determine the store aerodynamic loads (or the reaction forces) because the motion is already defined by the strapdown equations. It may be useful, however, to evaluate just the no-aero reaction load requirements. This can be accomplished by assuming zero aerodynamic forces in Eq. (4.3.10.9) (Note that this is an accurate assumption for pre-launch support loads on stores which are carried in closed weapons bays):

$$\begin{vmatrix} RXB_{INERTIA} \\ RYB_{INERTIA} \\ RZB_{INERTIA} \end{vmatrix} = m \begin{vmatrix} AXBBI \\ AYBBI \\ AZBBI \end{vmatrix} - \begin{vmatrix} WXB \\ WYB \\ WZB \end{vmatrix} \quad (4.3.10.10)$$

Equation (4.3.10.10) represents the reaction loads to which the store support structures must be designed in order to support the store inertia and weight during the maneuver. The reaction moments necessary to support the store inertia (again assuming no aerodynamic moments) can also be determined. First, the body-axis angular momentum and angular momentum derivatives at each pre-launch time step are determined from Eqs. (4.2.1.34) and (4.2.1.38). Then Eq. (4.2.2.43) [or (4.2.1.37)] can be rearranged to:

$$\begin{vmatrix} MXB \\ MYB \\ MZB \end{vmatrix}_{\text{about } B} + \begin{vmatrix} RLB \\ RMB \\ RNB \end{vmatrix} = [I]_{BB} \begin{vmatrix} DPBBI \\ DQBBI \\ DRBBI \end{vmatrix} + [\dot{\omega} BBI] \begin{vmatrix} HXBBI \\ HYBBI \\ HZBBI \end{vmatrix} + \begin{vmatrix} XBBH \\ YBBH \\ ZBBH \end{vmatrix} \times \begin{vmatrix} RXB \\ RYB \\ RZB \end{vmatrix} \quad (4.3.10.11)$$

For the pre-launch moment case, the $\{RLB\}$ vector is composed entirely of aerodynamic moments and if these are set to zero, the reaction moments are:

$$\begin{vmatrix} \text{RLB}_{\text{INERTIA}} \\ \text{RMB}_{\text{INERTIA}} \\ \text{RNB}_{\text{INERTIA}} \end{vmatrix} = [\mathbf{I}]_{\text{BB}} \begin{vmatrix} \text{DPBBI} \\ \text{DQBBI} \\ \text{DRBBI} \end{vmatrix} + [\tilde{\omega}_{\text{BBI}}] \begin{vmatrix} \text{HXBBI} \\ \text{HYBBI} \\ \text{HZBBI} \end{vmatrix} + \begin{vmatrix} \text{XBBH} \\ \text{YBBH} \\ \text{ZBBH} \end{vmatrix} \times \begin{vmatrix} \text{RXB} \\ \text{RYB} \\ \text{RZB} \end{vmatrix} \quad (4.3.10.12)$$

Note in Eq. (4.3.10.12) that if the {XBBH} vector is provided (and non-zero), strapdown reaction moments about the hook point are calculated; otherwise, moments about the store center of gravity are calculated.

4.4 INITIAL CONDITIONS FOR STORE SEPARATION TRAJECTORY SIMULATIONS

Because store separation simulations involve time integration they can be considered to be initial value problems and, in addition to the motion constraint boundary conditions must also have specified initial conditions. Mathematical descriptions for the initial conditions of a store released in free fall from a maneuvering aircraft are developed in Section 4.4.1. Initial conditions for a re-started (post-launch) trajectory are described in Section 4.4.2. Special cases in which initial conditions are specified relative to aircraft-fixed axes rather than inertial axes are then described in Section 4.4.3

4.4.1 Initial Conditions for Simulations from Carriage

Trajectories which are initiated from carriage positions on the aircraft must be initialized so that the store motion properties are consistent with the aircraft motion properties at the instant of release. Using the suffix "0" to denote the initial values, the following initial conditions can be defined for a simulation initiated at carriage.

The store body axes have not yet moved relative to inertial axes at first motion:

$$\begin{vmatrix} \text{XIBI0} \\ \text{YIBI0} \\ \text{ZIBI0} \end{vmatrix} = \begin{vmatrix} 0.0 \\ 0.0 \\ 0.0 \end{vmatrix} \quad (4.4.1.1)$$

The orientation of the body axes relative to inertial axes at first motion is a function of the store carriage attitude relative to the aircraft and the orientation of the aircraft relative to the flight path (because inertial and flight axes are coincident at the instant of first motion):

$$[\text{TRNBI0}] = [\text{TRNBA0}] \quad [\text{TRNAI0}] = [\text{TRNCA}] \quad [\text{TRNAI0}] = [\text{TRNCA}] \quad [\text{TRNAF}] = [\text{TRNCA}] \quad [\text{TRNy(ALPHAO)}] \quad [\text{TRNz(-BETA0)}] \quad (4.4.1.2)$$

At (and before) the instant of release the store is rigidly attached to the aircraft and must be translating at the aircraft velocity (the body-axis and flight-axis origins are coincident prior to release):

$$\begin{vmatrix} \text{UBBI0} \\ \text{VBBI0} \\ \text{WBBI0} \end{vmatrix} = [\text{TRNBI0}] \begin{vmatrix} \text{UIFI0} \\ \text{VIFI0} \\ \text{WIFI0} \end{vmatrix} \quad (4.4.1.3)$$

where $\{\text{UIFI0}\}$ comes from the aircraft maneuver (Section 4.3.1 or 4.3.8) and is zero for constant load factor maneuvers. At and before the instant of release, the store must also be rotating at the aircraft angular velocity:

$$\begin{vmatrix} \text{PBBI0} \\ \text{QBBI0} \\ \text{RBBI0} \end{vmatrix} = [\text{TRNBP0}] \begin{vmatrix} \text{PPPI0} \\ \text{QPPI0} \\ \text{RPPI0} \end{vmatrix} = [\text{TRNBI0}] [\text{TRNPI0}]^T \begin{vmatrix} \text{PPPI0} \\ \text{QPPI0} \\ \text{RPPI0} \end{vmatrix} \quad (4.4.1.4)$$

where $[\text{TRNPI0}]$ and $\{\text{PPPI0}\}$ are obtained from the aircraft maneuver (Section 4.3.1 or 4.3.8).

This completes the definition of initial conditions for standard simulations starting at the carriage point. The initial values are assigned to the store state variables before the first pass through the equation-of-motion/time integration procedures.

4.4.1.1 Initial Conditions for the Roll Structure of the Two-Body F-15 Pivot Model

For some complex pivot mechanisms such as the F-15 mechanism of Section 4.3.5, the store and pivot assemblies are modeled as two or more separate bodies. In such cases it is also necessary to initialize the state variables of the pivot assembly. In general, it can not be assumed that the state variables of the pivot structure can be initialized to the same values as the body structure state variables. This is especially true for an aircraft undergoing any type of rotational maneuver. At the release instant, for example, the initial accelerations at the body axis origin/store cg position and at the pivot axes will be different because of the different transfer distances from the aircraft rotation center. It is vitally important that the initial state values for the body and pivot structures be kinematically compatible, as, otherwise, the structures will tend to be pulled apart from one another as the simulation advances in time. Initialization of the second body in a two-body problem (in this case the roll structure of the F-15 pivot mechanism described in Section 4.3.5) will be described in the remainder of this section. The remainder of the equations in this section apply only to the F-15 two-body mechanism.

The initial orientation of the roll axes relative to inertial axes can be extracted from the initial orientation matrix for the body axes relative to carriage axes. First calculating $[\text{TRNBC0}]$ according to: [see Eq. (4.4.1.4)]

$$\begin{aligned} [\text{TRNBPO}] &= [\text{TRNBI0}] [\text{TRNPI0}]^T \\ [\text{TRNBC0}] &= [\text{TRNBI0}] [\text{TRNCI0}]^T \end{aligned} \quad (4.4.1.5)$$

The orientation angles for body axes relative to carriage axes (PSIBC0 , THABC0 , and PHIBC0) can then be extracted using the relations of Eq. (1.3.9). If it is assumed that all roll of the body axes occurs about the roll joint, then the initial angles for the roll axes relative to carriage axes are:

$$\begin{aligned} \text{PSIRC0} &= \text{PSIBC0} \\ \text{THARC0} &= \text{THABC0} \\ \text{PHIRC0} &= 0.0 \end{aligned} \quad (4.4.1.6)$$

The $[\text{TRNRC0}]$ matrix can then be built using the angles from Eq. (4.4.1.6) and the rotational transformation formula from Eq. (1.3.8). The initial orientation for roll axes is then given by:

$$[\text{TRNRI0}] = [\text{TRNRC0}] [\text{TRNCI0}] \quad (4.4.1.7)$$

The initial values for the $\{\text{URRI}\}$ vector are obtained by first rewriting Eq. (4.3.5.12) as:

$$\begin{vmatrix} \text{UBRI0} \\ \text{VBRI0} \\ \text{WBRI0} \end{vmatrix} = \begin{vmatrix} \text{UBBI0} \\ \text{VBBIO} \\ \text{WBBIO} \end{vmatrix} - [\tilde{\omega}] \begin{vmatrix} \text{XBBR} \\ \text{YBBR} \\ \text{ZBBR} \end{vmatrix} \quad (4.4.1.8)$$

Then:

$$\begin{vmatrix} \text{URRI0} \\ \text{VRRI0} \\ \text{WRRI0} \end{vmatrix} = [\text{TRNBR0}]^T \begin{vmatrix} \text{UBRI0} \\ \text{VBRI0} \\ \text{WBRI0} \end{vmatrix} \quad (4.4.1.9)$$

where $[\text{TRNBR0}]$ is obtained from:

$$[\text{TRNBR0}] = [\text{TRNBI0}] [\text{TRNRI0}]^T \quad (4.4.1.10)$$

The initial values for the terms in the $\{\text{PRRI}\}$ vector may be obtained from known initial values in the $\{\text{PBBI}\}$ and $\{\text{PPPI}\}$ vectors. First, noting that:

$$\begin{vmatrix} \text{PRBI0} \\ \text{QRBI0} \\ \text{RRBI0} \end{vmatrix} = \begin{vmatrix} \text{PRBR0} \\ \text{QRBR0} \\ \text{RRBR0} \end{vmatrix} + \begin{vmatrix} \text{PRRI0} \\ \text{QRRI0} \\ \text{RRRI0} \end{vmatrix} = [\text{TRNBR0}]^T \begin{vmatrix} \text{PBBI0} \\ \text{QBBI0} \\ \text{RBBI0} \end{vmatrix} \quad (4.4.1.11)$$

But since only roll occurs at the roll joint, the pitch and yaw rates of the body axes relative to roll axes must be zero:

$$\text{QRBR0} = \text{RRBR0} = 0.0 \quad (4.4.1.12)$$

Substituting Eq. (4.4.1.12) into Eq. (4.4.1.11) results in:

$$\begin{vmatrix} \text{PRBR0} + \text{PRRI0} \\ \text{QRRI0} \\ \text{RRRI0} \end{vmatrix} = \begin{vmatrix} \text{PRBI0} \\ \text{QRBI0} \\ \text{RRBI0} \end{vmatrix} \quad (4.4.1.13)$$

The QRRI0 and RRRI0 terms are defined by Eq. (4.4.1.13), but the PRRI0 term cannot be evaluated because PRBR0 is unknown. The value for PRRI0 can be deduced from the $\{\text{PPPI0}\}$ vector. Beginning with:

$$\begin{vmatrix} \text{PRCIO} \\ \text{QRCIO} \\ \text{RCPIO} \end{vmatrix} = \begin{vmatrix} \text{PRPIO} \\ \text{QRPIO} \\ \text{RRPIO} \end{vmatrix} = \begin{vmatrix} \text{PRRI0} \\ \text{QRRI0} \\ \text{RRRI0} \end{vmatrix} - \begin{vmatrix} \text{PRRC0} \\ \text{QRRC0} \\ \text{RRRC0} \end{vmatrix} = [\text{TRNRP0}] \begin{vmatrix} \text{PPPIO} \\ \text{QPPIO} \\ \text{RPPIO} \end{vmatrix} \quad (4.4.1.14)$$

and, since no roll occurs between carriage axes and roll axes:

$$\text{PRRC0} = 0.0 \quad (4.4.1.15)$$

Substituting into Eq. (4.4.1.14), the value for PRRI0 is:

$$\text{PRRI0} = \text{PRCI0} \quad (4.4.1.16)$$

The initial values are assigned to the store and roll structure state variables before the first pass through the equation-of-motion/time integration procedures.

4.4.2 Initial Conditions for Re-Started Simulations

Store simulations can also be started by initializing the primary state variables identified in the previous section using the results of another simulation. Such "post-launch" simulations are often performed for stores with deployable surfaces. The initial "launch" simulation may be performed using an aerodynamic model with stowed surfaces, for example, and the conditions at a particular time instant might be used to re-start a second simulation using a surface-deployed aerodynamic model. The initial time value must also be specified for a re-started simulation. Particular care must be taken in post-launch simulations to ensure that the effects of maneuvers are properly included in the initial angle and rate values. In simulations incorporating missile autopilots, initial values must also be provided for all time-dependent parameters in the autopilot model.

4.4.3 Initial Conditions for Simulations Started at End-of-Stroke or at Downrail Positions

An alternate method of trajectory initialization has been developed for simulations of the ejection of stores from weapons bays in wind tunnel trajectory studies. The alternate methodology is necessary because physical limitations of the wind tunnel support hardware often do not allow trajectories to be initialized at carriage within a bay because the support hardware cannot physically place the store model at the carriage position (often because of physical interferences of the store sting support with the back wall of the bay). In such cases, it is often necessary to initialize the wind tunnel trajectory simulations using conditions at some point external to the bay. Such problems also exist in some rail-launch simulation cases where it is desirable to initialize the trajectory with the missile at a downrail position. It is, of course, possible in such situations to perform computational "launch" simulations (which are not limited by test hardware) and then to initialize the wind tunnel "post-launch" runs with state values from the launches (as in Section 4.4.2). Unfortunately, if it is necessary to initialize wind tunnel simulations at a wide range of maneuver load factors, then separate off-line initial condition simulations at each load factor must be generated. As an approximation, however, it can be noted that although the initial velocities and angular velocities of the store relative to inertial space are highly variable, the conditions relative to the aircraft itself are relatively independent of the aircraft maneuver for many cases. For example, the downrail velocity of an AIM-9 type missile relative to the aircraft at the point where the middle hanger leaves the rail is about 80 ft/sec and is relatively independent of aircraft flight condition and maneuver load factor. Similarly, the vertical end-of-stroke velocity of an ejected store relative to the aircraft is also often a relatively maneuver-independent quantity. This

suggests that it might be desirable in some specialized cases to specify initial conditions using velocity and position terms for the store relative to some aircraft-fixed trajectory axes (such as carriage axes) rather than specifying the state variable directly relative to inertial axes. The equations for the conversion of input motion quantities defined relative to carriage axes to the standard input quantities defined relative to inertial axes (which are the state variables that are actually integrated in a motion simulation) are developed in this section.

It is assumed that the input initial condition variable provided to the simulation include the initial time, the initial orientation of the body axes relative to carriage axes [TRNBC0], the initial position of the body axes relative to carriage axes {XCBC0}, and the initial linear and angular velocities of the body relative to carriage axes {UCBC0} and {PCBC0}. For a downrail initialization, for instance, XCBC0 and UCBC0 might represent the downrail position and velocity of the store. For a simulation initialized at the ejector end of stroke, ZCBC0 and WCBC0 might represent the end of stroke position and velocity.

The orientation of the body axes relative to inertial axes at initialization is a function of the store initial attitude relative to carriage axes, and the initial orientation of carriage axes relative to inertial axes:

$$[TRNBI0] = [TRNBC0] [TRNCI0] \quad (4.4.3.1)$$

where [TRNCI0] comes from the aircraft maneuver (Section 4.3.1 for constant load factor maneuvers or Section 4.3.9 for arbitrary maneuvers). The inertial-axis components of the initial body position are:

$$\begin{vmatrix} XIBI0 \\ YIBI0 \\ ZIBI0 \end{vmatrix} = [TRNCI0]^{-1} \begin{vmatrix} XCBC0 \\ YCBC0 \\ ZCBC0 \end{vmatrix} + \begin{vmatrix} XIFI0 \\ YIFI0 \\ ZIFI0 \end{vmatrix} \quad (4.4.3.2)$$

where the {XIFI0} vector comes from the aircraft maneuver and it is noted that {XIFI} = {XICI} because flight and carriage axes have a common origin. The body-axis projections of the initial body inertial velocity are obtained from the velocity of the body relative to carriage axes and the velocity of the carriage axes (again flight and carriage origins are coincident) relative to inertial axes:

$$\begin{vmatrix} UBBIO \\ VBBIO \\ WBBIO \end{vmatrix} = [TRNBC0] \begin{vmatrix} UCBC0 \\ VCBC0 \\ WCBC0 \end{vmatrix} + [TRNBI0] \begin{vmatrix} UIFIO \\ VIFIO \\ WIFIO \end{vmatrix} \quad (4.4.3.3)$$

where {UIFIO} is defined in Section 4.3.1 or 4.3.8. Finally, the inertial rotational velocities are obtained from the rotational velocities of carriage axes relative to inertial and body axes relative to carriage:

$$\begin{vmatrix} PBBI0 \\ QBBI0 \\ RBBI0 \end{vmatrix} = [TRNBP0] \begin{vmatrix} PPPI0 \\ QPPI0 \\ RPPI0 \end{vmatrix} + [TRNBC0] \begin{vmatrix} PCBC0 \\ QCBC0 \\ RCBC0 \end{vmatrix} \quad (4.4.3.4)$$

where $\{PPPI0\}$ comes from the aircraft maneuver and it is noted that $\{PBCI0\} = \{PBPI0\}$.

5.0 DATA REDUCTION EQUATIONS FOR CALCULATION OF TRADITIONAL MOTION PROPERTIES FROM MEASUREMENTS OF FORWARD- AND AFT-MOUNTED ACCELEROMETERS

The data reduction equations for converting the output from instrumented free-drop tank models into positions and orientations and their corresponding velocities and accelerations are developed in this section. The data reduction equations are presented after Section 4.0 on the numerical equations of motion because some concepts used in equation-of-motion simulations are necessary for reducing the data from the instrumented models. Several different mixtures of instrumentation can be used to measure the rotational and translational accelerations of a free-drop model. The instrumentation selected for the first use of the instrumented model technique in a July 1994 drop test of releases of the F-22 fuel tank is assumed in the data reduction equations developed in this section. The F-22 tank instrumentation consists of forward- and aft-mounted three-axis (but not quite tri-axial) accelerometer packages and a single rotational rate sensor aligned with the longitudinal tank body axis. The selected instrumentation does not necessarily represent the optimum instrument configuration, but it was the one with the smallest mass then available (which is extremely important for dynamic scaling of an empty fuel tank) and all the instrumentation was readily available to support the tight schedule for the F-22 test. For the developments in this section, the designation "T" which formerly signified "Transducer" axis will be taken to mean "Tail" accelerometer axes and the new designation "N" will be used for "Nose" accelerometer axes. The equations are basically derived for the special case of idealized tri-axial Nose and Tail accelerometer packages but are then expanded to account for the six independent measurements where possible. Because of space limitations within the tank, both the forward and aft accelerometer packages were rotated 45 deg in roll relative to the tank body axes. The F-22 drop tank instrumentation axes are illustrated in Fig. 29.

The equations for linear and rotational transfer of measured accelerations from tail transducer axes to body axes for idealized "tri-axial" accelerometers were formerly developed as Eq. (3.0.8) of Section 3.0. If Eq. (3.0.8) is solved for $\{AXBBI\}$:

$$\begin{vmatrix} AXBBI \\ AYBBI \\ AZBBI \end{vmatrix} = [TRNTB]^{-1} \begin{vmatrix} AXTTI \\ AYTTI \\ AZTTI \end{vmatrix} - [\tilde{\omega}_{BBI}] [\tilde{\omega}_{BBI}] \begin{vmatrix} XBTB \\ YBTB \\ ZBTB \end{vmatrix} - [D\tilde{\omega}_{BBI}] \begin{vmatrix} XBTB \\ YBTB \\ ZBTB \end{vmatrix} \quad (5.0.1)$$

A similar equation can also be written for the Nose accelerometers:

$$\begin{vmatrix} AXBBI \\ AYBBI \\ AZBBI \end{vmatrix} = [TRNNB]^{-1} \begin{vmatrix} AXNNI \\ AYNNI \\ AZNNI \end{vmatrix} - [\tilde{\omega}_{BBI}] [\tilde{\omega}_{BBI}] \begin{vmatrix} XBNB \\ YBNB \\ ZBNB \end{vmatrix} - [D\tilde{\omega}_{BBI}] \begin{vmatrix} XBNB \\ YBNB \\ ZBNB \end{vmatrix}$$

(5.0.2)

Subtracting Eq. (5.0.1) from Eq. (5.0.2) and rearranging:

$$\begin{aligned}
 & -[\text{TRNNB}]^{-1} \begin{vmatrix} \text{AXNNI} \\ \text{AYNNI} \\ \text{AZNNI} \end{vmatrix} + [\text{TRNTB}]^{-1} \begin{vmatrix} \text{AXTTI} \\ \text{AYTTI} \\ \text{AZTTI} \end{vmatrix} \\
 & = [\tilde{\omega} \text{ BBI}] \begin{vmatrix} \text{XBTB} \\ \text{YBTB} \\ \text{ZBTB} \end{vmatrix} - [\tilde{\omega} \text{ BBI}] \begin{vmatrix} \text{XBNB} \\ \text{YBNB} \\ \text{ZBNB} \end{vmatrix} \\
 & \quad + [D\tilde{\omega} \text{ BBI}] \begin{vmatrix} \text{XBTB} \\ \text{YBTB} \\ \text{ZBTB} \end{vmatrix} - [D\tilde{\omega} \text{ BBI}] \begin{vmatrix} \text{XBNB} \\ \text{YBNB} \\ \text{ZBNB} \end{vmatrix} \\
 & = [\tilde{\omega} \text{ BBI}] \begin{vmatrix} \text{XBTB} - \text{XBNB} \\ \text{YBTB} - \text{YBNB} \\ \text{ZBTB} - \text{ZBNB} \end{vmatrix} + [D\tilde{\omega} \text{ BBI}] \begin{vmatrix} \text{XBTB} - \text{XBNB} \\ \text{YBTB} - \text{YBNB} \\ \text{ZBTB} - \text{ZBNB} \end{vmatrix} \\
 & = [\tilde{\omega} \text{ BBI}] \begin{vmatrix} \text{XBTN} \\ \text{YBTN} \\ \text{ZBTN} \end{vmatrix} + [D\tilde{\omega} \text{ BBI}] \begin{vmatrix} \text{XBTN} \\ \text{YBTN} \\ \text{ZBTN} \end{vmatrix} \tag{5.0.3}
 \end{aligned}$$

Recall, however, that an accelerometer does not sense the acceleration of gravity so that {AXNNI} and {AXTTI} are not actually measured:

$$\begin{vmatrix} \text{AXTTI} \\ \text{AYTTI} \\ \text{AZTTI} \end{vmatrix} = \begin{vmatrix} \text{AXMTTI} \\ \text{AYMTTI} \\ \text{AZMTTI} \end{vmatrix} + [\text{TRNTE}] \begin{vmatrix} 0.0 \\ 0.0 \\ \text{GG} \end{vmatrix} = \begin{vmatrix} \text{AXMTTI} \\ \text{AYMTTI} \\ \text{AZMTTI} \end{vmatrix} + [\text{TRNTB}] [\text{TRNBE}] \begin{vmatrix} 0.0 \\ 0.0 \\ \text{GG} \end{vmatrix} \tag{5.0.4}$$

and

$$\begin{vmatrix} \text{AXNNI} \\ \text{AYNNI} \\ \text{AZNNI} \end{vmatrix} = \begin{vmatrix} \text{AXMNNI} \\ \text{AYMNNI} \\ \text{AZMNNI} \end{vmatrix} + [\text{TRNNE}] \begin{vmatrix} 0.0 \\ 0.0 \\ \text{GG} \end{vmatrix} = \begin{vmatrix} \text{AXMNNI} \\ \text{AYMNNI} \\ \text{AZMNNI} \end{vmatrix} + [\text{TRNNB}] [\text{TRNBE}] \begin{vmatrix} 0.0 \\ 0.0 \\ \text{GG} \end{vmatrix} \tag{5.0.5}$$

Substituting Eqs. (5.0.4) and (5.0.5) into Eq. (5.0.3):

$$\begin{aligned}
 & -[\text{TRNNB}]^{-1} \begin{vmatrix} \text{AXMNNI} \\ \text{AYMNNI} \\ \text{AZMNNI} \end{vmatrix} - [\text{TRNBE}] \begin{vmatrix} 0.0 \\ 0.0 \\ \text{GG} \end{vmatrix} \\
 & + [\text{TRNTB}]^{-1} \begin{vmatrix} \text{AXMTTI} \\ \text{AYMTTI} \\ \text{AZMTTI} \end{vmatrix} + [\text{TRNBE}] \begin{vmatrix} 0.0 \\ 0.0 \\ \text{GG} \end{vmatrix} \tag{5.0.6}
 \end{aligned}$$

$$\begin{aligned}
 &= -[\text{TRNNB}]^{-1} \begin{vmatrix} \text{AXMNNI} \\ \text{AYMNNI} \\ \text{AZMNNI} \end{vmatrix} + [\text{TRNTB}]^{-1} \begin{vmatrix} \text{AXMTTI} \\ \text{AYMTTI} \\ \text{AZMTTI} \end{vmatrix} \\
 &= [\tilde{\omega} \text{BBI}] [\tilde{\omega} \text{BBI}] \begin{vmatrix} \text{XBTN} \\ \text{YBTN} \\ \text{ZBTN} \end{vmatrix} + [\text{D}\tilde{\omega} \text{BBI}] \begin{vmatrix} \text{XBTN} \\ \text{YBTN} \\ \text{ZBTN} \end{vmatrix}
 \end{aligned}$$

Accelerometers are normally calibrated for output in units of g's rather than ft/sec². Defining a new term GAXM to mean AX measured in g's:

$$\{GAXMTTI\} = \{AXMTTI\} / 32.174 \text{ and } \{GAXMNNI\} = \{AXMNNI\} / 32.174 \quad (5.0.7)$$

and substituting into Eq. (5.0.6) yields the final form of the data reduction equations for tri-axial accelerometers:

$$\begin{aligned}
 &- 32.174 [\text{TRNNB}]^{-1} \begin{vmatrix} \text{GAXMNNI} \\ \text{GAYMNNI} \\ \text{GAZMNNI} \end{vmatrix} + 32.174 [\text{TRNTB}]^{-1} \begin{vmatrix} \text{GAXMTTI} \\ \text{GAYMTTI} \\ \text{GAZMTTI} \end{vmatrix} \\
 &= [\tilde{\omega} \text{BBI}] [\tilde{\omega} \text{BBI}] \begin{vmatrix} \text{XBTN} \\ \text{YBTN} \\ \text{ZBTN} \end{vmatrix} + [\text{D}\tilde{\omega} \text{BBI}] \begin{vmatrix} \text{XBTN} \\ \text{YBTN} \\ \text{ZBTN} \end{vmatrix} \quad (5.0.8)
 \end{aligned}$$

Note that the terms involving [TRNBE] and the gravity vector drop out of Eq. (5.0.8) so that the vector equation represents three scalar equations in six unknowns (<{PBBI, QBBI, RBBI} and {DPBBI, DQBBI, DRBBI}). Given the measured accelerations at each time step, Eqs. (5.0.8) can be solved for one of the unknown vectors only if the values of the other vector are known. Note, however, that the two unknown vectors are related to one another because the first vector is the integral of the second. This means that the equations can be solved for the angular velocity derivatives at any time step provided the velocity derivatives from previous time steps are integrated to determine the angular velocities at that time step. The needed integration process is exactly analogous to integration of the equations of motion in a wind tunnel simulation.

It is undesirable to solve Eqs. (5.0.8) directly for DPBBI, however, because the nose and tail accelerometers are not positioned at significant distances from the tank longitudinal body axis and the corresponding mathematical problem is not well posed because of the small moment arms. For this reason a separate roll rate sensor which measures PBBI is mounted within the tank in addition to the Nose and Tail accelerometer packages. The measured roll rate must be differentiated to determine DPBBI for use in evaluating Eqs. (5.0.8). Given the value of DPBBI and the entire rotational rate vector <{PBBI, QBBI, RBBI}, Eq. (5.0.8) can then be easily solved for DQBBI and DRBBI at each time step. After defining temporary parameters:

$$\begin{vmatrix} \text{AXMBTI} \\ \text{AYMBTI} \\ \text{AZMBTI} \end{vmatrix} = 32.174 [\text{TRNTB}]^{-1} \begin{vmatrix} \text{GAXMTTI} \\ \text{GAYMTTI} \\ \text{GAZMTTI} \end{vmatrix} \quad (5.0.9)$$

$$\begin{vmatrix} AXMBNI \\ AYMBNI \\ AZMBNI \end{vmatrix} = 32.174 [TRNNB]^{-1} \begin{vmatrix} GAXMNNI \\ GAYMNNI \\ GAZMNNI \end{vmatrix} \quad (5.0.10)$$

and

$$\begin{vmatrix} OOXBTN \\ OYOYBTN \\ OOZBTN \end{vmatrix} = [\tilde{\omega} BBI] \begin{vmatrix} XBTN \\ YBTN \\ ZBTN \end{vmatrix} \quad (5.0.11)$$

Equations (5.0.8) can then be expressed as:

$$\begin{aligned} - \begin{vmatrix} AXMBNI \\ AYMBNI \\ AZMBNI \end{vmatrix} + \begin{vmatrix} AXMBTI \\ AYMBTI \\ AZMBTI \end{vmatrix} - \begin{vmatrix} OOXBTN \\ OYOYBTN \\ OOZBTN \end{vmatrix} &= [D\tilde{\omega} BBI] \begin{vmatrix} XBTN \\ YBTN \\ ZBTN \end{vmatrix} \\ &= \begin{bmatrix} 0 & -DRBBI & DQBBI \\ DRBBI & 0 & -DPBBI \\ -DQBBI & DPBBI & 0 \end{bmatrix} \begin{vmatrix} XBTN \\ YBTN \\ ZBTN \end{vmatrix} \end{aligned} \quad (5.0.12)$$

Which can be solved for DQBBI and DRBBI as:

$$DRBBI = (-AYMBNI + AYMBTI - OYOYBTN + DPBBI*ZBTN) / XBTN \quad (5.0.13)$$

and:

$$DQBBI = -(-AZMBNI + AZMBTI - OOZBTN - DPBBI*YBTN) / XBTN \quad (5.0.14)$$

Only one angular rate sensor is used to measure the body roll rate to minimize weight of the instrumentation. Because of this, great care must be taken that it be as closely aligned with the store longitudinal body axis as possible in order to obtain an accurate measurement of PBBI. In the data reduction equations, the roll rate must, therefore, be assumed to be measured without misalignment. This is, of course, not the case with the nose and tail accelerometers because all three orthogonal components are measured and an interaction matrix may be included in the instrument calibration to account for misalignment. Careful physical alignment should be adequate for the roll sensor.

Up to this point, the data reduction equations have been developed for the special case of tri-axial nose and tail accelerometer packages. In the actual telemetry model, three separate linear accelerometers mounted to forward and aft cubic mounting blocks to ensure orthogonality were used for the measurements. Each accelerometer was, therefore, mounted at slightly different positions within the body and (at the small size of the drop model) the position offsets could not be ignored. To accommodate the finite position offsets, Eqs. (5.0.8) (and the equations leading up to them) must be rewritten for each pair of nose/tail accelerometers individually. For the nose and tail accelerometers which are aligned with the body longitudinal axis:

$$\begin{aligned}
 & -32.174 [\text{TRNNx}B]^{-1} \begin{vmatrix} GAXMNxNxI \\ GAYMNxNxI \\ GAZMNxNxI \end{vmatrix} + 32.174 [\text{TRNTx}B]^{-1} \begin{vmatrix} GAXMTxTxI \\ GAYMTxTxI \\ GAZMTxTxI \end{vmatrix} \\
 & = [\tilde{\omega} \text{ BBI}] [\tilde{\omega} \text{ BBI}] \begin{vmatrix} XBTxNx \\ YBTxNx \\ ZBTxNx \end{vmatrix} + [D\tilde{\omega} \text{ BBI}] \begin{vmatrix} XBTxNx \\ YBTxNx \\ ZBTxNx \end{vmatrix} \quad (5.0.15)
 \end{aligned}$$

Note in Eq. (5.0.15) that separate T and N axis systems are specified for the positions of the "x" accelerometers. Note also that the "Y" and "Z" components of the acceleration are shown in italics because single accelerometers aligned with the "x" axes of the Tx and Nx systems would not measure y and z components. Equations (5.0.8) must also be written for the separate "y" and "z" accelerometers:

$$\begin{aligned}
 & -32.174 [\text{TRNNy}B]^{-1} \begin{vmatrix} GAXMNyNyI \\ GAYMNyNyI \\ GAZMNyNyI \end{vmatrix} + 32.174 [\text{TRNTy}B]^{-1} \begin{vmatrix} GAXMTyTyI \\ GAYMTyTyI \\ GAZMTyTyI \end{vmatrix} \\
 & = [\tilde{\omega} \text{ BBI}] [\tilde{\omega} \text{ BBI}] \begin{vmatrix} XBTyNy \\ YBTyNy \\ ZBTyNy \end{vmatrix} + [D\tilde{\omega} \text{ BBI}] \begin{vmatrix} XBTyNy \\ YBTyNy \\ ZBTyNy \end{vmatrix} \quad (5.0.16)
 \end{aligned}$$

and:

$$\begin{aligned}
 & -32.174 [\text{TRNNz}B]^{-1} \begin{vmatrix} GAXMNzNzI \\ GAYMNzNzI \\ GAZMNzNzI \end{vmatrix} + 32.174 [\text{TRNTz}B]^{-1} \begin{vmatrix} GAXMTzTzI \\ GAYMTzTzI \\ GAZMTzTzI \end{vmatrix} \\
 & = [\tilde{\omega} \text{ BBI}] [\tilde{\omega} \text{ BBI}] \begin{vmatrix} XBTzNz \\ YBTzNz \\ ZBTzNz \end{vmatrix} + [D\tilde{\omega} \text{ BBI}] \begin{vmatrix} XBTzNz \\ YBTzNz \\ ZBTzNz \end{vmatrix} \quad (5.0.17)
 \end{aligned}$$

Equations (5.0.15), (5.0.16), and (5.0.17) can then be combined into a single large matrix equation:

$$\begin{array}{c}
 -32.174 \quad \left[\begin{array}{cccccc} 0 & 0 & 0 & 0 & 0 & 0 \\ [TRNNx_B]^{-1} & 0 & 0 & 0 & 0 & 0 \\ & 0 & 0 & 0 & 0 & 0 \\ 0 & 0 & 0 & 0 & 0 & 0 \\ 0 & 0 & 0 & [TRNNy_B]^{-1} & 0 & 0 \\ 0 & 0 & 0 & 0 & 0 & 0 \\ 0 & 0 & 0 & 0 & 0 & 0 \\ 0 & 0 & 0 & 0 & 0 & 0 \\ 0 & 0 & 0 & 0 & 0 & 0 \end{array} \right] \quad \left| \begin{array}{l} GAXMNxNxI \\ GAYMNxNxI \\ GAZMNxNxI \\ GAXMNyNyI \\ GAYMNyNyI \\ GAZMNyNyI \\ GAXMNzNzI \\ GAYMNzNzI \\ GAZMNzNzI \end{array} \right. \\ +32.174 \quad \left[\begin{array}{cccccc} 0 & 0 & 0 & 0 & 0 & 0 \\ [TRNNx_B]^{-1} & 0 & 0 & 0 & 0 & 0 \\ 0 & 0 & 0 & 0 & 0 & 0 \\ 0 & 0 & 0 & 0 & 0 & 0 \\ 0 & 0 & 0 & [TRNNy_B]^{-1} & 0 & 0 \\ 0 & 0 & 0 & 0 & 0 & 0 \\ 0 & 0 & 0 & 0 & 0 & 0 \\ 0 & 0 & 0 & 0 & 0 & 0 \\ 0 & 0 & 0 & 0 & 0 & 0 \end{array} \right] \quad \left| \begin{array}{l} GAXMTxTxI \\ GAYMTxTxI \\ GAZMTxTxI \\ GAXMTyTyI \\ GAYMTyTyI \\ GAZMTyTyI \\ GAXMTzTzI \\ GAYMTzTzI \\ GAZMTzTzI \end{array} \right. \\ = \quad \left[\begin{array}{cccccc} 0 & 0 & 0 & 0 & 0 & 0 \\ [\tilde{\omega}BBI]^2 & 0 & 0 & 0 & 0 & 0 \\ & 0 & 0 & 0 & 0 & 0 \\ 0 & 0 & 0 & 0 & 0 & 0 \\ 0 & 0 & 0 & [\tilde{\omega}BBI]^2 & 0 & 0 \\ 0 & 0 & 0 & 0 & 0 & 0 \\ 0 & 0 & 0 & 0 & 0 & 0 \\ 0 & 0 & 0 & 0 & 0 & 0 \end{array} \right] \quad \left| \begin{array}{l} XBTxNx \\ YBTxNx \\ ZBTxNx \\ XBTyNy \\ YBTyNy \\ ZBTyNy \\ XBTzNz \\ YBTzNz \\ ZBTzNz \end{array} \right. \\ + \quad \left[\begin{array}{cccccc} 0 & 0 & 0 & 0 & 0 & 0 \\ [D\tilde{\omega}BBI] & 0 & 0 & 0 & 0 & 0 \\ & 0 & 0 & 0 & 0 & 0 \\ 0 & 0 & 0 & 0 & 0 & 0 \\ 0 & 0 & 0 & [D\tilde{\omega}BBI] & 0 & 0 \\ 0 & 0 & 0 & 0 & 0 & 0 \\ 0 & 0 & 0 & 0 & 0 & 0 \\ 0 & 0 & 0 & 0 & 0 & 0 \end{array} \right] \quad \left| \begin{array}{l} XBTxNx \\ YBTxNx \\ ZBTxNx \\ XBTyNy \\ YBTyNy \\ ZBTyNy \\ XBTzNz \\ YBTzNz \\ ZBTzNz \end{array} \right. \end{array} \quad (5.0.18)$$

At this point, the expressions on the left of the equality in Eq. (5.0.18) cannot be evaluated because the italicized acceleration terms were not actually measured. An approximation must, therefore, be made. The closest approximation to the italicized non-measured values is, of

course, the nearest available measurement from the accelerometer which is aligned in the proper direction, thus: $GAYMTxTxI \sim GAYMTyTyI$, $GAZMTxTxI \sim GAZMTzTzI$, etc. When this substitution is made, the system becomes:

$$\begin{array}{l}
 \begin{array}{c}
 \boxed{\begin{array}{cccccc} 0 & 0 & 0 & 0 & 0 & 0 \\ [TRNNx_B]^{-1} & 0 & 0 & 0 & 0 & 0 \\ & 0 & 0 & 0 & 0 & 0 \\ 0 & 0 & 0 & & & 0 \\ 0 & 0 & 0 & [TRNNy_B]^{-1} & 0 & 0 \\ 0 & 0 & 0 & & 0 & 0 \\ 0 & 0 & 0 & 0 & 0 & 0 \\ 0 & 0 & 0 & 0 & 0 & [TRNNz_B]^{-1} \\ 0 & 0 & 0 & 0 & 0 & 0 \end{array}} \quad \begin{array}{l} GAXMNxNxI \\ GAYMNyNyI \\ GAZMNsNzI \\ GAXMNxNxI \\ GAYMNyNyI \\ GAZMNsNzI \\ GAXMNxNxI \\ GAYMNyNyI \\ GAZMNsNzI \end{array} \\
 - 32.174
 \end{array} \\
 \begin{array}{c}
 \boxed{\begin{array}{cccccc} 0 & 0 & 0 & 0 & 0 & 0 \\ [TRNNx_B]^{-1} & 0 & 0 & 0 & 0 & 0 \\ & 0 & 0 & 0 & 0 & 0 \\ 0 & 0 & 0 & & & 0 \\ 0 & 0 & 0 & [TRNNy_B]^{-1} & 0 & 0 \\ 0 & 0 & 0 & & 0 & 0 \\ 0 & 0 & 0 & 0 & 0 & 0 \\ 0 & 0 & 0 & 0 & 0 & [TRNNz_B]^{-1} \\ 0 & 0 & 0 & 0 & 0 & 0 \end{array}} \quad \begin{array}{l} GAXMTxTxI \\ GAYMTyTyI \\ GAZMTzTzI \\ GAXMTxTxI \\ GAYMTyTyI \\ GAZMTzTzI \\ GAXMTxTxI \\ GAYMTyTyI \\ GAZMTzTzI \end{array} \\
 + 32.174
 \end{array} \\
 = \begin{array}{c}
 \boxed{\begin{array}{cccccc} 0 & 0 & 0 & 0 & 0 & 0 \\ [\tilde{\omega}BBI]^2 & 0 & 0 & 0 & 0 & 0 \\ & 0 & 0 & 0 & 0 & 0 \\ 0 & 0 & 0 & & & 0 \\ 0 & 0 & 0 & [\tilde{\omega}BBI]^2 & 0 & 0 \\ 0 & 0 & 0 & & 0 & 0 \\ 0 & 0 & 0 & 0 & 0 & 0 \\ 0 & 0 & 0 & 0 & 0 & [\tilde{\omega}BBI]^2 \\ 0 & 0 & 0 & 0 & 0 & 0 \end{array}} \quad \begin{array}{l} XBTxNx \\ YBTxNx \\ ZBTxNx \\ XBTyNy \\ YBTyNy \\ ZBTyNy \\ XBTzNz \\ YBTzNz \\ ZBTzNz \end{array} \\
 + \begin{array}{c}
 \boxed{\begin{array}{cccccc} 0 & 0 & 0 & 0 & 0 & 0 \\ [D\tilde{\omega}BBI] & 0 & 0 & 0 & 0 & 0 \\ & 0 & 0 & 0 & 0 & 0 \\ 0 & 0 & 0 & & & 0 \\ 0 & 0 & 0 & [D\tilde{\omega}BBI] & 0 & 0 \\ 0 & 0 & 0 & & 0 & 0 \\ 0 & 0 & 0 & 0 & 0 & 0 \\ 0 & 0 & 0 & 0 & 0 & [D\tilde{\omega}BBI] \\ 0 & 0 & 0 & 0 & 0 & 0 \end{array}} \quad \begin{array}{l} XBTxNx \\ YBTxNx \\ ZBTxNx \\ XBTyNy \\ YBTyNy \\ ZBTyNy \\ XBTzNz \\ YBTzNz \\ ZBTzNz \end{array}
 \end{array}
 \end{array}
 \tag{5.0.19}$$

where the italics have been left in place to indicate when an available measurement has been substituted for a true value. Errors associated with such an approximation are sometimes referred to as finite position errors, but should be relatively small since the three accelerometers at the nose and tail positions are as closely spaced to one another as possible. An examination of Eq. (5.0.19) reveals that (with the approximate substitution) the system is now over determined with respect to the measured accelerations, i.e., nine equations are not necessary when only three acceleration measurements are available. The entire system can be simplified by selecting only the first, fifth, and last equations in the system. In so doing the system reduces to:

$$\begin{aligned}
 -32.174 & \begin{vmatrix} \text{TRNNxB}(1,1) & \text{TRNNxB}(2,1) & \text{TRNNxB}(3,1) \\ \text{TRNNyB}(1,2) & \text{TRNNyB}(2,2) & \text{TRNNyB}(3,2) \\ \text{TRNNzB}(1,3) & \text{TRNNzB}(2,3) & \text{TRNNzB}(3,3) \end{vmatrix} \begin{vmatrix} \text{GAXMNxNxI} \\ \text{GAYMNyNyI} \\ \text{GAZMNgNzI} \end{vmatrix} \\
 +32.174 & \begin{vmatrix} \text{TRNTxB}(1,1) & \text{TRNTxB}(2,1) & \text{TRNTxB}(3,1) \\ \text{TRNTyB}(1,2) & \text{TRNTyB}(2,2) & \text{TRNTyB}(3,2) \\ \text{TRNTzB}(1,3) & \text{TRNTzB}(2,3) & \text{TRNTzB}(3,3) \end{vmatrix} \begin{vmatrix} \text{GAXMTxTxI} \\ \text{GAYMTyTyI} \\ \text{GAZMTzTzI} \end{vmatrix} \\
 & = [\tilde{\omega} \text{ BBI}] [\tilde{\omega} \text{ BBI}] \begin{vmatrix} \text{XBTxNx} \\ \text{YBTyNy} \\ \text{ZBTzNz} \end{vmatrix} + [\text{D} \tilde{\omega} \text{ BBI}] \begin{vmatrix} \text{XBTxNx} \\ \text{YBTyNy} \\ \text{ZBTzNz} \end{vmatrix}
 \end{aligned} \tag{5.0.20}$$

Note that the matrices applied to the measured acceleration readings in Eq. (5.0.20) are not traditional rotational transformations, because each row contains terms associated with a different accelerometer axis system. The terms in the Eq. (5.0.20) transformations must be determined by a process of calibration. The calibration for the accelerometer packages is analogous to the process used to calibrate strain-gage balance systems for use in measuring forces and moments in more-traditional wind tunnel testing and is described in Ref. 14. In simplified terms, calibration for the accelerometer packages is accomplished by applying known accelerations in known directions to the store just as force balance calibration is accomplished by applying known forces to the store. In actual application, it is not even necessary to convert the measured accelerometer data to units of g's as specified in Eq. (5.0.20) as the excitation voltages, biases, and scale factors for each accelerometer can also be empirically included within the calibration matrices. Using calibration matrices, Eq. (5.0.20) can be written in final form as:

$$\begin{aligned}
 -32.174 [\text{CTRNNB}]^{-1} & \begin{vmatrix} \text{CAXMNxNxI} \\ \text{CAYMNyNyI} \\ \text{CAZMNgNzI} \end{vmatrix} + 32.174 [\text{CTRNTB}]^{-1} \begin{vmatrix} \text{CAXMTxTxI} \\ \text{CAYMTyTyI} \\ \text{CAZMTzTzI} \end{vmatrix} \\
 & = -32.174 \begin{vmatrix} \text{GAXMBNxI} \\ \text{GAYMBNyI} \\ \text{GAZMBNzI} \end{vmatrix} + 32.174 \begin{vmatrix} \text{GAXMBTxI} \\ \text{GAYMBTyI} \\ \text{GAZMBTzI} \end{vmatrix} = - \begin{vmatrix} \text{AXMBNxI} \\ \text{AYMBNyI} \\ \text{AZMBNzI} \end{vmatrix} + \begin{vmatrix} \text{AXMBTxI} \\ \text{AYMBTyI} \\ \text{AZMBTzI} \end{vmatrix} \\
 & = [\tilde{\omega} \text{ BBI}] [\tilde{\omega} \text{ BBI}] \begin{vmatrix} \text{XBTxNx} \\ \text{YBTyNy} \\ \text{ZBTzNz} \end{vmatrix} + [\text{D} \tilde{\omega} \text{ BBI}] \begin{vmatrix} \text{XBTxNx} \\ \text{YBTyNy} \\ \text{ZBTzNz} \end{vmatrix}
 \end{aligned} \tag{5.0.21}$$

where the CAXMNNI and CAXMTTI terms denote raw digital counts from the telemetry packages and the calibrated transformations, $[CTRNNB]^{-1}$ and $[CTRNTB]^{-1}$, include the matrices from Eq. (5.0.20) and the conversions from digital counts of transmitted output to g's. Finally, Eqs. (5.0.21) can then be solved for DQBBI and DRBBI as:

$$DRBBI = (-AYMBNyI + AYMBTyI - OGYBTN + DPBBI * ZBTzNz) / XBTxNx \quad (5.0.22)$$

and:

$$DQBBI = -(-AZMBNzI + AZMBTzI - OOZBTN - DPBBI * YBTyNy) / XBTxNx \quad (5.0.23)$$

Where Eq. (5.0.11) is rewritten for the non-triaxial accelerometers as:

$$\begin{vmatrix} OOXBTN \\ OGYBTN \\ OOZBTN \end{vmatrix} = [\tilde{\omega} BBI] [\tilde{\omega} BBI] \begin{vmatrix} XBTxNx \\ YBTyNy \\ ZBTzNz \end{vmatrix} \quad (5.0.24)$$

This completes the derivation of the primary data reduction equations for the telemetry model.

The roll rate sensor and the six accelerometers transmit measured, encoded information from the tank at each data-cycle step of the instrument package (currently 10,000 samples per sec). The data are received, decoded, and stored directly to memory of the data acquisition computer (a 486 PC). After all the data for a particular drop are received, lab calibrations on the instrumentation are applied to the raw digital data to determine the Time, PBBI, {CAXMNNI}, and {CAXMTTI} values. At this point, post-drop data reduction of the data can begin as outlined in the remainder of this section.

Some filtering of the measured data such as removal of low-frequency "tones" near the structural frequencies of the drop tank are accomplished by the instrumentation system. Additional filtering of the raw data to eliminate unwanted "noise" may then be performed before final data reduction. When the final raw data are available, the measured body-axis roll rate (PBBI) as a function of time is differentiated using the Akima spline technique to determine roll velocity derivatives (DPBBI) as a function of time during the drop. The accelerometer data are then used in an iterative equation-of-motion solution which is analogous to the integration process used in wind tunnel and off-line simulations. Beginning with initial values of the {UBBI}, {PBBI}, and {XIBI} vectors, the initial DPBBI value from the Akima spline fit, and the initial [TRNBI] matrix, Eqs. (5.0.22) and (5.0.23) are solved for the values of DQBBI and DRBBI at the first time instant. Given the initial {PBBI} and {DPBBI} vectors at that time instant, Eqs. (5.0.1) can then be rewritten to allow for non-triaxial accelerometers and then solved for the accelerations of the body axis origin {AXBBI}:

$$\begin{aligned}
 \begin{vmatrix} AXBBI \\ AYBBI \\ AZBBI \end{vmatrix} &= \begin{vmatrix} AXMBTxI \\ AYMBTxI \\ AZMBTxI \end{vmatrix} - [\tilde{\omega} BBI] [\tilde{\omega} BBI] \begin{vmatrix} XBTxB \\ YBTxB \\ ZBTxB \end{vmatrix} - [D\tilde{\omega} BBI] \begin{vmatrix} XBTxB \\ YBTxB \\ ZBTxB \end{vmatrix} \\
 &\quad + [TRNBE] \begin{vmatrix} 0.0 \\ 0.0 \\ GG \end{vmatrix} \\
 \begin{vmatrix} AXBBI \\ AYBBI \\ AZBBI \end{vmatrix} &= \begin{vmatrix} AXMBTyI \\ AYMBTyI \\ AZMBTyI \end{vmatrix} - [\tilde{\omega} BBI] [\tilde{\omega} BBI] \begin{vmatrix} XBTyB \\ YBTyB \\ ZBTyB \end{vmatrix} - [D\tilde{\omega} BBI] \begin{vmatrix} XBTyB \\ YBTyB \\ ZBTyB \end{vmatrix} \quad (5.0.25) \\
 &\quad + [TRNBE] \begin{vmatrix} 0.0 \\ 0.0 \\ GG \end{vmatrix} \\
 \begin{vmatrix} AXBBI \\ AYBBI \\ AZBBI \end{vmatrix} &= \begin{vmatrix} AXMBTzI \\ AYMBTzI \\ AZMBTzI \end{vmatrix} - [\tilde{\omega} BBI] [\tilde{\omega} BBI] \begin{vmatrix} XBTzB \\ YBTzB \\ ZBTzB \end{vmatrix} - [D\tilde{\omega} BBI] \begin{vmatrix} XBTzB \\ YBTzB \\ ZBTzB \end{vmatrix} \\
 &\quad + [TRNBE] \begin{vmatrix} 0.0 \\ 0.0 \\ GG \end{vmatrix}
 \end{aligned}$$

where the non-italicized equations are used for each term of {AXBBI} because the italicized terms were not measured. The body-axis accelerations from Eq. (5.0.25) are then projected to derivatives of body-axis velocities {DUBBI} according to Eq. (4.1.1.10). At this point, the {DUBBI} and {DPBBI} acceleration vectors at the time step are known, the {UBBI} vector can be projected to {UIBI} form according to Eq. (4.1.1.7), and the [TRNBI] derivative can be calculated from Eq. (1.4.6) (or, preferably, from the equivalent Quaternion form as outlined in Section 4.2.3). A numerical time integration may then be performed to determine the new position {XIBI}, orientation [TRNBI], velocity {UBBI}, and angular velocity {PBBI} at the time step for the next set of data in the telemetry data file. This process is then repeated for each time step of recorded data just as in a numerical trajectory simulation.

The final piece of the telemetry data reduction process is the determination of initial conditions for the numerical time integration. Initial conditions are particularly easy for wind tunnel drop testing. The aircraft model for drop testing is rigidly mounted in the tunnel and is, therefore, non-maneuvering and the store must be released from carriage so that its initial translational and rotational velocities are zero.

The store body axes have not yet moved relative to inertial axes at the instant of release:

$$\begin{vmatrix} XIBIO \\ YIBIO \\ ZIBIO \end{vmatrix} = \begin{vmatrix} 0.0 \\ 0.0 \\ 0.0 \end{vmatrix} \quad (5.0.26)$$

The velocities of body axes and inertial axes are identical at release:

$$\begin{vmatrix} \text{UBBI0} \\ \text{VBBI0} \\ \text{WBBI0} \end{vmatrix} = \begin{vmatrix} 0.0 \\ 0.0 \\ 0.0 \end{vmatrix} \quad (5.0.27)$$

The orientation of the body axes relative to inertial axes at first motion is a function of the store carriage attitude relative to the aircraft and the orientation of the aircraft relative to the tunnel centerline (inertial tunnel axes and earth axes are assumed coincident for drop testing):

$$[\text{TRNBI0}] = [\text{TRNBA0}] [\text{TRNAI0}] = [\text{TRN(IY, IP, IR)}] [\text{TRN}(-\text{BETA0}, \text{ALPHA0}, 0.0)] \quad (5.0.28)$$

At (and before) the instant of release the store is rigidly attached to the aircraft and (since the aircraft is not rotating in the tunnel):

$$\begin{vmatrix} \text{PBBI0} \\ \text{QBBI0} \\ \text{RBBI0} \end{vmatrix} = \begin{vmatrix} 0.0 \\ 0.0 \\ 0.0 \end{vmatrix} \quad (5.0.29)$$

It is also possible that measured accelerations obtained before the instant of release can provide an alternate source for some components of the initial orientation which can augment the orientation matrix determined purely from the geometric relations of Eq. (5.0.28). The measured accelerations would be sensitive to any possible misalignment errors of the model hardware in the tunnel and deflections of the aircraft attributable to flow loads. Measured accelerations can be used because the accelerometers are not sensitive to gravitational acceleration and sense one "g" of reaction acceleration when at rest. The measured components of that one "g" can be used to define corresponding terms in the [TRNBI0] direction cosine transformation matrix. At rest the accelerometer should sense:

$$[\text{TRNBI0}] \begin{vmatrix} 0.0 \\ 0.0 \\ -\text{GG}/32.174 \end{vmatrix} = \begin{vmatrix} \text{GAXMBTxIO} \\ \text{GAYMBTyIO} \\ \text{GAZMBTzIO} \end{vmatrix} = [\text{CTRNTB}]^{-1} \begin{vmatrix} \text{CAXMTxTxIO} \\ \text{CAYMTyTyIO} \\ \text{CAZMTzTzIO} \end{vmatrix} \quad (5.0.30)$$

or:

$$\begin{bmatrix} \text{TRNBI0(1,1)} & \text{TRNBI0(1,2)} & \text{TRNBI0(1,3)} \\ \text{TRNBI0(2,1)} & \text{TRNBI0(2,2)} & \text{TRNBI0(2,3)} \\ \text{TRNBI0(3,1)} & \text{TRNBI0(3,2)} & \text{TRNBI0(3,3)} \end{bmatrix} \begin{vmatrix} 0.0 \\ 0.0 \\ -\text{GG}/32.174 \end{vmatrix} = \begin{vmatrix} \text{GAXMBTxIO} \\ \text{GAYMBTyIO} \\ \text{GAZMBTzIO} \end{vmatrix} \quad (5.0.31)$$

Performing the matrix multiplication discloses that:

$$\begin{aligned} \text{TRNBI0(1,3)} &= -\text{GAXMBTxIO} * 32.174/\text{GG} \\ \text{TRNBI0(2,3)} &= -\text{GAYMBTyIO} * 32.174/\text{GG} \\ \text{and} \\ \text{TRNBI0(3,3)} &= -\text{GAZMBTzIO} * 32.174/\text{GG} \end{aligned} \quad (5.0.32)$$

which can be used with the relations of Eq. (1.3.9) to determine the body inertial pitch and roll angles:

$$\text{THABI0} = \sin^{-1} \{-\text{TRNBI0}(1,3)\} = \sin^{-1} \{\text{GAXMBTxI0} * 32.174/\text{GG}\} \quad (5.0.33)$$

and

$$\text{PHIBI0} = \tan^{-1} \{\text{TRNBI0}(2,3)/\text{TRNBI0}(3,3)\} = \tan^{-1} \{\text{GAYMBTyI0}/\text{GAZMBTzI0}\} \quad (5.0.34)$$

It is not possible, however, to determine the yaw angle (PSIBI0) from the accelerometers because only the last column of the transformation can be determined from the measurements and therefore yaw must always be extracted from the geometric relationship of Eq. (5.0.28). Some normalization of the measured accelerations (such as division of the $\{\text{GAXMBTI0}\}$ vector by its magnitude and time averaging a range of acceleration measurements before the drop) may be necessary before applying Eq. (5.0.32).

6.0 APPROXIMATING DYNAMIC STORE SEPARATION EVENTS USING STEADY-STATE WIND TUNNEL FORCE AND MOMENT MEASUREMENTS

Although store separation trajectories are dynamic motion events, wind tunnel force and moment (load) measurements on the separating store are typically made in a steady-state or quasi-steady manner as described in this section. The use of steady-state load measurements necessitates that approximations be made in the store and aircraft placement for "on-line" wind tunnel trajectory simulations. The two major approximations are the "induced angle" approximation used to account for the translational aerodynamics of the store as it moves through the aircraft flow field and the necessary approximations of the curved flight path of a maneuvering aircraft when curved flow is not available in the wind tunnel. These two approximations are described in Sections 6.0.1 and 6.0.2. Section 6.0.3 then describes how aerodynamic data from an "on-line" wind tunnel simulation can be extracted for use in "off-line" simulations.

6.1 FLOW-FIELD, TRANSLATIONAL, AND ROTATIONAL AERODYNAMICS - THE "INDUCED-ANGLE" APPROXIMATION

The aerodynamic forces and moments on the store are needed along with external forces such as thrust, weight, and ejectors as input to a separation simulation. Aerodynamic loads are caused by three separate aerodynamic phenomena. Only one of those phenomena can be directly simulated in a wind tunnel test. Total aerodynamic loads consist of (1) loads induced by the local flow angles and local flow velocities in the aircraft flow field, (2) loads induced by the relative translational motion of the store through the flow field, and (3) loads induced by the relative rotational motion of the store within the aircraft flow field. The three contributions are illustrated conceptually in Fig. 30.

Flow-field loads are generated by the store response to the local velocities and flow angles in the aircraft interference flow field. This portion of the total store aerodynamic loads may be measured in the wind tunnel using a dual support technique. A model of the aircraft is mounted

in the wind tunnel on the primary support and an instrumented model of the store is mounted separately on the computer-controlled Captive Trajectory Support (CTS). The CTS is a robotic mechanism capable of positioning the store in all six degrees of freedom in the vicinity of the aircraft. The CTS testing technique can be used in two basic modes. The first is a trajectory point-prediction mode coupled with an equation-of-motion package in which the CTS model is placed at calculated positions and orientations relative to the aircraft model obtained from solution of the store equations of motion for previous time steps. The loads used in the next evaluation of the equations of motion are measured at each new position. Such trajectories are often called "on-line" or "captive" trajectories. The second CTS mode is the "grid" mode. In grid testing, flow-field loads on the store are measured at a spatial array or grid of predetermined positions and orientations relative to the aircraft model. Store trajectories may then be generated "off-line" based on appropriate interpolation of the grid data to determine the flow-field loads at each point in the trajectory.

The second contributor to the total aerodynamic loads on the store arises from the relative translational motion of the store as it moves through the aircraft flow field. For instance, the solution of the store equations of motion at a particular time step in the trajectory might indicate that the store is moving downward at a relatively large vertical velocity, WBBI, in response to gravity and ejection forces as shown in Fig. 30. An observer fixed relative to the store would, therefore, sense an upwash velocity of magnitude WBBI (ignoring flow-field and rotational contributions). This apparent upwash velocity (referred to as "induced" upwash velocity) causes store aerodynamic loads which tend to resist the downward motion of the store. Translational motion effects cannot be rigorously modeled in "on-line" wind tunnel captive simulations because the solving of the store equations of motion and movement of the CTS-mounted store model cannot be performed in real time. An approximate technique has been developed to allow inclusion of some of the translational effects in on-line captive wind tunnel simulations by using "induced-angle" corrections. The induced angle correction basically involves replacing the true orientation of the store relative to inertial axes which is obtained from the equations of motion, with an adjusted orientation. The CTS rig is then commanded to place the store at the adjusted orientation for the load measurements in on-line trajectories. The induced angle approximation involves some loss in the accuracy of the flow-field portion of the total aerodynamic loads (because the store is placed at an adjusted orientation) for the added gain of a better model of the translational loads in on-line trajectory simulations. Better models of the flow-field and translational loads which do not involve compromising one component of the aerodynamic loads in favor of another are available for "off-line" grid simulations as will be described in a later paragraph. First, however, the on-line induced-angle approximation will be described in more detail in the next several paragraphs.

The concept of induced angles is most easily presented using a representative example. Figure 31a presents an illustrative case for a missile rail launch from an aircraft flying at 337 ft/sec at a rather large angle of attack of 45 deg relative to the air mass. At the end-of-rail point the equation-of-motion solution indicates a missile downrail velocity of 90 ft/sec in response to its rocket thrust. Figure 31b represents a vector summation of the missile velocity relative to the inertial system with the flight velocity of the inertial axes relative to the air mass to determine the resultant true velocity of the missile relative to the air mass. Note that this resultant velocity vec-

tor is rotated slightly from the inertial XI direction. This rotation of the resultant store velocity vector relative to the aircraft velocity vector is the so-called "induced" angle which reduces the store aerodynamic angle of attack to 35.98 deg even though the aerodynamic angle of the aircraft is 45 deg. The paradox which arises in store separation wind tunnel testing is that both velocities cannot be set in the wind tunnel at the same time. Control of only the free-stream velocity is available in the wind tunnel and the moving air mass in the tunnel is always aligned with the tunnel centerline so that it is impossible to set a store velocity different in magnitude and direction from the aircraft velocity. A compromise is therefore necessary which is illustrated in Fig. 31c. As shown in Fig. 31c, the store is rotated so that it is at the correct aerodynamic angle relative to the only wind velocity vector which is available in the tunnel - the aircraft free-stream velocity. The store is, as a result, at the "wrong" geometric attitude relative to the adjacent aircraft hardware but this "bias" in the flow-field loads is generally less than errors which would result from ignoring translational effects.

The actual calculations used to implement the induced-angle procedure in "on-line" wind tunnel simulations are outlined in the next several equations. First PSIBI, THABI, and PHIBI are extracted from the [TRNBI] matrix obtained from the equations of motion using the expressions of Eq. (1.3.9). Then the body axis components of the velocity of the inertial axis system relative to the air mass in the tunnel are calculated according to:

$$\begin{vmatrix} \text{UBIW} \\ \text{VBIW} \\ \text{WBIW} \end{vmatrix} = [\text{TRNBI}] \begin{vmatrix} \text{UIIW} \\ 0.0 \\ 0.0 \end{vmatrix} \quad (6.1.1)$$

where UIIW is the free-stream flight velocity of the aircraft at the instant of release (i.e., the tunnel free-stream velocity). The body-axis components of the "idealized" velocity of the body axis system relative to the air mass are then:

$$\begin{vmatrix} \text{UBBW} \\ \text{VBBW} \\ \text{WBBW} \end{vmatrix} = \begin{vmatrix} \text{UBIW} \\ \text{VBIW} \\ \text{WBIW} \end{vmatrix} + \begin{vmatrix} \text{UBBI} \\ \text{VBBI} \\ \text{WBBI} \end{vmatrix} \quad (6.1.2)$$

The inertial-axis components of the "idealized" velocity of the body-axis system relative to the air mass can be determined from applying the [TRNBI] transformation to the {UBBW} vector of Eq. (6.1.2) or by the alternate relation:

$$\begin{vmatrix} \text{UIBW} \\ \text{VIBW} \\ \text{WIBW} \end{vmatrix} = \begin{vmatrix} \text{UIIW} \\ 0.0 \\ 0.0 \end{vmatrix} + \begin{vmatrix} \text{UIBI} \\ \text{VIBI} \\ \text{WIBI} \end{vmatrix} \quad (6.1.3)$$

The {UIBW} and {UBBW} vectors are "idealized" in the sense that they represent the total velocity of the store relative to the undisturbed air mass far away from the aircraft. (The local velocity disturbances caused by the near-field presence of the parent aircraft are ignored.) The idealized aerodynamic angles of attack and sideslip of the store body relative to the wind mass are then:

$$\text{ALPHAS} = \tan^{-1} \{ \text{WBBW}/\text{UBBW} \} \quad (6.1.4)$$

and

$$\text{BETAS} = \sin^{-1} \{ \text{VBBW}/\text{VTOTBW} \} \quad (6.1.5)$$

where VTOTBW is a new addition to the nomenclature representing the total magnitude of the velocity of the body relative to the wind mass:

$$\begin{aligned} \text{VTOTBW} &= \sqrt{\text{UBBW}^2 + \text{VBBW}^2 + \text{WBBW}^2} \\ &= \sqrt{\text{UIBW}^2 + \text{VIBW}^2 + \text{WIBW}^2} \end{aligned} \quad (6.1.6)$$

The CTS rig orientations may then be calculated with adjusted rotations to include induced effects as follows (first assuming that the CTS mechanism is commanded in a yaw-pitch-roll modified Euler sequence such as is used in the AEDC 16T and 16S tunnels):

$$\begin{aligned} \text{PSI_I} &= \text{PSIBI} - \tan^{-1} \{ \text{VIBW}/\text{UIBW} \} \\ \text{THA_I} &= \text{THABI} + \tan^{-1} \{ \text{WIBW}/(\text{UIBW} \cdot \cos(\text{PSIBI}) + \text{VIBW} \cdot \sin(\text{PSIBI})) \} \\ \text{PHI_I} &= \text{PHIBI} \end{aligned} \quad (6.1.7)$$

In the AEDC 4-ft tunnel where the CTS rig is commanded in pitch/yaw/roll sequence, the command angles are:

$$\begin{aligned} \text{NU_I} &= \text{NUBI} + \tan^{-1} \{ \text{WIBW}/\text{UIBW} \} \\ \text{ETA_I} &= \text{ETABI} - \tan^{-1} \{ \text{VIBW}/(\text{UIBW} \cdot \cos(\text{NUBI}) - \text{WIBW} \cdot \sin(\text{NUBI})) \} \\ \text{OMEG_I} &= \text{OMEGBI} \end{aligned} \quad (6.1.8)$$

The character "_" is used to denote the induced test orientation at which the body "B" axes are actually positioned in the tunnel. The fact that the "_I" angles are actually set in wind tunnel captive trajectory simulations is transparent to the test user - all output parameters from the test are based on the actual "BI" values from the true equation-of-motion simulation. In other words, if measured tunnel forces and moments are plotted or tabulated as a function of THABI or the pitch angle relative to any other system (such as THABF, THABA, or THABP), there is no indication in the data that (as part of the induced angle approximation) the measurements were actually made at a pitch angle of THA_I. The fact that the angles output from an on-line wind tunnel simulation differ from the angles at which the aerodynamic data were actually measured has important implications when attempts are made to extract aerodynamic data from tunnel captive trajectories to provide input to off-line simulations at other conditions.

The induced angle adjustments for most trajectory simulations range from zero to about 1.5 deg. The Fig. 31 rail-launch example case which had extremely large induced angles of as much as 9 deg represents a case which, until the introduction of high-angle-of-attack fighters such as the F-22 had never been encountered in the wind tunnel. In a recent F-22 test, however, physical conflict between the missile hardware and the adjacent launch rail hardware caused by the induced angle adjustments necessitated the removal of the launcher hardware from the aircraft

model to allow testing. An alternate method for accounting for translational motion in on-line simulations for high-angle-of-attack launches must, therefore, be implemented. "Off-line" simulations using grid data are able to account for translational effects without compromising the flow-field loads. In grid simulations, the grid data can be obtained at orientations that are unbiased by translational effects. When performing trajectory simulations, the grid database can be searched and interpolated as a function of the true geometric orientations of the store relative to the aircraft (from the [TRNBI] matrix) and, thus, remain unbiased. The induced translational effects can be determined by then adding a free-stream increment based on the load differences at the true aerodynamic angles of attack and sideslip [defined by Eqs. (6.1.4) and (6.1.5)], and the geometric angles of attack and sideslip [obtained when the relative translational velocity vector {UBBI} is set to zero in Eqs. (6.1.2) through (6.1.5)]. Some of the advantages of the off-line grid method could conceivably be realized in on-line captive simulations by incorporating a store free-stream database and associated interpolator into the on-line program so that the "false-positioning" using the [TRN_I] matrix would not be necessary. Such a capability is being studied to allow future extreme high-alpha testing on the F-22.

In addition to "adjusting" the orientation of the store so that it is at its proper aerodynamic angle relative to the tunnel velocity, it is also necessary to correct for the differences in the magnitudes of the aircraft and resultant store flight velocities. In the Fig. 31 example case, for instance, the resultant velocity of the store had a magnitude of VTOTBW = 406.57 ft/sec whereas the aircraft velocity was UIIW = 337.5 ft/sec. Corrections for the different velocity magnitudes in the simulations are implemented by using appropriate velocity terms as the measured store forces and moments are scaled from wind tunnel conditions to true flight conditions. This scaling is accomplished by reducing the measured wind-tunnel forces and moments to non-dimensional coefficient form based on the tunnel flow dynamic pressure (a measure of the energy available in the flow defined by $Q_{\infty} = 1/2 \rho_{\infty} V_{\infty}^2$) and appropriate reference areas and lengths. The force and moment coefficients derived from the wind tunnel measurements take the following forms (using normal force and pitching moment as examples):

$$CN = FN' / (1/2 * \rho_{\infty}' * UIIW^2 * S') \quad (6.1.9)$$

and

$$C_m = M_m' / (1/2 * \rho_{\infty}' * UIIW^2 * S' * l_m') \quad (6.1.10)$$

where the primed quantities denote model parameters measured at wind tunnel conditions and S' and l_m' are the reference area and length at model scale. The velocity used to define the wind tunnel dynamic pressure in Eqs. (6.1.9) and (6.1.10) is the flight velocity of the aircraft (UIIW) as simulated in the tunnel. The density used is the free-stream air density in the tunnel. When, however, the force and moment coefficients are re-scaled at the simulated altitude, the resultant total velocity of the store (VTOTBW) is used in the determination of flight Q_{∞} rather than just the aircraft velocity, and the full-scale forces and moments are:

$$F_N = C_N * (1/2 * \rho_\infty * V_{TOTBW}^2 * S) \quad (6.1.11)$$

and

$$M_m = C_m * (1/2 * \rho_\infty * V_{TOTBW}^2 * S * l_m) \quad (6.1.12)$$

For the re-dimensionalization, the free-stream air density at the simulated altitude and full-scale reference lengths are used.

The final contributors to the overall aerodynamic loads acting on a store are the store rotational roll, pitch, and yaw angular velocities (PBBI, QBBI, and RBBI). The effects of pitch rate, for example, are illustrated in Fig. 31. Because of the nose-up pitching rotation in Fig. 30, an observer fixed at the store nose would sense a downwash velocity and an observer at the store tail would sense an upwash velocity. This velocity distribution induces moments that tend to resist the rotational motion of the store. Rotational motion effects also cannot be rigorously modeled in the wind tunnel because the CTS rig movement is not performed in real time. Rotational effects are approximated in on-line wind tunnel trajectories and many forms of off-line trajectories using input values of the primary free-stream rate damping derivatives. The PBBI, QBBI, and RBBI rates obtained at each evaluation of the store equations of motion are combined with the moment damping derivatives (C_{lp} , C_{mq} , C_{nr}) to determine induced rotational moments. These moments are then added to the measured moment values at each point in the trajectory for the next evaluation of the equations of motion. Rate-damping force terms (such as normal force caused by pitch rate, C_{Nq}) and cross-coupling terms (such as normal force caused by yaw rate, C_{Nr}) are not accounted for. The free-stream C_{lp} , C_{mq} , and C_{nr} derivatives are input as constants to the equations of motion and must be determined prior to the trajectory simulation. Fortunately, most store trajectories are not particularly sensitive to rotational loads, and extreme accuracy in the damping derivative values is not critical. Sophisticated computational trajectory techniques such as the AEDC-developed Flow-field Loads Influence Prediction Trajectory Generation Program (FLIP TGP) (Ref. 15) actually compute rotational loads directly by superimposing the equivalent rotational flow field illustrated in Fig. 30 onto the store.

6.2 THE "NON-ROTATING AIRCRAFT" APPROXIMATION FOR CONSTANT LOAD-FACTOR MANEUVERS

As was previously pointed out in Section 4.3.1, a capability for simulating store separations during constant load-factor aircraft maneuvers in the pitch plane can be implemented in wind tunnel simulations because the aircraft angle of attack remains constant during such maneuvers. Some approximations are necessary, however, because a true maneuver involves a curving flight path whereas curved free-stream flow is not available in the wind tunnel.

The true flight maneuver situation and the wind tunnel approximation are illustrated in Fig. 32. In the idealized constant load-factor maneuver, the magnitude of the aircraft free-stream velocity (UFFW) remains constant relative to the air mass (with magnitude equal to UIIW) but the aircraft pitches by an amount $\Delta\theta = QFFI * Time$ relative to inertial axes as outlined in Eq. (4.3.1.6). The free-stream velocity of the aircraft relative to the air mass is, therefore, a

curved vector lined up with the XF axis at any instant in time as shown in the left portion of Fig. 32. In the wind tunnel, however, the tunnel free-stream velocity vector is always aligned with the tunnel centerline and cannot be curved. As a result, the aircraft cannot be rotated through the THAFI angle in the tunnel and still remain at the correct angle of attack relative to the wind tunnel flow. In other words, (much as was the case for the store induced-angle approximation) the aircraft cannot be placed at the correct orientation relative to the wind in the tunnel and the correct geometric orientation relative to the inertial axes at the same time. A wind tunnel approximation is necessary for "on-line" trajectories in which the aircraft rotation during the maneuver is ignored in the tunnel simulations. The aircraft is thereby placed at the correct attitude relative to the wind so that its flow field is properly generated. But, as illustrated in Fig. 32, the store is not placed at exactly the correct geometric position and orientation within the aircraft flow field and, again, the flow-field loads are somewhat biased.

Once again (as was the case with the translational effects in Section 6.1), a more rigorous model of the aerodynamics during maneuvering store separations is possible when simulations are generated in the "off-line" grid mode than is available for "on-line" trajectories. For off-line simulations, the grid data can be searched and interpolated as a function of angles relative to the aircraft which include the angular rotations of the aircraft during its maneuver. The improvement in the trajectory accuracy is rather minimal, however, because the aircraft curved flight path generally has an extremely large radius and the angle change during the time duration of a typical store separation [Eq. (4.3.1.6)] is rather small.

The fact that the aircraft model is not actually rotated during a maneuvering on-line wind tunnel captive trajectory is transparent to the test user. Output from on-line wind tunnel simulations includes the THAFI factor in all calculated orientation angles of the body relative to aircraft-fixed systems (such as THABF, THABA, and THABP) although the load measurements in the tunnel were actually made with THAFI = 0. The fact that the angles between the store body and the aircraft which are output from an on-line wind tunnel maneuvering simulation differ from the angles at which the aerodynamic data were actually measured also has implications when attempts are made to extract aerodynamic data from tunnel captive trajectories to provide input to off-line simulations at other conditions.

6.3 EXTRACTION OF TESTED MODEL ORIENTATIONS FROM WIND TUNNEL CAPTIVE TRAJECTORIES

As pointed out in Sections 6.1 and 6.2, in order to simulate some of the aerodynamic phenomena associated with store trajectories during an "on-line" captive trajectory properly, steady-state measurements of store forces and moments must be made with the store and aircraft placed at orientations in the tunnel that are not consistent with the physical geometry of the true dynamic situation. On occasion, it is desirable to extract the angles at which a store was actually placed during a wind tunnel test so that databases of aerodynamic data as a function of store attitudes can be available for off-line simulations. The data from a captive tunnel trajectory can thus be used as a one-dimensional "pseudo-grid" for generation of other trajectories. Such a technique, for instance, has been used for parametric F-22 tank studies using various tank-restrained motion options. In the F-22/tank case, each existing tunnel trajectory was treated as a pylon-axis

"pitch" grid sweep for re-computed trajectories using several different types of pivot devices. The equations used to define the true "as-tested" orientations from "on-line" CTS trajectory data are outlined in this section.

To extract the true test orientations of the store relative to the aircraft, it is necessary to retrieve the values of PSIBI, THABI, PHIBI, and the {UBBI} vector from the "on-line" test trajectory data file at each time step (or other values from which these parameters can be calculated). The true test orientations of the model relative to any of the primary aircraft-fixed trajectory axes can then be developed using the following relations.

The [TRNBI] matrix is first determined from the PSIBI, THABI, and PHIBI values retrieved from the "on-line" trajectory according to Eq. (1.3.8). The {UIBI} vector is then determined from the retrieved {UBBI} vector using Eq. (4.1.1.7). The actual rig set angles PSI_I, THA_I, and PHI_I or NU_I, ETA_I, and OMEG_I may then be determined from Eqs. (6.1.7) or (6.1.8), depending on which AEDC tunnel the captive simulations were generated in. The [TRN_I] matrix is then calculated from the adjusted angles using the relations of Eq. (1.3.8) again.

At this point all the information necessary to determine the test orientations of the store model relative to inertial axes is defined. Most implementations of the grid method, however, interpolate the grid data as a function of the angles between the store model and one of the aircraft-fixed trajectory axis systems. The equations for the orientations of the non-rotating flight, aircraft, pylon, and carriage axes relative to inertial axes must also be developed. Because the selection of which aircraft-fixed trajectory axis is used to sort and interpolate the grid data for a particular application is at the discretion of the analyst, relations for all four primary systems will be developed in this section. The transformations for the trajectory axes were previously defined in Eqs. (4.3.2.1), (4.3.2.2), and (4.3.2.3), but all will be repeated here for clarity. The transformation for aircraft axes relative to flight axes [TRNAF] is derived from the angles:

$$\begin{aligned} \text{PSIAF} &= -\text{Beta} \\ \text{THAAF} &= \text{Alpha} \\ \text{PHIAF} &= 0.0 \end{aligned} \quad (6.3.1)$$

where Alpha and Beta are the angles of attack and sideslip of the aircraft relative to the wind mass which do not vary with time in constant load-factor wind tunnel simulations. The transformation for pylon axes relative to aircraft axes [TRNPA] is derived from the angles:

$$\begin{aligned} \text{PSIPA} &= \text{IY} \\ \text{THAPA} &= \text{IP} \\ \text{PHIPA} &= 0.0 \end{aligned} \quad (6.3.2)$$

and the transformation for carriage axes relative to aircraft axes [TRNCA] is derived from the angles:

$$\begin{aligned} \text{PSICA} &= \text{IY} \\ \text{THACA} &= \text{IP} \\ \text{PHICA} &= \text{IR} \end{aligned} \quad (6.3.3)$$

where IY, IP, and IR are the installed incidence angles of the store body axes relative to the aircraft at its carriage orientation. Without the non-rotating aircraft and induced-angle approximations, the true orientations of the body axes relative to flight, aircraft, pylon, or carriage axes would be extracted from [TRNBF], [TRNBA], [TRNBP], or [TRNBC], respectively, which are obtained from:

$$\begin{aligned} [\text{TRNBF}] &= [\text{TRNBI}] [\text{TRNFI}]^T \\ [\text{TRNBA}] &= [\text{TRNBI}] [\text{TRNAI}]^T \\ [\text{TRNBP}] &= [\text{TRNBI}] [\text{TRNPI}]^T \\ [\text{TRNBC}] &= [\text{TRNBI}] [\text{TRNCI}]^T \end{aligned} \quad (6.3.4)$$

where:

$$\begin{aligned} [\text{TRNAI}] &= [\text{TRNAF}] [\text{TRNFI}] \\ [\text{TRNPI}] &= [\text{TRNPA}] [\text{TRNAF}] [\text{TRNFI}] \\ [\text{TRNCI}] &= [\text{TRNCA}] [\text{TRNAF}] [\text{TRNFI}] \end{aligned} \quad (6.3.5)$$

and [TRNFI] represents the rotation of the aircraft during the maneuver.

With the induced-angle and non-rotating approximations, Eqs. (6.3.4) are rewritten as:

$$\begin{aligned} [\text{NRTRN_F}] &= [\text{TRN_I}] [\text{NRTRNFI}]^T \\ [\text{NRTRN_A}] &= [\text{TRN_I}] [\text{NRTRNAI}]^T \\ [\text{NRTRN_P}] &= [\text{TRN_I}] [\text{NRTRNPI}]^T \\ [\text{NRTRN_C}] &= [\text{TRN_I}] [\text{NRTRNCI}]^T \end{aligned} \quad (6.3.6)$$

where names like [NRTRNPI] are a special addition to the nomenclature denoting the direction cosine transformation matrix of "non-rotating" axes relative to inertial axes and the CTS test orientations of the body axes relative to the non-rotating trajectory axes. The non-rotating axis transformations are defined by rewriting Eqs. (6.3.5) as:

$$\begin{aligned} [\text{NRTRNFI}] &= \text{matrix identity} \\ [\text{NRTRNAI}] &= [\text{TRNAF}] \\ [\text{NRTRNPI}] &= [\text{TRNPA}] [\text{TRNAF}] \\ [\text{NRTRNCI}] &= [\text{TRNCA}] [\text{TRNAF}] \end{aligned} \quad (6.3.7)$$

since the [TRNFI] matrix in Eq. (6.3.5) is an identity for non-rotating axes. Finally, the actual tested store angles relative to any of the primary trajectory axis systems can be extracted from the appropriate Eq. (6.3.6) transformation using the relations of Eq. (1.3.9).

7.0 CONCLUDING REMARKS

The equations of motion used to numerically model free-flight, pivot-restricted, ejector-restricted, and rail releases of stores from arbitrarily maneuvering aircraft are developed. These equations are currently implemented in the AEDC off-line separation programs, and many of the capabilities are also implemented in AEDC wind tunnel separation simulations. Also, the equations modeling the operation, transfer of measurements, and data reduction necessary for fully instrumenting flight and drop models for store separation are developed and presented herein. The equations of motion as presented here include features not previously available in AEDC analytical and wind tunnel simulations such as arbitrary aircraft maneuvers, more rigorous models of the specific pivot hardware used by current aircraft, and downrail motions with all components of kinematic acceleration (including Coriolis effects) modeled.

REFERENCES

1. Carman, J. B., Jr., Hill, D. W., Jr., and Christopher, J. P. "Store Separation Testing Techniques at the Arnold Engineering Development Center, Volume II - Description of Captive Trajectory Store Separation Testing in the Aerodynamic Wind Tunnel (4T)." AEDC-TR-79-1 (AD-A087561), June 1980.
2. Newton, Sir Isaac. *"Principia."* (1687) translated and revised by F. Cajori, University of California Press, 1934.
3. Etkin, Bernard. *"Dynamics of Flight - Stability and Control."* John Wiley & Sons, 1982. (Second Edition).
4. Euler, L. *"Novi Commentari Academiae Petropolitanae."* Vol. 15, Petrograd Accademy, 1770.
5. Euler, L. *"Novi Commentari Academiae Petropolitanae."* Vol. 20, Petrograd Accademy, 1776.
6. Hamilton, W. R. "On a New Series of Imaginary Quantities Connected with a Theory of Quaternions." *Proceedings of the Royal Irish Academy, Dublin*, Vol. 2, No. 13, 1843, pp. 424-434.
7. Hamilton, W. R. *"Lectures on Quaternions."* Hodges and Smith, Dublin, 1853.
8. Hamilton, W. R. *"Elements of Quaternions."* Dublin, 1865, Longman's, Green, and Co., London, 1899 (Second Edition).

9. Robinson, A. C. "On the Use of Quaternions in Simulation of Rigid Body Motion." USAF Wright Air Development Center, TR-58-17, Dayton, OH, December 1958.
10. Klein, F. and Summerfield, A. "*Über die Theorie des Kreisels . . . mit 143 figuren im text.*" Vol. 1, Leipzig, Germany, B. G. Teubner, 1897.
11. Wilson, G. G. and Sundberg, W. D. "Quaternion Representation of Rigid-Body Finite Rotations." Sandia Laboratories Report SC-TM-72 (AD-905395), April 1972.
12. "Recommended Practice for Atmospheric and Space Flight Vehicle Coordinate Systems." American National Standard ANSI/AIAA R-004-1992, Approved Feb. 28, 1992 American National Standards Institute.
13. Akima, Hiroshi. "A New Method of Interpolation and Smooth Curve Fitting Based on Local Procedures." *Journal of the Association for Computing Machinery*, Vol. 17, No. 4, October 1970, pp. 589-602.
14. Marquart, E. J., Davis, K. I., Walker, G. P., and Dix, R. E. "Kinematic Telemetry from Small-Scale Wind Tunnel Models." AEDC-TR-94-13, January 1995.
15. Morgret, C. H. "Engineering Methods for Analytical Simulation of Store Separation from Weapons Bays." AEDC-TR-92-9, October 1992.

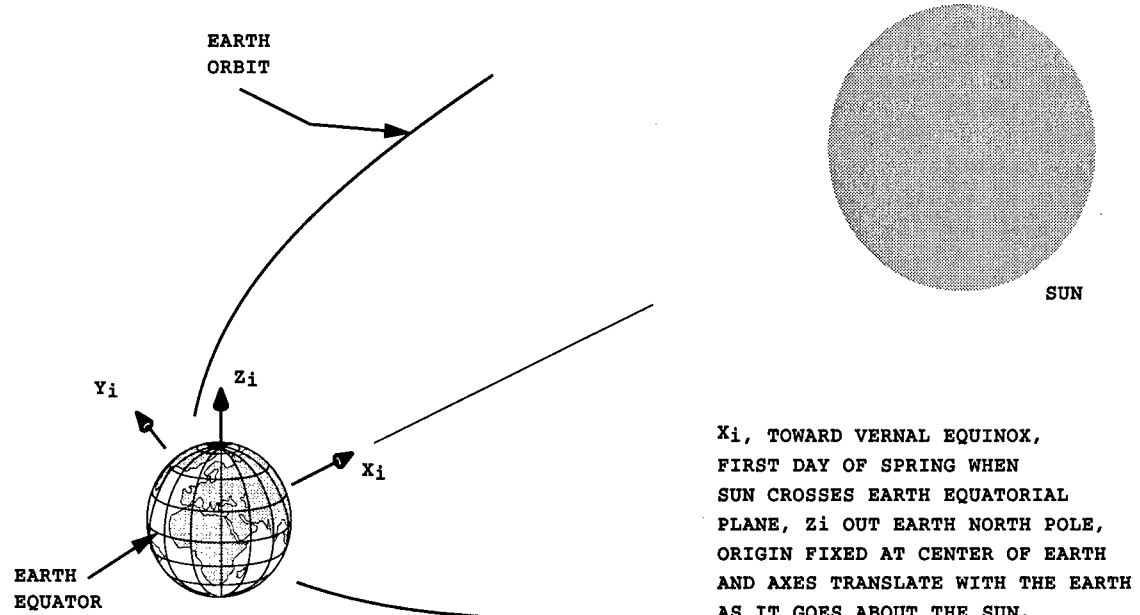
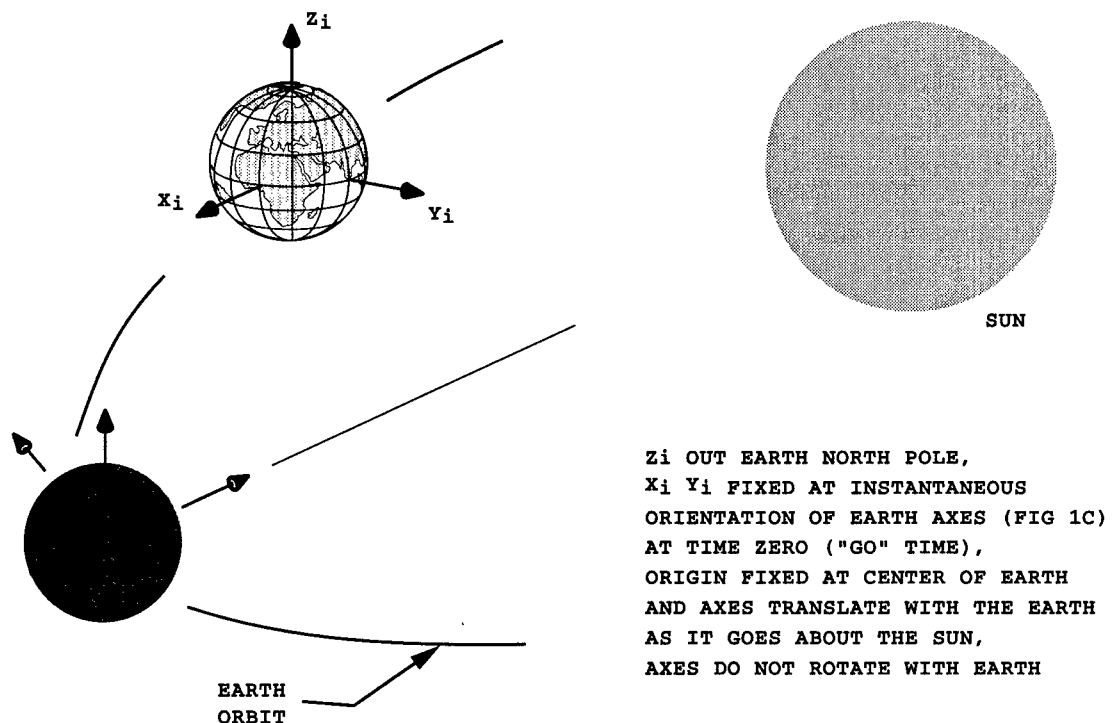
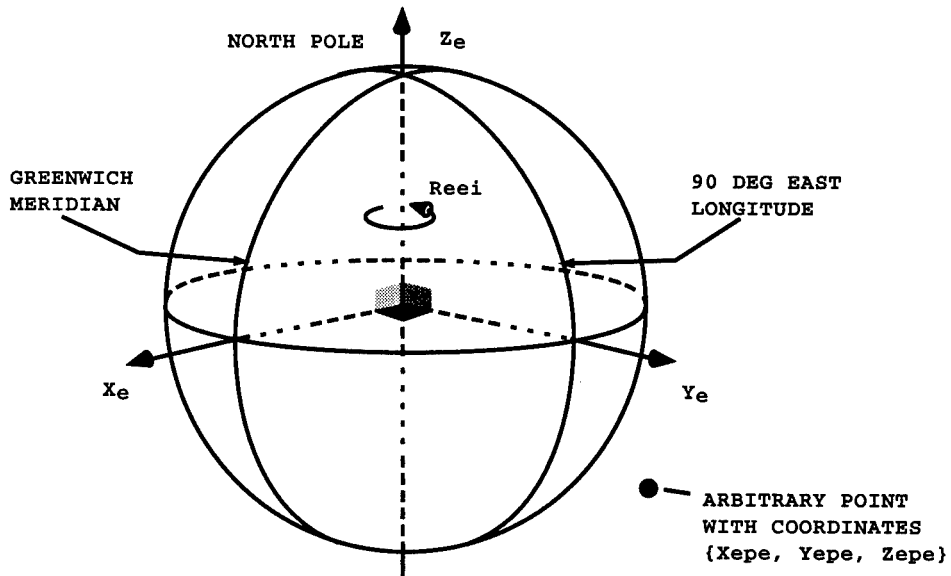
**a. Geocentric inertial axes****b. Go-inertial axes (alternate geocentric inertial axes)**

Figure 1. Operationally inertial axis systems for atmospheric motion simulations.



ORIGIN AT INTERSECTION OF MEAN EQUATORIAL PLANE
WITH PLANETARY POLAR AXIS

$$\bar{\omega}_{eei} = \begin{vmatrix} P_{eei} \\ Q_{eei} \\ R_{eei} \end{vmatrix} = \begin{vmatrix} 0.0 \\ 0.0 \\ 7.29211508E-05 \text{ rad/sec} \end{vmatrix} \approx \begin{vmatrix} 0.0 \\ 0.0 \\ 2\pi \text{ rad/day} \end{vmatrix}$$

GEOCENTRIC POLAR COORDINATES OF POINT $\{X_{epe}, Y_{epe}, Z_{epe}\}$

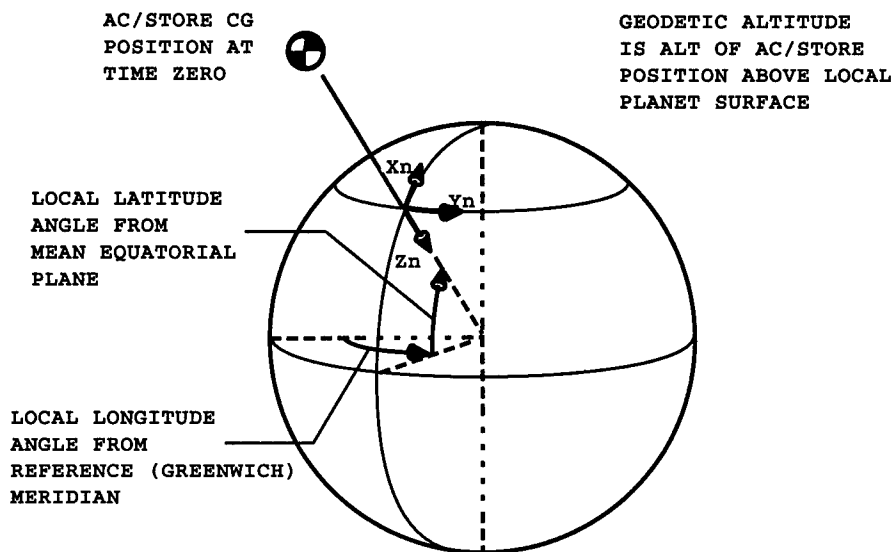
GEOCENTRIC ALTITUDE $R = \sqrt{X_{epe}^2 + Y_{epe}^2 + Z_{epe}^2}$

LATITUDE = $\sin^{-1}(Z_{epe}/R)$

LONGITUDE = $\tan^{-1}(Y_{epe}/X_{epe})$

c. Geocentric earth-fixed axes

Figure 1. Continued.



x_n POSITIVE GEOGRAPHIC NORTH ALONG PLANET LONGITUDE

y_n POSITIVE GEOGRAPHIC EAST ALONG PLANET LATITUDE

z_n ALONG NEGATIVE TO LOCAL NORMAL TO PLANET SURFACE
(NORMAL TO GEOID)

ORIGIN AT INTERSECTION OF GEOID WITH A LINE NORMAL TO THE
GEOID THROUGH THE AC/STORE CG AT TIME ZERO POSITION

PLANET SURFACE (GEOID) MAY BE SPHERICAL, ELLIPTICAL,
OR HIGHER ORDER DEPENDING ON ACCURACY REQUIREMENTS
(IF SPHERICAL THEN z_n GOES THROUGH PLANET CENTER AS SHOWN)

d. Normal earth-fixed (navigation) axes

Figure 1. Concluded.

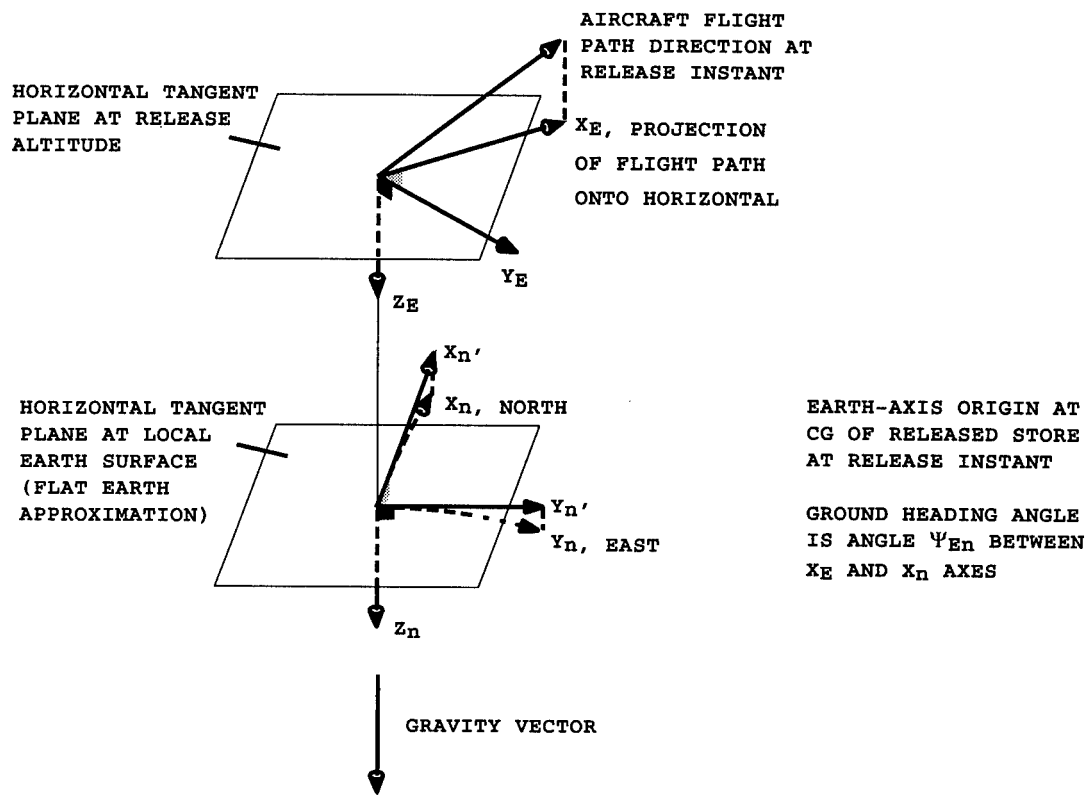
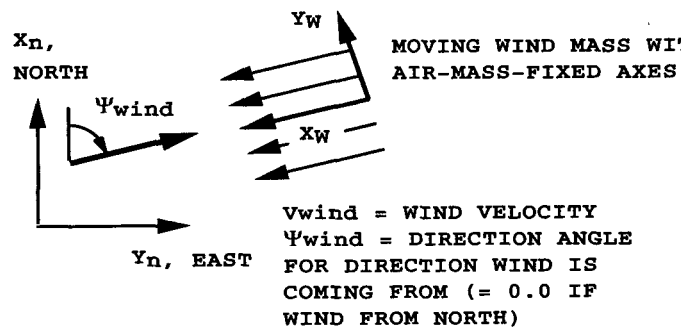


Figure 2. The "earth" axis system for store separation.



WIND MEASUREMENTS USUALLY OBTAINED
BY SOUNDING BALLOON RELEASED ON TEST
RANGE SOME TIME BEFORE THE FLIGHT TEST

DIRECTION WIND MASS IS MOVING IN RELATIVE TO
EARTH-FIXED NAVIGATION AXES:

$$\Psi_{wn} = \Psi_{wind} + 180$$

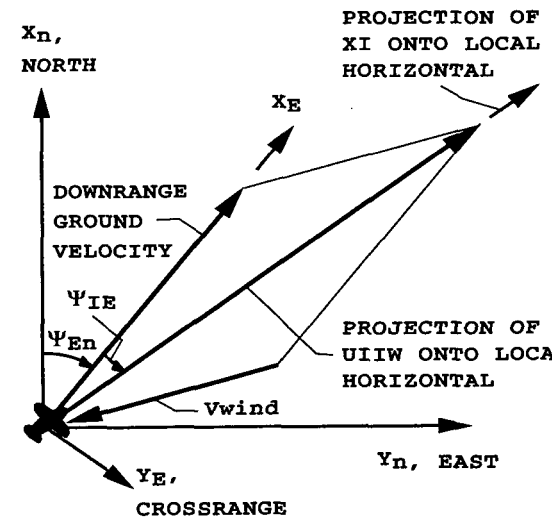
NAVIGATION-AXIS COMPONENTS OF VELOCITY OF MOVING WIND
MASS RELATIVE TO NAVIGATION AXES (NOTE: $U_{WWn} = v_{wind}$)

$$\begin{vmatrix} U_{nWE} \\ V_{nWE} \\ W_{nWE} \end{vmatrix} = \begin{vmatrix} U_{nWn} \\ V_{nWn} \\ W_{nWn} \end{vmatrix} = \begin{vmatrix} U_{WWn} * \cos(\Psi_{wn}) \\ U_{WWn} * \sin(\Psi_{wn}) \\ 0.0 \end{vmatrix} = \begin{vmatrix} -v_{wind} * \cos(\Psi_{wind}) \\ -v_{wind} * \sin(\Psi_{wind}) \\ 0.0 \end{vmatrix}$$

ORIENTATION OF WIND VECTOR RELATIVE TO EARTH AXES
 $\Psi_{WE} = \Psi_{wn} - \Psi_{En}$

EARTH-AXIS COMPONENTS OF VELOCITY OF MOVING WIND
MASS RELATIVE TO EARTH AXES

$$\begin{vmatrix} U_{WE} \\ V_{WE} \\ W_{WE} \end{vmatrix} = \begin{vmatrix} U_{EWn} \\ V_{EWn} \\ W_{EWn} \end{vmatrix} = \begin{vmatrix} U_{WWn} * \cos(\Psi_{WE}) \\ U_{WWn} * \sin(\Psi_{WE}) \\ 0.0 \end{vmatrix}$$



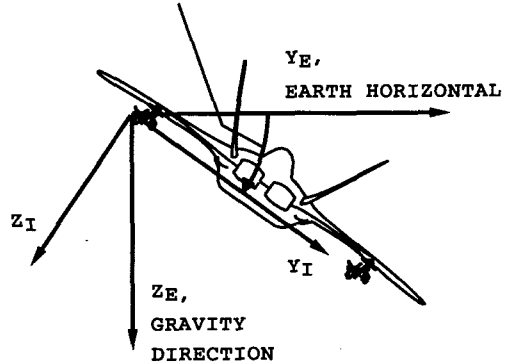
SHOWN AT RELEASE INSTANT

Ψ_{En} = GROUND HEADING ANGLE

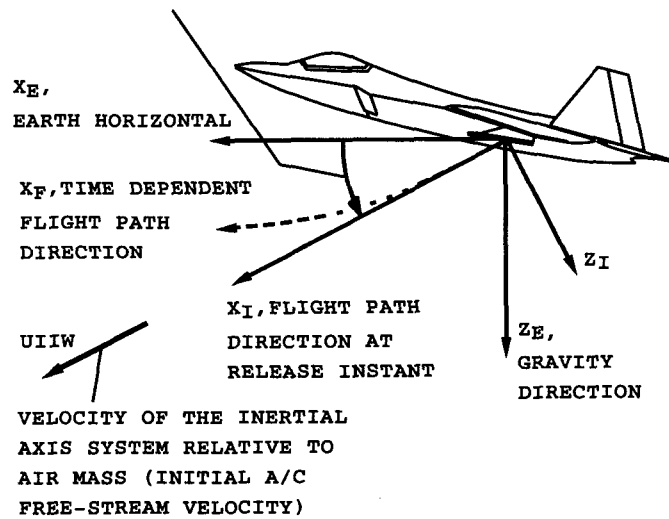
Ψ_{IE} = AIRCRAFT INERTIAL FLIGHT HEADING
SO THAT VELOCITY OF AIRCRAFT RELATIVE TO
WIND MASS AT RELEASE INSTANT AND VELOCITY
OF WIND MASS RELATIVE TO EARTH CAUSE A
GROUND TRACK IN THE x_E DIRECTION

a. Heading of inertial axes relative to earth and navigation axes (view looking down Z_E axis)

Figure 3. Store separation inertial axes.

Φ_{IE} , INERTIAL BANK ANGLE

SHOWN FOR ZERO CLIMB ANGLE CASE

 Θ_{IE} , INERTIAL DIVE/CLIMB ANGLE

SHOWN FOR ZERO BANK ANGLE CASE

BOTH VIEWS SHOWN AT RELEASE INSTANT
(INERTIAL AND EARTH ORIGINS COINCIDENT)

b. Dive and bank angles of inertial axes relative to earth axes
Figure 3. Concluded.

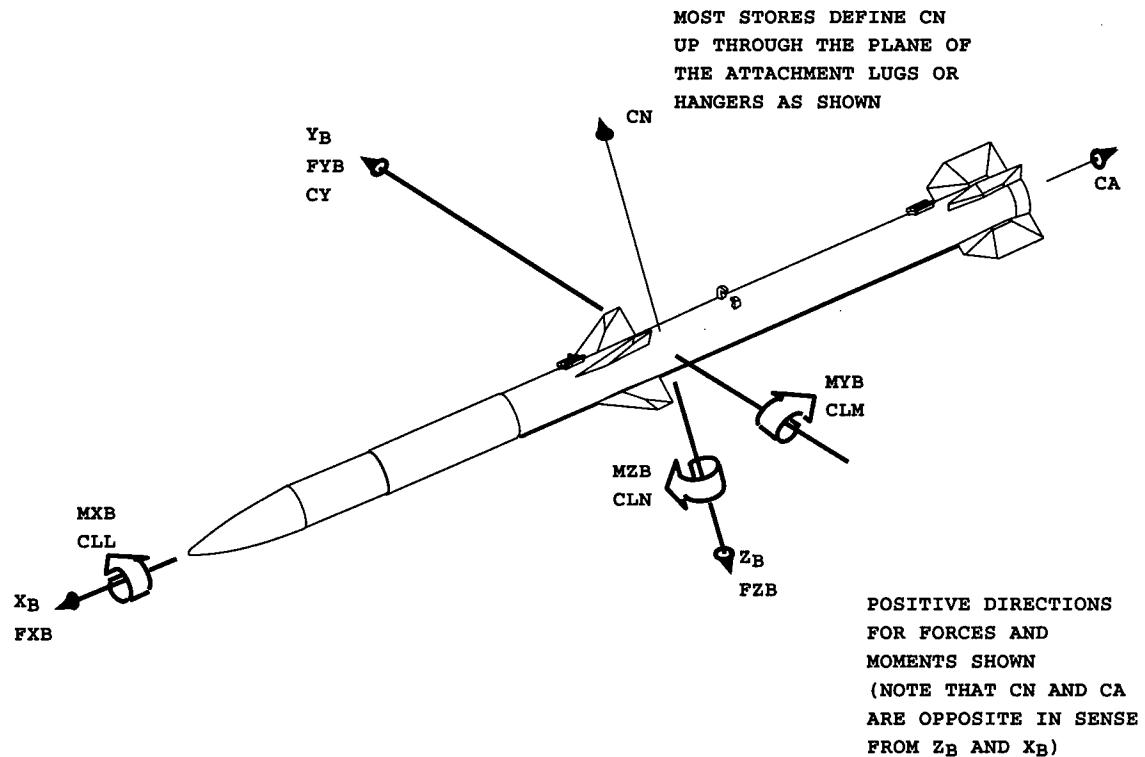


Figure 4. Store body-axis coordinate system.

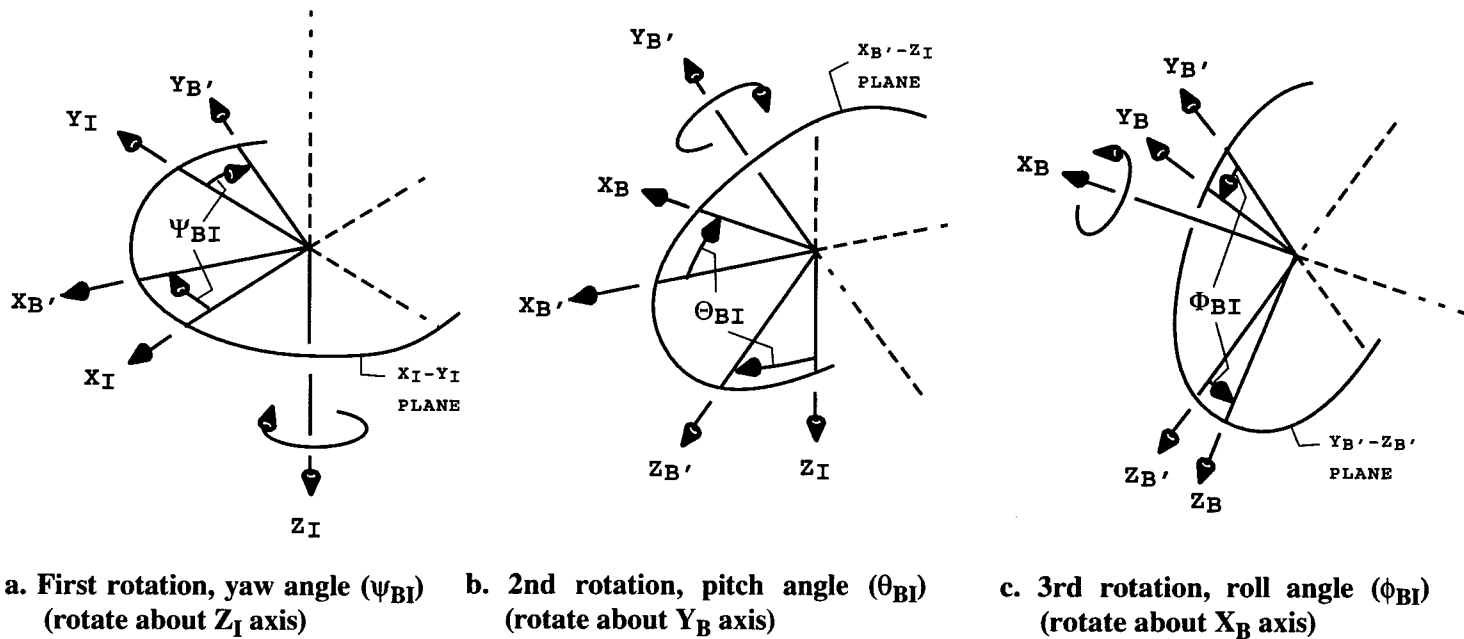
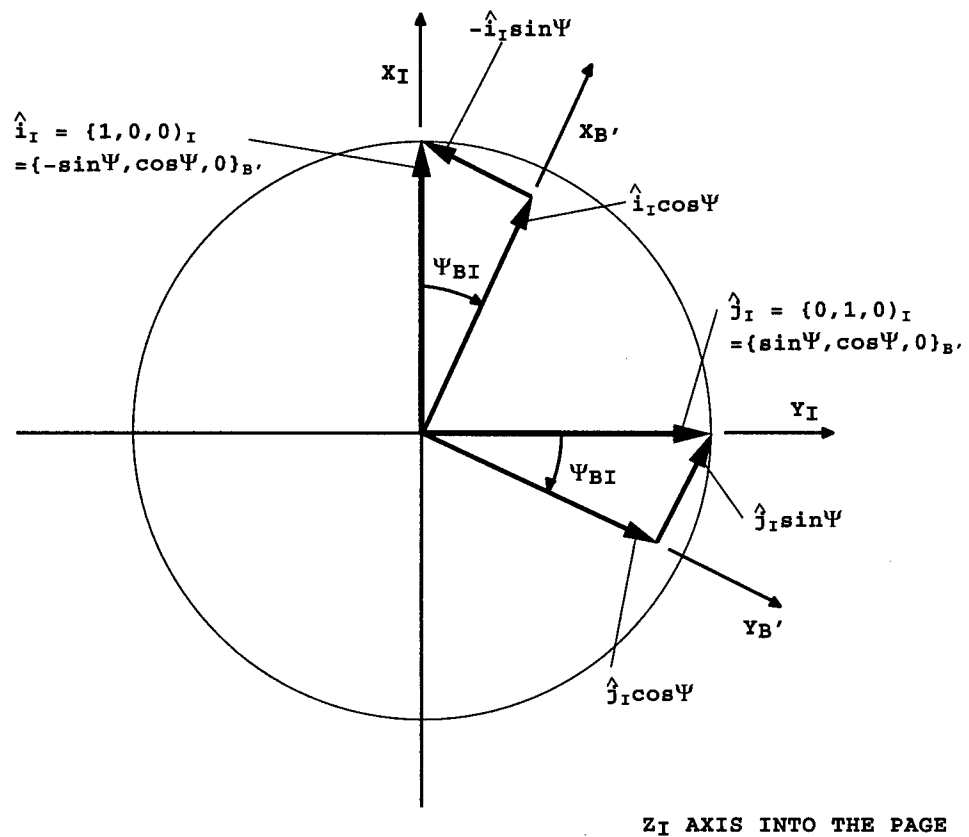
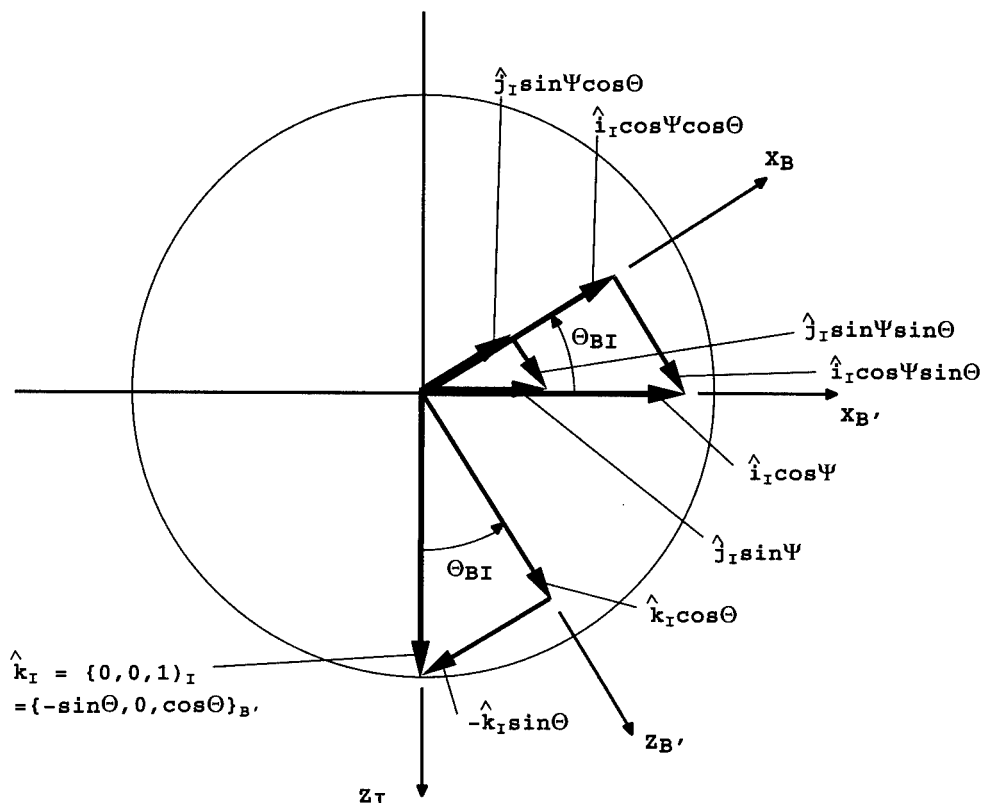


Figure 5. Yaw-pitch-roll rotation sequence.



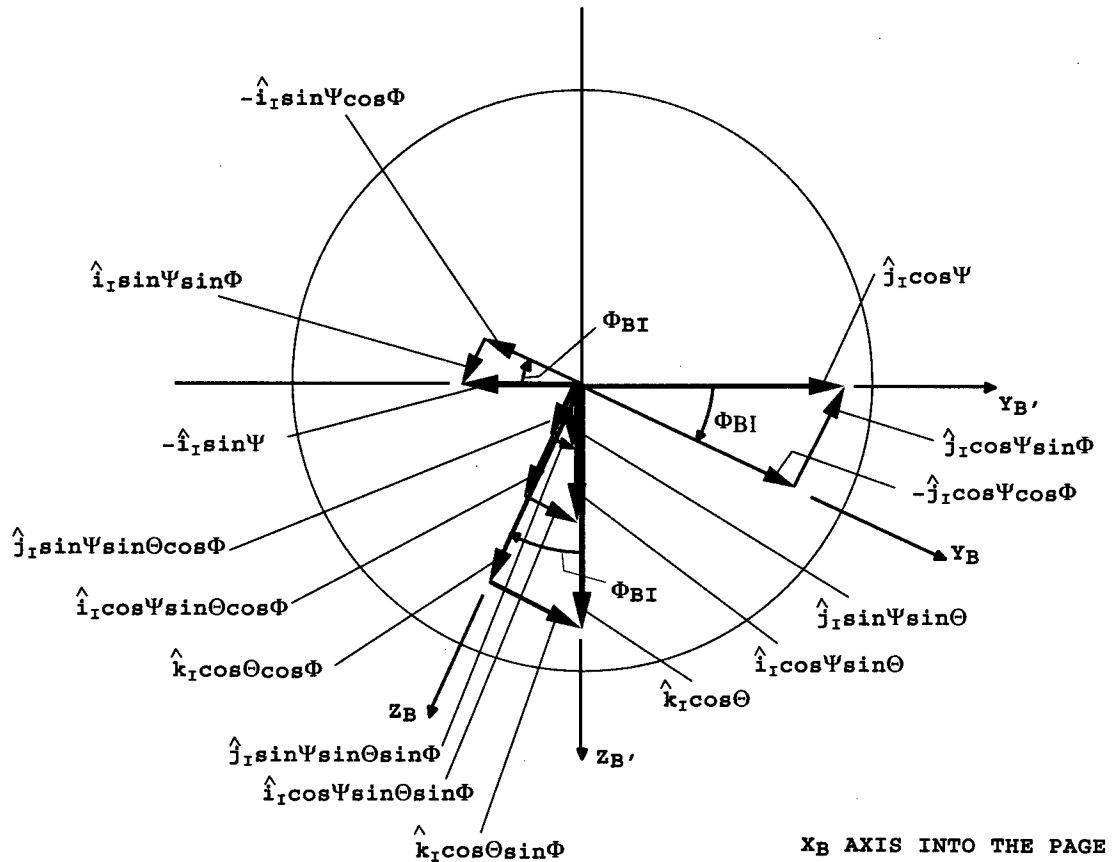
a. First rotation - yaw about \$Z_I\$ axis
Figure 6. Yaw-pitch-roll rotation sequence shown on a unit sphere.



$Y_{B'}$ AXIS OUT OF THE PAGE

b. Second rotation - pitch about $Y_{B'}$ axis

Figure 6. Continued.



c. Third rotation - roll about XB axis

Figure 6. Concluded.

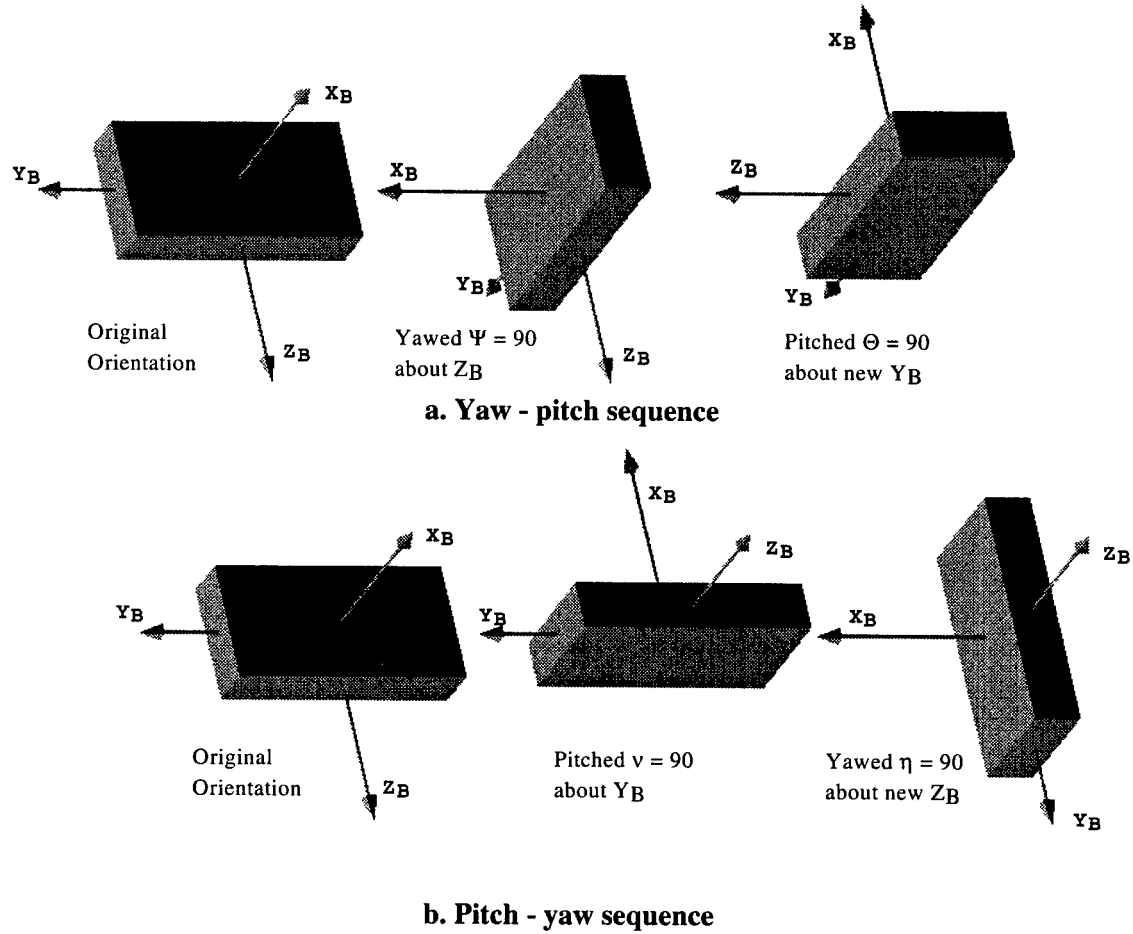


Figure 7. The effects of two rotations performed in opposite orders.

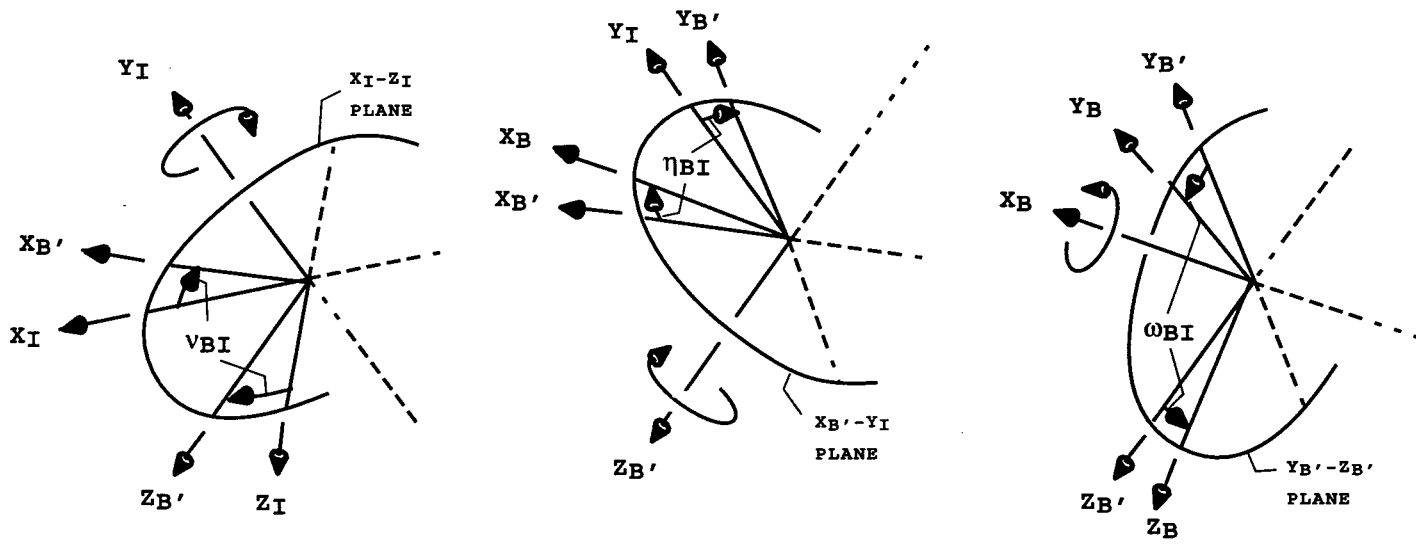


Figure 8. Pitch-yaw-roll rotation sequence.

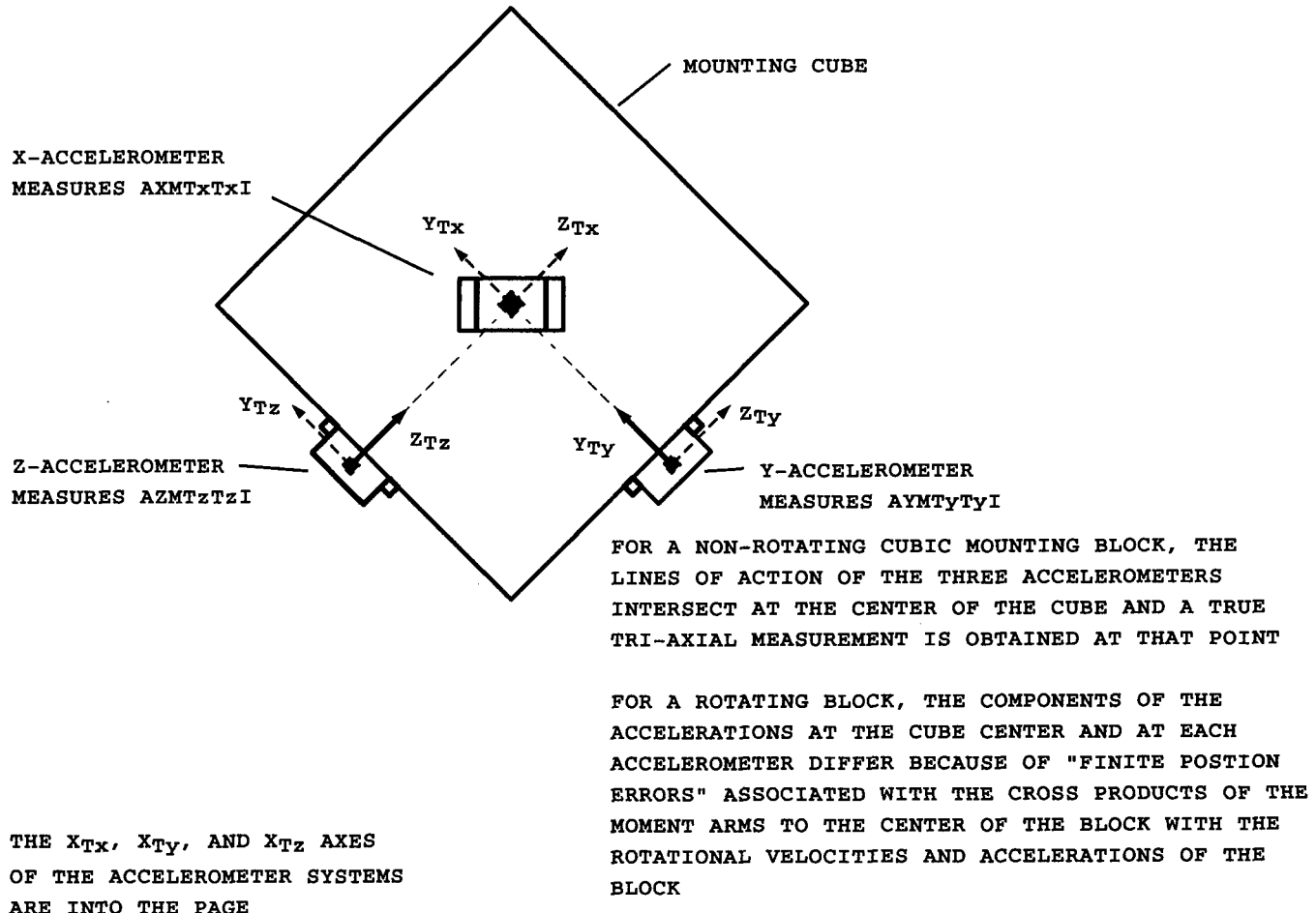


Figure 9. Physical approximation of a "tri-axial" accelerometer.

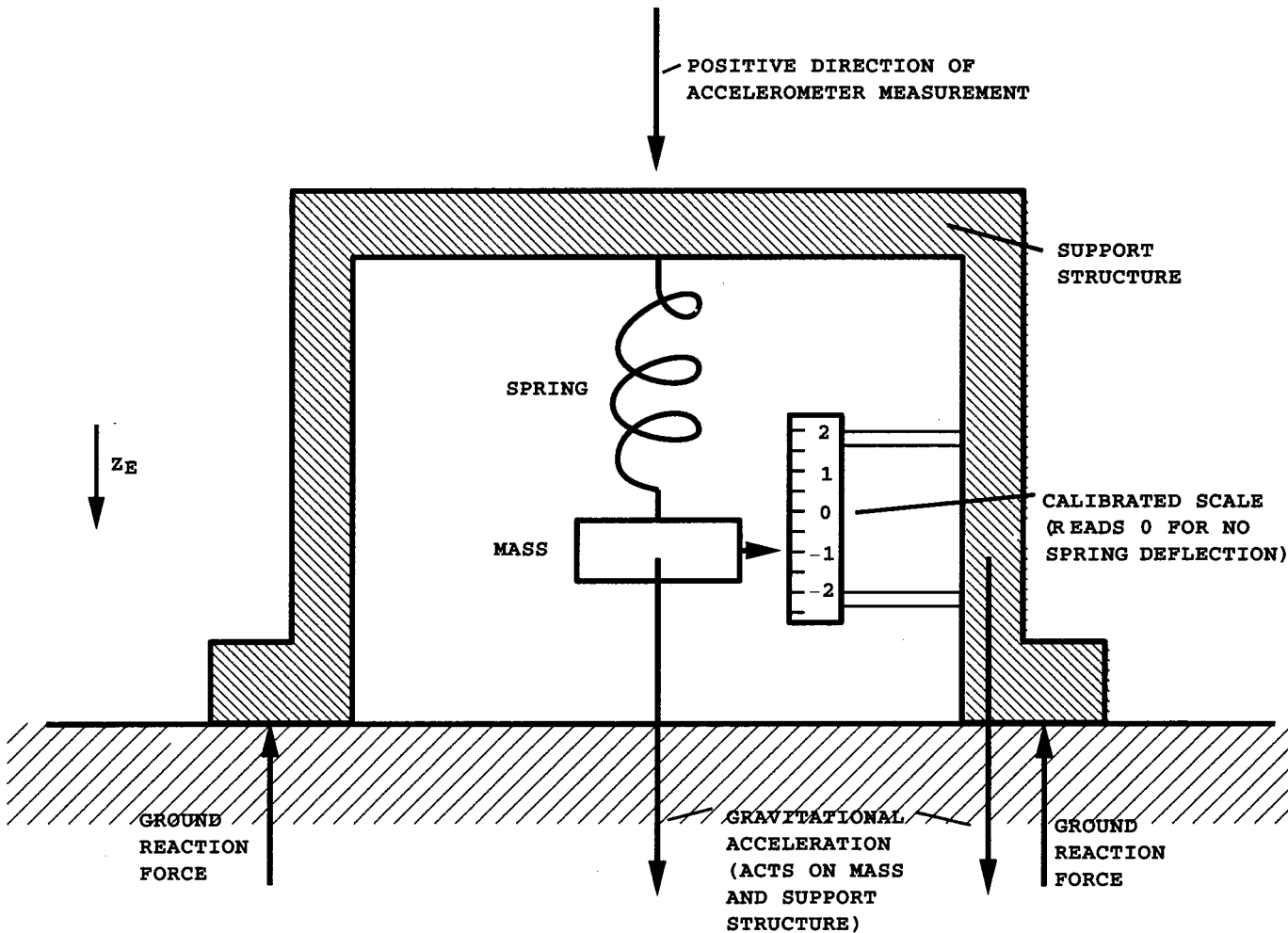


Figure 10. An idealized accelerometer.

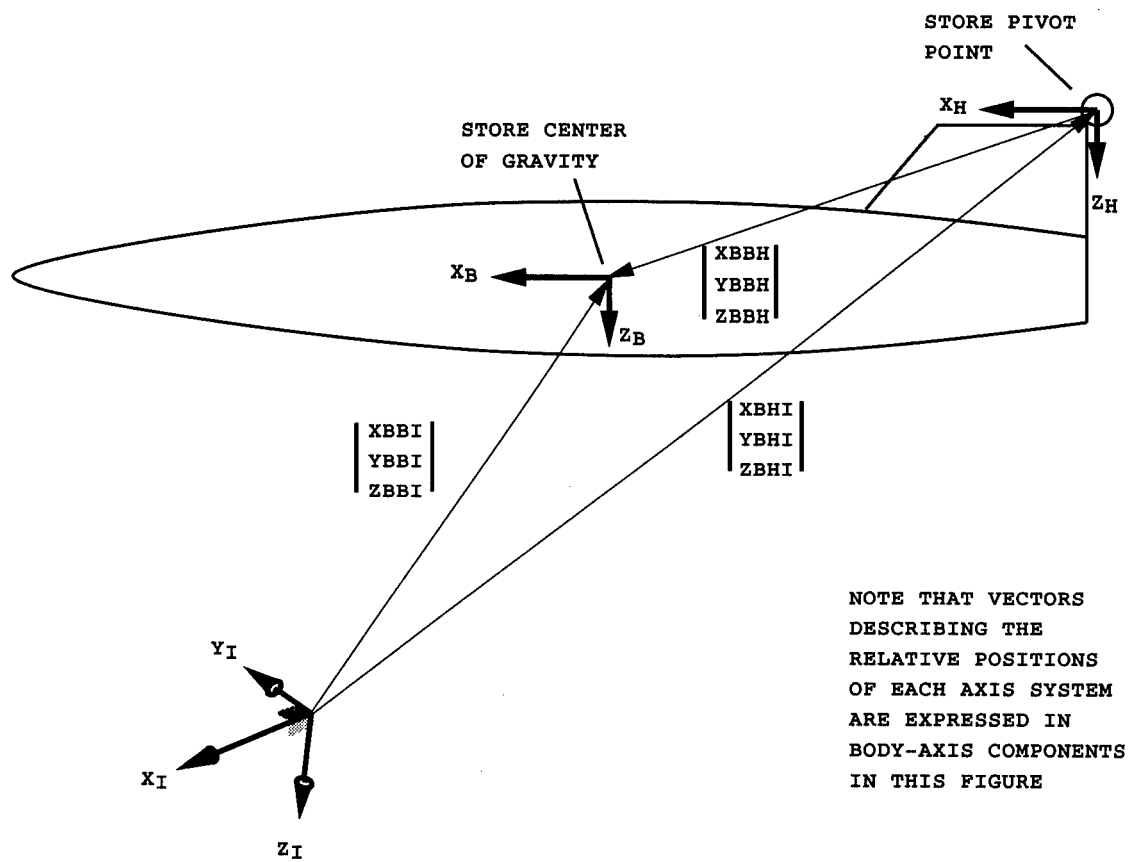


Figure 11. Body, hook, and inertial axis systems.

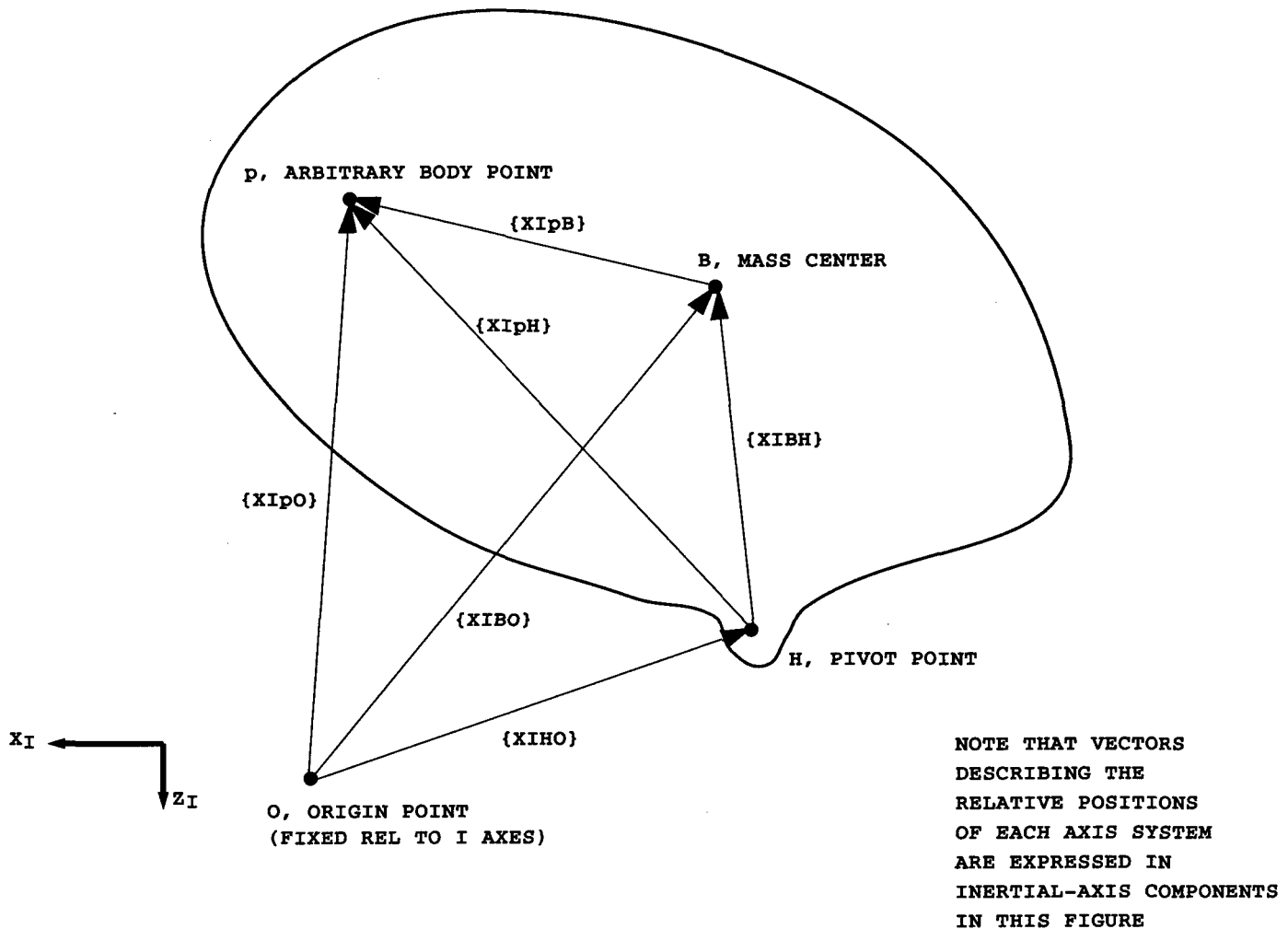


Figure 12. Moment arms of point p relative to body, hook, and inertial axes.

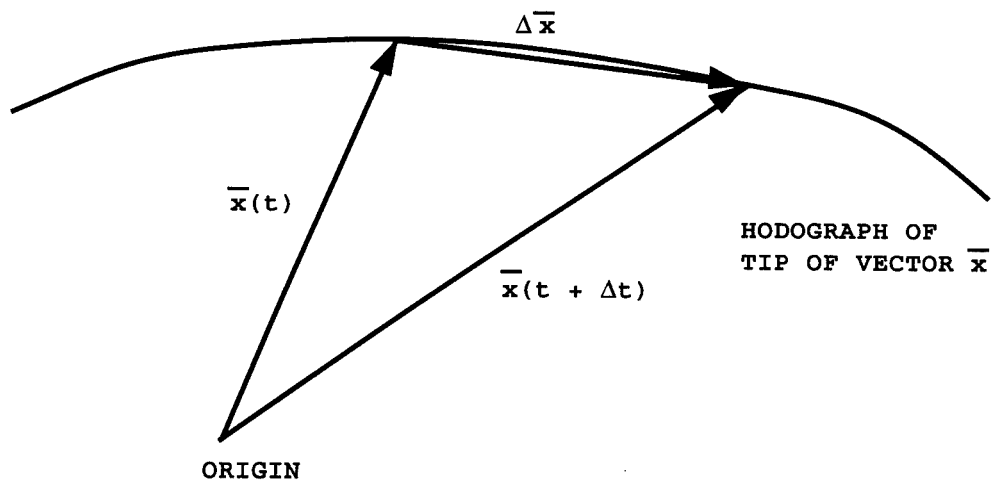


Figure 13. Schematic of the derivative of a vector.

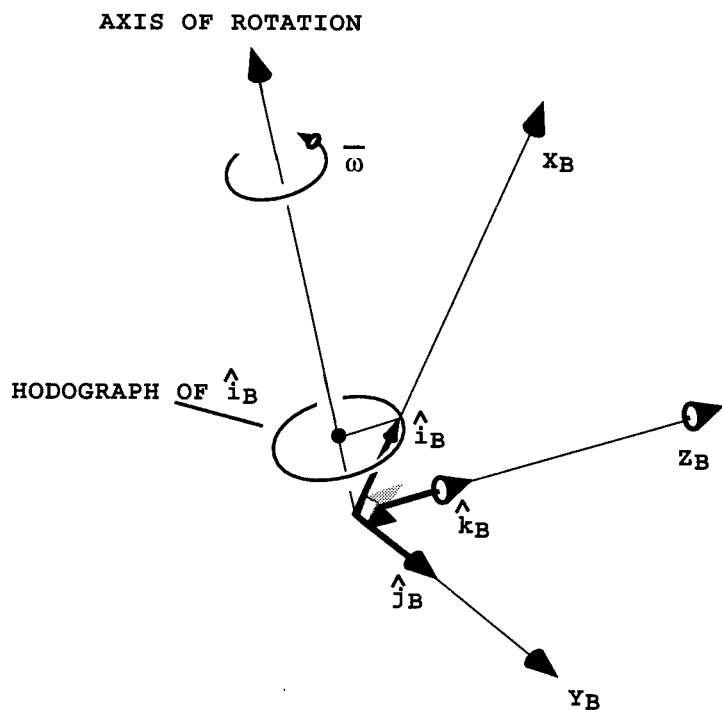


Figure 14. Velocities of unit vectors fixed in a rotating body.

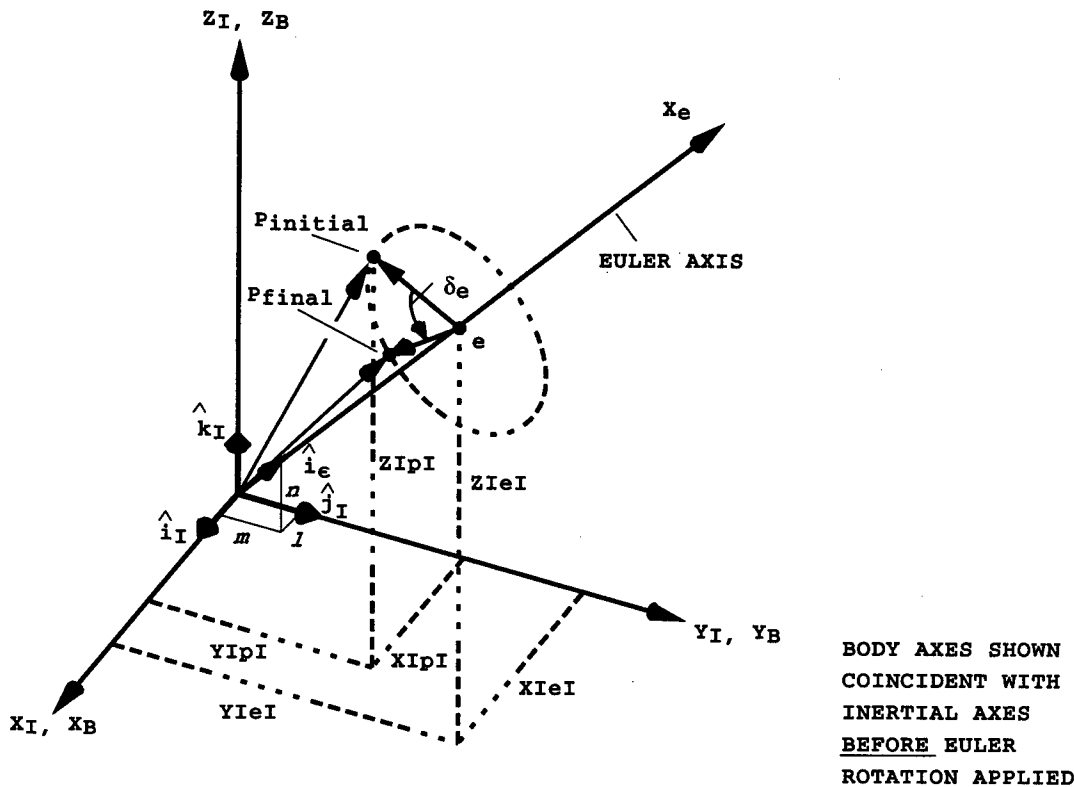


Figure 15. Depiction of Euler axis and arbitrary point "P" before and after Euler rotation.

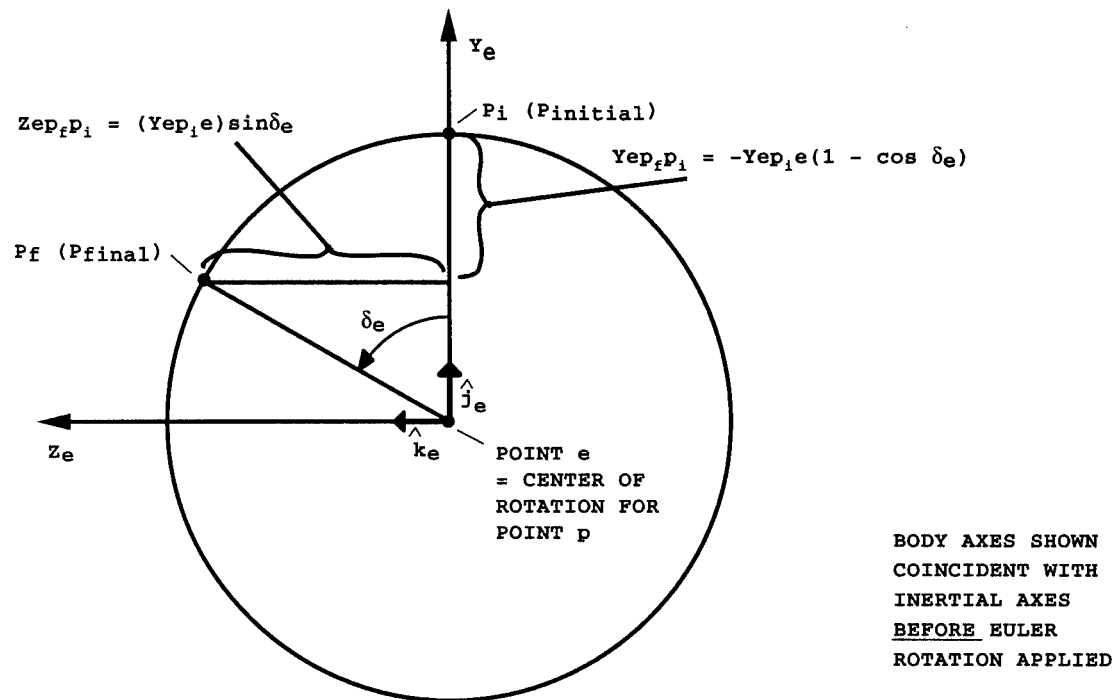


Figure 16. View of Euler rotation looking down Euler axis.

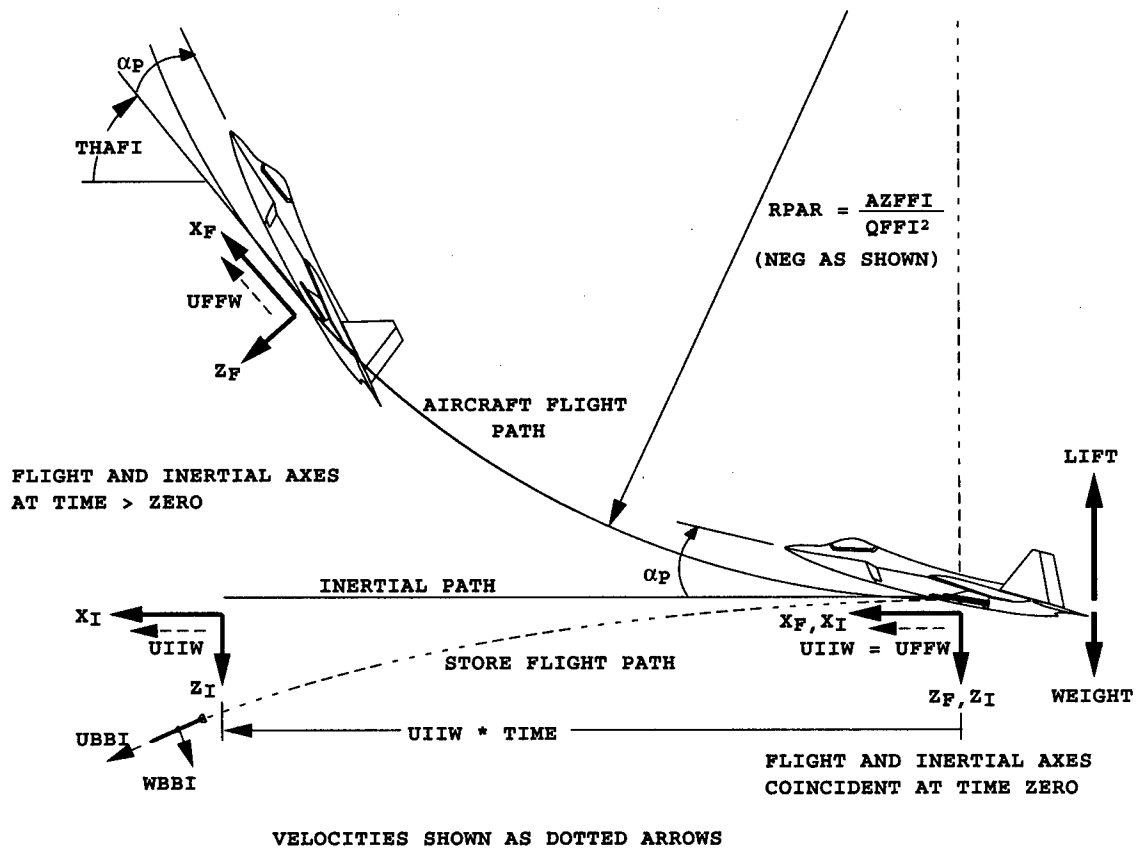
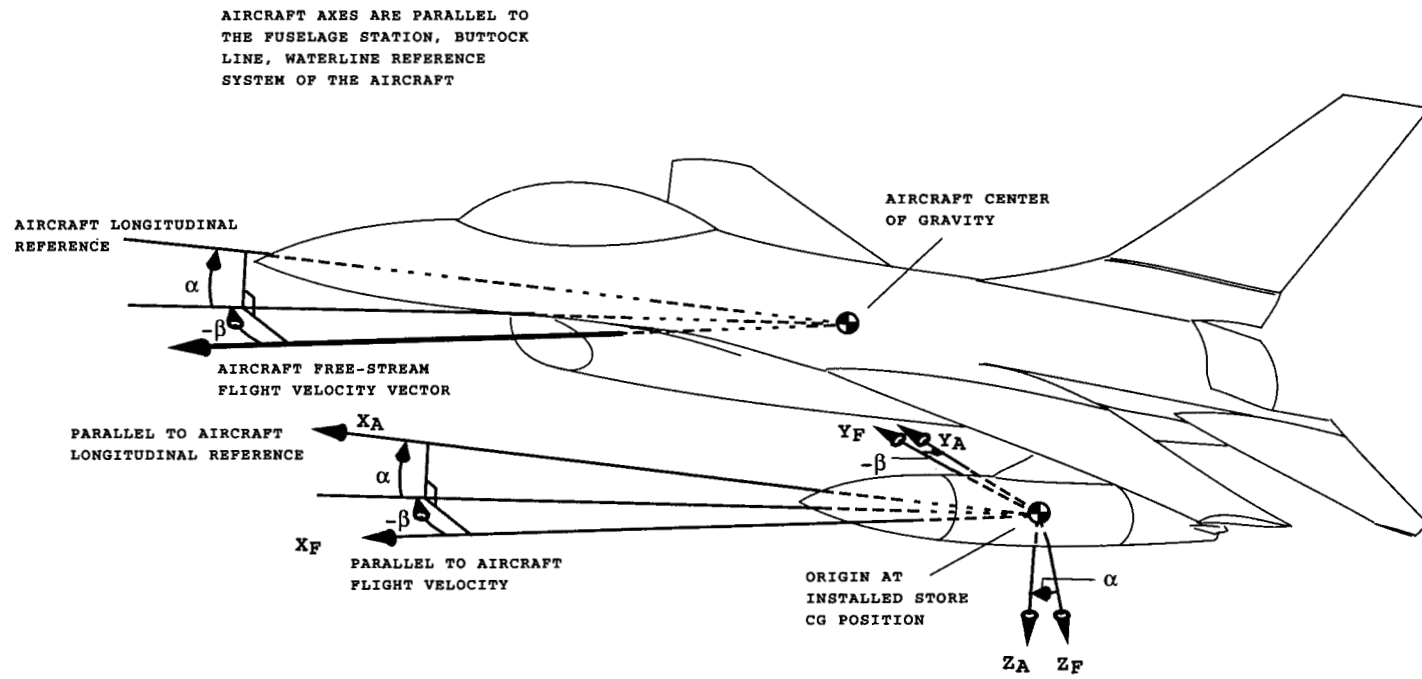
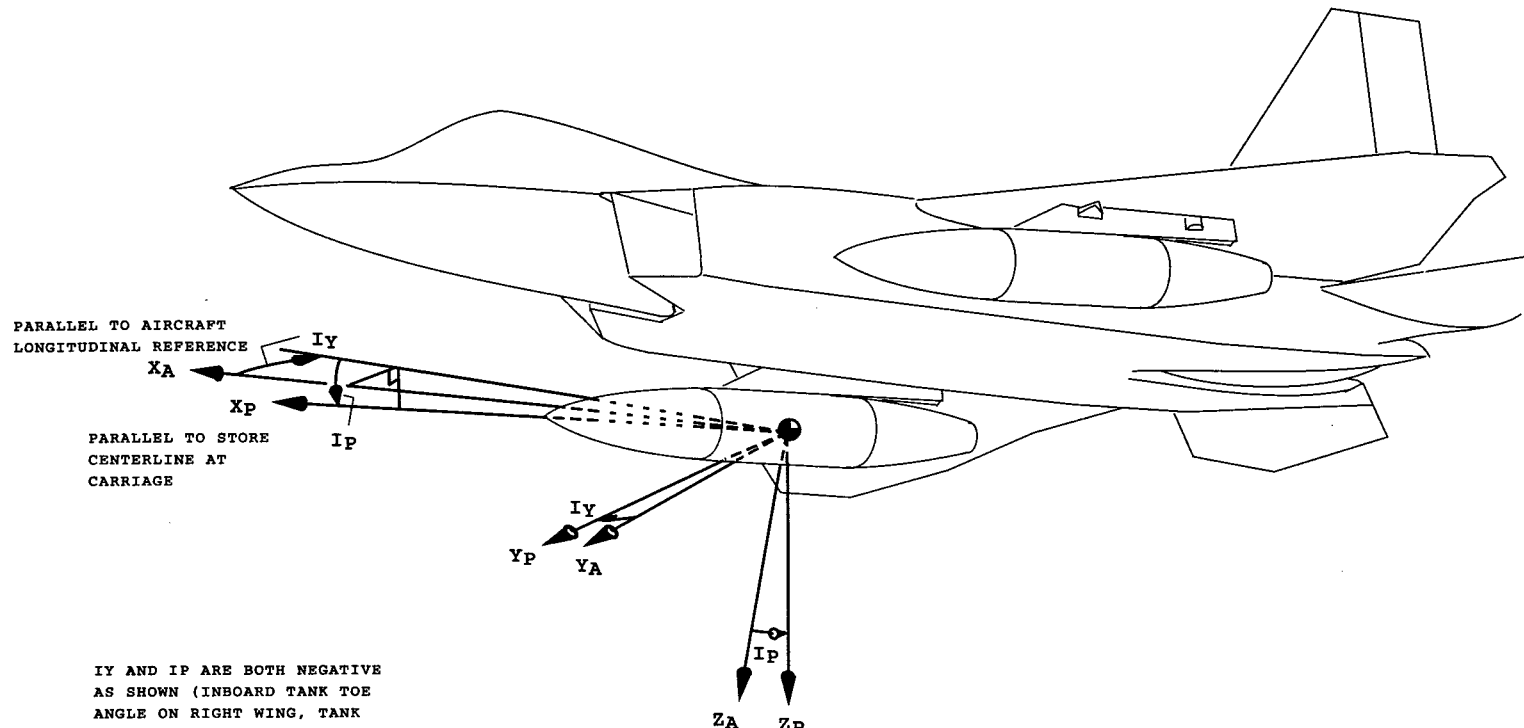


Figure 17. Idealized constant-load-factor maneuvers.

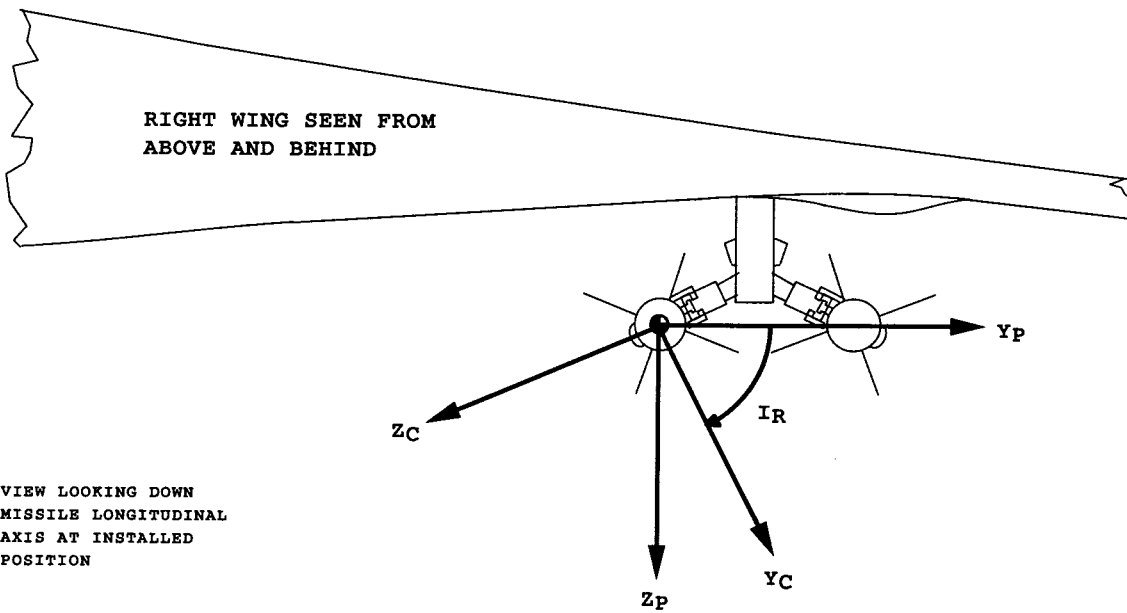


a. Relationship between flight axes and aircraft axes
Figure 18. Trajectory axis coordinate directions.



b. Relationship between aircraft axes and pylon axes.

Figure 18. Continued.



c. Relationship between pylon axes and carriage axes.
Figure 18. Concluded.

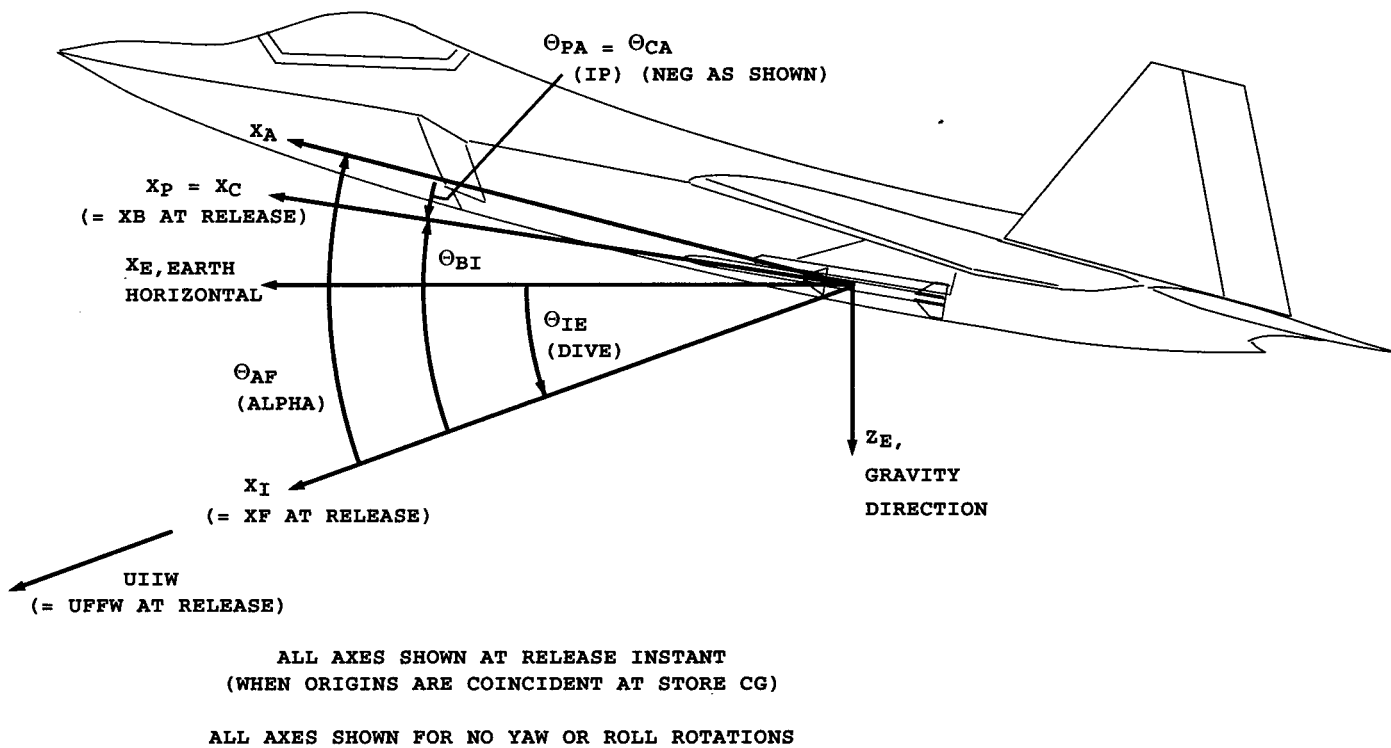


Figure 19. Relationship between various trajectory axes for pitch-plane-only rotations.

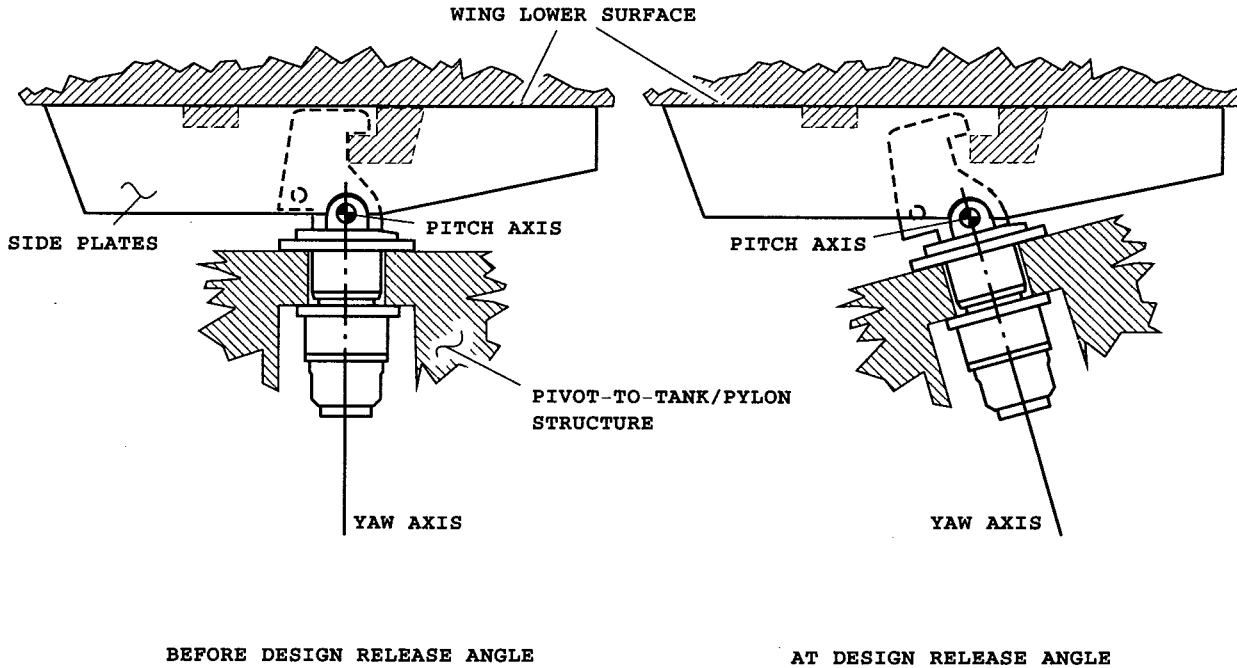


Figure 20. F-16 pivot fitting.

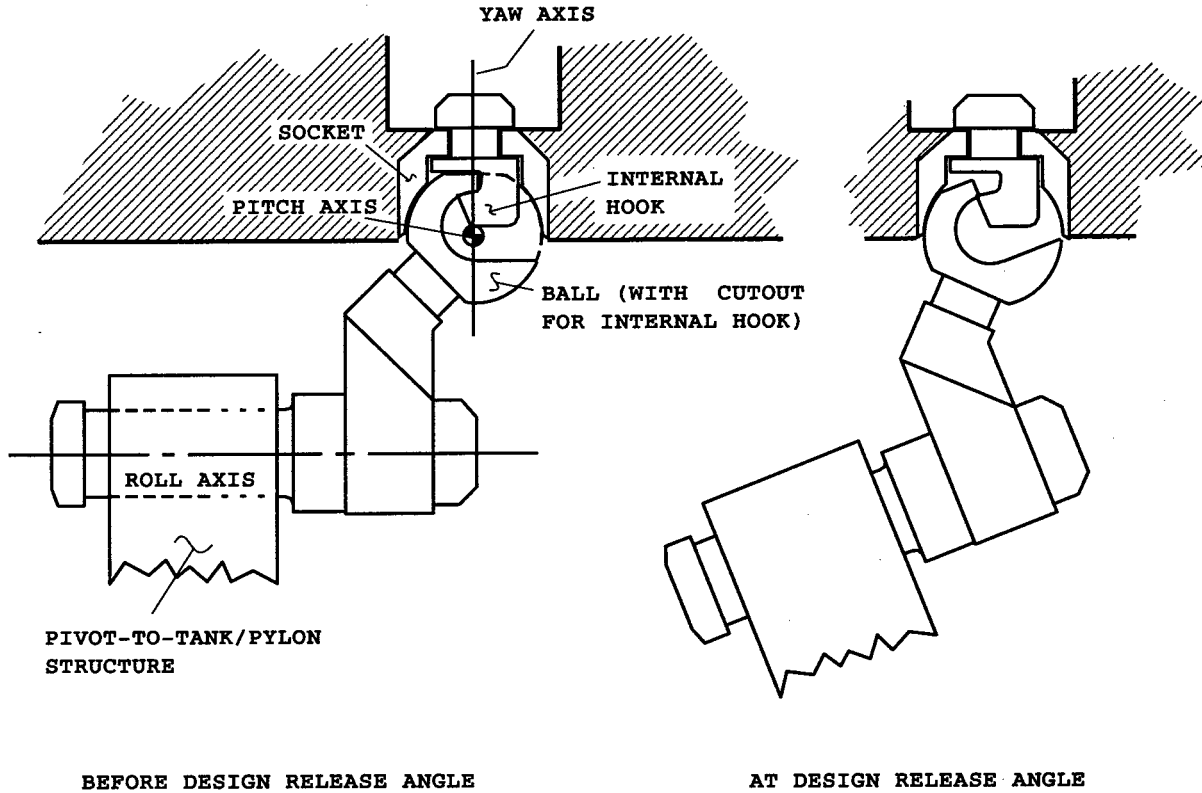
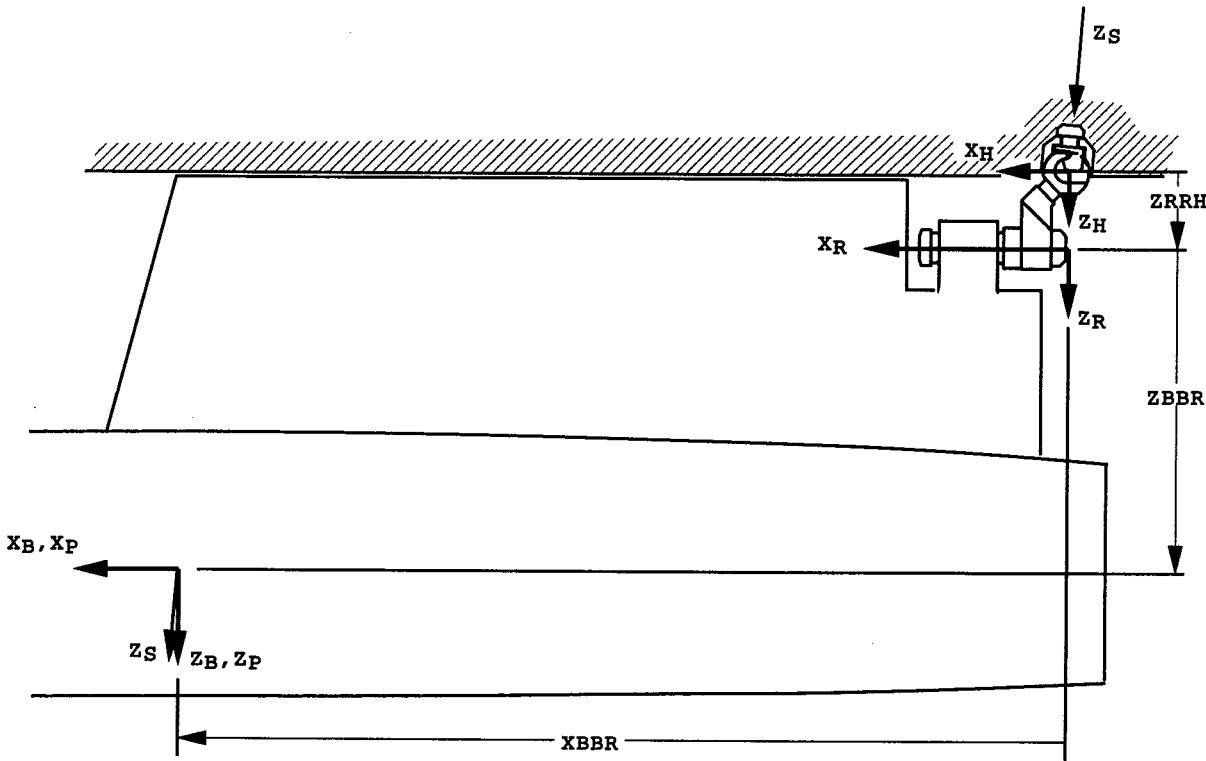


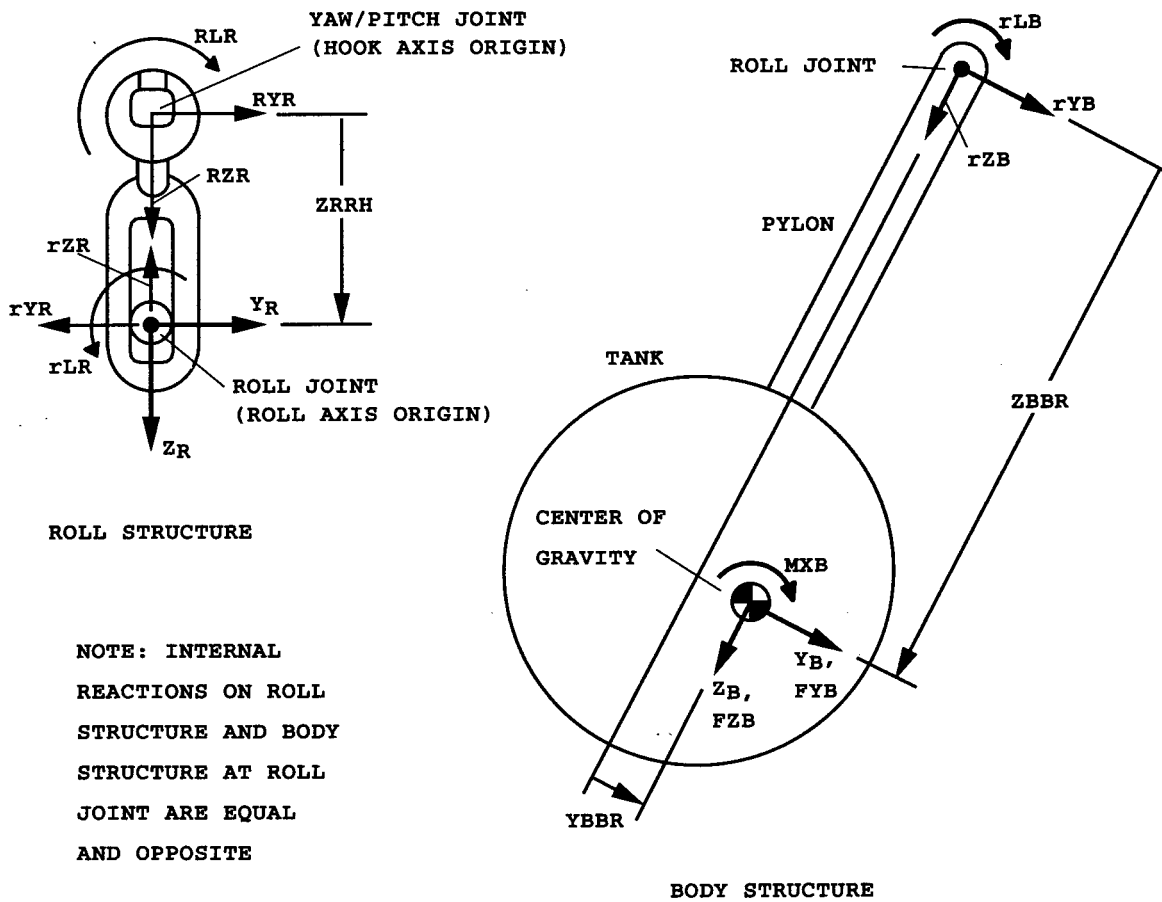
Figure 21. F-15 pivot fitting.

212

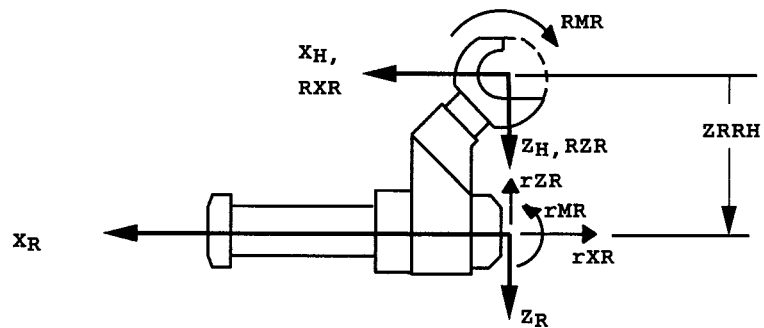


SIDE VIEW FOR STORE AT INSTALLED POSITION

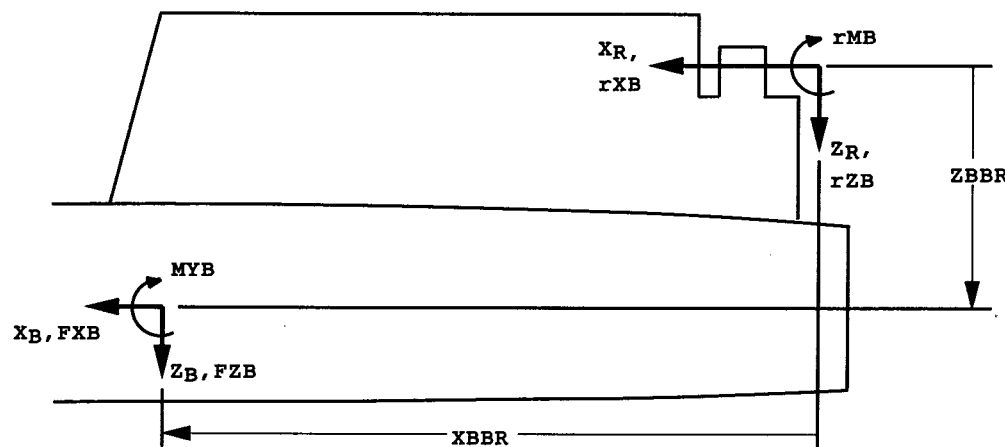
Figure 22. Relationship between body, roll, and hook axes for F-15 pivot.



a. Rear views looking forward along XB and XR axes
 Figure 23. Free-body diagram for F-15 pivot.



VIEW LOOKING ALONG YR AXIS OF ROLL STRUCTURE



VIEW LOOKING ALONG YB AXIS OF BODY STRUCTURE

b. Side views

Figure 23. Concluded.

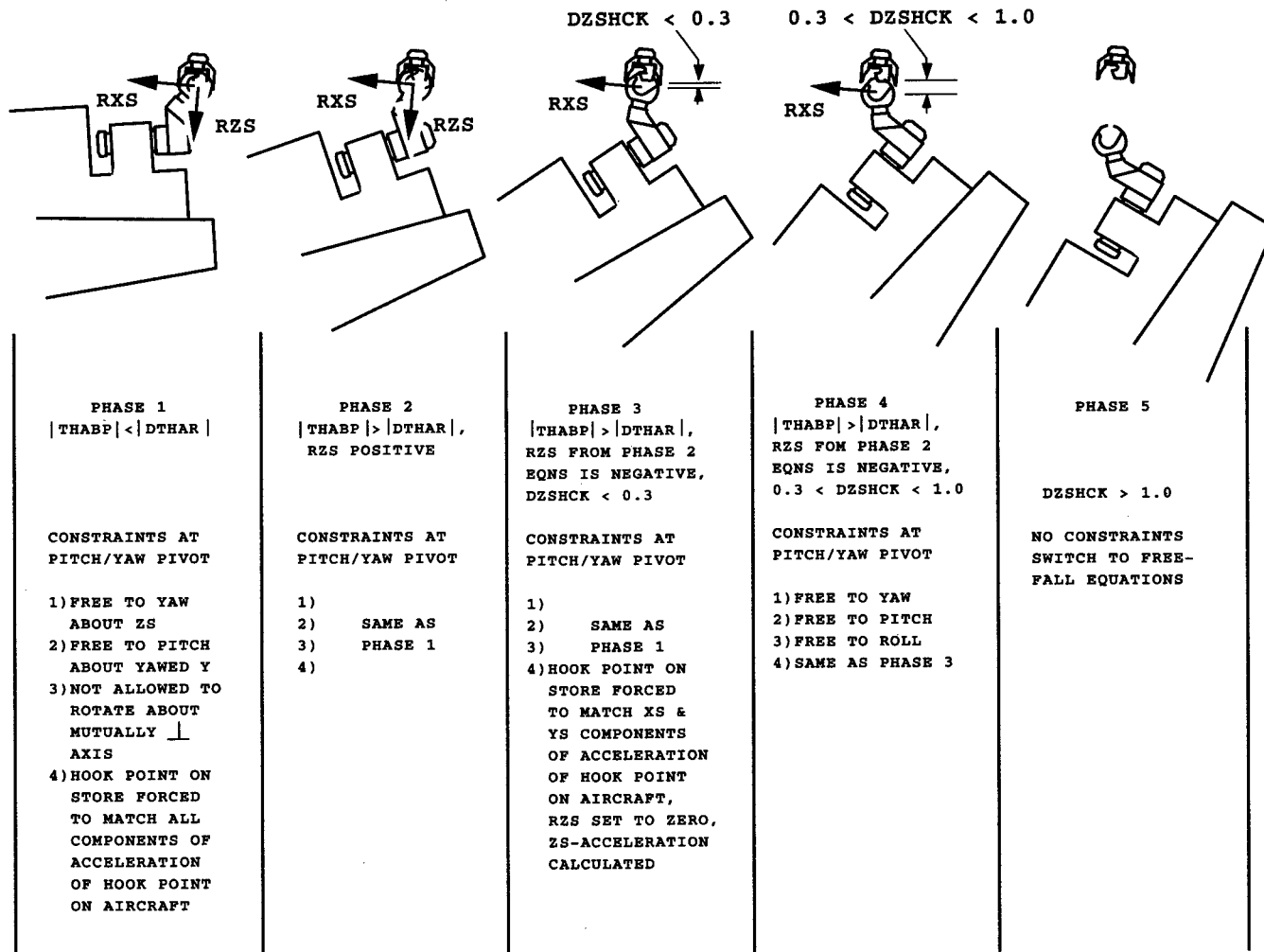
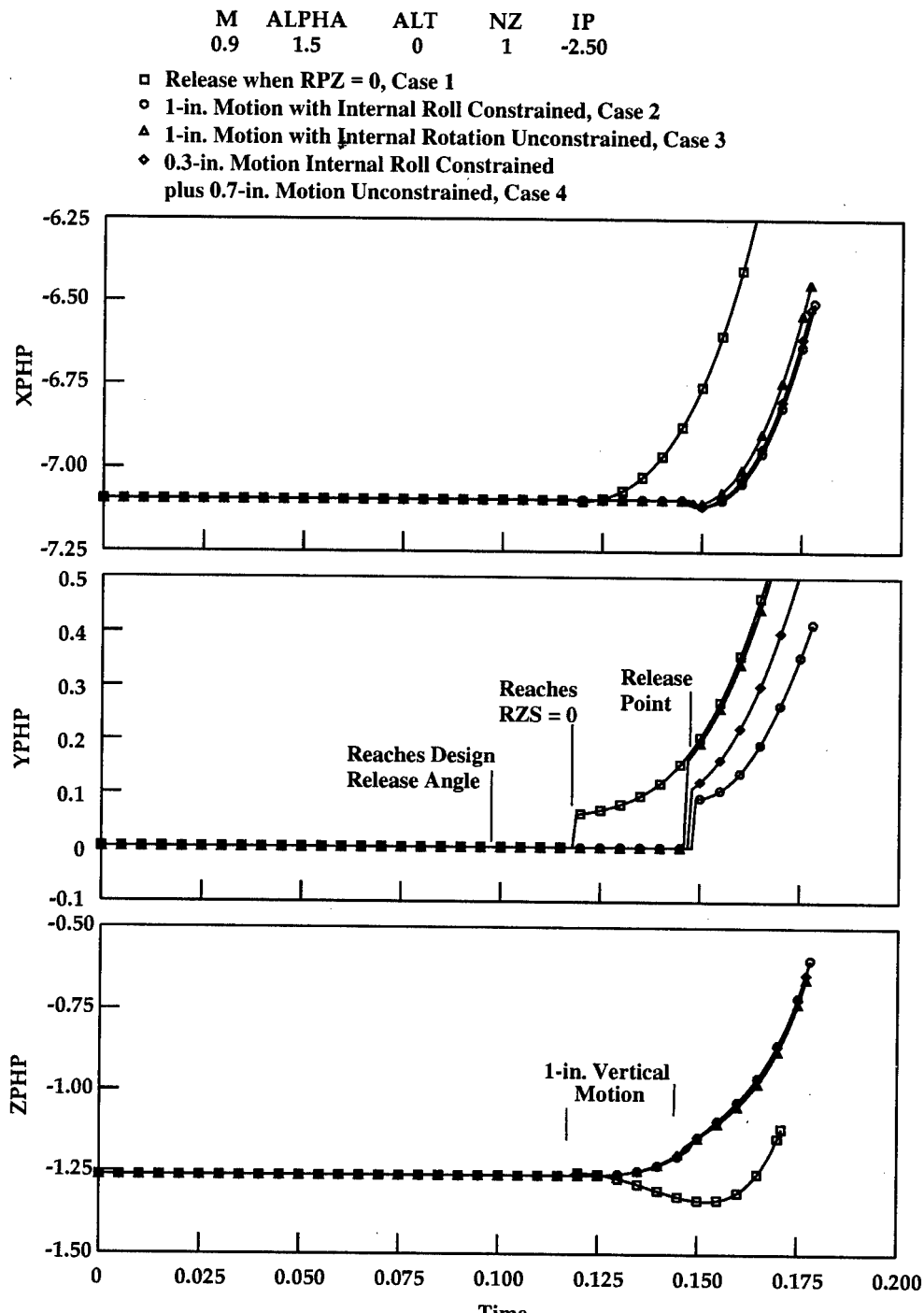
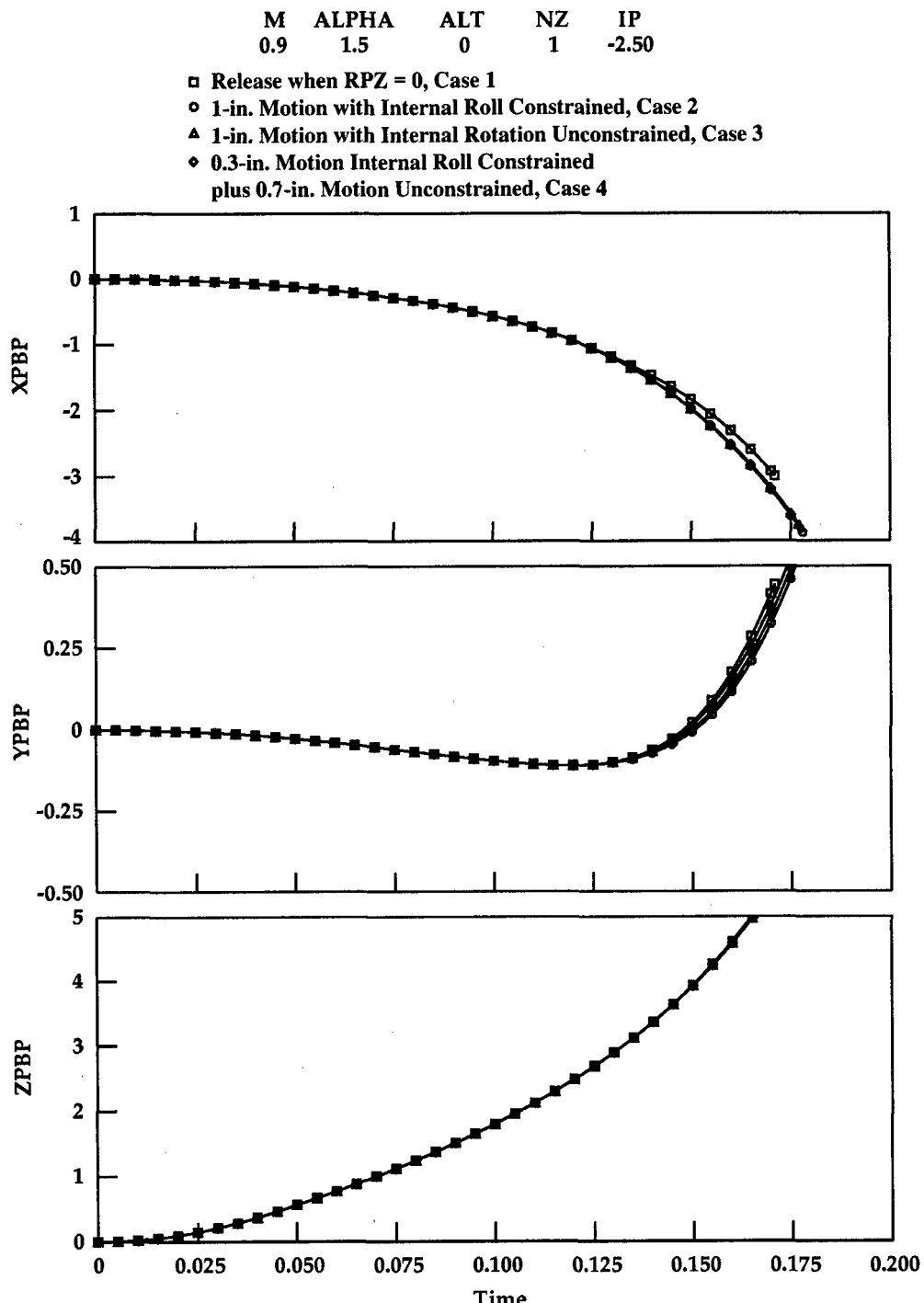


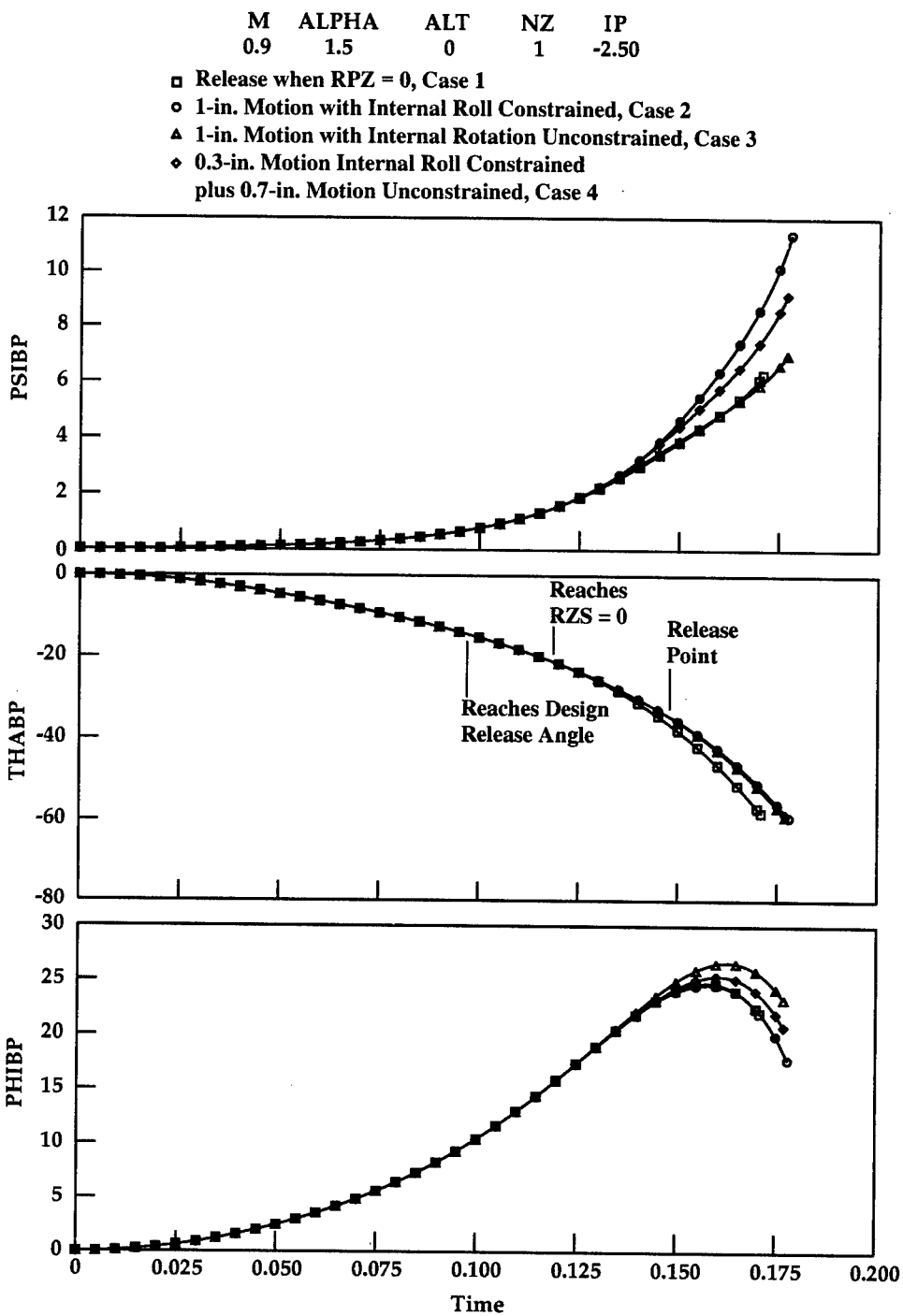
Figure 24. Phases of release motion for F-15 pivot mechanism.



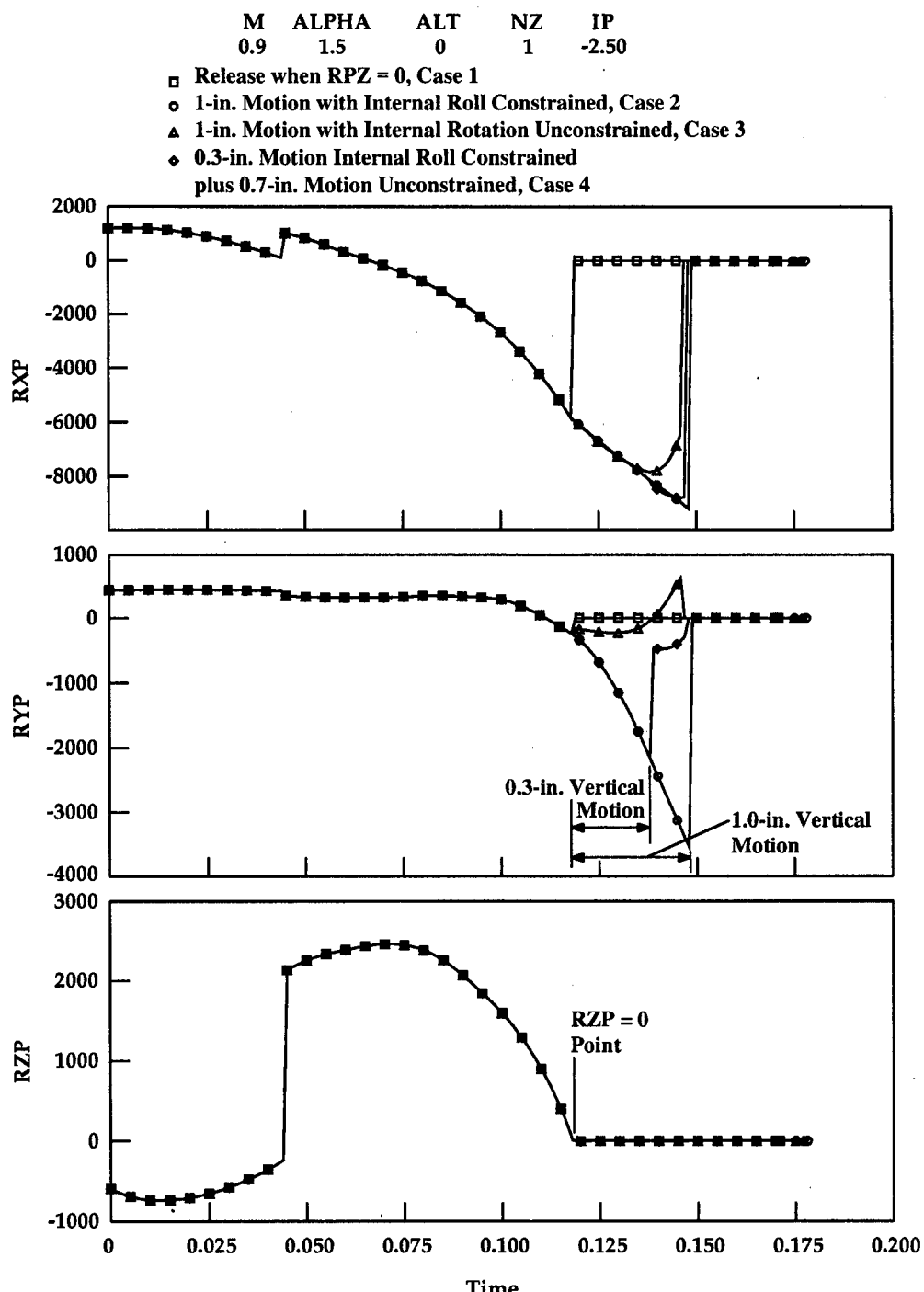
a. Pylon axis components of hook position
Figure 25. Motion parameters for numerical experiment.



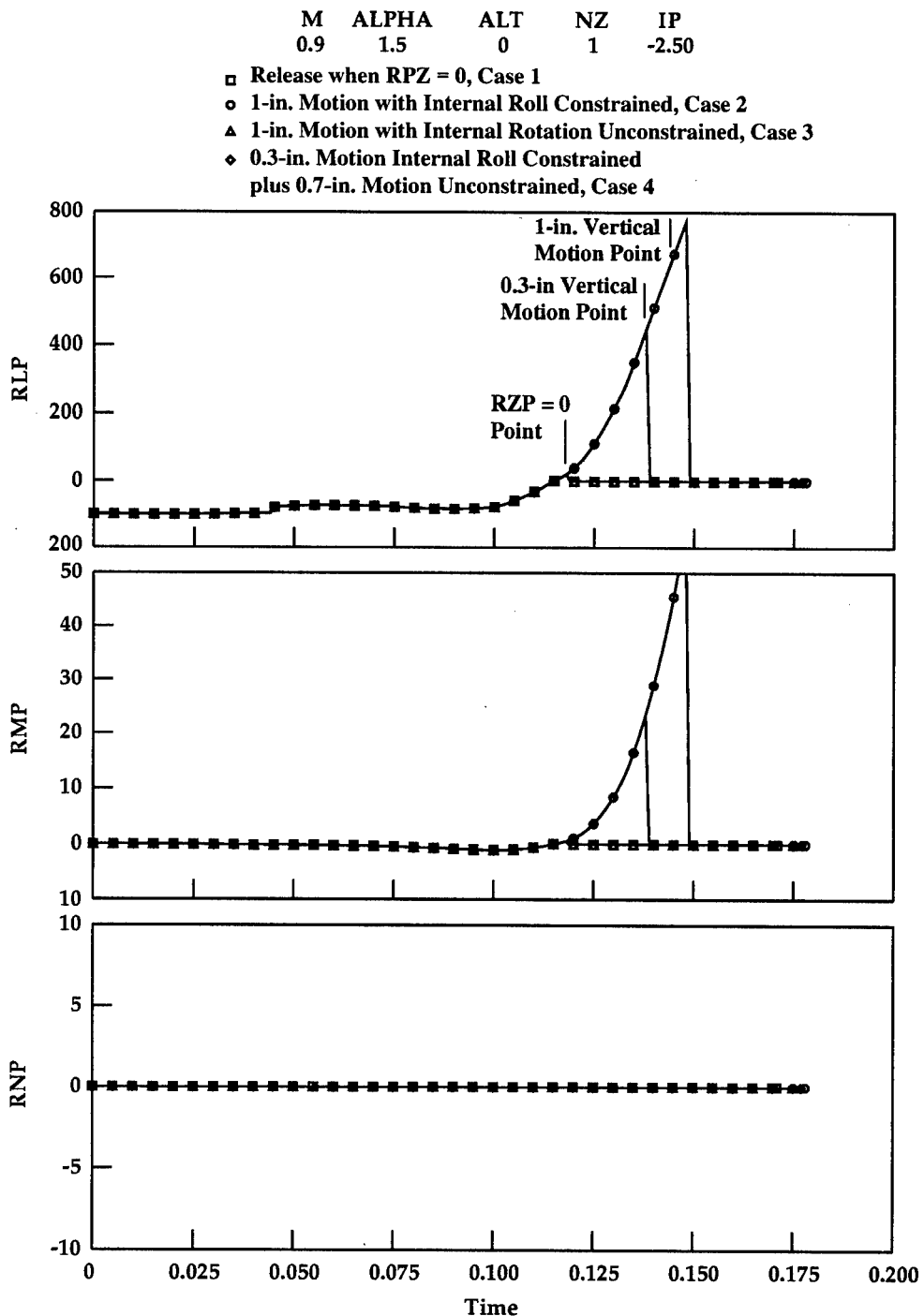
b. Pylon axis components of cg position
 Figure 25. Continued.



c. Tank angular orientations
 Figure 25. Continued.



d. Pylon axis components of reaction forces
Figure 25. Continued.



e. Pylon axis components of reaction moments
Figure 25. Concluded.

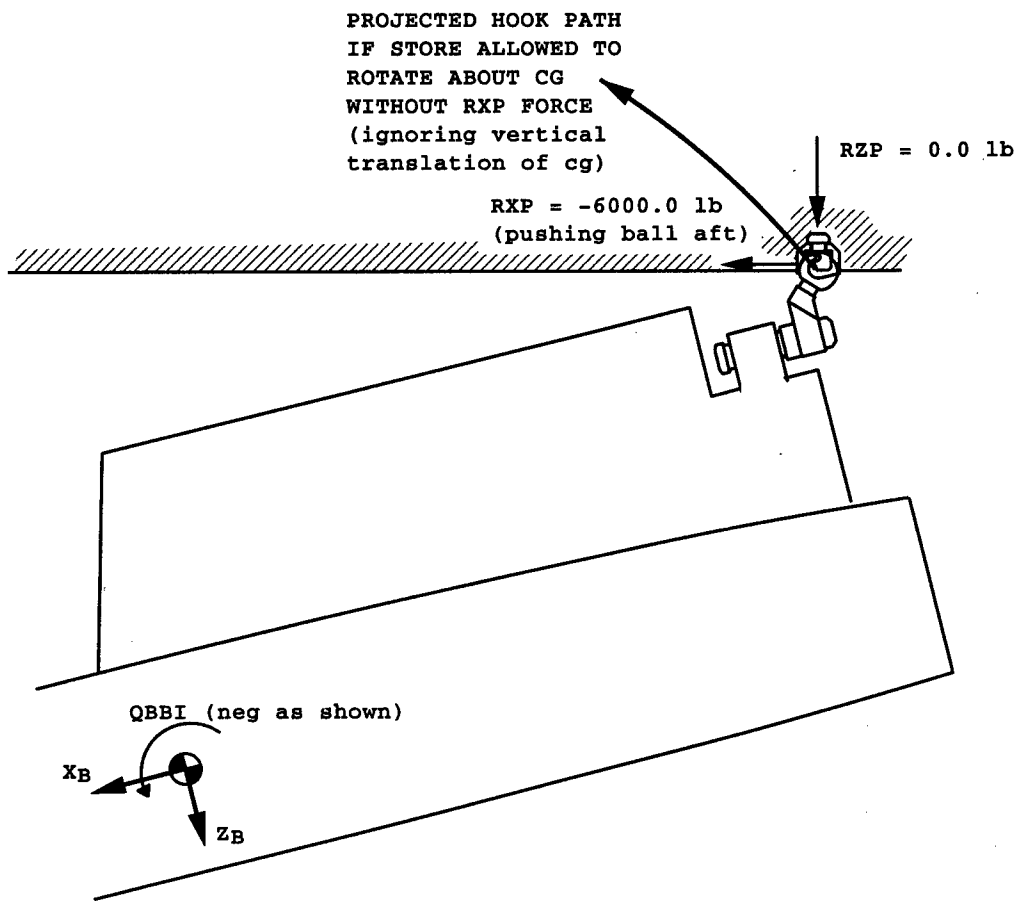
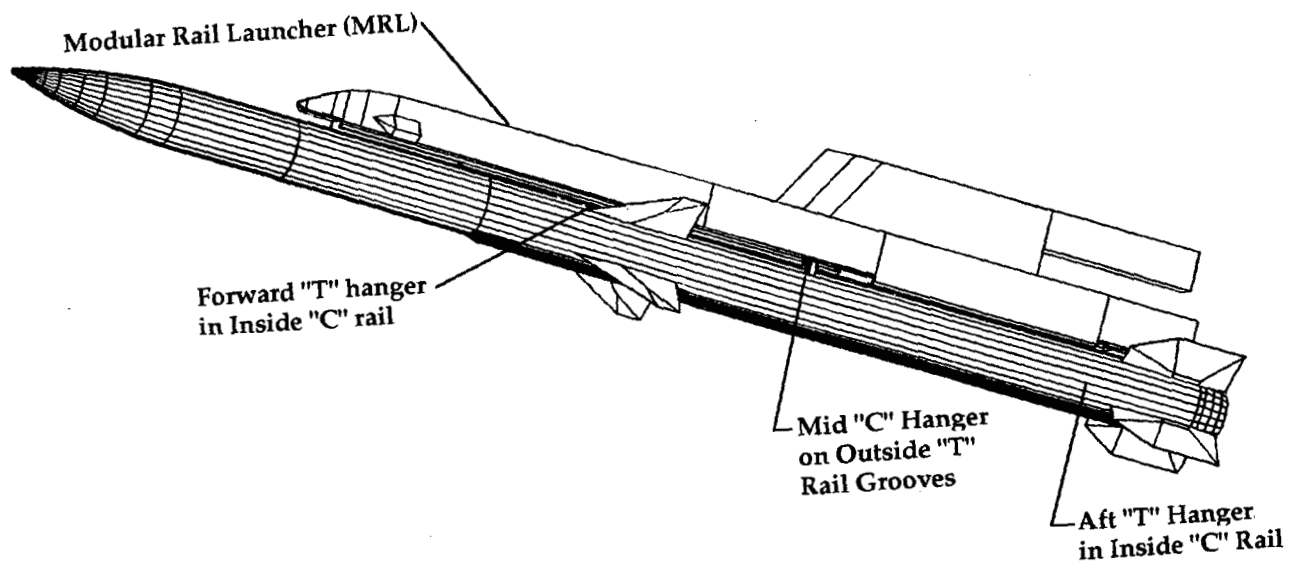
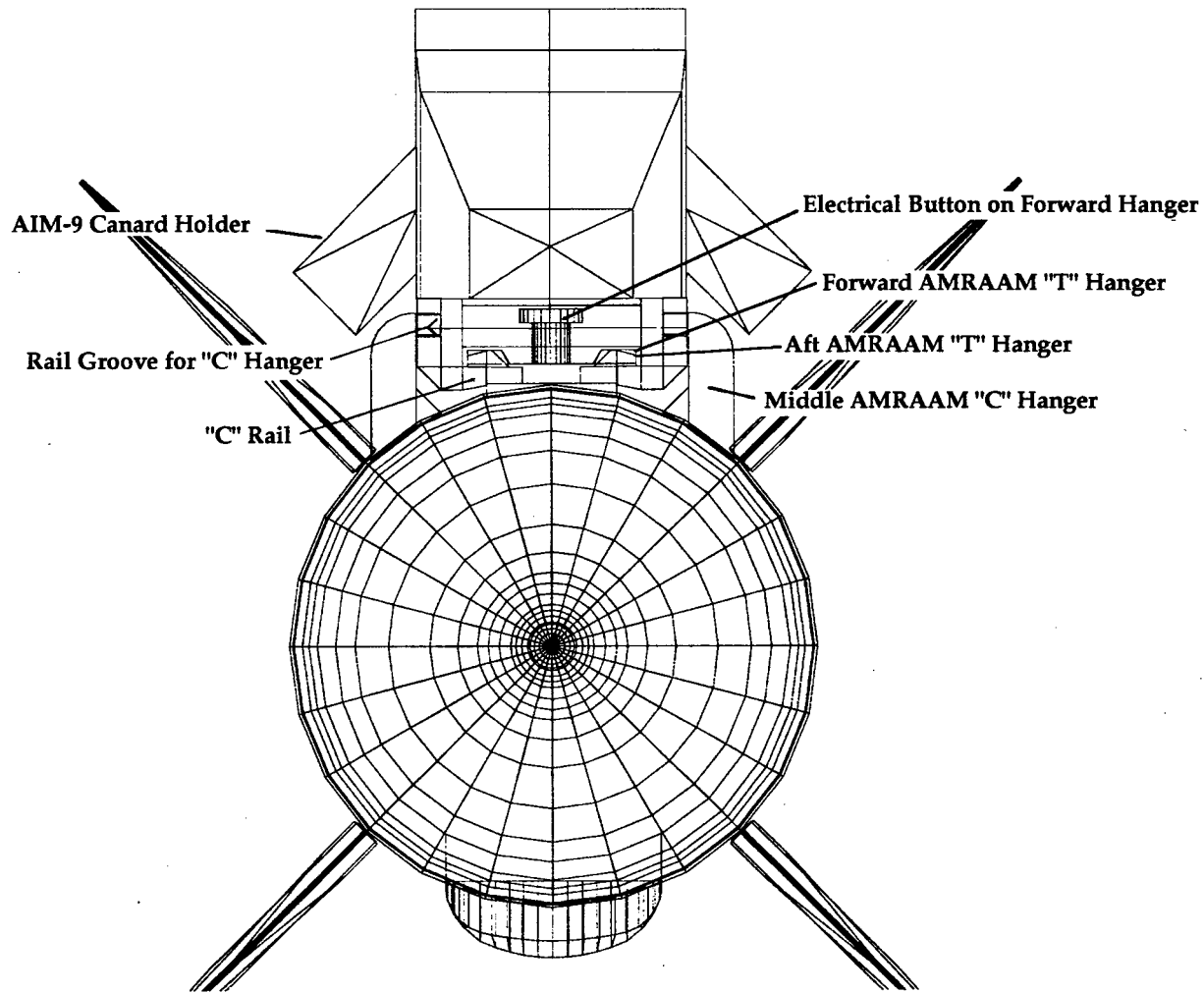


Figure 26. Free body diagram of tank at instant $RZS = 0.0$.



a. Installed carriage position
Figure 27. AMRAAM/MRL physical interface.



b. Front view
Figure 27. Concluded.

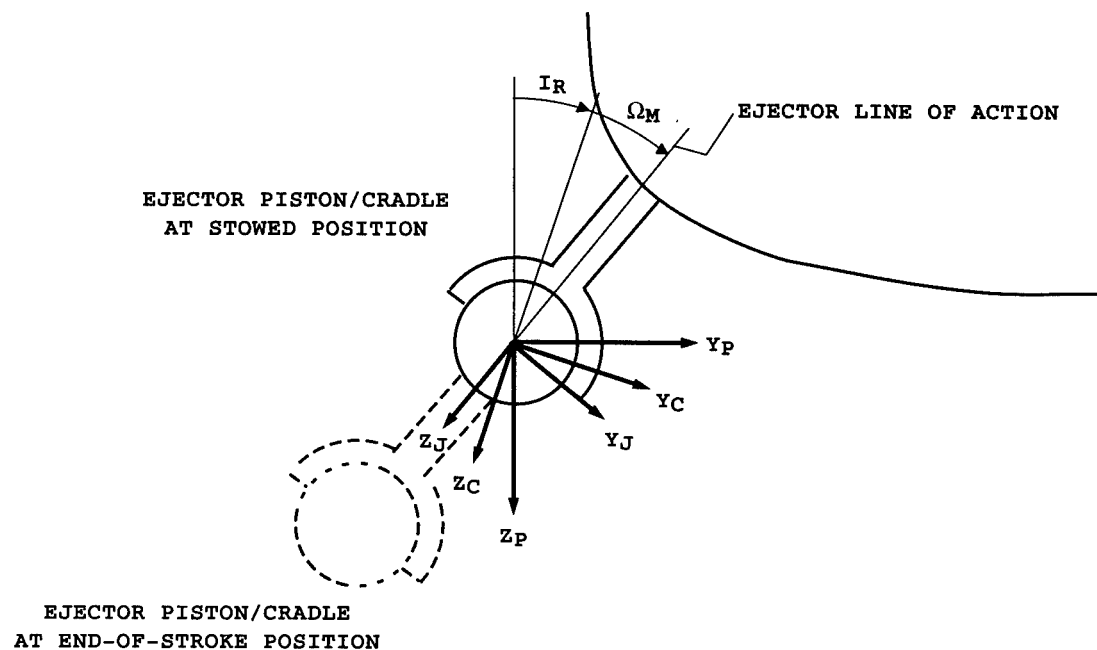


Figure 28. Ejector plane motion.

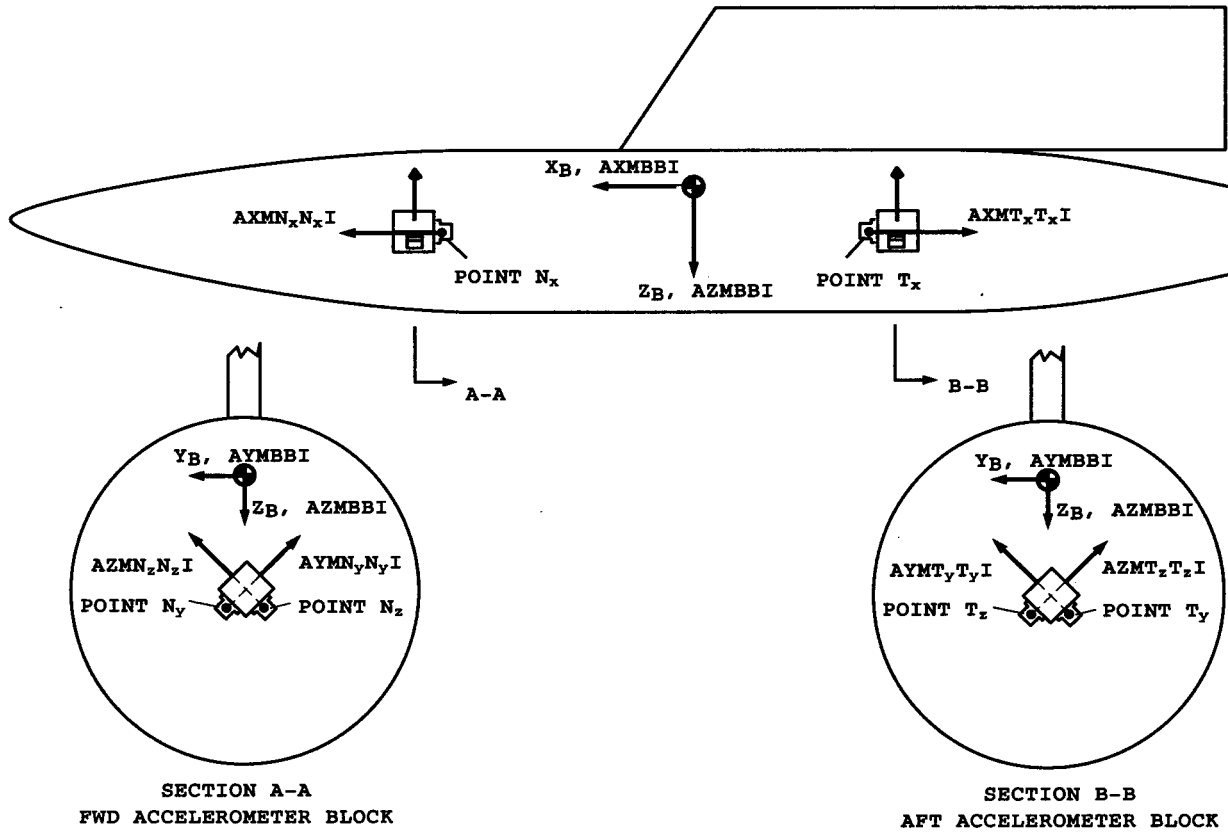


Figure 29. Instrumentation axes for F-22 drop tanks.

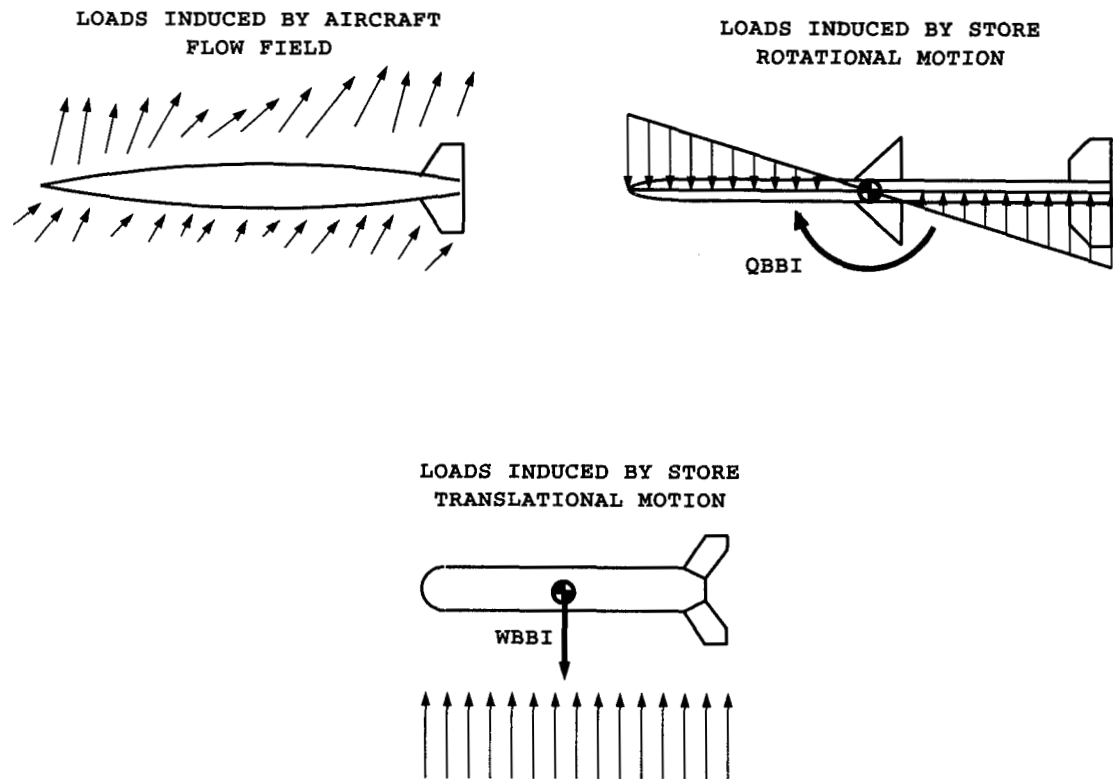
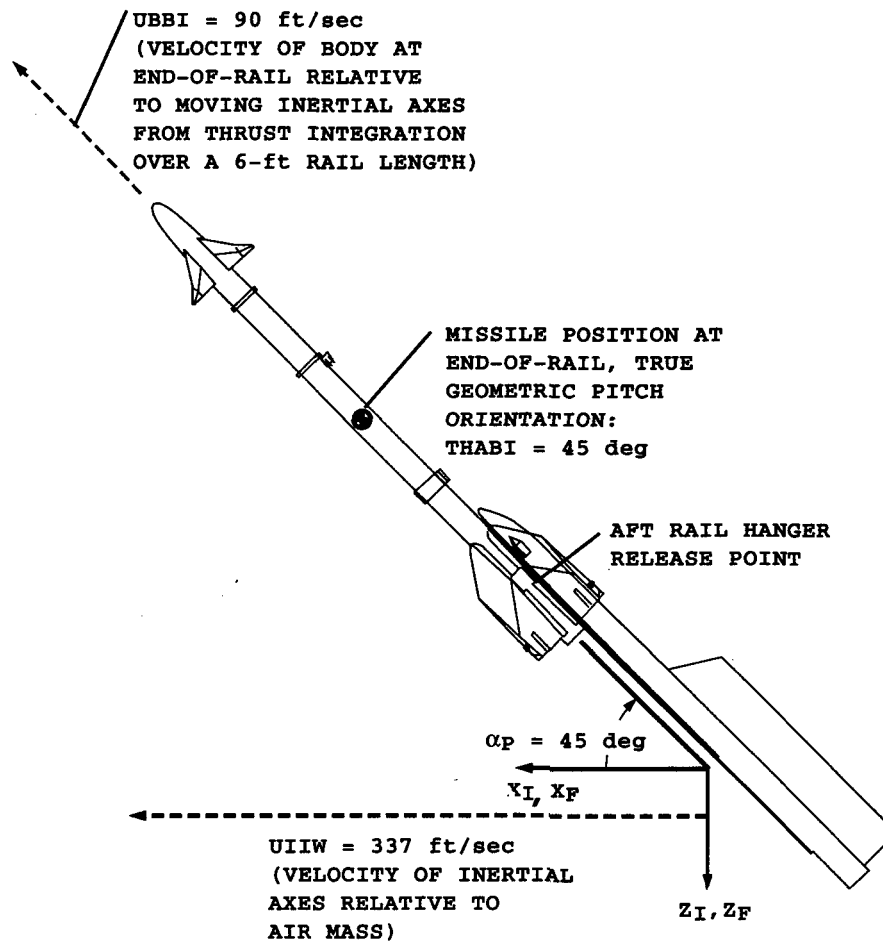
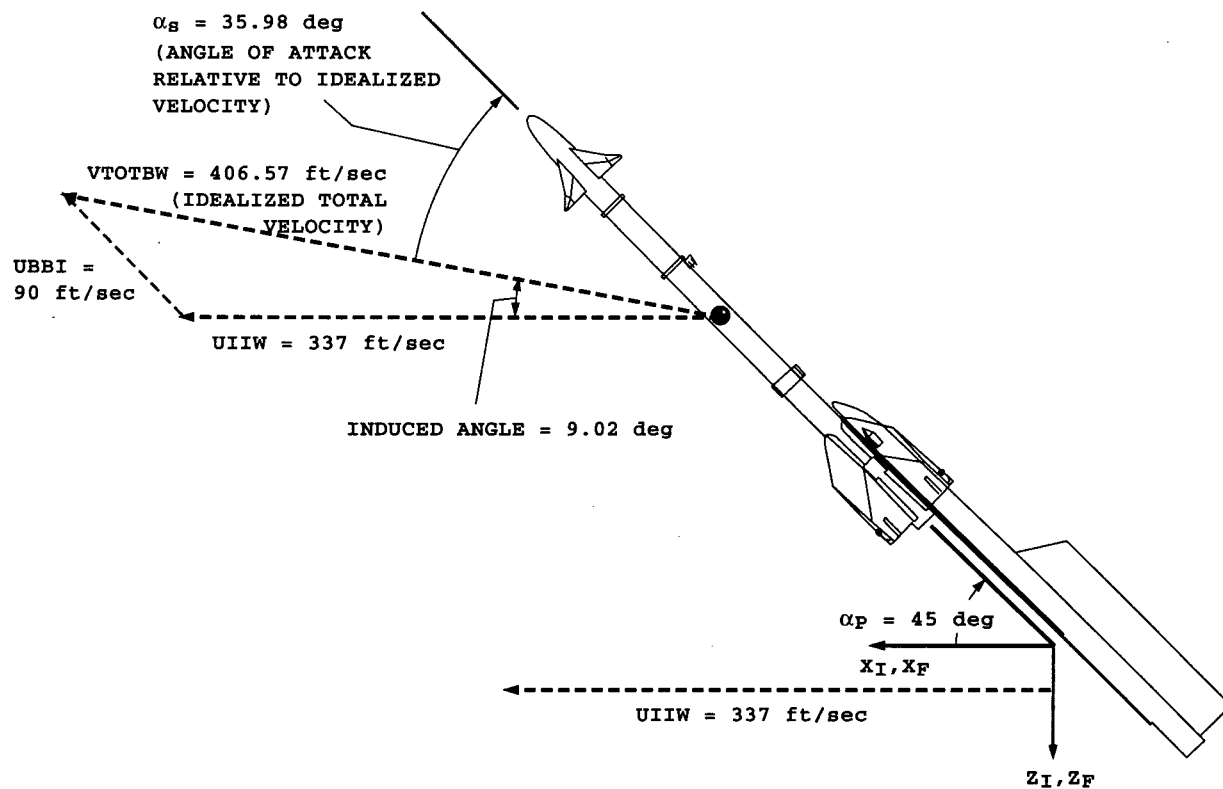


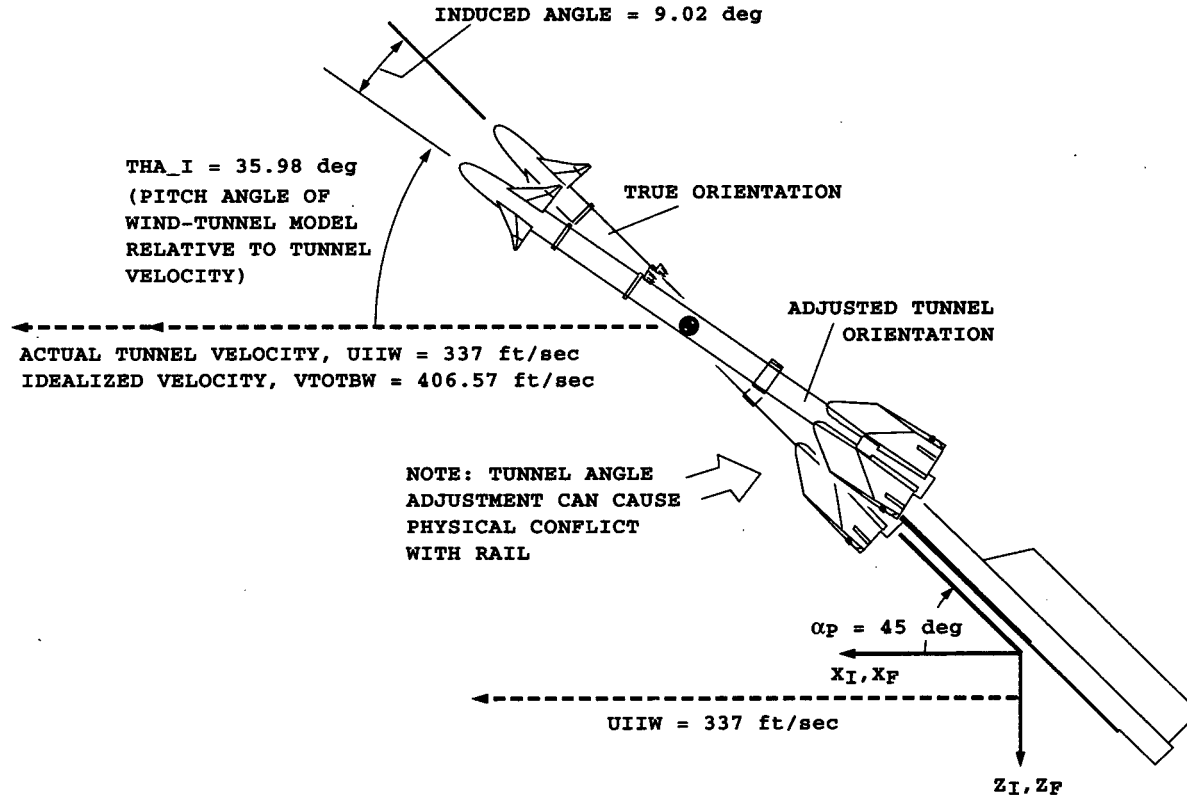
Figure 30. Sources of store aerodynamic loads.



a. True geometric downrail position and orientation
Figure 31. Example of "induced angle" approximation.



b. Velocity vector summation at store CG
Figure 31. Continued.



c. Adjusted test orientation
Figure 31. Concluded.

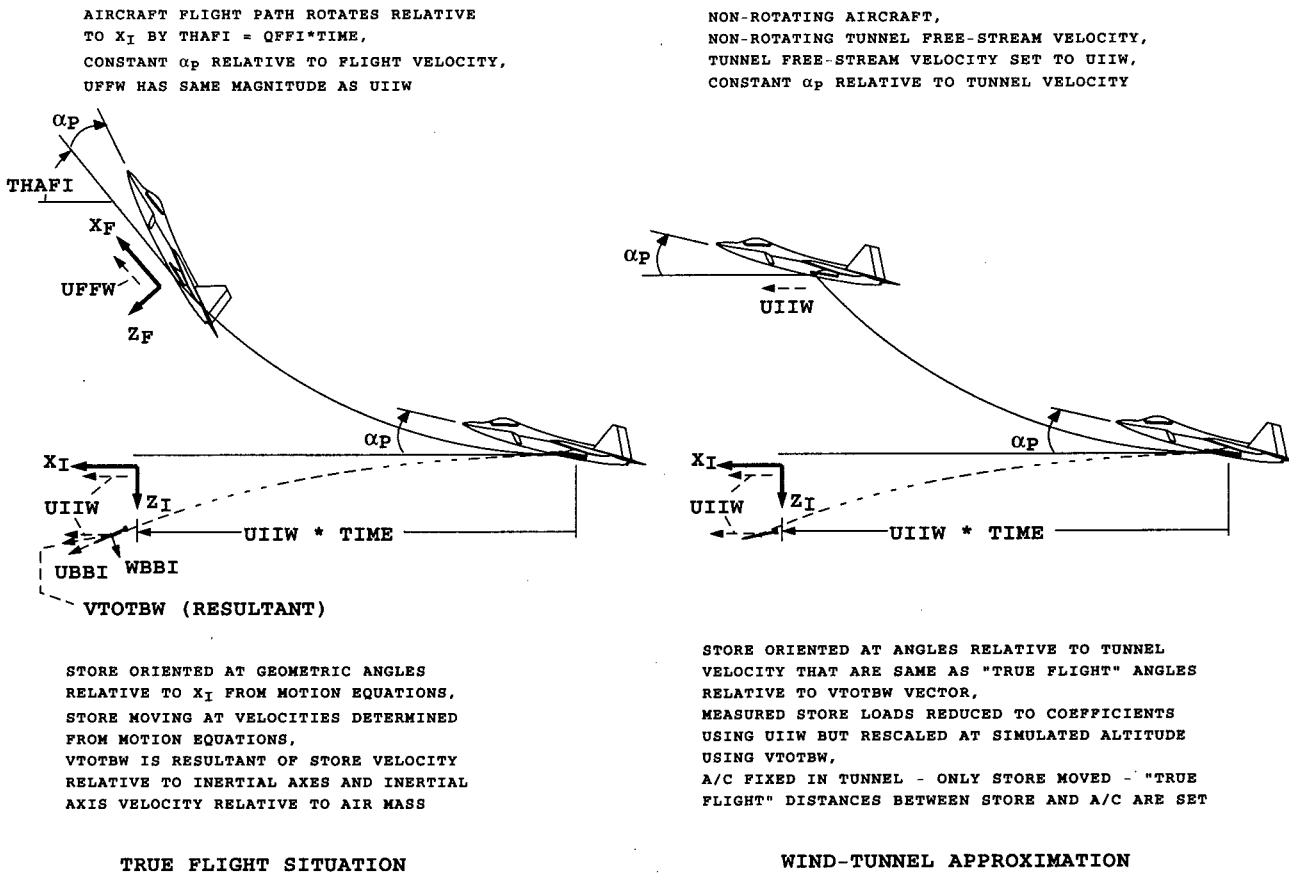


Figure 32. Non-rotating aircraft approximation.